Mangrove cover dynamics and community zonation in Gulf of Kachchh – A study based on synergistic use of optical and microwave satellite data

A Thesis Submitted to

Nirma University

In Partial Fulfilment of the Requirements for

The Degree of

Doctor of Philosophy

In

Science

BY

Mohit Kumar

(Reg. No. 12EXTPHDS40)

Institute of Science

Nirma University

Ahmedabad-382481

Gujarat, India

August, 2018

Affectionately

Dedicated

to

My Mother

CERTIFICATE

This is to certify that the thesis entitled "**Mangrove Cover Dynamics and Community Zonation in Gulf of Kachchh – A Study Based on Synergistic Use of Optical and Microwave Satellite Data**" has been prepared by **Mr. Mohit Kumar** under my supervision and guidance. The thesis is his own original work completed after careful research and investigation. The work of the thesis is of the standard expected of a candidate for Ph.D. Programme in Science and I recommended that it be sent for evaluation.

डॉ. ए.एस. राजावत / Dr. A.S. Rajawat
ग्रुप निदेशक / Group Director
भू-विज्ञान, जल विज्ञान, हिममंडल विज्ञान एवं उपयोग समूह/ईपीएसए
Geo-Sciences, Hydrology, Cryosphere Sciences & Application Group/EPSA
अंतरिक्ष उपयोग केन्द्र (इसरो) / Space Applications Centre (ISRO)
भारत सरकार / Government of India
अहमदाबाद / Ahmedabad - 380 015

Date: 18/08/2018

Signature of the Guide

Forwarded by:

Name and Signature of the
Head of the Department (If Any)

Director
Institute of Science
Nirma University
Ahmedabad

Name and Signature of the
Dean Faculty of Science

23-8-18

Name and Signature of the Dean
Faculty of Doctoral Studies and Research

23/8/18

Executive Registrar

ABSTRACT

This research work has demonstrated efficacy of digital classification techniques using both optical as well microwave satellite data in inventory and monitoring of mangrove cover and community classes of the mangrove covered regions of the Gulf of Kachchh, Gujarat, India and has attempted to understand causes for changes in the mangrove habitats.The present work has utilized optical and microwave satellite data for studying mangrove cover dynamics and community zonation in the Gulf of Kachchh, Gujarat, India.The Gulf of Kachchhis a semi-enclosed basin situated in the north-west part of the Indian coast in the state of Gujarat. Occupying an area of approximately 7300km^2, this region is characterized by the presence of shoals, channels, inlets, creeks, mudflats, islands, mangroves and coral reefs. The Gulf of Kachchh is a highly energetic macro-tidal system of the northeastern Arabian Sea. The tidal ranges in the Gulf of Kachchh reach upto 7.2 m. The region is characterized by arid/semi-arid climate with an average annual rainfall of 50 cm. The mangroves in the Gulf show spatial variability in extent, composition and condition based on dominant coastal processes, geomorphological setting and amount of protection from anthropogenic influences.Mangrove cover dynamics has been studied for five mangrove occupying regions of the Gulf *viz*., i) around Kori creek along north-west coast, ii) around Mundra along northern coast, iii) around Kandla along northern coast, iv) around Satsaida bet in north-eastern coast, and v) Marine National Park and Sanctuary (MNP&S) along southern coast of the Gulf of Kachchh.This study has observed that in all the five study regions mentioned above, *Avicennia marina*is the only dominant species, with smaller patches of *Rhizophora mucronata*, *Rhizophora apiculata, Acanthus ilicifolius* and *Ceriops tagal*. It has been possible to digitally classify mangroves as per density for all the regions. Based on existing knowledge about various classes in the inter-tidal zone, and understanding of spectral signatures, field visits, seven classes were chosen for supervised classification *viz*., Mangrove Dense (MD), Mangrove Sparse (MS), Mangrove Degraded (MDeg), Intertidal Mudflat (IM), Subtidal Mudflat (SM), Salt Encrustation (SE) and Sea Water (SW). Class separability has been evaluated using transformed divergence method, which involves computation of spectral distance between

signatures of various classes by taking into account their statistical parameters such as mean, variance and covariance. Class separability value is well above the threshold 1700 (i.e., 1823.6 – 2000) for all seven classes used in this study. In fact mostly the range in near to 2000, except locations where attempt to discriminate mangrove species within MNP&S was made, the value is relatively lower (1823.6). Accuracy assessment for all the classified images shows overall accuracy range 89%-97.64% and corresponding Kappa values ranges 0.87-0.96. Temporal changes in extent and condition of mangrove classes during time frame 2011 and 2017 have been quantified based on the corresponding classified Landsat images. The results show that mangrove covered area in the entire Gulf of Kachchh has increased by 254.73 sq km during time frame 2011-2017. Mangrove covered area mapped is 963.62 sq km for 2011 and 1218.35 sq km for 2017 for the entire study area. Out of five regions, Satsaida bet and environs has shown 57.18 % increase, Kori creek and environs 18.81 % increase, Marine National Park and Sanctuary 10.70 % increase, Kandla and environs 7.33 % increase and Mundra and environs 5.98 % increase in mangrove cover. In general, there is decrease in area under degraded mangrove class and increase in area under sparse mangrove class. Primary reason of increase in mangrove cover is due to serious plantation efforts carried out by various agencies such as Gujarat Forest Department, Marine National Park (MNP) authorities, Gujarat Ecology Commission etc. in collaboration with local communities and organizations. There has been lot of developmental activities along the inter-tidal region of Gulf of Kachchh, major ones being development of Ports such as Mundra and massive expansion of salt industry, which led to destruction of mangroves at some locations prior to 2011, however as per this study, efforts and care being taken on mangrove plantation is resulting into positive results and there is substantial increase in mangrove cover during current decade.

There has been an increase of about 48 sq km of mangroves around Kori Creek in 2017 compared to 2011. Dense mangroves have increased by about 18 sq km, sparse mangroves have shown an increase of about 27 sq km and mangroves under degraded class have increased by 2.5 sq km. The increase is more in the category of dense mangroves (63% increase) which reflects concomitant improvement of mangrove density in this region.It seems that due to lot of nutrients being brought out along with the sediments of Indus river and less anthropogenic activities due to its proximity to International border, growth of mangroves in this region is more due to natural processes rather than plantation efforts. Around Mundra, an increase of about 15 sq km of mangroves was observed during the period 2011-2017, largely because of approx. 17 sq km of increase in the sparse mangrove category, which is probably result of plantation activities. However, around1sq km of dense mangroves and 0.69 sq km of degraded mangroves were destroyed in this region due to expansion of port-related activities. In Kandla region, there has been an increase of roughly 19 sq km of sparse mangroves during 2011 and 2017, which is also probably result of plantation activities. However, the study has also observed decline of about half sq km of dense mangroves in this region because of port-related activities and construction of saltpans. The mudflats around Satsaida bet showed an increase of 145.62 sq km of mangrove during the mapping period of 2011-2017, which is around 57.18 % increase among the five regions studied. Here, the increase is mainly because of increase of 201 sq km of sparse mangroves. However, the study also observed reduction of approx. 20 sq km of dense mangroves due to construction of saltpans. The area under 'mangrove degraded' category declined by about 36 sq km as their condition improved and they were categorized as sparse mangroves in 2017. Mangrove cover in the Marine National Park and Sanctuary (MNP&S), located along southern coast of the Gulf of Kachchh is 190.52 sq km in 2011 and 217.85 sq km in 2017. There has been an increase in mangrove cover of about 27.23 sq km (10.69% among five regions studied). The increase is mainly in *Avicennia*sparse mangrove class (~ 25 sq km). The increase is observed mainly on islands such as Pirotan, Mundeka-Dideka, Kalubhar, Dhani and on coastal belts adjoining Balachadi, Jodiya, near Hansthal Creek and Sikka. Cause of increase in mangrove cover is primarily due to plantation efforts by authorities of the MNP&S. These plantations were carried out under various schemes such as Cher Plantation, Coastal Border Plantation etc.

An attempt has been made to evaluate potentials of C-band HH RISAT-1 MRS (Medium Resolution ScanSAR mode) data in conjunction with Resourcesat-2 LISS-IV (Linear Imaging Self Scanner-IV) datafor identifying mangrove communities in Jindra-Chhad Island complex located within Marine National Park and Sanctuary (MNP&S), with a primary focus on developing approach for improving discrimination of mangrove communities by synergistic use of microwave and optical data.Three different approaches were used to combine the SAR and optical data to explore the synergistic potential of the SAR data with optical data, for discriminating different mangrove communities in the study region. The study has carried out supervised classification for mangrove community zonation using Maximum Likelihood Classifier i) using LISS-IV data, ii) using RISAT-1 SAR data, iii) Integrating RISAT-1 SAR and three LISS-IV bands, iv) Merging RISAT-1 SAR and LISS-IV using IHS method and v) Integrating RISAT-1 to the band ratios derived from LISS-IV bands and has subsequently evaluated the results qualitatively as well quantitatively. All approaches resulted into classified images showing seven classes viz., *Avicennia* Dense (AD), *Avicennia* Sparse (AS), *Rhizophora-Ceriops* Dense (RCD), Intertidal Mudflat (IM), Hightidal Mudflat (HM), Sand and Sea. Quantitative evaluation of classified images was done through class separability analysis using transformed divergence method and accuracy assessment. The results indicate that addition of RISAT-1 SAR significantly improves the class separability. All the combinations employing optical and SAR data, have shown increased class separability compared to either LISS-IV or RISAT-1 when used alone. In addition, when all the four channels (two visible, one NIR and one microwave) are integrated and used together, the separability and accuracy obtained is highest. Replacing hue with SAR data yielded image that provided better class separability value (1847.51) than replacing either intensity (1811.78) or saturation (1829.72).The band ratio approach which segregated the non-vegetative component from the vegetative one in the image, yielded image with relatively lower class separability value (1867.27) than those obtained by integration method, but this approach provided relatively higher class separability value than those obtained by IHS method.The study demonstrated that the synergistic use of RISAT-1 C-band MRS and Resourcesat-2 LISS-IV data improves mangrove community discrimination. The mangrove communities discriminated are *Avicennia* Dense, *Avicennia* Sparse, and *Rhizophora-Ceriops* Dense. Among the different approaches of merging SAR with optical data, maximumseparability among mangrove community classes could be obtained by integrating SAR data with Red, Green and NIR bands of optical data.

The work provides the latest estimates for mangroves in the Gulf of Kachchh. In addition, the community zonation done through synergistic use of microwave and optical data provides new approach for mangrove studies using disparate datasets.

DECLARATION

I, Mr. **Mohit Kumar**, registered as Research Scholar, bearing Registration No. **12EXTPHDS40** for Doctoral Programme under the **Faculty of Science** of Nirma University do hereby declare that I have completed the course work, pre-synopsis seminar and my research work as prescribed under R. Ph.D. 3.5.

I do hereby declare that the thesis submitted is original and is the outcome of the independent investigation/research carried out by me and contains no plagiarism. The research is leading to the discovery of new facts/techniques/correlation of scientific facts already known. This work has not been submitted to any other University or Body in quest of a degree, diploma or any other kind of academic award.

I do hereby further declare that the text, diagrams or any other material taken from other sources (including but not limited to books, journals and web) have been acknowledged, referred and cited to the best of my knowledge and understanding.

Date: 21/08/2018

Mohit Kumar

Signature of the Student:

डॉ. ए.एस. राजावत / Dr. A.S. Rajawat
ग्रुप निदेशक / Group Director
भू-विज्ञान, जल विज्ञान, हिममंडल विज्ञान एवं उपयोग समूह/ईपीएसए
Geo-Sciences, Hydrology Cryosphere Sciences & Application Group/EPSA
अंतरिक्ष उपयोग केन्द्र (इसरो) / Space Applications Centre (ISRO).
भारत सरकार / Government of India
अहमदाबाद / Ahmedabad - 380 015

ACKNOWLEDGEMENTS

I express my sincere and heartfelt gratitude to my Research guide and supervisor, **Dr. A.S. Rajawat**, Scientist G and Group Director, Geo-Sciences, Hydrology, Cryosphere Sciences and Applications Group (GHCAG), Earth, Ocean, Atmosphere, Planetary Sciences and Applications Area (EPSA), Space Applications Centre (SAC), Indian Space Research Organization (ISRO), Ahmedabad, for his inspiring guidance, continuous support, constant encouragement and also for providing data and necessary facility. His positive approach and friendly attitude led to completion of the writing of this thesis.

I convey my heartfelt gratitude to the **Director**, Space Applications Centre (SAC), Indian Space Research Organization (ISRO), Ahmedabad, for granting me permission to pursue my Ph. D. study.

I would like to express my sincere gratitude to **Dr. Ajai**, Emeritus Professor, CSIR and former Group Director, SAC, for constant guidance and encouragement throughout my career so far.

I am extremely grateful to **Nirma University**, Ahmedabad for providing me an opportunity to pursue PhD. I owe my deep sense of gratitude to the **Director General**, the **Deputy Registrar (Ph.D. Section)**, the **Dean, Faculty of Doctoral Studies & Research**, and the **Dean, Faculty of Science**, of Nirma University, for allowing me to register as a Ph. D. student and for all the support to carry out Ph.D. study. I am also thankful to the administrative staff of Ph.D. Section, Nirma University, Ahmedabad for providing guidance related to various matters from time to time.

I am extremely grateful to **Dr. Jyoti Parikh**, Executive Director, and **Mr Rohit Magotra**, Deputy Director, Integrated Research and Action for Development (IRADe), New Delhi, for valuable support and encouragement.

I sincerely acknowledge the guidance and support given by **Dr H B Chauhan** and **Mr Ratheesh Ramakrishnan** of SAC throughout my tenure at SAC. Most of the time at SAC, I used to work with either of these two eminent scientists.

I also acknowledge the support received at various stages from other scientists of EPSA/SAC, Ahmedabad, *viz.* **Dr Gaurav Jain, Dr Nandini Ray Chaudhury, Dr Tanumi Kumar** and **Mr. Ritesh Agrawal.**

I wish to place on record the valuable assistance provided by my colleagues at SAC, Ahmedabad especially **Ms Yashee Joshi, Mrs. Veera Panchal, Dr Manik Mahapatra, Ms Mitali Gautam, Mr Parixit Vala, Mr Hiren Bhatti, Ms Preeti Rajput, Ms Dimpal Sanghavi, Ms Richa Tiwari** and **Mrs Dhara Shah.** In addition, I would like to thank **Ms Vanya Bajpai, Dr Prabhjot Kaur, Dr Varunika Jain, Dr. Sriram Saran Bairavarasu, Dr Revati More, Dr Suvarna Punalekar, Dr Arunima Dasgupta, Dr Inderpreet Kaur, Dr Jagat Singh Bisht, Dr. Guneshwar Thangjam, Dr. Shashikant Patel, Ms Koyel Sur, Dr. Durgesh Nandan Piyush, Dr. Swapnil Sunil Vyas** and all Research Fellows for their support and friendship during my tenure at SAC.

I also thank my colleagues at IRADe: **Mr Pushkar Pandey** and **Mrs Asha Kaushik** for their assistance and support at IRADe.

I thank **Mr Shyamal Tikadar**, Chief Conservator of Forests (CCF), MNP Circle, Jamnagar for providing permission, boat and other necessary facilities for ground visit. He was kind enough to accompany me during the field visit.

I also thank **Dr H S Singh**, Ex-PCCF, Gujarat Forest Department and **Mr Bharat Pathak**, former Director, GEER Foundation, Gandhinagar for accompanying me during the field visit and for fruitful discussions during the course of this work.

I am greatly thankful to **Dr. Sarvesh Palria**, Former Head, Department of Remote Sensing and Geo-informatics, Maharshi Dayanand Saraswati University, Ajmer for his guidance and encouragement during the course of my PhD.

Finally, I would like to acknowledge my family members, my parents Late **Smt Sapna Devi Bakhru and Shri Raj Kumar Bakhru** who were always there for me and the thesis would never have been completed without their blessings and support; and my sister **Mrs Meeta Jotwani** who is younger to me but has taught me many things. I also thank my brother-in-law **Mr Vijay Jotwani** for his support. I also owe gratitude to my wife **Prof. Sarika Keswani** for helping me in arranging the references of my thesis.

I dedicate this Ph.D. to my mother who passed away during the course of this PhD but will always be with me in the form of her blessings and encouragement.

Mohit Kumar

Ahmedabad (Mohit Kumar)

CONTENTS

LIST OF TABLES

LIST OF FIGURES

LIST OF ABBREVIATIONS

AD	*Avicennia* Dense
AISA	Airborne Imaging Spectrometer for Applications
AGB	Above Ground Biomass
A&N	Andaman and Nicobar
ALOS	Advanced Land Observation Satellite
ANOVA	Analysis of Variance
AR	Apparent Reflectance
AS	*Avicennia* Sparse
ASTER	Advanced Space borne Thermal Emission and Reflection Radiometer
AVIRIS	Airborne Visible/Infrared Imaging Spectrometer
AVNIR	Advanced Visible Near Infrared Radiometer
AWiFS	Advanced Wide Field Sensor
CA	Consumer's Accuracy
CASI	Compact Airborne Spectral Imager
CBH	Circumference at Breast Height
CCF	Chief Conservator of Forests
CIR	Colour Infrared
CRS	Coarse Resolution ScanSAR
CRZ	Coastal Regulation Zone
CZIS	Coastal Zone Information System
dB	Decibels
DBH	Diameter at Breast Height
DEM	Digital Elevation Model

DN	Digital Number
DOC	Dissolved Organic Carbon
EMR	Electro-magnetic Radiation
EMS	Electro-magnetic Spectrum
ENVI	Environment for Visualization of Images
EO	Earth Observation
ERDAS	Earth Resource Data Analysis System
ERS-1	European Remote Sensing Satellite-1
ESRI	Environmental Systems Research Institute
ESZ	Eco Sensitive Zone
ETM	Enhanced Thematic Mapper
FCC	False Colour Composite
FFT	Fast Fourier Transform
FOTO	Fourier-based Textural Ordination
FRS	Fine Resolution Stripmap
FSI	Forest Survey of India
GE	Google Earth
GEC	Gujarat Ecology Commission
Geo-TIFF	Geographic Tagged Image File Format
GIS	Geographic Information Systems
GLCM	Grey Level Co-occurrence Matrix
GPS	Global Positioning System
GoI	Government of India
GoK	Gulf of Kachchh
Gt	Gigaton
ha	Hectares

HH	Horizontal Transmit, Horizontal Receive
HM	Hightidal Mudflat
HTL	High Tide Line
HV	Horizontal Transmit, Vertical Receive
IFoV	Integrated Field of View
IHS	Intensity-Hue-Saturation
IM	Intertidal Mudflat
InSAR	Interferometric Synthetic Aperture Radar
IR	Infrared
IRADe	Integrated Research and Action for Development
IRS	Indian Remote Sensing Satellite
IUCN	International Union of Conservation of Nature and Natural Resources
ISRO	Indian Space Research Organization
JAXA	Japan Aerospace Exploration Agency
JERS-1	Japan Earth Resources Satellite-1
JD	Julian Day
JM	Jeffries-Matusita
LAI	Leaf Area Index
LISS	Linear Imaging Self-Scanner
LSU	Linear Spectral Unmixing
MD	Mangrove Dense
MDeg	Mangrove Degraded
MLA/MLC	Maximum Likelihood Algorithm/ Maximum Likelihood Classifier
MNP	Marine National Park
MNP&S	Marine National Park and Sanctuary
MPA	Marine Protected Area

MRS	Medium Resolution ScanSAR
MS	Marine Sanctuary, Mangrove Sparse
MSS	Multispectral Scanner
NCC	Natural Colour Composite
NDVI	Normalized Difference Vegetation Index
NIR	Near Infrared
OA	Overall Accuracy
OB	Optical Brightness
OBIA	Object Based Image Analysis
OLI	Optical Land Imager
PA	Producer’s Accuracy
PALSAR	Phased Array L-band Synthetic Aperture Radar
PAN	Panchromatic
PCA	Principal Components Analysis
QGIS	Quantum GIS
RADAR	Radio Detection and Ranging
RCD	*Rhizophora-Ceriops* Dense
RGB	Red, Green, Blue
RISAT	Radar Imaging Satellite
RMSE	Root Mean Square Error
RS	Remote Sensing
SAC	Space Applications Centre
SAR	Synthetic Aperture Radar
SAM	Spectral Angle Mapper
SBM	Single Buoy Moorings
SCP	Semi-automatic Classification Plugin

SE	Salt Encrustation
SEZ	Special Economic Zone
SM	Subtidal Mudflat
SPOT	Satellite Pour l’ Observation de la Terre
SR	Simple Ratio, Surface Reflectance, Saturation Radiance
SRTM	Shuttle Radar Topographic Mission
SW	Sea Water
SWIR	Short-Wave Infrared
TD	Transformed Divergence
TM	Thematic Mapper
TSX	Terra SARX
UA	User’s Accuracy
UNESCO	United Nations Educational, Scientific and Cultural Organization
USA/US	United States of America/United States
UTM	Universal Transverse Mercator
UV	Ultra Violet
VH	Vertical Transmit, Horizontal Receive
VV	Vertical Transmit, Vertical Receive
WGS	World Geodetic System
XS	Multi-spectral

Chapter 1

Introduction

1.1 Mangroves

Mangroves are taxonomically diverse associations of woody trees and shrubs, which grow in the intertidal and adjacent communities along tropical and sometimes subtropical coasts (Tomlinson, 1986). These are shrubs and trees of medium height that grow between 25^0–30^0S up to 25^0–30^0N and are able to survive in brackish water, sea water, and salty evaporation pools with up to twice the salinity of ocean water. The term “mangrove” often refers to both the plants and the forest community. The term “mangrove” is also used as an adjective, as in “mangrove tree” or “mangrove fauna.” Mangrove forests are sometimes called “tidal forests”, “coastal woodlands”, or “oceanic rain forests.” Mangroves build communities parallel to the shoreline. Mangrove forests are extremely important coastal resources, which are vital to our socio-economic development. A vast majority of human population lives in coastal areas, and most communities depend on these local resources for their livelihood. The mangroves are sources of highly valued commercial products and fishery resources and are also the sites for developing a burgeoning eco-tourism industry. Of about 110 known mangrove species, about 54 species in 20 genera from 16 families constitute the group of true mangroves occurring only in mangrove habitats.

Most of the mangrove genera and families are not closely related to each other, but what they do have in common is their highly developed morphological, biological, physiological and ecological adaptability to extreme environmental conditions. The most important characteristic to achieve this kind of adaptability are pneumatophoric roots (*Avicennia*, *Sonneratia* species) (Figure 1.1), stilt roots (*Rhizophora*, *Brugueria*, *Ceriops* species) (Figure 1.2), salt excreting leaves (*Aegiceras* species) and viviparous water dispersed propagules (*Brugueria*species).

Figure 1.1: Pneumatophores in *Avicennia*

Figure 1.2: Stilt roots in *Rhizophora*

1.2 Significance of mangroves

Some of the commercial benefits accrued from mangroves (Kathiresan, 2012) are:

- The mangroves supply forestry products (firewood, charcoal, timber, honey etc.) and fishery products (fish, prawn, crab, mollusk etc.). The mangrove wood with high content of tannin is used as timber for its durability. The pneumatophores are used to make bottle stoppers and floats. *Nypa* leaves are used to thatch roofs, mats and baskets. Shells of mangrove molluscs are used to manufacture lime.
- Mangroves attract honey bees and facilitate apiculture activities in some areas. For instance, the Sundarbans provide employment to 2000 people engaged in extracting 111 tons of honey annually and this accounts for about 90% of honey production among the mangroves of India.
- Mangroves and especially *Avicennia* form cheap and nutritive feed for buffaloes, sheep, goats and camels. To cite an example, about 16,000 camels are herded into the mangroves of Indus delta of Pakistan.
- Mangrove extracts are used in indigenous medicine; for example, *Bruguiera* species (leaves) are used for reducing blood pressures and *Excoecariaagallocha* for the treatment of leprosy and epilepsy.
- The mangroves provide seeds for aquaculture industries. To cite an example, 40,000 fishers get an annual yield of about 540 million seeds of *Penaeus monodon* for aquaculture, in the Sundarban mangroves of West Bengal.

Some of the ecological benefits accrued from mangroves (Kathiresan, 2012) are:

- Mangroves possess mechanisms to deal with intense sunrays and solar UV ‐ B radiation. The mangrove foliage produces flavonoids that serve as UV ‐ screen compounds. This ability of mangroves makes the environment free from the deleterious effects of UV ‐ B radiation (Kathiresan, 2012).
- Mangroves,like other plants, remove CO_2 from the atmosphere through photosynthesis. This,in turn, reduces the problems associated with the ′green house gases’ and global warming. They fix greater amounts of CO_2 per unit area, than what the phytoplankton do

in the tropical oceans. For example, the ability of *Rhizophora* forest to divert carbon belowground is remarkably high. A 20-year old plantation of mangroves stores 11.6 kg per m^2 of carbon (C) with C burial rate of 580 g m ‑ 2 yr ‑ 1 (Fujimoto, 2000). Because the mangroves fix and store significant amounts of carbon, their loss may have impact on global carbon budget. Cebrain (2002) estimated that a loss of about 35% of the world's mangroves has resulted in a net loss of 3.8 x 10^{14}g C stored as mangrove biomass.

- Mangrove forests protect all types of coastal communities from the fury of cyclones and storms. Recent example is the cyclone Phailin that struck the coast of Odisha in India. It has been reported that the damage was less in the regions which were behind the mangrove forests. Mangroves like *Rhizophora*sp. seem to act as a protective force towards this natural calamity (McCoy *et al.*, 1996).
- Mangroves help in mitigating the fury of tsunami, e.g., during the tsunami of December 26, 2004, the monstrous waves devastated Andaman and Nicobar Islands and southeast coast of India, but spared the areas that were colonized with luxuriant mangroves.
- Mangrove systems offer protection to the coastline against the flood, which are often caused by tidal waves or due to heavy rainfall associated with storms. The ability of mangroves in flood control is due to the response of their root system to have a larger spread in areas prone to tidal inundation, and their roots to promote sedimentation.
- The mangrove systems minimize the action of waves and thus prevent the coast from erosion. The reduction of waves increases with the density of vegetation and the depth of water. Mangroves function as 'live seawalls', and are very cost effective as compared to the concrete seawall and other structures for the protection of coastal erosion.
- One of the important functions of mangroves is trapping of sediments, and thus acting as sinks to the suspended sediments. The mangrove sediments have the ability to retain nutrients.
- Mangrove ecosystems are important for fish production. They serve asnursery, feeding and breeding grounds for many fishes and shellfishes.Nearly 80% of the fish catches are directly or indirectly dependent onmangrove and other coastal ecosystems worldwide.Besides fishes,the mangroves support a variety of wildlife such as the Royal Bengal tiger,crocodiles, deer, pigs, snakes, fishing cats, insects and birds.

- The influx ofnutrients generated by the mangroves supports other sensitive habitatslike the coral reefs, seaweeds and seagrass beds.
- Mangrove sediments have a high capacity for absorbing and holding heavy metals thereby preventing the spread of metal pollution in coastal areas.

Thus, conclusively, it can be said that mangroves serve a diversity of functions which are all very important from ecological point of view. Economically also they have been found to be of immense monetary benefits in comparison to agricultural landscapes such as rice fields. According to an estimate the annual economic value of mangrove ecosystems is US $9,990/ha (Costanza et al., 1997). Sathirathai and Barbier (2001) rated the economic value much higher: between US $27,264 and $35,921/ha, calculated for mangroves in a local community in Thailand.

1.3 Distribution of mangroves

1.3.1 Global scenario

Globally, mangroves cover approx. 137,760 km^2 (Giri et al., 2011). This area comes out to be 0.1% of earth's surface (Cornforth et al., 2013). These plants are distributed in 118 countries and territories in the tropical and subtropical regions of the world (Giri et al., 2011). Approximately 75% of world's mangroves are found in just 15 countries (Table-1.1), and only 6.9% are protected under the existing protected areas network (IUCN I-IV) (Giri et al., 2011).

Though these plants occupy only 0.1% of earth's continental surface, they account for 11% of the total input of terrestrial carbon into the ocean (Jennerjahn & Ittekot, 2002) and 10% of the terrestrial dissolved organic carbon (DOC) exported to the ocean (Dittmar et al., 2006).

According to Table 1.2, India ranks at 11th place in the world in terms of mangrove cover, however, as per the work of SAC (2012) the mangrove cover in the country is 4956.20 sq km which puts India at 7th place.

Table-1.1: Global distribution of mangroves (Source: Giri et al., 2011)

S No	**Country**	**Area (ha)**	**% of global total**	**cumulative %**	**Region**
1	Indonesia	3112989	22.6	22.6	Asia
2	Australia	977975	7.1	29.7	Oceania
3	Brazil	962683	7	36.7	South America
4	Mexico	741917	5.4	42.1	North and Central America
5	Nigeria	653669	4.7	46.8	Africa
6	Malaysia	505386	3.7	50.5	Asia
7	Myanmar	494584	3.6	54.1	Asia
8	Papua New Guinea	480121	3.5	57.6	Oceania
9	Bangladesh	436570	3.2	60.8	Asia
10	Cuba	421538	3.1	63.9	North and Central America
11	India	368276	2.7	66.6	Asia
12	Guinea Bissau	338652	2.5	69.1	Africa
13	Mozambique	318851	2.3	71.4	Africa
14	Madagascar	278078	2	73.4	Africa
15	Philippines	263137	1.9	75.3	Asia

1.3.2 Indian Scenario

India with a long coastline of about 8414 km, including the island territories, but excluding the length of mouths of estuary, river and creek (Rajawat et al.,2015), has a mangrove cover of about 4740 km^2 (Table-1.2). This area covers 0.14% of country's total geographic area (FSI, 2015). These mangrove habitats (69°E-89.5°E longitude and 7°N-23°N latitude) comprise three distinct zones: East coast habitats facing Bay of Bengal, West coast habitats facing Arabian sea, and Island Territories. In India, the states like West Bengal, Odisha, Andhra Pradesh, Tamil Nadu, Andaman and Nicobar Islands, Kerala, Goa, Maharashtra, and Gujarat occupy vast area of Mangroves.The area under mangroves in Gujarat (1107 sq km) is the second largest along the Indian coast, after Sunderbans in West Bengal (2106 sq km). Gujarat has about 23 percent of India's estimated mangrove cover of 4.74 lakh ha. Of the total mangrove cover in the state, the coastal districts of Gulf of Kachchh cover almost 90%. Mangroves in India account for about 3% of the global mangroves (FSI, 2015). About 60% of the mangroves occur on the east coast along the Bay of Bengal, 27% on the west coast bordering the Arabian Sea, and 13% on Andaman & Nicobar Islands.Mangrove cover has been categorised into very dense (canopy density of more than 70%), moderately dense (canopy density between 40-70%) and open mangrove cover (canopy density between 10-40%).

Table-1.2: Mangrove cover in India (FSI, 2015)

(All figures in sq. Km)

S No.	State/Uts	Very Dense Mangrove	Moderately Dense Mangrove	Open Mangrove	Total Mangrove
1	Andhra Pradesh	0	129	238	367
2	Goa	0	20	6	26
3	Gujarat	0	174	933	1107
4	Karnataka	0	3	0	3
5	Kerala	0	5	4	9
6	Maharashtra	0	79	143	222
7	Odisha	82	95	54	231
8	Tamil Nadu	1	18	28	47
9	West Bengal	990	700	416	2106
10	A & N Islands	399	168	50	617
11	Daman & Diu	0	0	3	3
12	Puducherry	0	0	2	2
	Total	1472	1391	1877	4740

1.4 Threats on mangroves

Mangroves are declining worldwide at an alarming rate (Valiela et al., 2001, Alongi, 2002; Myint et al., 2008). Globally, 36,000 km^2 of mangroves have been lost since 1980, primarily due to conversion to agriculture and aquaculture, urbanization, and timber extraction (Asbridge et al., 2016).This damaging scenario is common to many countries, making mangrove degradation a global issue with worldwide consequences (Giri et al., 2011; Polidoro et al., 2010). In addition, lack of specific laws applicable to protect and to allow sustainable exploitation of this ecosystem increases the probability for expanding degradation of mangrove forests (Beys-da-Silva et al., 2014).

In Indian context, main causes of mangrove destruction are (Sahu et al., 2015):

- **Aquaculture and agriculture expansion:** A large fraction of the mangroves in India has been destroyed due to aquaculture and agriculture expansion. In India and Bangladesh, about 1,50,000 ha of mangroves were destroyed for agricultural purposes during the past 100 years (Sahu et al., 2015). Mangroves are destroyed and reclaimed with rain water for reducing the salinity of the soil. Then, these areas were protected from soil water intrusion by forming embankments. After salt is leached from soil, these areas are used for raising plantation of coconut or paddy. These activities are very common in South Indian states of Goa, Karnataka and Andhra Pradesh (Bhatt and Kathiresan, 2011; Swain and Rao, 2013; Tarakanadha et al., 2013).
- **Harvesting of mangroves for timber, fuel and charcoal:** Because of high calorific value of mangrove wood and high strength, mangroves are harvested for firewood, charcoal and timber collection (Tarakanadha et al., 2013). Mangrove wood is highly suitable for chipboard and paper industry. So due to its industrial value, forests are cleared annually for these purposes.
- **Pollution:** Mangrove patches in cities such as Mumbai and Kolkata are affected by discharge of large amounts of solid wastes and effluents from various sources. Pollution has made it difficult for mangrove survival and growth (Vyas, 2013).
- **Natural calamities:** Frequent occurrences of tropical cyclones, storms and tsunamis, have damaged the mangroves of India. To cite an example, in the east coast of Odisha during the year 1999, a major cyclone devastated a large area of mangroves (Das and

Vincent, 2009). It has been estimated that the total mangrove area fell from 30,766 ha to 17,900 ha during the super cyclone. The tsunami that occurred in 2004 caused extensive damage of mangroves in the south coast of India and Andaman and Nicobar Islands (Roy & Krishnan, 2005; Ramchandran et al., 2005; Sridhar et al., 2006).

- **Reduction of fresh water and tidal water flows:** Mangroves are well established in areas where there is good amount of fresh water inflow. Dam and barricade construction on upper portion of rivers reduces fresh water flow into mangrove swamps. Embankment construction and siltation at the river mouth obstruct tidal water flow in to mangrove swamps. Reduction in fresh water and tidal water inflow increases the salinity of these areas, resulting in poor germination, growth and regeneration of mangroves. In Sundarbans, due to reduction in fresh water inputs, species such as *Heritierafomes* and *Nypafruticans* are reducing in their population (Bhatt &Kathiresan, 2011).
- **Invasive species:** Most mangrove regions in India are suffering from invasive species which disrupt the ecological balance and dynamics of the mangrove ecosystem. For example, in Tamil Nadu and Andhra Pradesh, there is rapid invasion of *Prosopis*species (Sahu et al., 2015). In Sundarbans, colonization of the twiner *Derris trifoliata* and other aquatic weeds *Eichhorniacrassipes* and *Salvinia* in mangrove water negatively affecting the natural flora of mangrove ecosystems (Bhatt and Kathiresan, 2011).
- **Climate change:** Climate change is also an important environmental issue impacting mangroves in India. It results in increase in temperatures, rising sea level, increasing the frequency of tropical storms and tsunamis. Due to sea level rise mangroves tend to move landward, but human encroachment prevents this and consequently, the width of the mangroves decreases (Gilman et al., 2006). It has been reported that as a consequence of sea level rise two islands in Indian Sundarbans- Suparibhanga and Lohacharra have submerged and a dozen of other islands are also facing the same problem (Sahu et al., 2015).

These anthropogenic and natural threats not only affect mangrove plants but also have an effect on marine life and on terrestrial biological diversity. In addition, disturbance to mangrove ecosystems also disturbs adjacent ecosystems such as sea grass beds and coral reefs. As a consequence of the loss of mangroves, the natural tidal system is altered or totally disturbed: tidal creeks are blocked, fisheries decline, sedimentation rates decrease, and toxic waste pollution, such as antibiotic impact from aquaculture, grows. Additional problems that surface as a result of mangrove degradation include salinization of coastal soils, increased erosion, land subsidence, land degradation, and extended exposure of coastlines to wave surges (Kuenzer et al., 2011).

1.5 Rationale for monitoring mangroves using satellite data

Because of high ecological and economical values associated with mangroves, there are worldwide efforts going on to study the dynamics of mangrove ecosystem. Earlier studies mostly relied on cumbersome on-field observations. It is extremely difficult to work in inter-tidal, muddy environments along with threats of wild life, therefore there are increasing efforts to develop satellite data based techniques for mangrove studies, which have obvious advantages of providing more reliable and accurate information due to synoptic view, multispectral, multi-temporal capabilities. Moreover, advancements in digital image processing, availability of GIS techniques and use of GPS while collecting ground truth data at selected locations have further facilitated research work in the mangrove eco-systems. A large number of such investigations have been carried out (details are provided in Chapter-2).

A long term systematic inventory, mangrove change dynamics and detailed investigations on understanding causes for the changes has not been carried out so far for the entire region of the Gulf of Kachchh and in particular Kori creek region. There are limited studies attempting community zonation of mangroves, using microwave data alone or employing a combination of microwave and optical data (Chakraborty et al., 2013).

1.6 Scope and objectives of the present study

The scope of the present work is to utilise and develop remote sensing and GIS based techniques for mangrove cover dynamics and community zonation studies in the Gulf of Kachchh region of Gujarat, India.

Major objectives of the present research work are as follows:

i) To study mangrove cover dynamics and understand causes of changes
ii) To develop techniques for mangrove community zonation by synergistic use of optical and microwave satellite data

1.7 Outline of the thesis

The thesis consists of six chapters.

Chapter One provides introduction of mangrove ecosystem, significance of mangrove ecosystems, distribution of mangroves globally as well as in India, threats on mangrove ecosystem, advantages of utilising satellite data and gap areas. The chapter concludes with the scope and objectives of the research and provides outline of the thesis.

Chapter Two primarily discusses state-of-art of remote sensing for mangrove studies based on extensive literature survey. Previous work carried out on mangroves in the Gulf of Kachchh is also provided. The chapter justifies the scope and objectives of the present research based on the literature survey.

Chapter Three describes the study area. This chapter provides geographic and ecological settings of the Gulf of Kachchh, with particular focus on regions where mangroves are found.

Chapter Four provides details about the materials and methods used in the study. It provides details about various remote sensing approaches (including fusion of satellite data) used to characterize mangroves through synergistic use of optical and microwave data.

Chapter Five highlights mangrove cover dynamics in the Gulf of Kachchh, Gujarat, India. This chapter provides details of changes in mangrove ecosystem over the years in five mangrove occupying regions of the Gulf of Kachchh based on spectral classifications applied on optical satellite data and attempts to understand causes of such changes.

Chapter Six describes details of community zonation of mangroves in the Gulf of Kachchh Marine National Park and Sanctuary (MNP&S) studied utilizing microwave as well as optical data.

Chapter Seven summarizes the study and provides conclusions and further recommendations. This chapter also enumerates the limitations of the study.

The list of various references used in the study is appended at the end of the thesis.

Chapter 2

Literature Review

2.1 Remote Sensing

Remote sensing is the science of acquiring, processing, and interpreting data obtained from aircraft and satellites that record the interaction between matter and electromagnetic radiations (Sabins, 1997). Acquiring images refers to the technology employed, processing refers to the procedures that convert the raw data into images and interpreting images is the most important step because it converts an image into information that is meaningful and valuable for a wide range of users. The interaction between matter and electromagnetic energy is determined by the physical properties of the matter, and the wavelength of the electromagnetic energy that is remotely sensed.

The Electro Magnetic Radiation (EMR) is the energy transmitted through space in the form of electric and magnetic waves. Electromagnetic radiation (Table 2.1) spans a large spectrum of wavelengths right from very short wavelength gamma rays (10^{-10} m) to long radio waves (10^{6} m). In remote sensing, the most useful regions are the visible (0.4 to 0.7 μm), the reflected IR (0.7 to 3 μm), the thermal IR (3 to 5 μm and 8 to 14 μm) and the microwave regions (0.3 to 300 cm).

Table 2.1: Electromagnetic spectral regions (Source: Sabins, 1997)

Region	Wavelength	Remarks
Gamma-ray	< 0.03 nm	Incoming radiation completely absorbed by the upper atmosphere
X-ray	0.03 to 30 nm	Completely absorbed by the atmosphere
Ultraviolet	0.03 to 0.4 μm	Incoming wavelengths less than 0.3 um completely absorbed by ozone in the upper atmosphere
Photographic UV band	0.3 to 0.4 μm	Transmitted through the atmosphere. Atmospheric scattering is severe
Visible	0.4 to 0.7 μm	Imaged with film and photo detectors
Infrared	0.7 to 100 μm	Interaction with matter varies with wavelength.
Reflected IR	0.7 to 3.0 μm	Reflected solar radiation
Thermal IR	3 to 5 um, 8 to 14 μm	Principal atmospheric windows in the thermal region.
Microwave	0.1 to 100 cm	All weather capability. Active as well passive sensing
Radio	> 100 cm	Longest-wavelength portion of the electromagnetic spectrum

The sun is the important source of electromagnetic radiation used in conventional optical remote sensing in the visible and infrared regions. Energy in the visible and near-infrared region (0.3 to 3 μm) is mostly due to reflectance while the energy in the 3.0 to 15 μm wavelength region is predominantly due to thermal emission of the earth. Remote sensors are made up of detectors that record specific wavelengths of the electromagnetic spectrum. Various types of sensors mounted on aircraft or satellite platforms record the reflected/emitted radiation.

Sensors and Resolutions

Most of the sensors record the solar energy and are called passive sensors. However, sensors, which send their own energy to the terrain such as radar, lidar etc. are called as active sensors and are independent of solar radiation. These sensors have day and night capability and can also provide data under cloudy conditions. Thermal infrared sensors detect heat emitted from the earth's surface and also have day and night capability. For earth observing sensors, the information collected is supposed to identify and map various earth surface features. Thus, the performance evaluation of the sensors will involve assessing the classification and map accuracy provided by it. Thus a sensor is characterized by:

- its ability to identify/distinguish objects on the ground (Spatial Resolution)
- how many bands it employs and the interval of each band (Spectral Resolution)
- how much it can differentiate among the emittances/reflectances recorded (Radiometric Resolution)
- how often it can visit a particular area (Temporal Resolution)

In general, while designing a sensor a trade-off is being accepted among four resolution parameters. This is because it is not possible to achieve best of all the four. For example, to achieve a high spatial resolution, the IFOV (Instantaneous Field of View) has to be reduced, which in turn reduces the amount of energy collected by the sensor. This will lead to poor signal-to-noise ratio, which will provide a poor radiometric resolution. On the other hand, for the same spatial resolution, radiometric resolution can be improved by increasing the bandwidth which will enable more energy to be collected. However, increasing the bandwidth will result in poor spectral resolution.

Table-2.2 gives characteristics of the major Earth Observation Satellites.

Table 2.2: Characteristics of major Earth Observation Satellites

Satellite	**Sensor**	**Bands (µm)**	**Spatial Resolution (m)**	**Swath (km)**	**Repitivity (days)**
Landsat-1, 2, 3 1972, 73, 78 (USA)	MSS	1. 0.5-0.6 2. 0.6-0.7 3. 0.7-0.8 4. 0.8-1.1	79	185	18
Landsat-4, 5 1982, 1985 (USA)	MSS	---Same---	Same	Same	16
	TM	1. 0.45-0.52 2. 0.52-0.60 3. 0.63-0.69 4. 0.76-0.90 5. 1.55-1.75 6. 10.40-12.50 7. 2.08-2.35	30 (120 for band 6)	185	16
SPOT-1, 2 1986, 1990 (France)	HRV	1. 0.50-0.59 2. 0.61-0.68 3. 0.79-0.89	20	60	26
	PAN	0.51-0.73	10	60	26
IRS-1A, 1B 1988, 1991	LISS-I	1. 0.45-0.52 2. 0.52-0.59	72.5	148	22

(India)	LISS-II	3. 0.62-0.68 0.77-0.86 ---Same---	36.25	74	22
ERS-1 1991	SAR	C-band VV	25-100	5-500	3-35
JERS-1 1992 Japan	SAR	L-band HH	18	75	44
Landsat-6 1993 (USA)	MSS ETM PAN	1. 0.5-0.6 2. 0.6-0.7 3. 0.7-0.8 4. 0.8-1.1 5. 10.5-12.5 --Same as L5- 0.50-0.90	80 (240 for Band 5) -Same as L5- 15	185 185	16 16
SIR-C 1994 (USA, Germany, Italy)	L-band SAR C-band SAR X-band SAR	Fully Polarimetric Fully Polarimetric VV	30 30 30	15.90 15.90 15.40	

Radarsat-1 1995 (Canada)	SAR	C-band HH	8-100	45-500	24
IRS-1C, 1D 1995, 1997 (India)	WiFS LISS-III PAN	1. 0.62-0.68 0.77-0.86 1. O.52-0.59 2. 0.62-0.68 3. 0.77-0.86 4. 1.55-1.70 1. 0.55-0.75 (Stereo)	188 23.5 (70.5 for band 4) 5.8	810 141 (148 for band 4) 70	5 24 5
Landsat-7 1998 (USA)	TM ETM+ MRMSI	B 1-5 VNIR B 7 MIR B6 TIR PAN 0.50-0.90 -Same as L5- PAN 0.50-0.90	28.5 (120 TIR) 15 -Same as L5- 5 10		16

		1. 0.45-0.52 2. 0.52-0.60 3. 0.63-0.69 4. 0.76-0.90			
SPOT 4 1998 (France)	HRVIR VEGETATION	1. 0.50-0.59 2. 0.61-0.68 3. 0.78-0.89 4. 1.58-1.75 5. 0.61-0.68 (PAN) 1. 0.43-0.47 2. 0.61-0.68 3. 0.79-0.89 4. 1.58-1.75	20 (VNIR) 10 (PAN) 1165	60 to 80 2250	26 1
Oceansat-1 (IRS-P4) 1999 (India)	OCM MSMR	1. 0.402-0.422 2. 0.433-0.453 3. 0.480-0.500 4. 0.500-0.520 5. 0.545-0.565 6. 0.660-0.680 7. 0.745-0.785 8. 0.845-0.885 6.6, 10.6, 18 & 21 GHz	360 120, 80, 40, 40	1420 1360	2 2

Terra 1999 (USA/Japan)	ASTER	14 VNIR	15-90	60	16
IKONOS 1999 (USA)		1. 0.44-0.51 2. 0.51-0.59 3. 0.63-0.69 4. 0.76-0.85 5. 0.45-0.90 (PAN)	4 (VNIR) 1 (PAN)	11.3	3
SRTM 2000 (USA)	SAR	C-band SAR	30-90	225	NA
EO-1 2000 (USA)	ALI Hyperion	1. 0.43-0.45 2. 0.45-0.51 3. 0.52-0.60 4. 0.63-0.69 5. 0.78-0.80 6. 0.84-0.89 7. 1.20-1.30 8. 1.55-1.75 9. 2.08-2.35 10. 0.48-0.69 (PAN) 0.4-2.5 (total 220 bands)	30 (VNIR) 10 (PAN) 30	37 7.5	16
QuickBird 2001 (USA)		1. 0.45-0.52 2. 0.52-0.60 3. 0.63-0.69	2.4 (VNIR)	16.8	3.5

		4. 0.76-0.90 5. 0.45-0.90 (PAN)	0.65 (PAN)		
SPOT 5 2002 (France)	HRG HRS VEGETATION 2	1. 0.50-0.59 2. 0.61-0.68 3. 0.78-0.89 4. 1.58-1.75 (MIR) 5. 0.51-0.73 (PAN) 1. 0.51-0.73 (PAN) 1. 0.43-0.47 2. 0.61-0.68 3. 0.79-0.89 4. 1.58-1.75	10 (VNIR)- 20 (MIR) 5 (PAN) 10 1165	60-80 120 2250	26 1
ENVISAT 2002 (ESA)	ASAR	C-band Full Polarimetry	25-150	5-400	35
Resourcesat -1 (IRS-P6) 2003 (India)	AWiFS LISS-III	4 VNIR & SWIR 4VNIR & SWIR	59 23.5	700 141	5 24

	LISS-IV	3 VNIR	5.8	23.5	24
Cartosat-1 2005 (IRS-P5) (India)	PAN	2 PAN + 26 deg _ 5 deg along track tilt	2.5	27.5 in stereo mode & 55 in monoscopic mode	5
ALOS PALSAR 2006 (Japan)	PRISM AVNIR-2 PALSAR	PAN 4 VNIR L-band	2.5 10 7-100 (depending on mode)	70 70 20-350 km (depending on mode)	46
Cartosat-2 2007 (India)	PAN	PAN	Better than 1	10 (Less than 10)	10
Radarsat-2 2007 (Canada)	SAR	C-band Full Polarimetry	3-100	50-170	24
WorldView 2	WV60	PAN: 0.45-0.90	0.50	17.6	1.7

2007 (USA)					
Cartosat-2A 2008 (India)	PAN	PAN	Better than 1	10 (Less than 10)	4
GeoEye-1 2008 (USA)		1. 0.45-0.51 2. 0.51-0.58 3. 0.65-0.69 4. 0.78-0.92 5. 0.45-0.80 (PAN)	2 (VNIR) 0.41 (PAN)	15.2	1-3
Oceansat-2 2009 (India)	OCM Scatterometer	8 VNIR	360 50 km footprint for scatterometer	1420	2
WorldView 2 2009 (USA)		1. 0.40-0.45 2. 0.45-0.51 3. 0.51-0.58 4. 0.58-0.63 5. 0.63-0.69 6. 0.70-0.74 7. 0.77-0.89 8. 0.86-1.04	2 (VNIR) 0.5 (PAN)	16.4	2.7

		9. 0.45-0.80 (PAN)			
Cartosat-2B 2010 (India)	PAN	PAN	Better than 1	10 (Less than 10)	4
Resourcesat -2 2011 (India)	AWiFS LISS-III LISS-IV	4 VNIR & SWIR 4VNIR & SWIR 3 VNIR	59 23.5 5.8	700 141 23.5	5 24 24
RISAT-1 2012 (India)	SAR	C-band	1-50 (depending on mode)	25-235 (depending on mode)	25
Landsat-8 2013 (USA)	OLI TIRS	B 1-5 VNIR B 6,7&9 SWIR B 8 PAN B 10&11	30 30 15 100 (resampled to 30)	170X183	16
ALOS-2	PAL SAR-2	L-band SAR	1-100 m (depending on mode)	25-490 (depending	14

2014 (Japan)				on mode)	
Sentinel-1A 2014 (Europe)	SAR	C-band	5-100 (depending on mode)	20-400 (depending on mode)	12
Cartosat 2C 2016 (India)	PAN HRMX	0.50-0.85 1. 0.43-0.52 2. 0.52-0.61 3. 0.61-0.69 4. 0.76-0.90	0.65 (PAN) 2 (VNIR)	10 10	7 7

Note: AWiFS: Advanced Wide Field Sensor; **LISS**: Linear Imaging Self Scanner; **VNIR**: Visible and Near Infra Red; **WiFS**: Wide Field Sensor; **PAN**: Panchromatic; **SWIR**: Short Wave Infra Red; **SAR:** Synthetic Aperture Radar **V:** Visible; **TIR:** Thermal Infra Red; **VNIR**: Visible and Near Infra Red; **HRVIR**: High Resolution Visible and Infrared; **HRG**: High Resolution Geometrical; **ALI**: Advance Land Imager; **SIR**: Space-borne Imaging Radar; **ERS**: European Remote-Sensing Satellite; **JERS**: Japanese Earth Resources Satellite; **ASAR**: Advanced Synthetic Aperture Radar; **RISAT**: Radar Imaging Satellite; **PALSAR**: Phased Array L-band Synthetic Aperture Radar; **WV**: World View; **HH**: Horizontal Transmit, Horizontal Receive; **VV**: Vertical Transmit, Vertical Receive; **HRMX**: High Resolution Multi Spectral Radiometer: **NA**: Not Applicable

Satellite data processing and interpretation

Remote sensing data analysis is primarily carried out using digital processing/enhancements followed by on screen visual interpretation and/or adopting different digital classification techniques. Visual interpretation is primarily carried out by developing interpretation keys based on basic elements of visual interpretation like, tone, colour, texture, shape, size, association etc. Ground truth data collection for developing interpretation keys, classification system, validation and accuracy assessment are integral parts of the process.

2.2 Geographical Information System (GIS)

A Geographic Information System (GIS) is an organized collection of computer hardware and software, with supporting data and personnel, that captures, stores, manipulates, analyzes, and displays all forms of geographically referenced information (Sabins, 1997). Thus Geographic Information System, is a computer modeling system that allows for the integration and collective analysis of geospatial data from multiple sources including satellite imagery, GPS (Global Positioning System) recordings and textual (non-spatial) attributes associated with a particular space/location. One of the biggest advantages of GIS is the seamless integration of spatial and non-spatial data. GIS provides an environment in which spatial as well as non-spatial information can be combined and organized in an appropriate format, for the further retrieval, manipulation and analysis. Specifically, organizing the remote sensing data in the GIS environment makes data integration and manipulation very convenient. Thus, GIS primarily deals with spatial and attribute data in an organized manner using computer hardware and associated software.

2.3 State-of-art of remote sensing for mangrove studies

Mangroves grow mostly at the junction between land and sea, in the inter-tidal regions. These inter-tidal areas are difficult to access frequently using ground based methods. Remote sensing, especially through satellites, provides a cost-effective, safe and frequent source of data and information about such difficult locations.

A review of all the work related to applications of remote sensing data for mangrove ecosystem mapping, numerous methods and techniques used for data analysis, their potential and limitations have been provided by Kuenzer et al. (2011) and Rhyma et al. (2016).

According to these authors, typically, mangroves grow in intertidal areas which are frequently inundated, and often difficult to access on foot. Therefore, traditional field observations and survey methods are highly intensive in terms of cost, labour and time. Therefore, there is an increasing requirement of large-scale, long-term and cost-effective monitoring methods such as those provided by remote sensing technologies. Remote sensing techniques have demonstrated a high potential to detect, identify, map, and monitor mangrove conditions and changes during past two and half decades which is reflected by large number of scientific papers published on this topic. These studies have demonstrated the efficacy of remote sensing in providing spatio-temporal information on mangrove ecosystem distribution, species differentiation, health status, and ongoing changes of mangrove populations.

The pixels in remotely sensed images of mangrove areas captured through space-borne and airborne platforms mainly contain the spectral information about three components: vegetation, soil, and water. In addition, any mixture of the individual surface appearance is also influenced by seasonal and diurnal intertidal interactions. These circumstances greatly influence the spectral characterization of the image components (Kuenzer et al., 2011). Also, the diversity of mangrove species in Asia is much higher than in the tropical or subtropical regions of the New World (Ramsey and Jensen, 1996). These circumstances aggravate discrimination difficulties as the result of a higher amount of spectrally unique species. Therefore, many researchers employ different sensors to take synergistic advantages of them for studying different aspects of mangroves. The selection of the appropriate sensor depends mainly on the purpose of the investigation, the attainable final map scale, the discrimination level required, the time frame to be covered, special characteristics of the geographic region, and the funds and training level of personnel available for the envisioned study (Kuenzer et al., 2011).

Among the different data sources pertaining to optical remote sensing technology, aerial photographs, medium resolution satellite images and high resolution satellite images have been used profusely for mangrove studies.

2.3.1 Aerial data

Aerial photography is suitable for detailed mapping in very small and narrow coastal environments. Prior to satellite data availability, aerial images were the only information source on the extent and condition of mangroves. After the availability of satellite data, they are often used to track temporal changes. The particular properties of high spatial resolution provided by aerial photography allow mapping of even narrow coastal areas with fringing stands, which are typical for these ecosystems. Aerial data helps in the accurate assessment of classification procedures performed on other, lower-resolution data. However, the feasibility of obtaining appropriate images depends on flight conditions, local weather, and the occurrence of clouds, which are typical in tropical and subtropical latitudes. A summary of studies conducted using aerial photographs in mangrove environment is provided in Table 2.3. Benefits and limitations of various aspects related to aerial photographs are summarised in Table 2.4.

Table 2.3: Studies conducted using aerial photographs in mangrove environment

Author (s)	**Data Used**	**Study Area**	**Brief about Work Done (Methods/Classification Approach/Outcomes/Accuracy)**
Patterson, 1986	Colour Infrared (CIR) Photographs	Marco Island, Florida, USA	• Mangrove boundary delineation and areal change detection through digital image processing.
Everitt et al., 1989, 1991, 1996, 2007	CIR Video, CIR Photographs	Texas Gulf Coast	• Studied the degradation of black mangroves through visual interpretation and pixel based digital classification approaches. • Black mangroves showed a high spectral distinction from other forms of vegetation and thus could be distinctly differentiated on CIR video and photographs.
Dale et al., 1996	CIR Photographs	Moreton Bay, Australia	• Investigation of anthropogenic impacts in mangrove habitat through pixel-based classification approach.
Manson et al., 2001	Colour photographs	Northern Australia	• A layer stack of low-pass filtered bands and principal component bands were created to which an unsupervised ISODATA

			classification approach was applied to estimate the extent of narrow fringe mangroves. • This mapping approach yielded very high accuracy compared to field data.
Dahdouh-Guebas et al., 2002	Aerial Photographs	Galle, Sri Lanka	• Change detection in mangrove environment in Galle, Sri Lanka during 1956-1994 through visual interpretation of aerial photographs. • An identification key, developed through intensive field work, was employed for visual demarcation of mangroves at genus level.
Kairo et al., 2002	Aerial Panchromatic Photographs	Kiunga Marine National Reserve, Kenya	• A discrimination key, developed through field work, was used to visually demarcate mangroves into two categories, productive and non-productive mangroves, including information about tree density and tree height on the species level.
Lucas et al., 2002	Digital ortho-mosaics derived from black- and – white photographs taken in 1950, and coloured stereo	Along West Alligator River, Australia	• An unsupervised ISODATA classification approach was used on digital ortho-mosaics to generate a mangrove canopy digital terrain model (DTM). • The DTM derived from coloured stereo photographs were more in agreement with field-derived canopy height information compared to the DTM derived from black-and-white photographs.

	photographs taken in 1991		
Fromard et al., 2004	Aerial images	Sinnamary Estuary in French Guiana	• Created time-series images using aerial photographs to track changes from 1951-1991 in the mangrove forests. The changes were related to coastline changes to understand the natural processes affecting the mangroves.
Benfield et al., 2005	Digitized aerial black and white photographs	Punta Mala Bay, Panama	• Assessed the changes in mangrove environment before and after road construction and establishment of water-treatment plants
Binh et al., 2005	Aerial photographs	Vietnam	• Used 58 aerial photographs of 1968 and 154 images of 1992, and assembled them into a photographic overview mosaic to identify land cover changes between 1968 and 2003 in the Ca Mau Province in Vietnam.

Table 2.4: Benefits and limitations of aerial photography for mangrove mapping (Kuenzer et al., 2011).

Aerial photography	**Benefits**	**Limitations**
1. Spectral resolution	Red–near-infrared spectral information with red-edge slope	None at all or very low (R,G,B;near-infrared)
2. Spatial resolution	Very high (centimeter to meter range)	Only small area is covered

3.Temporal resolution	Always available on demand	Complex acquisition of equipment and flight campaign planning is needed
4. Costs	Low costs for small areas	Increasing costs with increasing spatial coverage; high costs if professional flight campaign planning and multispectral camera
5. Long-term monitoring	Data available for >50 years	
6. Purposes	Local maps of mangrove ecosystems, parametrization, change detection	Only local-scale studies
7. Discrimination level	Species communities, density parameters	Sometimes too much detail (hampering unbiased image processing)
8. Methods	Visual interpretation with on-screen digitizing and object-oriented approaches	Automatization usually not possible; considerable analyst bias and, thus, hampered transferability or comparability
9. Other	Valuable additional information source to support field survey, image interpretation, or accuracy assessments. If overlapping pictures are acquired (stereo pairs), it is possible to derive canopy elevation model	

2.3.2 Medium resolution optical (multi-spectral) data

The availability of commercial medium resolution multi-spectral space-borne satellite images have led to plethora of research activities in mangrove environment over the last three decades. Data under this category most commonly stems from Landsat MSS, Landsat-5 TM, SPOT, Landsat-7 ETM+, the Indian Remote Sensing Satellite (IRS) LISS III, and the Advanced Spaceborne Thermal Emission and Reflection Radiometer (ASTER). Medium-resolution satellite imagery is suitable for mapping mangrove areas on a regional scale. The spectral and spatial resolution of satellite data are sufficient for many purposes. On a regional mapping level, mangrove–non-mangrove vegetation classes, density differences, condition status and, in some cases, mangrove community-dominating species could be clearly discriminated (Kuenzer et al., 2011). Some national agencies are more interested in updated overview information on a regional or even a country-wide scale, for their spatial planning and conservation-planning tasks, and the reporting of status and trends. The advantages of using medium-resolution imagery, for example, are that it delivers appropriate coverage and information depth in a cost-effective manner.

A summary of studies conducted using medium resolution multi-spectral satellite data in mangrove environment is provided in Table 2.5. Benefits and limitations of various aspects related to usage of medium resolution multi-spectral satellite data are summarised in Table 2.6.

Table 2.5: Studies conducted using medium resolution multispectral satellite data in mangrove environment

Author (s)	**Sensor Used**	**Study Area**	**Brief about Work Done (Methods/Classification Approach/Outcomes/Accuracy)**
Nayak et al., 1989	Landsat MSS	Gulf of Kachchh Marine National Park & Sanctuary, Jamnagar, Gujarat, India	• Mapping and change detection of mangroves using visual interpretation of satellite data.

Blasco et al., 1992	SPOT XS	Sunderbans, Bangladesh	• Mapping of post-cyclone flooding extent in Sunderbans using visual interpretation method. • Results demonstrated importance of mangroves as a protective shield against cyclones. • However, temporal resolution of the data was found to be a limitation as cloud-free optical image could be acquired after 5-10 weeks of the cyclone.
Gang and Agatsiva, 1992	SPOT XS	Mida Creek, Kenya	• Mapping the extent and status of mangroves using visual interpretation of satellite data
Aschbacher et al., 1995	SPOT XS	Phangnga Bay, Thailand	• Assessment of ecological status of mangroves
Rasolofoharinoro et al., 1998	SPOT XS	Mahajamba Bay, Madagascar	• Pixel-based classification method used for inventory of mangroves
Nayak and Bahuguna, 2001	IRS and Landsat	Indian coast	• Mapping of mangroves using pixel-based supervised classification method
Blasco et al., 2001 and Blasco and Aizpuru, 2002	SPOT XS	Bay of Bengal	• Pixel-based classification approach used for mangrove ecosystem mapping
Wang et al., 2003	Landsat TM and ETM+	Tanzania	• Visual interpretation of satellite images to identify changes in the mangrove area and distribution

Selvam et al., 2003	Landsat TM and IRS LISS III	Tamil Nadu, India	• Assessment of success of mangrove restoration efforts based on visual interpretation of satellite images.
Nayak et al., 2003	IRS LISS	Selected habitats along Indian coast	• Digital pixel-based supervised maximum likelihood classification approach used for community zonation of mangroves
Tong et al., 2004	SPOT XS	Mekong Delta, Vietnam	• Analysis of the impact of shrimp aquaculture on mangrove ecosystem using pixel-based classification approach
Shah et al., 2005	IRS LISS III	Gulf of Kachchh Marine National Park & Sanctuary, Gujarat, India	• Zoning and monitoring of dominant mangrove communities using supervised maximum likelihood classification method
Seto and Fragkias, 2007	Landsat MSS and TM	Red River Delta, Vietnam	• Mapping of extent and density of mangroves using neural network approach. • A methodology was presented for systematic monitoring of the area in the context of Ramsar Convention on Wetlands.
Conchedda et al., 2008	SPOT XS	Low Casamance, Senegal	• Object-based classification approach used for land cover mapping in mangrove ecosystem
Giri et al., 2011	Landsat	Entire globe	• Mapping of world's mangrove areas

Kumar et al., 2012	IRS LISS III and Landsat ETM+	Kori Creek, Gujarat, India	• Study of changes in mangrove environment over a period of 45 years using old topographic sheets and satellite images. • Visual interpretation of images was done for mapping mangroves and studying the changes.
Ajai et al., 2013	IRS LISS III	Entire Indian coast	• Community zonation of mangroves using pixel-based maximum likelihood classification method. • Accuracy achieved was between 85-90%.
Rahman et al., 2013	Landsat	Sunderbans, Bangladesh	• Assessment of different mangrove classification approaches
Kanniah et al., 2015	Landsat TM, ETM+ and OLI	Malaysia	• Monitoring of mangroves over a period of 25 years
Sari and Rosalina, 2016	Landsat	Bangka Belitung Islands, Indonesia	• Mapping of mangrove densities

Table 2.6: The advantages and disadvantages of medium resolution multispectral satellite data for mangrove studies (Source: Rhyma et al., 2016, Kuenzer et al., 2011)

Parameters	Advantages	Disadvantages
1. Spectral Resolution	Several multispectral bands, usually displayed using red, green and near-infrared or shortwave-infrared bands; thermal band is also used sometimes	Skilled trained personnel required to extract the information
2. Spatial Resolution	Good for mapping at regional scale	Too coarse for local observation requiring in-depth species differentiation and parameterization
3. Temporal Resolution	Frequent mapping (e.g., rainy season and dry season within 1 year; or repeated annual mapping) is possible	Repetition rate may be too low to record impact of extreme events (e.g., cyclones, floods, tsunami); furthermore, very weather dependent (clouds) = critical in subtropical and tropical regions
4. Cost	Depending on sensor, freely available (e.g., Landsat), very cost efficient (ASTER), or expensive (e.g., SPOT); but all are cost efficient compared with field surveys and airborne campaigns.	Software for image processing need (common software, such as ERDAS IMAGINE, ENVI and ArcGIS have high license fees)
5. Long-term monitoring	Data availability over three decades	Depending on the future duration of the systems and

		subsequent comparable sensors
6. Purposes	Inventory and status maps; change detection, such as assessment of impact damages; assessment of forestation and conservation success	For some species-oriented botany-focused studies, resolution may prove to be too coarse
7. Discrimination Level	Mangrove-non mangrove, density variations, condition status, mangrove zonation, in some cases community/species discrimination	High regional differences; classification result depends highly on the ecosystem conditions, such as biodiversity, heterogeneity of forest, adjacent targets; dominant community/species identification is possible
8. Methods	Visual interpretation with on-screen digitization; pixel-based, object-based and hybrid classification approaches; image transformation and analyses (PCA, TCT, HIS, Indices etc.)	Skilled analysts required to exploit the complete potential of the data.
9. Other	Data easy to access or order; best explored data type and therefore most literature available	

2.3.3 High resolution optical (multi-spectral) data

The main advantage of using high-resolution optical imagery (spatial resolution mostly <10 m) is identification to the species level or of species associated with different conditions with regard to their location (Kuenzer et al., 2011). The species identification and mapping is vital to assess the variety of ecosystem functions, processes, and relationships concerning single species or assemblages to better understand the history of mangrove growth and diversity and to predict future developments (Vaiphasa et al., 2006; Rodriguez et al., 2004; Neukermans et al., 2008; Saleh, 2007). Availability of textural features also makes high resolution optical imagery more attractive for mangrove studies as canopy textural differences may be employed for species discrimination. The advent of high resolution multispectral images began with the successful launch of IKONOS-2 (in 1999) and QuickBird (in 2001) satellites (Kuenzer et al., 2011). In the context of mangrove studies, these high resolution images have been used for spatial distribution and current state assessment, species zonation, biomass estimation, Leaf Area Index (LAI) calculation, change detection, and assessment of protective role of mangroves for protection of the coast (Kuenzer et al., 2011). However, there have been rather limited studies conducted using high resolution multispectral satellite images compared to the ones performed using medium resolution space-borne optical images. One of the reasons could be free or relatively low-cost availability of the latter. Then spectral resolution of high resolution optical images is usually limited compared to similar medium resolution images (Kuenzer et al., 2011). This makes it rather difficult to spectrally discriminate individual mangrove species from one another (for example, to discriminate *Rhizophora* from *Avicennia*). One of the approaches to overcome this limitation is to synergistically employ images from two different regions of electromagnetic spectrum, as attempted in the present thesis. There are a variety of image fusion algorithms which could be employed and the resulting fused images are qualitatively and quantitatively assessed.

A summary of studies conducted using high resolution multi-spectral satellite data in mangrove environment is provided in Table 2.7. Benefits and limitations of various aspects related to usage of high resolution multi-spectral satellite data are summarised in Table 2.8.

Table 2.7: Studies conducted using high resolution multispectral satellite data in mangrove environment

Author (s)	Sensor Used	Study Area	Brief about Work Done (Methods/Classification Approach/Outcomes/Accuracy)
Wang et al., 2004	IKONOS and QuickBird	Panama	• Comparison of two high resolution optical data for mapping mangroves. • Mapping was done using maximum likelihood pixel-based method, object-based classification approach and a hybrid approach integrating both pixel based and object-based methods. • IKONOS provided better results on account of greater spectral details than QuickBird data using maximum likelihood method. • For IKONOS data, both the approaches yielded acceptable accuracies (maximum likelihood: 88.9%, object-based: 80.4%), with maximum likelihood yielding better accuracy. • The hybrid approach provided an accuracy of 91.4% indicating that synergistic application of both pixel-based and object-based method might provide best

			results in mangrove classification studies.
Rodriguez and Feller, 2004	IKONOS	Twin Cays Archipelago, Belize	• IKONOS images were used along with aerial panchromatic image to study the changes during 1986-2003. • Image transformations were performed using Principal Component Analysis (PCA), NDVI and IHS (Intensity, hue and Saturation) methods to facilitate on-screen digitization. • Seven land cover classes were identified including two mangrove classes (black and red mangroves). • These authors further provided more detailed mangrove maps showing seven subclasses of black mangroves and eight subclasses of red mangroves, on the basis of a classification scheme which incorporated details such as height and density of the mangrove forests and tidal influences.
Kovacs et al., 2004	IKONOS	Agua Brava Lagoon System of Nayrit, Mexico	• Biomass estimation of mangroves through regression analysis of ground measured LAI (Leaf Area Index) and NDVI and

			SR (simple ratio) calculated using satellite data.
Kovacs et al., 2005	IKONOS	Agua Brava Lagoon System of Nayrit, Mexico	• Generation of LAI map based on NDVI calculated using satellite data. The LAI map had four mangrove classes: red, healthy white, poor condition white and dead mangroves.
Dahdouh-Guebas et al., 2005	IKONOS	Pambala, Sri Lanka	• Mangrove mapping at the assemblage and species level using various image composites and image transformations: true- and false-colour composites (FCCs) at 4m resolution, pan-sharpened 1m resolution FCC, Tasselled Cap transformation and PCA. • Pixel-based unsupervised (ISODATA) and supervised (parallelepiped, minimum distance, Bayesian) classification approaches were used and tested against visual interpretation method. • Among all the methods tried, pan-sharpened FCC provided best discrimination of mangrove species assemblages using visual interpretation method.

Olwig et al., 2007	IKONOS and QuickBird	TN, India	• Evaluation of protective role of mangroves against 2004-Tsunami by mapping mangroves through visual interpretation of satellite data.
Proisy et al., 2007	IKONOS	French Guiana	• Above ground biomass estimation using FOTO (Fourier-based Textural Ordination) method.
Kanniah et al., 2007	IKONOS	Malaysia	• Mangrove species discrimination by combining textural information with the individual bands. • Two pixel-based supervised classification approaches were employed: maximum likelihood and minimum distance. • Minimum distance showed poorest results with 63.6% overall accuracy, compared to 68.2% accuracy achieved using maximum likelihood method. • The highest accuracy achieved was 81.8% when textural information was employed along with spectral bands. ,
Everitt et al., 2008	QuickBird	Texas, USA	• Mangrove community discrimination using unsupervised ISODATA clustering and maximum

			likelihood supervised classification approach. • More acceptable results were obtained using maximum likelihood approach.
Lee and Yeh, 2009	QuickBird	Taiwan	• Distinguished between mangrove and non-mangrove areas using maximum likelihood classification approach. High accuracies were obtained for both the mapped classes.
Leempoel et al., 2013	GeoEye-1	China	• Employed GeoEye-1 (for 2009) images along with Landsat ETM+ (for 2000) and Corona KH4B (for 1967) images for assessing mangrove cover dynamics in Gaoqiao in Southern China.

Table 2.8: Advantages and limitations of using high resolution multi-spectral satellite data for mangrove studies (Source: Rhyma et al., 2016)

Parameters	Advantages	Limitations
1. Spectral Resolution	Red-near-infrared spectral information with red-edge slope; usually panchromatic band allowing image fusion (pan-sharpening)	Relatively few spectral bands
2. Spatial Resolution	High resolution (0.5-4 m range) for mapping on a local scale	Only small area is covered

3. Temporal Resolution	Regular mapping is possible on demand	Weather dependent (clouds); cost intensive if repeated monitoring is required
4. Costs	Moderate costs for single acquisitions (depending on area)	Very high costs if repeated monitoring is requested. Also, high costs of object-oriented image processing software
5. Long-term monitoring	Theoretically possible, but usually not used because of expense. Sensors such as IKONOS, QuickBird etc. available since late 1990s/2000	Depending on the future duration of the systems and susbsequent comparable sensors. Only back to the late 1990s.
6. Purposes	Discrimination of mangrove species, spatial distribution and variability, health status, parameterization	Single tree species discrimination usually not possible.
7. Discrimination level	Down to species communities; detailed parameterization	Regional differences; classification result depends highly on the ecosystem conditions, such as biodiversity, heterogeneity of forests, adjacent targets
8. Methods	Visual interpretation with on-screen digitization; pixel-based, object-based and hybrid classification approaches	Skilled analysts needed to exploit the full potential of the data
9. Other	Valuable information source to support field survey and accuracy assessment. Easy to	In some (developing/emerging) countries, data of relevant sensors very difficult to

	close the scale gap to *in situ* investigations	purchase; few studies published based on the data type

2.3.4 Hyper-spectral data

Hyperspectral data provides a large number of very narrow bands (<10 nm) in the 0.38–2.5-µm range (Kuenzer et al., 2011). This enables characterization of all mangrove cover types. As hyperspectral data provides measurements beyond the non-photosynthetic spectral range, factors such as leaf water content, leaf chemistry and phenological changes could be employed for better mangrove discrimination. For example, it is possible to detect physiological stress in mangrove plants by measuring the spectral reflectance in hyperspectral data. This type of information is of high significance for mangrove monitoring and management. However, the disadvantage of hyperspectral data is large number of narrow bands which require time-intensive image-processing steps. Also, highly correlated bands may prove to be a noise than utility in hyperspectral images. Consequently, searching for the most useful bands for mangrove discrimination is necessary. Those spectral bands that are able to deliver the greatest spectral distinction among mangroves species are the most appropriate for consecutive mapping activities.

A summary of studies conducted using hyperspectral data in mangrove environment is provided in Table 2.9. Benefits and limitations of various aspects related to usage of hyperspectral data are summarised in Table 2.10.

Table 2.9: Summary of studies which employed hyperspectral data for mangrove studies

Author (s)	**Sensor Used**	**Study Area**	**Brief about Work Done (Methods/Classification Approach/Outcomes/Accuracy)**
Green et al., 1998	CASI (Compact Airborne Spectral Imager)	Turks and Caicos Islands	• Hyperspectral data was used for mangrove mapping and the results were compared with

			mapping done using SPOT XS data. • The eight spectral channels of CASI data were put to PCA (Principle Component Analysis) and band ratioing. • Supervised classification was then employed to classify the resulting images into nine mangrove habitats. • CASI data could be used to distinguish between species of homogeneous mangrove stands; however, it was not possible to identify species within mixed mangrove assemblages.
Ong et al., 2003	HyMap	Port Hedland, Australia	• Used airborne HyMap imagery to measure the effects of iron ore dust (chemically, iron oxide) on mangroves. • Iron oxide can be spectrally characterized by a broad absorption at 860 nm, and it is distinctive in the visible (iron oxide absorption band at 518 nm) and short-wave (1,700–2,500 nm) regions. • Therefore, simple band combinations within these spectral ranges could be used to

			distinguish between clean and dusty leaves.
Hirano et al., 2003	AVIRIS (Airborne Visible/Infrared Imaging Spectrometer)	Everglades National Park, USA	• The mapping done using AVIRIS data was compared with a pre-existing detailed GIS wetland vegetation database compiled by manual interpretation of 1:40,000-scale CIR aerial photographs. • It was found that accuracies for single-vegetation classes differed greatly, ranging from 40% for scrub red mangroves (*R. mangle*) to 100% for spike rush (*Eleocharis cellulosa*) prairies. • The authors attributed the low accuracies for mangroves to the relatively low spatial resolution, requirement of highly trained personnel for complex image-processing procedures, and a lack of stereo views which might be useful for canopy differentiation.
Demuro and Chisholm, 2003	EO-1 (Earth Observing-1) Hyperion	Minnamurra River estuary in New South Wales, Australia	• SAM (Spectral Angle Mapper) algorithm was applied on selected 105 noise free bands of Hyperion. • The resulting image depicted nine non-vegetation classes,

			two aggregated mangrove species classes and five other vegetation classes. • Overall accuracy obtained was 76.74%.
Vaiphasa et al., 2005	Hand-held spectroradiometer	Thailand	• Collected the spectra of 16 mangrove species in Chumporn, Thailand. • Four spectral bands (720, 1,277, 1,415, and 1,644 nm) were found to distinguish these 16 mangroves species most clearly, with the exception of members of the Rhizophoraceae family. • The spectral responses for members of the Rhizophoraceae family have been spectrally too similar among themselves and in conjunction with other species. Therefore, it is likely that this will cause difficulties using hyperspectral imagery to separate mangrove classes.
Wang and Sousa, 2009	Hand-held spectroradiometer	Punta Galeta, Panama	• Developed an optimal band-selection method aimed at optimizing the spectral separability of mangrove species.

			• A ratio of the 695/420 nm bands was found to distinguish between stressed and healthy mangrove vegetation.
Yang et al., 2009	AISA+ (Airborne Imaging Spectrometer for Applications)	Texas, USA	• AISA+ data having a resolution of 2.1 m was classified using four algorithms: Minimum Distance, Mahalanobis Distance, Maximum Likelihood and Spectral Angle Mapper (SAM). • The original hyperspectral data, containing 214 bands, was transformed into a dataset containing only 20 bands. Inverse minimum noise fraction was used to reduce the noise in the data. • It was concluded that SAM and minimum distance methods were not suitable for spectral discrimination of mangroves and maximum likelihood classification provided the most accurate results.
Kamal and Phinn, 2011	CASI-2	Australia	• The ability of CASI-2 data was evaluated for mangrove species mapping using pixel-based and object-based approaches • Three mapping techniques were used in this study: spectral

			angle mapper (SAM) and linear spectral unmixing (LSU) for the pixel-based approaches, and multi-scale segmentation for the object-based image analysis (OBIA). • The mapping results showed that SAM produced accurate class polygons with only few unclassified pixels (overall accuracy 69%, Kappa 0.57), the LSU resulted in a patchy polygon pattern with many unclassified pixels (overall accuracy 56%, Kappa 0.41), and the object-based mapping produced the most accurate results (overall accuracy 76%, Kappa 0.67).
Chakravortty, 2013	EO-1 (Earth Observing-1) Hyperion	Henry Island, Sunderbans, West Bengal	• Development of spectral library of 7 dominant mangrove species: *Excoeocaria agallocha*, *Avicennia officinalis*, *Ceriops decandra*, *Avicennia marina*, *Phoenix paludosa*, *Brugueira cylindrica*, and *Aegialitis*.
Kumar et al., 2013	EO-1 Hyperion	Bhitarkanika National Park, Odisha, India	• Identification of mangrove floristic composition classes was carried out using hyperspectral data.

			• Out of 196 calibrated bands of the image, 56 were selected for the classification. • Among the three full-pixel classifiers tested in the investigation, Support Vector Machine (SVM) produced the best results in terms of training pixel accuracy with overall precision of 96.85 %, in comparison to about 70-72.0 % for the other two classifiers. • A total of five mangrove classes were obtained - pure or dominant class of *Heritiera fomes*, mixed class of *H. fomes*, mixed *Excoecaria agallocha* with *Avicennia officinalis*, mixed class of fringing *Sonneratia apetala* and class comprising of mangrove associates with salt resistant grasses.
Manjunath et al., 2013	Hand-held spectroradiometer	Sunderbans, India	• Use of field-recorded spectra to discern mangrove species and mudflats in Indian Sunderbans. • 17 mangrove species, belonging to nine families, and four mudflat classes were spectrally characterized.

			• ANOVA (Analysis of Variance) was used to demonstrate the statistical separability of collected canopy spectra. • Discriminant analysis was performed in different combinations/cases to identify the bands for maximum separability. • The most significant bands reported for canopy discrimination were 960, 970, 1000, 1070, 1120, 1160, 2070, 2080, 2150, 2200, 2240 and 2340 nm; and for discrimination amongst mudflat classes and creek water were 540, 550, 730, 740, 770, 780, 880, 1190, 1290, 2010 and 2150 nm.
Chakravortty et al., 2014	Hand-held spectroradiometer	Sunderbans, India	• Analysis of classification accuracy of linear and non-linear unmixing models for discrimination of mangrove species was carried out. • The authors found that linear unmixing was successful in identification of mangrove species which exist as a pure patch whereas the non-linear

			model was better in discriminating species more accurately in a heterogeneous patch.
Chakravortty and Sinha, 2016	EO-1 Hyperion	Henry Island, Sunderbans, West Bengal, India	• Application of higher-order nonlinear models on EO-1 Hyperion data to identify heterogeneous mangrove stands. • Homogeneous mangrove areas could be identified through linear spectral unmixing, • However, in natural heterogeneous forests such as Sunderbans, nonlinear spectral unmixing models provided more accurate estimates of fractional abundance of mangrove species.

Table 2.10: Advantages and disadvantages of using hyperspectral satellite data for mangrove studies (Source: Kuenzer et al., 2011)

Parameters	**Advantages**	**Disadvantages**
1. Spectral Resolution	Very high, covering a broad range with narrow bandwidths	High data volume, bands with redundant information
2. Spatial Resolution	Usually very high (centimetre to meter range)	Very small area covered

3. Temporal Resolution	Spcaeborne: maximum monthly; airborne: on demand	Weather dependent (clouds); complex acquisition of equipment is needed; very cost intensive
4. Costs	None	Very high costs for airborne campaigns and sensor operations; very high costs for personnel working in airborne or spaceborne data
5. Long-term monitoring	Theoretically possible, practically not feasible	Unsuitable because of small areas covered and very high costs; will only be possible with a reliable spaceborne, operational sensor
6. Purposes	Maps of mangroves on species level; highly detailed parameterization; detailed analyses of status (vigor, health etc.)	No major limitation
7. Discrimination Level	Species, Communities	No major limitation
8. Methods	Typical hyperspectral data-analysis methods (spectral unmixing, SAM, MTMF etc.); partially also paired with object-oriented analyses	Specialized knowledge is needed for data analysis; experience in sound hyperspectral data processing often not available; hyperspectral analyses often lead to only seemingly quantitative results (e.g.., endmember fraction images)

9. Other	Detailed mapping of non-mangrove constituents also probably beneficial (e.g., different water classes, depending on sediment load, algae etc.; or soil types)	Relatively few studies have been conducted; still in a testing phase; very few spaceborne sensors available (Hyperion with questionable SNR, Sebas etc.)

2.3.5 Microwave remote sensing

The microwave region of the electromagnetic spectrum includes radiation with wavelengths longer than 1 mm. Solar radiation in this region is negligible, although the earth itself emits some microwave radiation. The energy characterizing microwave region of electromagnetic spectrum is capable of penetrating atmospheric conditions that render traditional space-borne optical/multispectral systems useless. Because of persistent cloud cover in the tropical and subtropical regions, radar imagery is an appropriate option compared to optical remotely sensed data for continuous monitoring of these regions. RADAR (Radio Detection and Ranging) is an active remote sensing system which carries its own energy source. Radar data provides information that is useful for characterizing the cover extent of mangrove surfaces, structural parameters, flooding boundaries, health status, deforestation status, and the amount of total biomass (Kuenzer et al., 2011). Imagery derived from radar systems, especially SAR (Synthetic Aperture Radar), is much more difficult to interpret than optical imagery. Here, the signal's intensity is measured in the form of a "backscatter coefficient (σ°)" in decibels (dB). Because microwaves can be transmitted under various configurations, varying in wavelength (P, L, S, C, X etc.) polarization of transmitted and received signals (HH, VV, HV, VH), and incidence angles, the same surface can yield different backscatter coefficients. This backscattering coefficient depends upon the interactions of different types of microwaves with different component of the mangrove (e.g. leaves, branches and trunks) of varying size, dimension, density, orientation and dielectrics constants (moisture contents) (Lucas et al., 2007). The longer L-band microwaves have a greater likelihood of penetrating the foliage and small branches of the upper canopies of the forest and interacting with woody trunk and larger branch components as well as the underlying surface (Lucas et al., 2004).

Studies have been conducted at different locations in various countries based on different radar data such as RADARSAT-1/2 SAR, ENVISAT ASAR, JERS-1, ERS-1 SAR, SIR-B, ALOS PALSAR, AIRSAR, SIR-C etc. The launch of RISAT-1 (Radar Imaging Satellite-1) on 26 April 2012 by Indian Space Research Organization (ISRO) has also offered new, exciting and cost-effective opportunities to conduct different experiments using SAR data to understand natural ecosystems. Several investigations have also been conducted by integrating radar data and optical remotely sensed imagery. Synergistic information on structure and composition derived from radar backscatter signals and the reflectance information from the optical imagery are most promising for vegetation-mapping applications. It is also possible to achieve increased level of classification detail and mapping accuracy by integrating radar data with hyperspectral data. However, all these advanced level of data processing requires highly skilled analysts which impose a practical restriction on widespread utilization of microwave data.

A summary of studies conducted using microwave satellite data in mangrove environment is provided in Table 2.11. Benefits and limitations of various aspects related to usage of microwave satellite data are summarised in Table 2.12.

Table 2.11: Summary of studies which employed microwave data for mangrove studies

Author (s)	**Sensor Used**	**Study Area**	**Brief about Work Done (Methods/Classification Approach/Outcomes/Accuracy)**
Mougin et al., 1999	AIRSAR	French Guiana	• The relationship between canopy parameters and radar backscattering at different wavelengths (P, L and C) were investigated. • Strong relationships were found between most forest parameters and radar data, with P-HV showing the greatest sensitivity to total biomass.

Proisy et al., 2000, 2002	AIRSAR	French Guiana	• Investigating the relationship between canopy parameters and radar backscattering at different wavelengths (P, L and C).
Simard et al., 2002	JERS-1 (Japan Earth Resources Satellite-1) and ERS-1 (European Remote-sensing Satellite-1)	West Gabon	• Combined L-band HH (Horizontal Transmit, Horizontal Receive) JERS-1 and C-band VV (Vertical Transmit, Vertical Receive) ERS-1 data to produce a land cover map for West Gabon which also included two mangrove classes. • The map produced using combined approach yielded 18% improvement in accuracy relative to that produced using either of the data alone.
Kovacs et al., 2006	RADARSAT-1	Agua Brava Lagoon, Mexico	• C-band HH RADARSAT-1 fine beam data obtained at two incidence angles were used to understand the interaction between mangrove stand parameters and radar backscattering. • A high degree of correlation between the backscatter coefficients and the estimated LAI and mean stem height was recorded.

Li et al., 2007	Radarsat-1	Guangdong, China	• The biomass obtained using Radarsat-1 fine mode images was compared with the results retrieved using Landsat TM data. • Results indicated that Radarsat images yielded significantly better accuracy than optical data. • The authors concluded that Radarsat images could provide more accurate trunk information about mangrove forests due to their higher resolution and side-looking geometry.
Kovacs et al., 2008	ENVISAT ASAR (Advanced Synthetic Aperture Radar)	Mexico	• Health monitoring of degraded mangrove forest was done. • The results indicate that polarization and, to a lesser extent, incidence angle play a significant role in the ability to estimate both leaf area index and mean tree height. • No significant linear coefficients of determination were observed between the recorded parameters and the backscatter coefficient from any of the co-polarized scenes.

			• The authors concluded that the inability of the co-polarized ENVISAT ASAR data to differentiate between dead mangrove stands and healthy ones is because of equally high backscatter resulting from strong scattering from trunk–ground double bounce and crown volume, respectively.
Wickramasinghe et al., 2012	ALOS (Advanced Land Observing Satellite) PALSAR (Phased Array L-band Synthetic Aperture Radar)	The Klias Peninsula, Malaysia	• Comparison of the results showed SAR data is more suited for mangrove mapping compared to optical data from ALSO/AVNIR-2. • The lack of Short Wave Infra-Red band in ALSO/AVNIR-2, made it difficult to apply ALOS/AVNIR-2 data for mangrove mapping.
De Santiago et al., 2013	ALOS PALSAR	Guinea, West Africa	• Assessed the accuracy of an object-based image analysis (OBIA) approach in classifying mangroves using both single (HH) and dual (HH+HV) polarized data. • The authors reported that at the first level of classification (mangroves from non-mangroves) it was possible to accurately separate mangrove

			areas from saltpan and water/shallow zones using both sets of SAR images. • At the second level of classification, separation among the three mangrove classes identified was most accurate when using the dual-polarized data, at an overall accuracy of only 63.4%. • Using the optimal combination of parameters, the extent to which a filter could be used to improve the accuracy was also examined. At this level, it was determined that the dual-polarized data, filtered with a 3 × 3 Lee speckle filter and a segmentation scale of 5, resulted in an overall accuracy of 64.9%.
Fatoyinbo and Simard, 2013	SRTM (Shuttle Radar Topography Mission)	Africa	• Employed a multi-sensor approach to derive three dimensional structure and biomass of mangroves of entire African continent. • The datasets used were: Landsat ETM+, ICESat/GLAS (Ice, Cloud, and Land Elevation Satellite/Geoscience Laser Altimeter System) and

			SRTM (Shuttle Radar Topography Mission). • The lidar measurements from the large footprint GLAS sensor were used to derive local estimates of canopy height and calibrate the interferometric synthetic aperture radar (InSAR) data from SRTM. • Then allometric equations were employed to relate canopy height to biomass in order to estimate AGB from the canopy height product. • The total mangrove area of Africa was estimated to be 25,960 km2 with 83% accuracy.
Kovacs et al., 2013	Radarsat-2	Mexico	• Studied the relationship between mangrove stand parameters and backscattering received from multi-polarized C-band Radarsat-2 data. • Results indicated that the selection of the spatial resolution (3 m vs. 8 m), the incidence angle (27–39°) and the polarimetric mode greatly influence the relationship between the SAR and mangrove structural data.

			• It was also observed that only models derived from the HH data are significant and that several of these were strong predictors of all but stem density.
Kovacs et al., 2013	ALOS PALSAR	Mexico	• Significant negative correlation coefficients were observed between filtered single polarization HH data (resolution 6.25 m) and Leaf Area Index (LAI). • Conversely, strong positive significant correlation coefficients were calculated between the cross-polarization HV backscatter and LAI. • The authors also used texture parameters derived from quad-pol data to develop mangrove LAI map of the study area which showed comparable spatial patterns of degradation to a map derived from higher spatial resolution optical data.
Chakraborty et al., 2013	RISAT (Radar Imaging Satellite)-1	Dhanchi Island, Sunderbans	• Published first study utilizing RISAT-1 C-band VV data for broad classification of mangrove ecosystem. • The broad categories used to classify mangrove ecosystem

			were mangrove forests, creeks/channels and mudflats. • The authors reported that intertidal mudflats appeared dark in the SAR image due to low backscatter and creeks/channels appeared bright due to high backscatter. • The mangrove forests registered backscatter values ranging from –12 to –7.5 Db
Cougo et al., 2015	Radarsat-2	Brazil	• Studied the relationship between radar backscattering of a multi-polarized Radarsat-2 C-band image with the structural attributes of mangrove vegetation. • Significant relationships between the linear σ° in VH (vertical transmit, horizontal receive) cross-polarization produced r2 values of 0.63 for the average height, 0.53 for the DBH (Diameter at Breast Height), 0.46 for the basal area (BA) and 0.52 for the AGB (Above Ground Biomass). • Using co-polarized HH (horizontal transmit, horizontal receive) and VV (vertical transmit, vertical receive), r2

			values increased to 0.81, 0.79, 0.67 and 0.79, respectively.
Darmawan et al., 2016	ALOS PALSAR	Southeast Asia (Myanmar, Thailand, Cambodia, Laos, Vietnam, Malaysia, Singapore, Brunei, Philippines, East Timor and Indonesia)	• Used 25-m resolution mosaics of ALOS-PALSAR data to generate an FCC with configuration: R=HH, G=HV and B= HH/HV. • Backscatter values of mangrove forest on HH images range from -10.88 Db to -6.65 Db and on HV images around -16.49 Db to -13.26 Db.

Table 2.12: Advantages and disadvantages of using RADAR data for mangrove studies (Kuenzer et al., 2011)

Parameters	Advantages	Disadvantages
1. Spectral Resolution	Active microwave radiation; delivers alternative information about the surface structure; various wavelengths and polarization are selectable	No spectral information
2. Spatial Resolution	Varies	None
3. Temporal Resolution	High; weather independent	None
4. Costs	Many data types available at low cost in the context of science proposals (ESA, JAXA, DLR, etc.)	Restricted access to data (certain number of scenes); also some data not sharable

		with certain developing countries (e.g., TSX)
5. Long-term monitoring	Good; long-duration systems	None
6. Purposes	Mangrove extent, condition, canopy properties, deforestation, biomass estimation	No information derivable from typical spectra (species differentiation not possible unless species vary in their structural appearance)
7. Discrimination Level	Age structure, forest parameters, biomass estimation	No discrimination between mangroves and other vegetation forms without *a priori* knowledge
8. Methods	Analyses of the backscatter signals using advanced image-processing techniques; very quantitative physics-based manner of image analysis	Extremely skilled analysts with experience in radar-image processing needed
9. Other	Most promising results when SAR data combined with optical imagery	Relatively few studies have been conducted; special software or modules are needed for radar-image processing

2.3.6 Synergistic applications of optical and microwave data

The highly complex interaction among mangrove species and between mangroves and the surrounding environment makes it difficult to characterize all aspects of these intertidal plants with sufficient accuracies. Synergistic exploitation of satellite data which record information in two different regions of electromagnetic spectrum could prove useful in such situations. For example, Synergistic information on structure and composition derived from radar backscatter signals and the reflectance information from the optical imagery may prove to be more promising for mangrove studies. Kuenzer et al. (2011) suggested that there is need for further investigation on synergistic data use for mangrove studies including joint analyses of multispectral and radar data, such as combined analyses based on high-resolution TerraSAR-X and QuickBird data, combined analyses based on TerraSAR-X and Rapid Eye data, combined analyses based on TerraSAR-X and SPOT data and combined analyses of Envisat ASAR and ASTER data.

A summary of studies conducted using microwave and optical satellite data in mangrove environment is provided in Table 2.13.

Table 2.13: Summary of studies which employed microwave and optical data synergistically for mangrove studies

Author (s)	**Sensor Used**	**Study Area**	**Brief about Work Done (Methods/Classification Approach/Outcomes/Accuracy)**
Giri and Delsol, 1993	SPOT XS and JERS-1	Phangnga Bay, Thailand	• Both optical and microwave data were synergistically employed to improve the discrimination between mangrove and non-mangrove classes. • The complementary use of both datasets led to a successful separation between pure *Rhizophora* and *Rhizophora*-dominated communities, which could not be discriminated using SPOT data alone.

Aschbacher et al., 1995	SPOT XS and ERS-1 SAR	Phangnga Bay, Thailand	• Used SAR data complementary to the classification previously done using SPOT data. • An increase was reported in the discrimination ability using the combined dataset for different age stages in a homogeneous *Rhizophora* community.
Raouf and Lichtenegger, 1997	Landsat TM and ERS-SAR	Karachi, Pakistan	• Developed a novel approach to integrate SAR and optical data. • The indices (NDVI: Normalized Difference Vegetation Index; and Optical Brightness) obtained using Landsat TM bands were layerstacked with speckle-filtered ERS data. • An FCC was prepared in which NDVI, Optical Brightness and SAR were displayed as 'Red, Green and Blue', respectively. • It was reported that integrated image provided more detailed land cover map than that produced using either data alone.
Dwivedi et al., 1999	ERS-1 SAR and IRS 1B LISS II	Sunderbans, West Bengal, India.	• The FCC (False Colour Composite) prepared by merging microwave and optical data was found to be better for the delineation of wetlands.

			• The cloud penetration capability of microwave data was also demonstrated by reporting features in merged data which were not discernible due to cloud cover in optical data.
Souza Filho and Paradella, 2002	Landsat TM and Radarsat-1	Bragança peninsula (North Brazil)	• Merged Landsat TM and Radarsat-1 data to map 19 different geomorphological and vegetation units of the Bragança peninsula. • It was concluded that the digital integration of Fine RADARSAT-1 and Landsat TM data sensitively highlighted geobotanical coastal features, providing a useful tool for a synoptic analysis of their natural and man-made changes.
Held et al., 2003	AIRSAR and CASI	Daintree River estuary in North Queensland, Australia	• Mapping the mangrove diversity by integrating NASA/JPL airborne polarimetric AIRSAR data with • MLC and hierarchical neural network (HNN)-derived results showed that the integrated approach achieved greater classification accuracies for

			species communities based on dominant species than did those achieved by each individual sensor. • HNN showed a slight improvement in overall classification accuracy of about 3% compared with the MLC result (76.5%).
Shanmugam et al., 2005	IRS-1D LISS III and ERS-2 SAR	TN, India	• Performed a sensor fusion between optical and SAR imagery and the properties of fused images and their ability to preserve spatial and spectral information of the original images were evaluated. • Four sensor fusion methods employed were: Multiplicative, Brovey Transform, Principal Component Analysis and Intensity-Hue-Saturation. In addition, authors presented a novel method of fusing images based on multiresolution wavelet transform. • It was concluded in the study that Brovey Transform yielded higher spatial and spectral details while merging disparate datasets such as microwave and optical. The wavelet transform

			was not identified as an efficient method to combine optical and microwave datasets because it essentially distorted the spatial details of the original images.
Souza Filho and Paradella, 2005	Landsat TM and Radarsat-1	Amazon Region (Brazil)	• Development of a novel scheme to merge Landsat TM bands with RADARSAT-1 fine mode data through the combination of principal components and IHS (Intensity- Hue-Saturation) transform for mapping geomorphology of a macrotidal mangrove coast. • The SPC-SAR (Selective Principal Component-SAR) product thus developed proved very useful for coastal geomorphological mapping, providing relevant information about geobotany and emergent and submergent coastal geomorphology. • It was reported that TM images contributed to the enhancement of vegetation and sedimentary environments based on the optical response whereas SAR data allowed the enhancement

			of differences between coastal vegetation heights and areas showing distinct moisture content.
Lucas et al., 2008	ALOS PALSAR, Landsat and SRTM	Selected tropical regions (northern Australia, Belize, French Guiana and Brazil)	• Use of ALOS PALSAR L-band HH data, in conjunction with Landsat and SRTM data for mapping and change detection of coastal ecosystems (including mangroves). • A rule-based classification was used for combining ALOS data with other layers (eg, Landsat-derived Foliage Projected Cover) for classification of forest structural types.
Monzon et al., 2016	ALOS PALSAR, JERS-1 and Landsat	Philippines	• Evaluated the synergistic use of time-series L-band SAR and optical data for mapping and monitoring mangroves. • The optical data were used for computing Normalized Difference Vegetation Indices (NDVIs). • SAR data were subjected to object-based image analysis. Image segmentation was implemented on the 25-meter ALOS/PALSAR image mosaics, in which the generated objects were

			subjected to statistical analysis using the software R. • In combination with selected Landsat bands, the class statistics from the image bands were used to generate decision trees and thresholds for the hierarchical image classification.

Above mentioned literature survey has revealed that mapping of mangroves is one of the most challenging tasks in remote sensing due to complexity of mangrove ecosystem. The image pixel containing 'mangrove' is usually comprised of different parts of mangrove plants, mudflats and water in different proportions. Apart from this, other parameters influencing signals emanating from mangroves include mangrove density and atmospheric conditions. In addition, choice of satellite data with respect to sensor parameters also determines the final outcome. All of this highlights the need to explore new sensors and digital analysis techniques using high resolution optical, microwave and hyperspectral data sets for improving the discrimination of mangrove communities and species. Also there is need to develop a uniform classification scheme and standardized data processing approaches for ease of comparison across different studies.

2.4 Previous work carried out on mangroves of Gulf of Kachchh

The earliest record regarding the mangroves of Jamnagar, situated at the southern coast of Gulf of Kachchh is the Imperial Gazette of India, Vol. XVIII (1908) wherein it has been documented that Jamnagar (then known as Navanagar State) had mangrove forests along the coastal belt and that these forests were largely used for firewood and pasture requirements (Singh, 2000; Singh et al., 2002). Later the Cher (local name for *Avicennia* sp.; also used synonymously for mangroves in general in Gujarat) forests of Okha Mandal (including 31 islands) were declared as Reserved Forests vide Notification No. 90 of the Baroda State, dated 24 April 1999 (Singh, 1994, Singh 2000, Singh et al. 2002). In 1955 and 1956, cher forests of Navanagar State were taken over by the Director of Marine Product, Government of Saurashtra and were notified as Forests (Singh, 2000). The Working Plan of Baroda (1977) provides the total mangrove notified area in Jamnagar district as 665.93 sq. km out of which 103.25 sq. km area was leased out to 21 salt industries (Singh, 2000; Singh 2002). Today, the mangroves in Jamnagar district are under the management control of MNP, Jamnagar (Singh, 2000).

Mangroves along the southern coast of GoK, in the past, extended from Okha in the west to Navlakhi in the east and continued further upto Surajbari creek (Singh, 2000). They were dense and fairy tall. Overall, they were in good condition though the species diversity was not very high (Singh, 2000). Integrated Research and Action for Development (IRADe), a Delhi based research and development organization, used satellite images of Landsat-1 MSS to map the mangrove cover for the year 1972, and the map of MNP&S prepared using these data is shown in Figure 2.1. For the year 1972, total mangrove area mapped is 175.36 sq. km and the total salt pan area mapped is 65.24 sq. km in MNP&S.

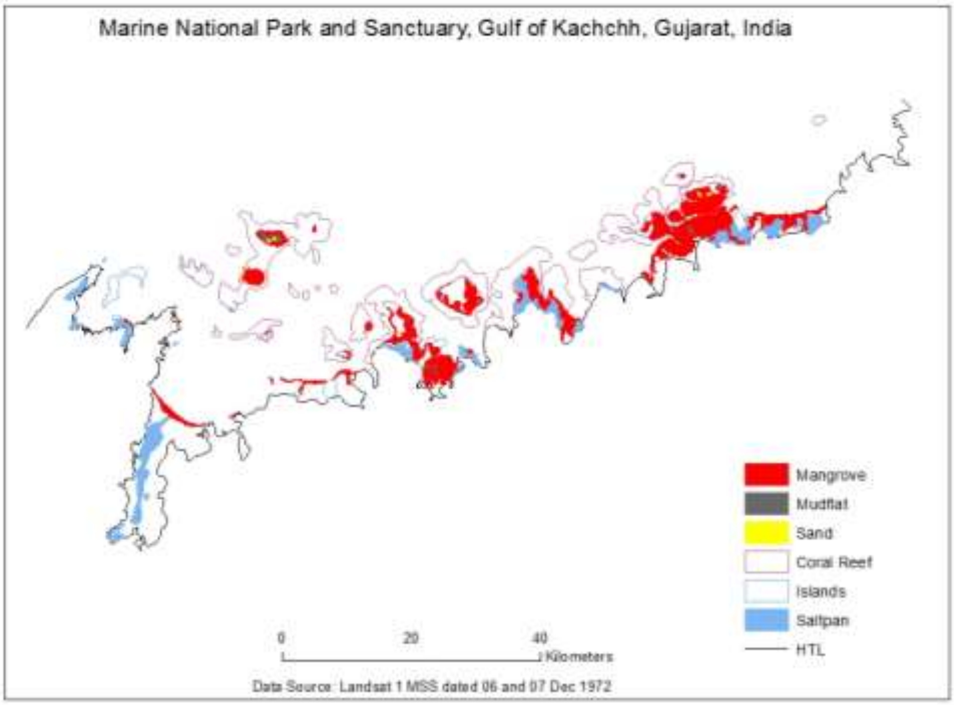

Figure 2.1**:** Mangrove extent during 1972 as mapped using Landsat MSS data covering MNP&S (Source: IRADe, 2016)

Considerable damage to mangroves took place during the period from 1973 to 1976 as these years were marked with drought and the entire coastal belt was declared open for collection of wood and fodder. Much of the mangrove degradation, however, was restricted to the fringing coastal areas, and the island mangroves were relatively less damaged. Nayak et. al. (1989) used satellite images to map mangroves and coral reefs of a stretch of MNP&S between Rozi and Vadinar, and reported the mangrove cover in 1975 to be 138.5 sq. km. Mangrove cover in this stretch reduced to 50 sq. km in 1982 and then to 33 sq. km in 1985 (Nayak et al., 1989). However, some improvement was reported in 1988 as the mangrove area in this stretch increased to 47 sq. km in this year (Nayak et al., 1989). The year 1983 saw the initiation of mangrove plantation activities in MNP&S (NCSCM & GEC, 2014). However, during the drought of 1986-88, the restrictions were released, and, grazing and exploitation were allowed which led to significant damage to the ecology of the area (Singh, 1994). Mostly mangroves were harvested for firewood and fodder collection by local villagers.

The grazing was mostly done by camels which would damage all the leading shoots of the plants and therefore such plants usually didn't grow further and remained stunted (Singh, 1994). These camels (Kharai breed) can even swim in low tides and reach up to nearby islands. Grazing by camels even damaged pneumatophores. Additionally, grazed vegetation don't produce flowers and fruits, thus their natural regeneration was severely affected. Another significant cause of mangrove destruction was the expansion of saltpans along the coast. Large portion of mangrove areas were leased out to industries for the creation of saltpans (Singh, 1994) which took a heavy toll on the ecology of MNP&S. The Government of Gujarat granted lease to 27 salt industries in Jamnagar, but some of these leases were later cancelled. Singh et al. (2002) reported that 21 salt industries are still operational in the intertidal areas and in June, 2001 around one lakh mangrove trees were fatally affected due to leakage of brine water from the pipelines of Tata Chemicals Ltd. near Poshitra. Singh (2000) estimated the mangroves in Jamnagar for 1998 as 141.44 sq. km. This includes 58.21 sq. km of mangrove cover on various islands.

Forest Survey of India has been mapping mangrove cover using satellite data and publishing the salient results since biannually since 1991. The salient results of mangrove cover mapped for the time frame 1987-89 to 2013-14 have been compiled for Jamnagar, Rajkot and Kachchh districts, Gujarat covering the coastal regions of the Gulf of Kachchh and are given in Table 2.14. There has been an increase in mangrove cover in Gulf of Kachchh of 606 sq km area during time frame 1987-89 to 2013-14. There has been enormous growth during time frame 1987-89 to 1996-98 from 357 sq km to 994 sq km. However, it reduced to 849 sq km in the year 2000 and probably this is due to cyclone of June 09, 1999 which severely damaged mangrove cover. In addition, there were recurring oil spill incidences in the Gulf of Kachchh during 1998-99, which also damaged the mangroves. In particular, the mangroves around Jindra Island suffered severe degradation due to recurring oil spill incidence in October, 1998 (Figure 2.2). An estimated 14.7 sq. km of mangrove cover in south-east of Jindra bet was considerably affected (Navalgund and Bahuguna 1999; SAC, 2003, Shah et al., 2005). There were more oil spill incidences in March, 1999 and November 1999 (SAC, 2003). Subsequently, there is steady growth of mangrove cover in the Gulf of Kachchh since 2002 from 892 sq km to 963 sq km in 2013-14.

It is quite evident that area under mangroves has increased because there have been serious plantation efforts carried out by Gujarat Forest Department, Marine National Park authorities, Gujarat Ecology Commission with support from local communities and Non-Government Organizations, e.g., mangrove plantation was initiated way back in 1983 by MNP authorities and by 2015 an area of 472.44 sq. km (Figure 2.3) of mangroves was planted at various locations within MNP&S. These plantations were carried out under various schemes such as Cher Plantation, Coastal Border Plantation etc. It is observed that there has been increase in area under mangrove sparse region due to plantation efforts (Figure 2.4).

Space Applications Centre, ISRO has been developing methods for mangrove inventory, monitoring and classifying them at dominant community level since past three decades using satellite data (Nayak et al., 1989, SAC, 1992, Nayak and Bahuguna, 2001, SAC, 2003, SAC, 2007, SAC, 2012, Ajai et al., 2013). Mangroves at community level have been recently mapped using IRS LISS-III data of 2005-07 timeframe on 1:25K for the entire country. The salient results for Gulf of Kachchh show that mangrove cover is 754.94 sq km. as mapped using LISS-III data of 2005-07 time frame (SAC, 2012, Ajai et al., 2013). This work has identified *Avicennia marina* as the major/dominant community (98% share of all the mangrove communities mapped for Jamnagar/Rajkot) along with scarce patches of *Rhizophora* and

Ceriops species. Coastal habitat maps for Marine Protected Areas have been prepared. A model for mangrove health assessment has also been developed.

Table 2.14: Mangrove cover mapped and published biannually (1991-2015) by Forest Survey of India (FSI) based on satellite data for Jamnagar, Rajkot and Kachchh districts, Gujarat covering the coastal regions of the Gulf of Kachchh

Year in which report was published	**Time-period of satellite images used**	**Mangrove area for Jamnagar (sq km)**	**Mangrove area for Rajkot (sq km)**	**Mangrove area for Kachchh (sq km)**	**Total Mangrove area (sq km)**
1991	1987-89	118	0	239	357
1993	1989-91	118	0	242	360
1995	1991-93	118	0	536	654
1997	1993-95	118	0	836	954
1999	1996-98	140	0	854	994
2001	2000	142	1	706	849
2003	2002	141	2	749	892
2005	2004	150	2	757	909
2009	2006	157	2	775	934
2011	2008-09	159	2	778	939
2013	2010-11	167	4	789	960
2015	2013-14	173	4	786	963

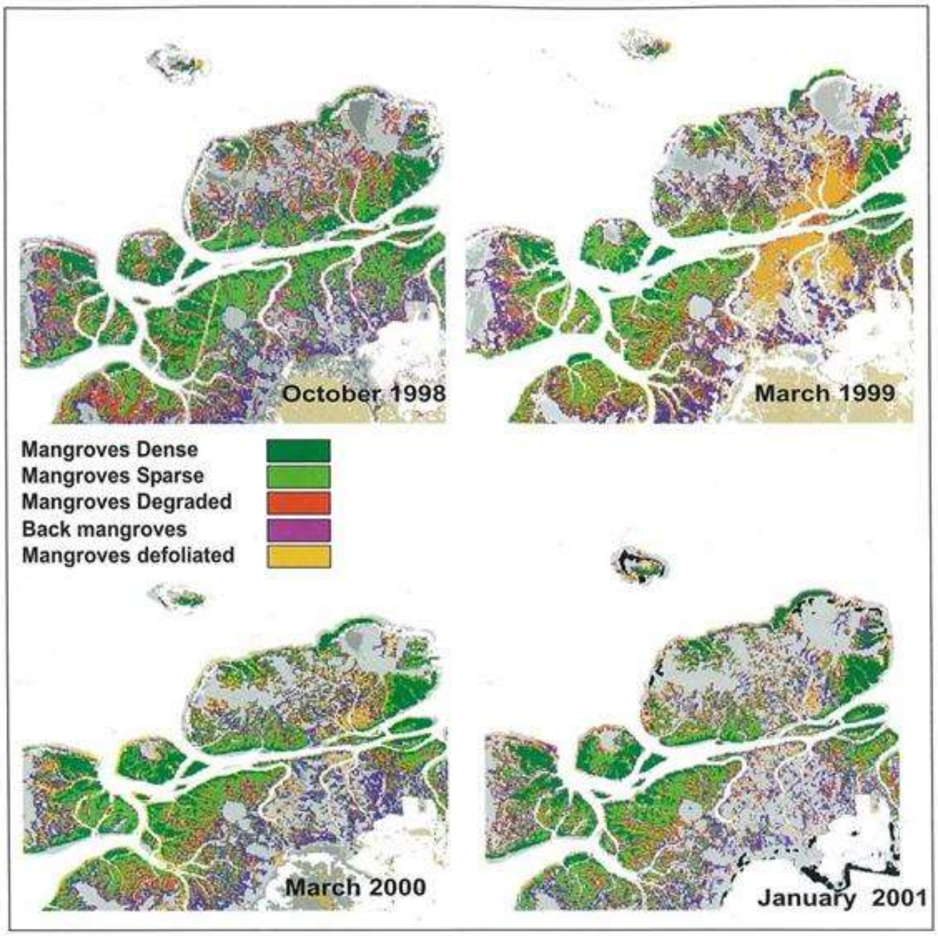

Figure 2.2: Impact of oil spill (defoliated mangroves) mapped for parts of Marine National Park & Sanctuary (MNP&S), Gulf of Kachchh using satellite data (Source: SAC, 2003)

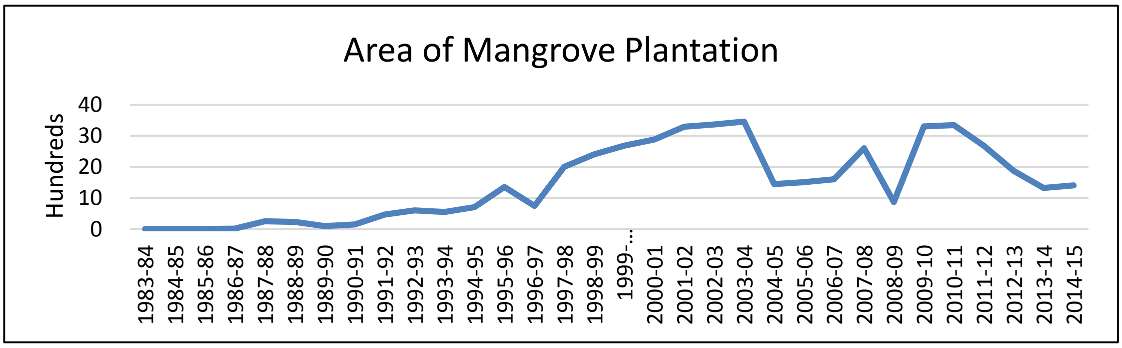

Figure 2.3: Area of mangrove plantation (ha)carried out during 1983-84 to 2014-15 in MNP&S (Source: IRADe, 2016)

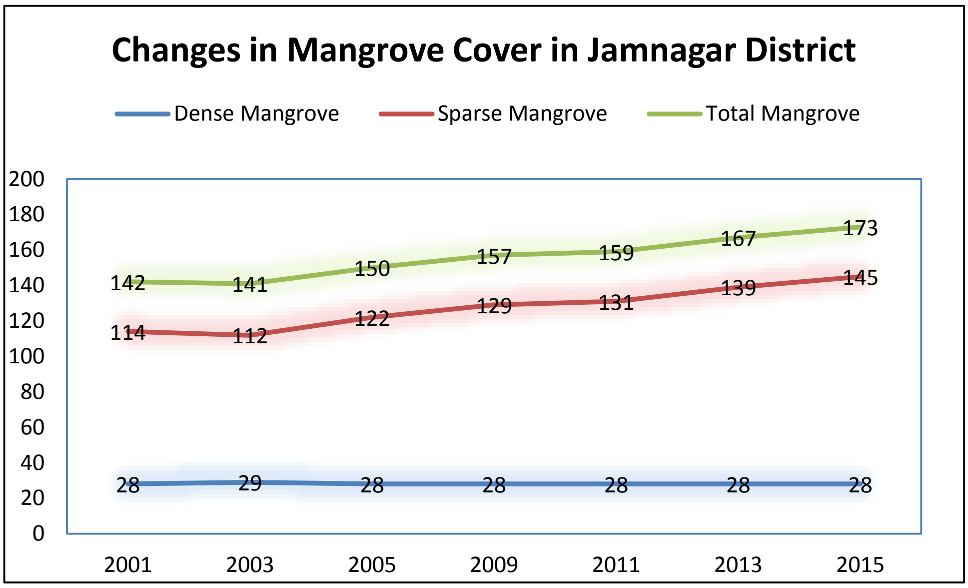

Figure 2.4: Variations in mangrove cover in sq km reported by FSI during time frame 2001-2015

The extensive literature review presented here show that mangrove ecosystem in the Gulf of Kachchh is under threat due to rapid developmental activities. These ecosystems need to be protected, conserved as well developed. In this context there is need to regularly monitor these ecosystems using satellite data. There is urgent need to develop new techniques of satellite data processing as well standardise classification systems aimed at achieving desired accuracy. There is a need to explore new sensors and digital analysis techniques using high resolution optical, microwave and hyperspectral data sets for improving the discrimination of mangrove communities and species.

Chapter 3

Study Area

3.1 General Characteristics of the Study Area

The study area selected for the present research work is Gulf of Kachchh, situated in the north-west part of the Indian coast in the state of Gujarat (Figure 3.1).The Gulf of Kachchh, popularly abbreviated as GoK in the literature, is a semi-enclosed basin located between 69˚46'E-69˚65'E and 22˚30'N-22˚40'N. Occupying an area of approximately 7300km^2, this region is characterized by the presence of shoals, channels, inlets, creeks, mudflats, islands, mangroves and coral reefs (Kunte et al., 2003). The Gulf of Kachchhis a highly energetic macro-tidal system of the northeastern Arabian Sea.The tidal ranges in the Gulf of Kachchhreach upto 7.2 m. Measuring approximately 180 km in length, the width of GoK decreases from nearly 70 km in the west to about a few hundred of meters near Navlakhi and Kandla ports (Vethamony and Babu, 2010). It further narrows down as a marshy land in the east. This marshy land is known as the Little Rann of Kachchh. The depth of GoK varies from nearly 60 m around its mouth to approx. 15 m in the central and western parts. The region is characterized by arid/semi-arid climate with an average annual rainfallof 50 cm.

The area has huge economic significance due to immense potential of industrial development. Major industries at present in the GoK include fertilizer, chemical, cement, power plants, minor and major ports, oil refineries and salt works. Most of these industries are concentrated along the southern shore of GoK. Administratively, the GoK encompass four districts. The entire northern coast is included in Kachchh district whereas there are three districts along the southern coast viz., Morbi, Jamnagar and Devbhumi Dwarka (GES, 2014).

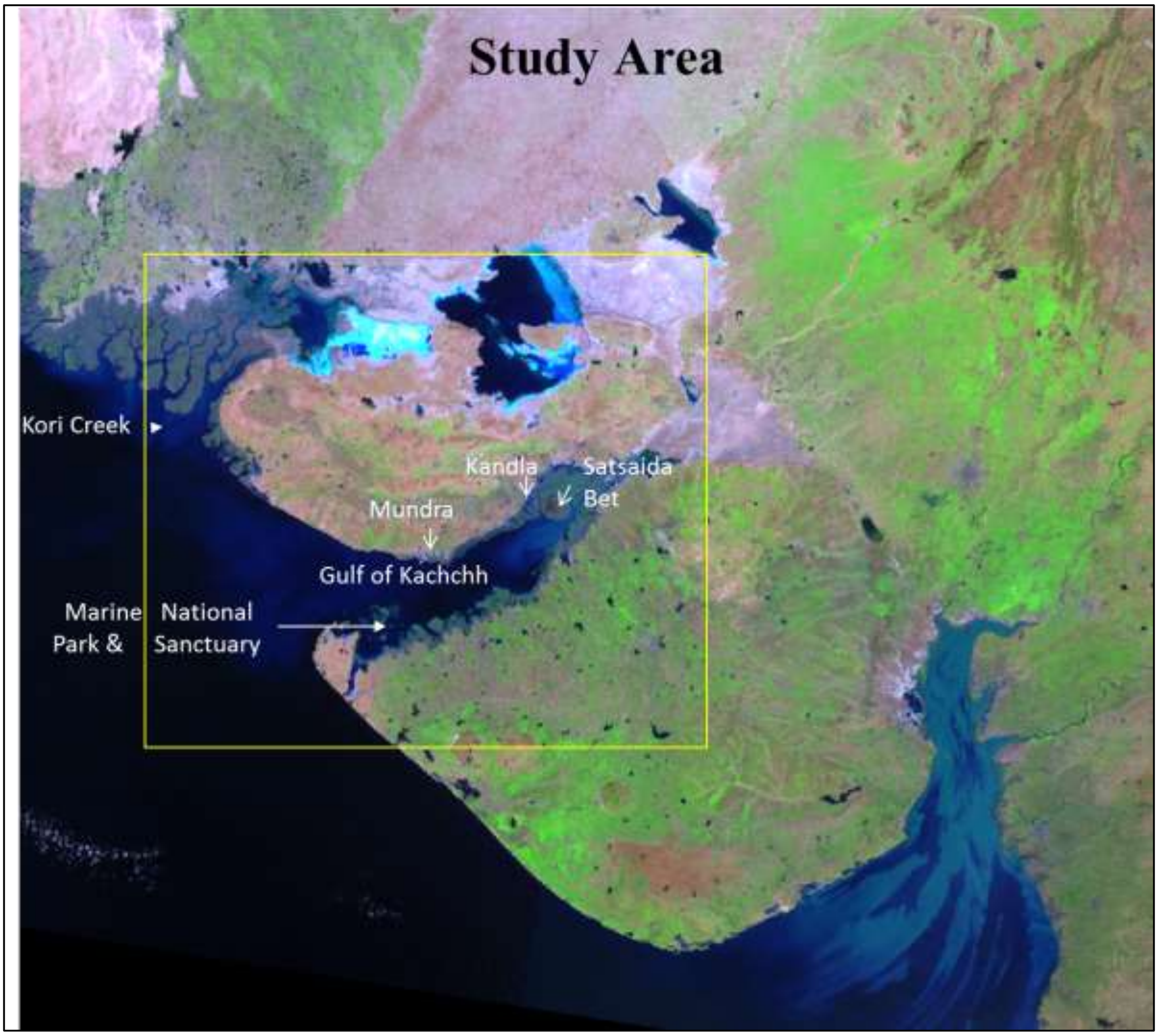

Figure 3.1: Natural Colour Composite image showing the Gulf of Kachchh and environs located in Gujarat, India. Location of five mangrove covered regions viz., Kori creek and environs, Mundra and environs, Kandla and environs, Satsaida bet and environs and Marine National Park and Sanctuary are shown.

There are five mangrove occupying regions taken up for the study viz., Kori creek and environs located in the north-western coast, Mundra and environs located along northern coast, Kandla and environs located along northern coast, Satsaida bet and environs located along north-eastern coast and Marine National Park and Sanctuary located along southern coast of Gulf of Kachchh.

3.1.1 Kori creek and environs

The Kori creek and surrounding area is part of lower Indus Deltaic plain, situated on the west of Great Rann of Kachchh, and north-west of Gulf of Kachchh in Gujarat state of India. This region has more than 65% of the total mangrove cover of the state. The mangrove ecosystem of this region is believed to be unique because it constitutes the largest area of arid climate mangroves in the world. The mangroves grow here in an environment characterized by extremely low rainfall, highly variable seasonal temperature and high evapotranspiration rate (146 mm per year). The annual average rainfall in the delta is 220 cm^2, so the mangroves depend almost completely on the Indus River for freshwater supplies. The diversity of mangroves in this region is low, comprising mostly of monospecific stands of *Avicennia marina*, with smaller patches of *Rhizophora mucronata*, *Rhizophora apiculata*, *Acanthus ilicifolius* and *Ceriops tagal* (Memon, 2005; Nayak and Bahuguna, 2001). Less availability of freshwater, over harvesting by local population coupled with coastal processes such as sedimentation and erosion are considered to be the factors responsible for reduced diversity of mangroves in this region (Shah et al., 2007).

3.1.2 Mundra region and environs

Mundra region is located along the northern coast of the Gulf of Kachchh. The northern coast of the GoK stretches about 300 km, with dissected coastline (GES, 2014). The important rivers of this region include Kali, Godhatad, Kehari, Mithi, Berachiya, Kankavati, Sai, Vingadi, Kharod, Rukmavati, Nagmati and Bhukhi.The northern coast of the Gulf, also known as Kachchh coast has wave as well as tide influenced landforms.

The inter-tidal zone in this region supports a unique marine ecosystem dominated by mangroves and natural creeks. A port has been developed in the region, known as Mundra

Port. The mangrove vegetation is found on the Navinal Island, Bocha Island and the adjoining inter-tidal mudflats.

3.1.3 Kandla region and environs

Kandla region has a small port town in Anjar taluka of Gujarat. Kandla Port is one of the major ports on the west coast of India. The area has two proposed Special Economic Zones (SEZs), one at Kandla and another southwest of Kandla near Tuna Port (GUIDE, 2015). The mudflats around Kandla and Tuna support *A. marina* only. The mangroves of Kandla and Tuna exist under heavy pressures from adjoining saltpans and port development activities.

3.1.4 Satsaida bet and environs

Satsaida bet region located in north-eastern parts of the Gulf of Kachchh has intricate network of creeks, dissecting large intertidal mudflats and has luxuriant growth of mangroves at many parts. This part of the Gulf is muddy in nature with extensive mud flats. This region is also called the Little Gulf of Kachchh. The mudflats along these creeks support sporadic mangrove growth. The coast is characterised by extensive inter-tidal zone along with development of salt pans all along the coastal mainland.

3.1.5 Marine National Park and Sanctuary (MNP&S)

Marine National Park and Sanctuary (MNP&S) is situated along the southern coast of Gulf of Kachchh in Morbi, Jamnagar, and DevbhumiDwarka districts between 20° 15’ N to 23° 40’ N latitudes and 68°20’ to 70°40’ E longitudes (Figure 3.2). There are 42 islands, out of which 37 islands are covered under National park and the rest 5 islands are covered under Sanctuary area. The State Government declared some part of southern coast of Gulf of Kachchhas Marine Sanctuary in 1980. In 1982, the area under marine sanctuary was expanded and some of the areas of the marine sanctuary were raised to the level of Marine National Park to provide more protection to these areas. Thus though Marine Sanctuary (MS) and Marine National Park (MNP) are two legal units, they are part of the same ecological area or Marine Protected Area (MPA in the Gulf (Singh, 2003). Marine Sanctuary (MS) covers an area of

457.92 sq. km whereas the Marine National Park (MNP) is established in an area of 162.89 sq. km.

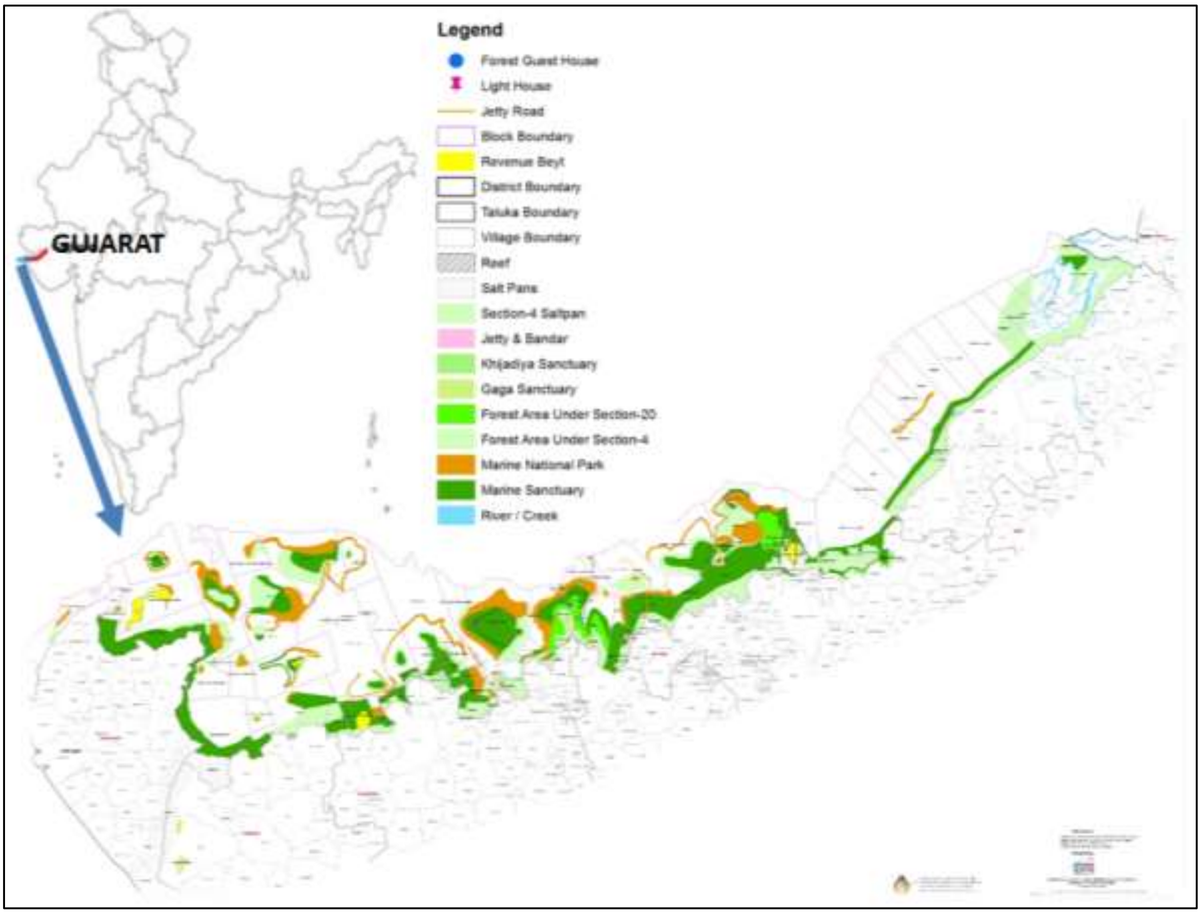

Figure 3.2: Location of Marine National Park and Sanctuary (MNP&S), along the southern shore of Gulf of Kachchh(GoK) in Gujarat state of India(Source: MNP, Jamnagar)

The MNP&S in Gulf of Kachchh supports a variety of marine biodiversity (Table 3.1) due to availability of a diversity of habitats *viz*. coral reefs, mangrove forests, sandy beaches, mudflats, creeks, rocky coast, sea grass beds etc. Marine National park and Sanctuary area of Jamnagar has been declared as Eco- Sensitive Zone (ESZ) by the Ministry of Environment, Forests and Climate Change (MoEFCC), Government of India. The MNP&S supports a bewildering diversity of flora and fauna: 7 core mangrove species (*A. marina, A. marina varaccutissma, A. officinalis, A. alba, R. mucronata, C. tagal, A. corniculatum*), 24 species of mangrove associated flora, more than 120 species of algae including some commercially important species of Agarophytes and Alginophytes, more than 70 species of sponges, 37 species of hard and soft corals (including sea anemones), 180 species of fishes, 8 types of sharks, 27 species of prawns, 30 species of crabs, 200 species of molluscs, 3 species of sea snakes, 3 species of sea turtles, 3 species of marine mammals, 94 species of aquatic birds and 78 species of terrestrial birds (Singh, 2000; Draft Notification Marine National Park, Ministry of Environment and Forests, Government of India, 2012).

Table 3.1: Biodiversity of Marine National Park& Sanctuary, Jamnagar (Source: Compiled from: www.mnpcs.gov.in, Adhavan et al. (2014), Kamboj (2014), Ingle et al. (2014), Dixit et al. (2010), Singh et al. (2002))

Flora/Fauna	**Species**
Algae	108
Sponges	70
Corals (Hard & Soft)	72
Fishes	200+
Prawns	27
Crabs	30
Seagrasses	4
Sea turtles	3
Sea mammals	3
Molluscs	200+
Mammals	3
Water Birds	94
Bivalves	92
Gastropods	55
Birds	78

Many species are in dire need of protection. As per Singh et al. (2002), 23 algal species, 26 coral species and 6 core mangrove species were classified as either ‘Rare’ or ‘Threatened’. Two core mangrove species *viz*. *Sonneratia apetala* and *Bruguiera gymnorrhiza* have become extinct (Singh et al., 2002). Among the marine mammals, Common Dolphin and Porpoise have been classified as ‘Threatened’ whereas Dugong has been classified as ‘Endangered’ (Singh et al., 2002). All the 8 species of sharks found in this region have been labelled as either ‘Rare’ or ‘Threatened’ (Singh et al., 2002). Among the turtles, Green and Olive Ridley

Turtles are 'Endangered' whereas the Leatherback Turtle is classified as 'Uncommon' (Singh et al., 2002). Among the seagrasses, *Halophila beccarii* was reported to be common while *Halodule uninervis*, *Halophila ovalis* and *Halophila ovata* were very rare (Kamboj, 2014).

The coral reefs of MNP&S are of immense importance and provide a range of goods and services for the benefit of the people and environment. As per the economic valuation done by Gujarat Ecological Commission (GEC) for Gulf of Kachchh (GoK) region, the total estimated annual value of the benefits from coral reefs is Rs. 2200.24 million (Dixit et al., 2010).

However, this region has also been extensively exploited for human development activities due to strategic location and importance of Gulf. Salt works, thermal power station, fertilizer plant, cement manufacturing unit, offshore oil terminal, soda ash industry, ship breaking yard, ports, jetties – all influence the area overlapping with the limits of MNP&S. In particular, the stretch between Vadinar and Salaya, is an area of intensive maritime activity characterized by three Single Buoy Moorings (SBMs), three oil handling jetties, one thermal power station and one oil refinery, in addition to many source effluent outlets originating from the nearby industries (Devi et al., 2014). Thus, MNP and other ecosystems are facing immense pressure due to industrialization, urbanization, tourism, shipping related activities and salt pans.

Some field photographs of mangroves along different regions of GoK are shown in Figure 3.3, 3.4, 3.5 and 3.6.

Figure 3.3: Mangroves near Koteshwar

Figure 3.4: Mangroves near Jakhau

Figure 3.5: Mangroves near Jodiya

Figure 3.6: Mangroves of MNP&S

Chapter 4

Materials and Methods

This study is based on utilising and developing remote sensing techniques and GIS tools for studying mangrove dynamics and community zonation. A variety of multi-sensor and multi-temporal satellite images have been used to map and characterize mangroves in the study area. The study has been substantiated with collection of extensive ground truth collected periodically. An attempt has been made to map mangrove cover in the Gulf of Kachchh in 2011 and 2017 and understand causes of the changes. The study has attempted to make synergistic use of optical and microwave satellite data for community zonation in Jindra-Chad Island complex of MNP&S.

4.1 Material used

In this study, a variety of datasets from Indian and foreign missions were used. Extensive ground surveys were carried out at different periods along the coast of GoK.

4.1.1 Satellite data

The satellite data used in this study primarily belong to Indian Remote Sensing Satellite (IRS) mission (Resourcesat-2, RISAT-1) and Landsat (5, 8). Various satellite data used in this study are given in Table 4.1 and their major characteristics have been previously summarised in Chapter 2, Table 2.2. Landsat datasets were downloaded from earth explorer website (http://www.earthexplorer.usgs.gov). Rest all satellite datasets were available in-house at SAC.

Table 4.1: Satellite data used in this study

Sr no.	Satellite	Sensor	Path	Row	Date of acquisition
1	Resourcesat-2	LISS-IV	90	56	25 Dec 2011
2	RISAT-1	C-band SAR	--	--	24 Sep 2012
3	Landsat 5	TM	151	44	04 Feb 2011
4	Landsat 5	TM	150	44	13 Feb 2011
5	Landsat 8	OLI	151	44	20 Feb 2017
6	Landsat 8	OLI	150	44	01 March 2017

In this study, Resourcesat-2 LISS-IV geo-referenced product with three channels i.e., Green (0.52-0.59 μm), Red (0.62-0.68 μm) and NIR (0.77-0.86 μm), spatial resolution of 5.8 m, 70 km swath and 10 bits quantisation was used. Georeferenced MRS product of RISAT-1 with 115 km swath, HH polarisation, 18 m spatial resolution, 36.548^0 incidence angle, descending pass and 10 bit quantisation was used.

Six channels of Landsat-5 TM i.e., Blue (0.45-0.52 µm), Green (0.52-0.60 µm), Red (0.63-0.69 µm), NIR (0.76-0.90 µm) and SWIR (1.55-1.75 µm & 2.08-2.35 µm) with 30 m spatial resolution and 185 km swath were used. Similarly, six channels of Landsat-8 OLI i.e., Blue (0.45-0.51 µm), Green (0.53-0.59 µm), Red (0.64-0.67 µm), NIR (0.85-0.88 µm) and SWIR (1.57-1.65 µm & 2.11-2.29 µm) with 30 m spatial resolution and 185 km swath were used. These are geo-referenced products with UTM projection and WGS-84 datum.

4.1.2 Ancillary data

- Coastal Zone Information System (CZIS) Data Base available at SAC (Coastal thematics maps e.g., coastal landuse/land cover maps, shoreline change maps etc.).
- Topographical maps
- High resolution satellite images available on Google Earth platform
- Published and unpublished literature (research papers, articles, project reports etc.) related to the present study collected from various sources including the world wide web (www) through internet.

4.1.3 Field data

In the present study, extensive ground truthing was carried out along the various coastal stretches in Gulf of Kachchh during the period of 2011-2016 for identifying mangroves, mangrove communities/species and accuracy checking of mangrove habitat/communities maps. On the northern coast of Gulf of Kachchh, sites visited are around Narayan Sarovar, Koteshwar, Jakhau, Mandavi and Luni. On the southern coast, sites visited are around Jodiya, Sikka, Salaya, Jamnagar, Pindara, Okha and Mithapur. In MNP, field work was carried out around core Marine National Park which includes the islands *viz.* Pirotan, Jindra, Chhad etc. and Narara. Sampling method was random as it is not possible to visit the region following a well laid down sampling strategy. The reason is that many parts of the area are inaccessible and are under protection by the State Environment Department, Port Trusts, Border Security Force, Coast Guards, Indian Navy (due to nearness to International border). Therefore, these areas were randomly and opportunistically visited as and when the permissions were granted for specific locations by the concerned authorities. Mangrove species were identified and their locations recorded using a GPS and a hand-held camera. High resolution satellite images available on Google Earth platform were used to recheck the ancillary coastal thematic maps as well as ground truth for some of the inaccessible areas.

4.1.4 Software used

A. Image processing software are as follows:
    ERDAS Imagine Version 8.5, 9.0, 9.3 and 10
    ENVI version 5.0

B. GIS software used are as follows:
    ESRI Arc Map 9.0, 9.3, 10, 10.1
    QGIS version 2.6.1

4.2 Methodology

4.2.1 Methodology adopted to study mangrove cover dynamics

The various steps employed for studying mangrove cover dynamics in the Gulf of Kachchh are depicted in Fig 4.1.

The stepwise details of method employed are presented below:

(a) Data downloading and conversion of DN to Apparent Reflectance (AR): Level 1 data products of both the images (Landsat 5 TM and Landsat 8 OLI) were downloaded from earthexplorer website (https://earthexplorer.usgs.gov/). The DN (Digital Number) values of optical datasets were converted to apparent reflectance values. Blue, Green, Red, NIR and SWIR bands (SWIR 1and 2) of both TM and OLI data were used in this study. The sensors of the EO satellites record the intensity of captured electromagnetic radiation (EMR) in the form of uncalibrated arbitrary units called digital numbers (DN) (Nayak et al., 2003). Therefore, it is important that to understand the behavior of earth surface features, the DN of image should be converted to more meaningful apparent reflectance values. Apparent reflectance is the ratio of upwelling radiance recorded at the sensor to the solar irradiance, and takes into calculation the solar elevation at the time of acquiring the image. It is the reflectance received at the top of the atmosphere and does not include the corrections for atmospheric attenuation of radiation. Though atmospheric corrections are necessary for studying the actual reflectance of target objects, it is not always possible to acquire scene-specific atmospheric parameters and field-derived reflectance values, to do the atmospheric corrections of optical images.

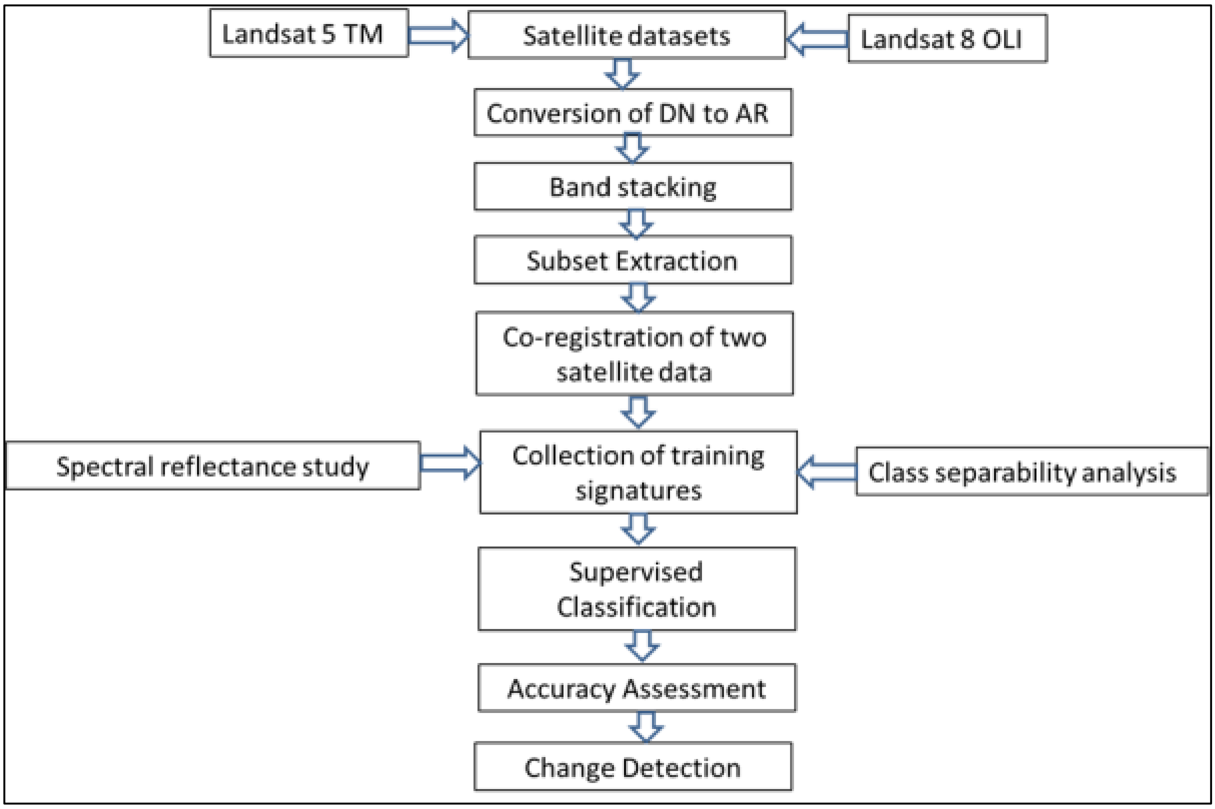

Figure 4.1: Flowchart depicting methodology adopted to study mangrove cover dynamics

In such cases, researchers have used apparent reflectance values to compare the behaviour of target objects in different optical regions of electromagnetic spectrum (Rahman et al., 2013; Nayak et al., 2003).

Conversion of DN image to AR image is a two-step process: first step involves conversion of DN to spectral radiance and the second step deals with conversion of spectral radiance to apparent reflectance.

Conversion of DN image to spectral radiance image: Radiance is the radiant flux emitted, reflected, transmitted or received by a surface, per unit solid angle whereas spectral radiance is the radiance of a surface per unit frequency or wavelength (https://en.wikipedia.org/wiki/Radiance). The SI unit of radiance is watt per m^2 per steradian

($W/m^2/sr$). The spectral radiance depends on several parameters such as time of the day, season, latitude etc. (Nayak et al., 2003). The conversion of DN to spectral radiance corrects the image for its sensor parameters. The equation used to retrieve radiance image from DN values is (Nayak et al., 2003):

$$L_{rad} = [(DN/\text{max grey}) * (L_{max} – L_{min})] + L_{min}$$

Where L_{rad} is the spectral radiance obtained, DN is the digital number, max grey is the maximum radiometric value recorded by the sensor (for example, it is 255 for 8-bit data), L_{max} is the maximum radiance value for a particular band and L_{min} is the minimum radiance value for a particular band.

Conversion of spectral radiance image to apparent reflectance image: The spectral radiance obtained in the above step only accounts for the radiance measured at the sensor. Therefore, it is converted to apparent reflectance (AR) image. AR is the ratio of radiance to irradiance. It provides a standardized measure that could be compared among different images. AR takes into account the solar elevation at the time of image acquisition. AR is also called exo-atmospheric reflectance as it is top of the atmosphere reflectance and thus does not allow the effects of atmospheric attenuation. The equation to calculate AR is (Nayak et al., 2003):

$$\rho = [\pi * L_{rad} * d^2] / E_{SUN} * \text{COS (SZ)}$$

where ρ is the unit-less AR, L_{rad} is the spectral radiance, d^2 is the earth-sun distance in the astronomical units [(1 – (0.01674 cos (0.9856 (JD-4)))] where JD is Julian Day, E_{SUN} is the mean solar exo-atmospheric spectral irradiance and SZ is the solar zenith angle at the time the scene was captured.

Apparent reflectance values were generated for Blue, Green, Red, NIR and Shortwave Infrared (SWIR) (1 & 2) bands of both the datasets. The parameters required for conversion of DN to radiance is derived from the metadata file provided with the satellite data. Semi-automatic Classification Plugin (SCP) of open source software QGIS (Quantum GIS) was employed for conversion of DN values of Blue, Green, Red, NIR and SWIR (1 & 2) bands of both the datasets to apparent reflectance (AR) values. Patches of dense mangroves regions were found to be pseudo-invariant spectral targets. “Reflectance database” of mangrove signatures from the same region generated by earlier studies (SAC, 2003; Shah et al., 2005; SAC, 2007) were utilised for the validation purpose. Therefore, these "reflectance signatures" are valid regardless the sensors or year of imagery acquisition. It was difficult to collect field derived spectra of pseudo-invariant spectral targets in the inter-tidal dynamic environment of Gulf of Kachchh.

(b) Layerstacking of individual bands: The AR bands were then stacked together separately for Landsat 8 OLI and Landsat 5 TM, i.e., blue, green, red, NIR and SWIR (1 & 2) bands of Landsat 8 OLI were stacked together and those bands of Landsat 5 TM were stacked together. Such a band composite helps to visualise the terrain features in those regions of electromagnetic spectrum which are invisible to human eyes.

(c) Subset extraction: The subset of the study area was then extracted from the two datasets separately. Thus we now have images of the study area corresponding to 2011 and 2017 years, comprising reflectance values in blue, green, red, NIR and SWIR (1 & 2) regions of the electromagnetic spectrum.

(d) Co-registration of the two datasets: These subsets of 2011 and 2017 were then co-registered with each other using 1^{st} order polynomial and at sub-pixel accuracy. Though the two Landsat images were well-aligned with each other, co-registration was done to generate more confidence in change detection analysis. Non-intertidal regions were then masked out from the subsets.

(e) Collection of training signatures: Next step was collection of signatures to classify the two images and assess the accuracy of the classified images. Ground visits were carried out with the GPS to collect the training signatures of intertidal categories. Training samples were collected according to a random approach. Specific strategy of sampling could not be followed as many parts of the area are inaccessible and are under protection by the State Environment Department, Port Trusts, Border Security Force, Coast Guards, Indian Navy (due to nearness to International border). Therefore, these areas were randomly and opportunistically visited as and when the permissions were granted for specific locations by the concerned authorities. In addition, we employed previous maps of this region developed by studies such as SAC (2003), SAC (2007), SAC (2012), Kumar et al. (2012) for collection of training signatures. The signatures were collected for following intertidal features: Mangrove Dense (MD), Mangrove

Sparse (MS), Mangrove Degraded (MDeg), Intertidal Mudflat (IM), Subtidal Mudflat (SM) and Salt Encrustation (SE). Mangroves were classified into three types based on the differences in their canopy closure: Mangrove Dense (> 40% canopy closure), Mangrove Sparse (10-40% canopy closure) and Mangrove Degraded (<10% canopy closure).

(f) Spectral reflectance study: The reflectance values of pixels corresponding to mangroves and other intertidal features were recorded and plotted against the visible/infrared regions of electromagnetic spectrum. The spectral reflectance profile thus generated of all the intertidal features were studied and compared with those provided in the literature. Any outliers encountered were removed from the final set of signatures. Many times the signatures of intertidal features overlap which results in spectral confusion. For example, there may be some confusion in the spectral signatures of mangrove sparse and intertidal mudflat or in the spectral signatures of mangrove sparse and mangrove degraded. Therefore, we employed Transformed Divergence (TD) method to assess the statistical separability among the various sets of signatures extracted for mentioned intertidal features.

(g) Class separability analysis: The class separability analysis was conducted using TD method. In the TD method, a covariance weighted distance between the mean values of signatures of two categories is compared to assess the separability between them. The class separability values may range from 0 to 2000. A separability value above 1700 indicates fairly good separability between the two categories. On the other hand, any value below 1500 is an indication of poor separability between the classes.

(h) Supervised classification: Once satisfied with the statistical separability of training signatures, the two images pertaining to 2011 and 2017 were classified using maximum likelihood classification (MLC) algorithm. Maximum Likelihood Classification has proven to be a robust classification for mangrove studies (Kuenzer et al., 2011). Further, it has been observed to provide higher accuracy as compared to Object based classification (Wang et al., 2004). Therefore, Maximum Likelihood Classification has been used in the present study. MLC is one of the most popular classification algorithm employed in supervised image classification studies. This algorithm uses a discriminant function to assign a pixel to the class with the highest likelihood. Statistical inputs for MLC like mean vector and covariance matrix are generated for the training signatures of each class. After the classification, accuracy assessment was performed for the two classified images.

(i) Accuracy assessment: Classification error occurs when a pixel belonging to one category is incorrectly classed to another category. Classification error could be either error of omission or error of commission. When a pixel is left out of its ‘correct’ class, then this type of error is called error of omission. On the other hand, when a pixel is incorrectly labeled to another category, then this type of error is called error of commission. An error of omission in one category will be counted as an error of commission in another category. Accuracy, in the context of classification assessment, is defined as the measure of agreement between a standard which is assumed to be correct and a classified image of unknown quality (Campbell, 2007). Accuracy assessment is performed by comparing the map created by remote sensing analysis to a reference map derived from a different information source.Quite often ground visit is used to collect the reference/standard information regarding the land use/land cover features using GPS and pixels in the image corresponding to features identified at the ground are matched for accuracy assessment. Accuracy of image classification is most often reported as percentages. The *overall accuracy* of the classified image represents percentage of the pixels correctly classified compared to the actual land cover conditions obtained from their corresponding ground truth data. The *consumer’s accuracy* (CA) or *user’s accuracy* (UA) is computed using the number of correctly classified pixels to the total number of pixels assigned to a particular category (https://www.e-education.psu.edu/geog883/node/524). It takes errors of commission into account by telling the consumer that, for all areas identified as category X, a certain percentage are actually correct. The *producer’s accuracy* (PA) informs the image analyst of the number of pixels correctly classified in a particular category as a percentage of the total number of pixels actually belonging to that category in the image (https://www.e-education.psu.edu/geog883/node/524). Producer’s accuracy measures errors of omission.This accuracy assessment is mostly presented in the form of a matrix called error matrix or confusion matrix. An error matrix compares the pixels classified in the image against the ground reference data.

Another technique of accuracy assessment is KAPPA (Cohen, 1960). The result of KAPPA analysis is KHAT statistics (which is an estimate of KAPPA) (Congalton, 1991). KHAT is computed using following equation (Congalton, 1991):

$$\hat{K} = \frac{N \sum_{i=1}^{r} x_{ii} - \sum_{i=1}^{r} (x_{i+} * x_{+i})}{N^2 - \sum_{i=1}^{r} (x_{i+} * x_{+i})}$$

where r is the number of rows in the matrix, x_{ii} is the number of observations in row i and column i, x_{i+} and x_{+i} are the marginal totals of row i and column i, respectively, and N is the total number of observations.

In the present study, both accuracy assessment as well as class separability analysis has been used to evaluate the results.

(j) Change detection: Post classification change detection was employed to study the changes in mangrove cover between 2011 and 2017. In addition, the changes in mangrove area were compared with earlier studies by SAC (2012), Kumar et al. (2012) and Ajai et al. (2013). The percentage change in the area of the three mangrove categories was computed and a change detection matrix was prepared documenting changes in mangrove dense, mangrove sparse and mangrove degraded during 2011 and 2017.

4.2.2 Methodology adopted for mangrove community zonation

The methodology adopted in the present study for mangrove community zonation includes following steps: 1) Processing of optical data, 2) Processing of microwave data, 3) Co-registration of optical and microwave data, 4) Fusion of optical and microwave data, 4) Classification of optical, microwave and fused images for mangrove community zonation, and 5) Qualitative and quantitative assessment of classified images. Figure 4.2 depicts the flow chart of the methodology adopted for mangrove community zonation. The various steps of this methodology are described below:

(a) Processing of optical data: This step involves conversion of DN (Digital Number) of satellite image into apparent reflectance (AR) image. The details about this step have already been described above in the section describing the methodology of studying mangrove cover dynamics. The three AR bands of LISS-IV data (Green, Red and NIR) were then stacked together, and the subset of the study area (Jindra-Chhad Island Complex) was extracted from the whole image.

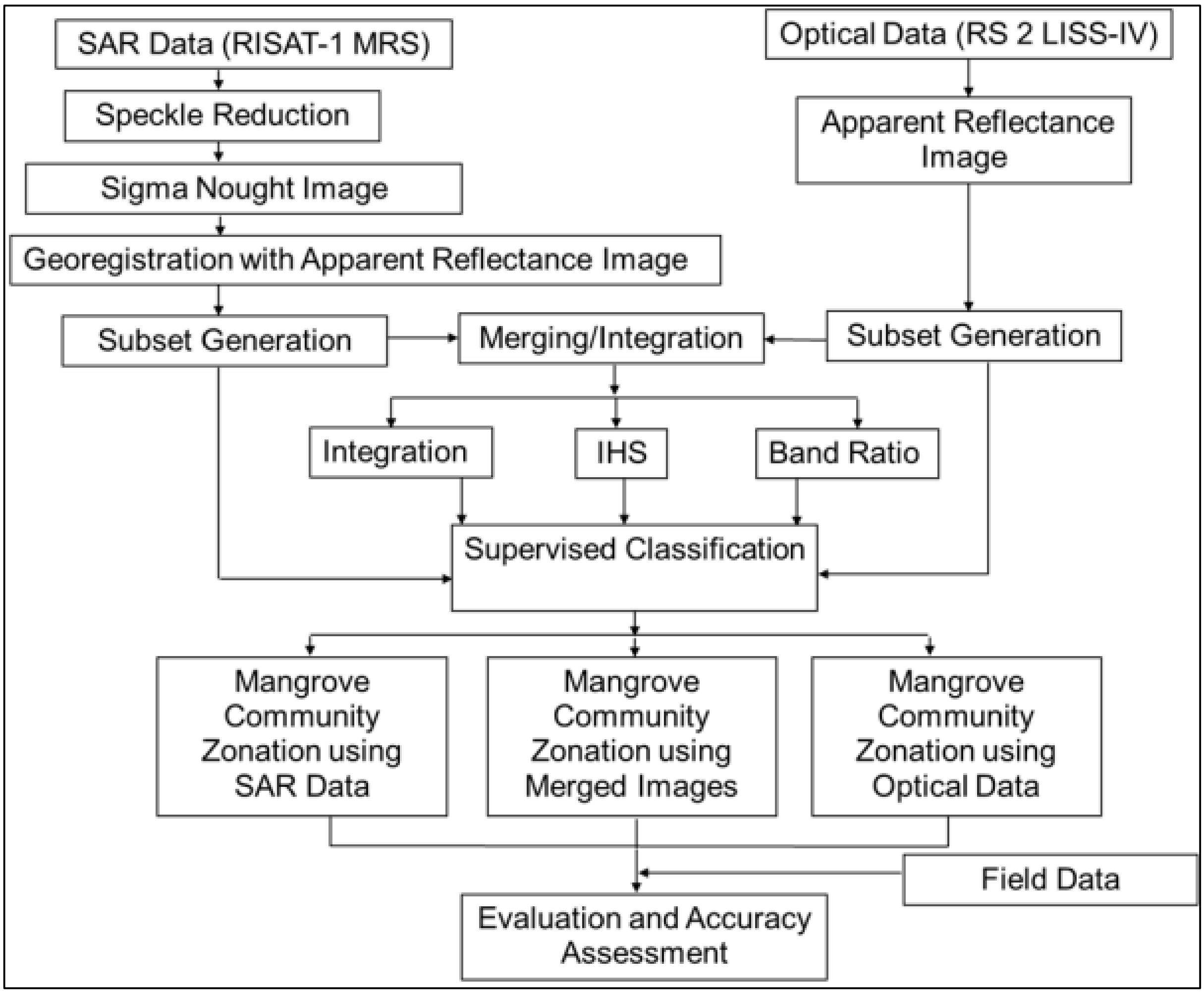

Figure 4.2: Methodology for mangrove community zonation using optical and SAR data

(b) Processing of microwave data: Microwave data processing involves speckle reduction and retrieval of sigma nought (σ^0) images:

Speckle Reduction: The backscattering received from different features being imaged in a microwave remote sensing system, is modified by a randomly distributed pattern of constructive and destructive interference, known as Speckle. For better analysis, the speckle content in the microwave data should be reduced before doing any further processing. Variation in backscatter from inhomogeneous cell generates speckle noise in SAR data. Due to speckle noise, the appearance of the SAR image is grainy (Raney, 1998). The spatial statistics of the underlying scene backscatter is also changed by the speckle noise which again, makes the classification of imageries difficult (Durand et al., 1987). Also, the presence of speckle makes the visual interpretation of SAR images relatively difficult. Therefore, it is important to filter the SAR data before doing any further analysis. Speckle reduction can be accomplished by applying different types of filters on the imagery. These filters are called the "spatial" filters and can be categorized as Adaptive or Non-adaptive (Mansourpour et al, 2006).

Non-adaptive filters do not consider the local properties of terrain backscatter or nature of sensor; they rather take the parameters of the whole image signal. These filters are not useful if the scene is non-stationary. One of the examples of such type of filters is Fast Fourier Transform (FFT) (Mansourpour et al, 2006). Adaptive filters consider changes in local properties of terrain backscatter and the nature of the sensor. Here, change in the mean backscatter due to change in the type of target is considered. Such filters preserve the edges while reducing the speckle and work on the principle of varying the contrast stretch of the DN (Digital Number) values in the surrounding moving kernel. Some of the adaptive filters are Mean, Median, Local Region, Lee, Lee-Sigma, Frost and Gamma-Map. In this study, Gamma-Map filter was used with 5 x 5 window size to reduce the speckle content in RISAT-1 SAR data.

Calculation of sigma nought (σ^0) image: Just as in optical data the uncalibrated arbitrary digital numbers need to be converted to reflectance values for further meaningful digital quantitative analysis; in the case of microwave data the DN needs to be converted into sigma nought (σ_0) values. Sigma nought is the normalized measure of the radar return from a distributed target, in the direction towards the radar (https://earth.esa.int/handbooks/asar/CNTR5-2.html). For example, for RISAT-1 data, sigma nought values were calculated using the following equation (Padia and Mehra, 2013):

$$\sigma^o=20\log_{10}(DN)-K_{db}+10\log_{10}(\sin(i_p)/\sin(i_{center}))$$

where,

DN = Digital Number per pixel

K_{db} = callibration constant in dB

i_p = incidence angle for pixel position p

i_c = incidence angle at the scene center

Co-registration of microwave data with optical data: The speckle-filtered sigma nought image was co-registered with AR image.

Subset extraction: Then the subset of the study area, Jindra-Chhad Island Complex, was extracted from the co-registered sigma nought image.

(c) Fusion of optical and microwave data: Co-registered AR and sigma nought images, were combined together to explore the synergistic potential of the SAR data with optical data, for discriminating different mangrove communities in the study region. Three different approaches were used to combine the SAR and optical data:

Integration approach: In this case, SAR data was integrated as an additional band to the three bands of LISS-IV data. Thus, the three, 3-band combinations generated employing SAR data were, *viz.*, SAR+Red+Green, SAR+NIR+Red, and SAR+NIR+Green.

IHS approach: Intensity-Hue-Saturation (IHS) is one of the most widely used technique to merge two different remote sensing images. The IHS transformation is effective in separating the spatial (I) and spectral components (HS) from an RGB (Red-Blue-Green) image (Pohl and Genderen, 1998). After separating an RGB image into IHS components, one of the components, *i.e.*, either I or H or S, is substituted with another image (which is to be merged) and the resultant image is then again transformed into RGB colour system. Mostly, the spatial component (Intensity, I) is replaced by another image having better spatial resolution. In the present study, all the three components, *i.e.*, I, H and S, retrieved from LISS-IV data were systematically replaced by RISAT-1 data, and the resulting images were then transformed into RGB colour space. Thus, the three possible combinations generated were: I+H+SAR, H+S+SAR and I+SAR+S.

Band ratio combination approach: Ratios of different bands of optical data have been employed to study the vegetative as well as sedimentary environments over the years. In particular, for mangroves this method has been found to be more useful for separating different communities than other approaches employing optical data (Shah et al., 2005). In our study, two optical band ratios, *viz.*, NDVI (Normalised Difference Vegetation Index) and OB (Optical Brightness) were generated from LISS-IV data, and these ratios were then integrated with RISAT-1 data. NDVI was computed by taking the ratio of (NIR-Red) to (NIR+Red) bands whereas for obtaining OB, averaging of red and green bands was done. Thus, a three band integrated image was generated comprising NDVI, OB and SAR, as individual bands.

(d) Classification of optical, microwave and fused images: The optical, microwave and fused images were classified digitally for community zonation of mangroves. For selection of training areas, the reflectance values of mangroves and mangrove species in optical data; and backscatter values of mangrove species in microwave data were studied. Field visit was also undertaken to identify the mangrove species on-site. Object based classification is best suited to be applied on very high resolution satellite data and for heterogeneous region. Maximum Likelihood Classification has proven to be a robust classification for mangrove studies (Kuenzer et al., 2011). Further, it has been observed to provide higher accuracy as compared to Object based classification (Wang et al., 2004). Therefore, Maximum Likelihood Classification has been used in the present study. The classification system developed by Nayak et al. (2003) was referred to for identification of mangrove environment categories (Table 4.2).

Table 4.2: Classification system for zoning mangrove communities (Source: Nayak et al., 2003)

Level I	**Level II**	**Level III**	**Level IV**
Onshore areas	Beach	Muddy Sandy	Fringe Tidal Mangroves No Mangroves
	Estuary	Sandy clay intertidal mudflat Silty clay intertidal mudflat	i) *Rhizophora, Sonneratia, Avicennia, Bruguiera*(pure/mixed communities) ii) Saline blanks i) *Avicennia, Rhizophora, Aegiceras, Sonneratia*(pure/mixed communities) ii) Salt marsh vegetation iii) Saline blanks

		Hightidal mudflat	i) Salt marsh vegetation ii) Saline blanks
		Freshwater zone	i) *Bruguiera, Excoecaria, Heritiera,* (pure/mixed communities) ii) Freshwater species
		Elevated estuarine area	Grass
	Deltaic complexes	Seaward margin of intertidal mudflats	*Avicennia marina*, *A. alba*, *A. officinalis* (pure)
		Intertidal mudflats	i) Pure communities of *Rhizophora*, *Sonneratia*, *Avicennia*, *Bruguiera* etc. ii) Mixed mangrove communities iii) Salt marsh vegetation iv) Grass/*Acanthus* v) Saline blanks
		Hightidal mudflats	i) Salt marsh vegetation ii) Saline blanks
		Muddy silt near river mouth	*Sonneratia, Bruguiera, Excoecaria, Heritiera* (pure/mixed communities)
		Recent alluvial soils	Grass
		Transitional areas	i) Saline blanks ii) Grassy banks iii) Trees/shrubs
	Gulf region	Sandy clay intertidal mudflat	Pure/mixed communities of *Rhizophora, Avicennia, Ceriops*

		Hightidal mudflats	i) Salt marsh vegetation ii) Grass/*Acanthus* iii) Saline blanks

(e) Qualitative and quantitative assessment of classified images

Qualitative Evaluation: This involves visual inspection of the images with a view to identify different categories of mangrove environment.Qualitative evaluation was used for fused images to see whether different mangrove habitat classes are visually distinct or not, and to see in particular which image fusion approach/algorithm provides most demarcation/differentiation among mangrove communities.

Quantitative Evaluation: In this study, two distinct methods were used for quantitative evaluation of classified images: Class separability analysis and Accuracy assessment.

Class Separability Analysis: A parametric signature comprises of a set of statistical parameters (such as mean and co-variance matrix) of the pixels. This information is then used to train the classifier for grouping the image pixels into desired set of clusters/classes. The information set comprising the parametric signature include:

- the number of bands in the input image.
- the minimum and maximum data value for each band, for each sample.
- the mean data value for each band, for each sample.
- the covariance matrix for each sample.
- the number of pixels in the sample.

These statistics of parametric signatures could be used to evaluate the separability among the various classification categories. Class separability analysis includes measures of separability which implies the ease with which patterns can be correctly associated with their classes using statistical pattern classification (Richard and Jia, 2006). Various separability measures have been evolved over the years to test the best combination of bands/images. These include divergence, transformed divergence, Jeffries-Matusita Distance, Bhattacharya Distance, M-statistic, Euclidean Distance etc. Here, Transformed Divergence (TD) was employed to assess the class separability obtained using different sets of images for mangrove communities as well as for intertidal categories.

Transformed Divergenceis a modified version of divergence and is defined as (https://wiki.hexagongeospatial.com/index.php?title=Evaluating_Signatures):

$$TD_{ij}= 2000\ (1 - e^{(-D_{ij}/8)})$$

Where TD_{ij} is the transformed divergence between spectral classes i and j, and D_{ij} is the divergence between spectral classes i and j. The advantages associated with the TD algorithm relative to similar other algorithms are:

- It takes into account the mean, variance and covariance of the classes while calculating the inter-class spectral distance whereas other methods such as Euclidean Distance do not.
- It represents the inter-class spectral distance on a transformed scale to enable comparisons from different such exercises.
- This method can work on multiple bands simultaneously, whereas other measures such as M-Statistics can work with only one band at a time.

The TD analysis provides separability values ranging from 0 to 2000. A separability value above 1700 indicates fairly good separability between the categories. On the other hand, any value below 1500 is an indication of poor separability between the classes. TD also shows a saturating behaviour like JM distance however, it is computationally more efficient than the latter (Jensen, 1996).

Accuracy Assessment: The details about accuracy assessment procedure have already been provided above in the section describing the methodology of studying mangrove cover dynamics. Overall accuracy, user's accuracy, producer's accuracy and Kappa coefficient were computed for each of the classified images (optical, SAR and merged images) to assess the accuracy yielded by the classification method for mangrove community zonation using different sets of images.

Chapter 5

Mangrove cover dynamics in Gulf of Kachchh

This chapter provides details of mangrove cover dynamics in five mangrove occupying regions of the Gulf of Kachchh viz., north-west parts around Kori creek, around Mundra and Kandla along northern coast, around Satsaida bet in north-eastern parts and southern coast of Gulf of Kachchh including Marine National Park and sanctuary. Observations are provided based on understanding of spectral properties, evaluating class separability, salient results of supervised classification, accuracy assessment and finally change detection. The mangroves in the GoK show spatial variability in extent, composition and condition based on dominant coastal processes, geomorphological setting and amount of protection from anthropogenic influences. The Gulf of Kachchh forms approx. 70 % of the total mangrove cover of Gujarat (FSI, 2015).

5.1 Mangrove cover dynamics around Kori Creek in north-western parts of the Gulf of Kachchh

One of the major mangrove cover region, which forms north-west parts of Gulf of Kachchh as well part of the Indus Delta falling in Indian Territory is around Kori Creek. This region comprises of number of islands dissected by an intricate system of creeks such as Pir Sunai, Sugar, Sir, Kharo, Pirsani, Kalichod, Sindhodic, Ramaria, Kori, Chukh, Kharia, Godia and Sethwara Bet creek. The region is west, north and south of nearby habitations such as Koteshwar, Narayan Sarovar, Jakhau in Kachchh district. The spatial extent of mangrove covered areas in this region are shown in (Figure 5.1).

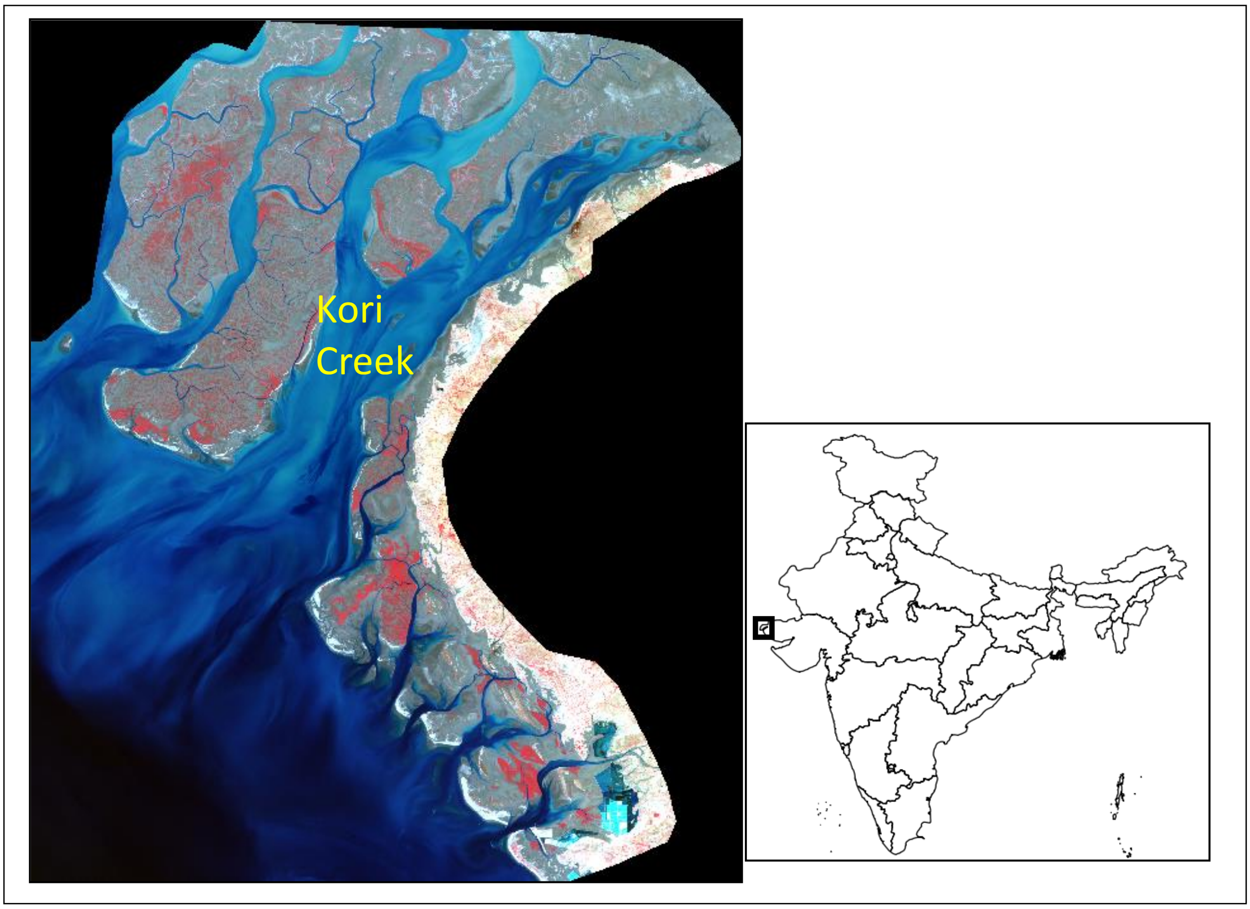

Figure 5.1: Spatial extent of mangrove covered area are seen as red tone on Landsat 8 OLI FCC of 20 February, 2017 around Kori creek in the north-western parts of the Gulf of Kachchh (the box on India's map shows the location of the study area)

5.1.1 Spectral characteristics of mangroves and associated features in the inter-tidal zone

First of all, an attempt was made to understand spectral characteristics of mangroves and associated features in the inter-tidal zone based on field observations and existing knowledge. Using the ground photographs (Figure 5.2, 5.3, 5.4) and the maps published by previous studies in this region (SAC 2012, Kumar et al., 2012), the intertidal categories were carefully identified in the satellite images and their reflectance was plotted in the visible, NIR and SWIR regions. Spectral reflectance curves of seven intertidal classes present in this study area are shown in Figure 5.5 and 5.6.

Figure 5.2: Dense *Avicennia* near Jakhau, NW parts of Gulf of Kachchh

Figure 5.3: Degraded mangroves near Jakhau, NW coast of Gulf of Kachchh

Figure 5.4: Saltpans near Jakhau, NW parts of Gulf of Kachchh

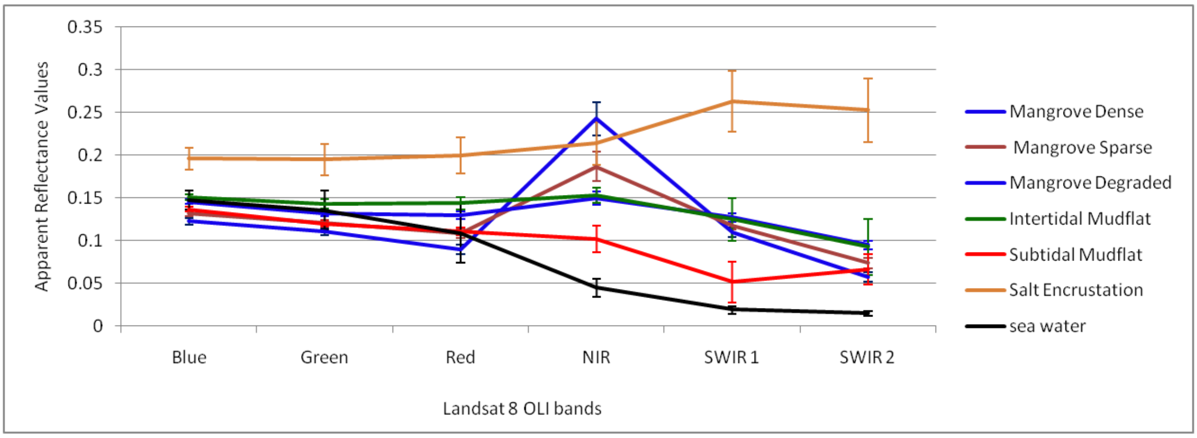

Figure 5.5: Mean spectral reflectance (along with standard deviation bar) of seven intertidal classes present in Kori creek and environs (north-western parts of the Gulf of Kachchh) derived from Landsat 8 OLI data of February 20, 2017

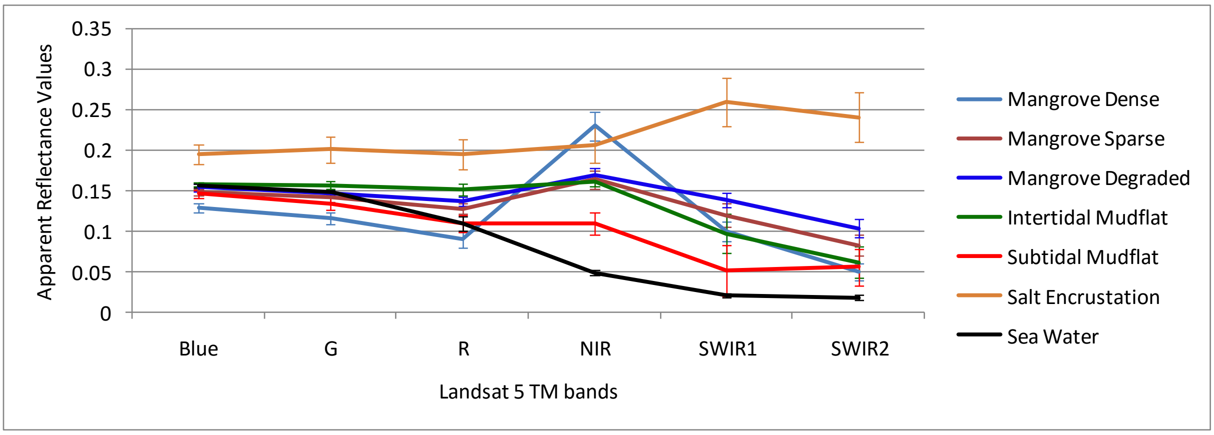

Figure 5.6: Mean spectral reflectance (along with standard deviation bar) of seven intertidal classes present in Kori creek and environs (north-western parts of the Gulf of Kachchh) derived from Landsat 5 TM data of February 04, 2011

It is observed that the three mangrove categories, *viz*., Mangrove Dense (MD), Mangrove Sparse (MS) and Mangrove Degraded (MDeg) are relatively more separable in NIR and SWIR region of electromagnetic spectrum. Dense mangroves show highest reflectance in the NIR region, followed by MS and then MDeg. These signatures were validated using the work published earlier by Nayak and Bahuguna (2001), SAC (2003), Shah et al. (2005) and SAC (2012) and ground truth data collection carried out in present work. Spectral response of vegetation communities, in the visible region of electromagnetic spectrum is affected by leaf pigmentation. In the NIR region, the internal structure of leaves and the stacking of leaves determine the spectral response whereas the leaf moisture content affects the behaviour in SWIR region (SAC 2003). Sparse and degraded mangroves show higher reflectance values relative to dense mangroves in SWIR regions. In addition, the overall reflectance of three mangrove classes may also be influenced by the humidity gradient in soil which in turn varies as per the tide levels (Blasco and Aizpuru 2002). As the space available among individual plants is more in MDeg and MS, the reflectance from wet ground also influences the overall reflectance of these mangrove classes. Intertidal mudflat shows higher reflectance than subtidal mudflat in all the studied electromagnetic regions. Other classes such as salt encrustation and sea water also show quite contrasting and distinct reflectance patterns.

5.1.2 Class separability analysis

Another test to determine separability of selected training data of different intertidal categories was conducted through Transformed Divergence (TD) method. TD method computes spectral distance between signatures of categories by taking into account their statistical parameters such as mean, variance and covariance (Kumar et al. 2017). As mentioned previously, the TD analysis provides separability values ranging from 0 to 2000. A separability value above 1700 indicates fairly good separability between the categories. On the other hand, any value below 1500 is an indication of poor separability between the classes. The spectral separability of training signatures of seven intertidal categories, *viz.*, Mangrove Dense (MD), Mangrove Sparse (MS), Mangrove Degraded (MDeg), Intertidal Mudflat (IM), Subtidal Mudflat (SM), Salt Encrustation (SE) and Sea Water (SW) is shown in Table 5.1 and 5.2.

Table 5.1: Class separability analysis for classified image of 2011 covering Kori creek and environs

Classes	MD	MS	MDeg	IM	SM	SE	SW
Mangroves Dense (MD)	0	1966.74	2000	2000	2000	2000	2000
Mangroves Sparse (MS)	1966.74	0	1914.36	1999.55	1999.99	2000	2000
Mangroves Degraded (MDeg)	2000	1914.36	0	1998.93	1998.32	2000	2000
Intertidal Mudflats (IM)	2000	1999.55	1998.93	0	1982.06	2000	2000
Subtidal Mudflats (SM)	2000	1999.99	1998.32	1982.06	0	1999.99	2000
Salt Encrustation (SE)	2000	2000	2000	2000	1999.99	0	2000
Sea Water (SW)	2000	2000	2000	2000	2000	2000	2000

Table 5.2: Class separability analysis for for classified image of 2017 covering Kori creek and environs

Classes	MD	MS	MDeg	IM	SM	SE	SW
Mangroves Dense (MD)	0	1896.97	1999.42	2000	2000	2000	2000
Mangroves Sparse (MS)	1896.97	0	1863.74	1999.99	2000	2000	2000
Mangroves Degraded (MDeg)	1999.42	1863.74	0	1999.94	2000	2000	2000
Intertidal Mudflats (IM)	2000	1999.99	1999.94	0	1978.17	2000	2000
Subtidal Mudflats (SM)	2000	2000	2000	1978.17	0	2000	2000
Salt Encrustation (SE)	2000	2000	2000	2000	2000	2000	2000
Sea Water (SW)	2000	2000	2000	2000	2000	2000	2000

The separability analysis gives fair amount of confidence regarding statistical separability of training data of intertidal categories. The separability values are relatively low among mangrove categories (MD, MS and MDeg) which is understandable as all these belong to similar vegetation communities whereas rest of the intertidal categories (IM, SM, SE and SW) are quite distinct among themselves as well as from mangroves.

5.1.3 Classification

In this study, maximum likelihood classification (MLC) algorithm has been used to classify the 2011 and 2017 subsets of Landsat images into seven intertidal classes *viz.*, Mangrove Dense, Mangrove Sparse, Mangrove Degraded, Intertidal Mudflat, Subtidal Mudflat, Salt Encrustation and Sea Water. Figure 5.7 shows the classified images of 2011 and 2017 respectively.

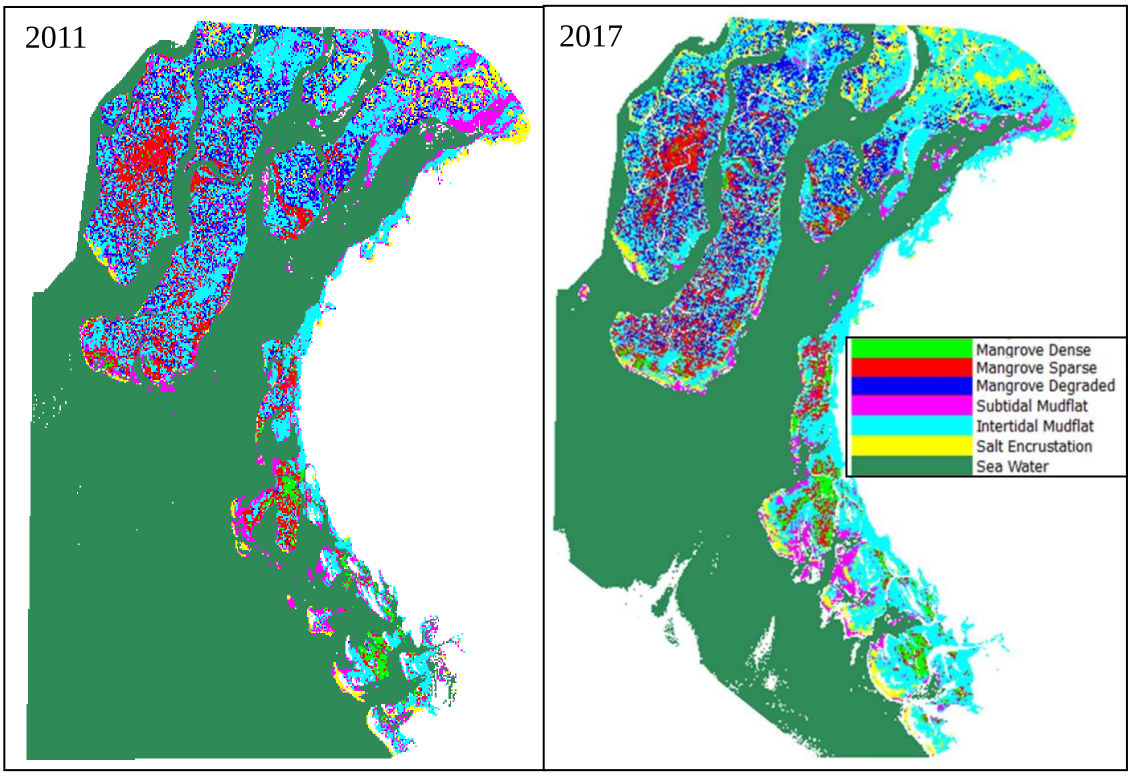

Figure 5.7: Mangrove and other inter-tidal classes as per supervised classification of Landsat data of 2011 and 2017 covering Kori creek and environs

5.1.4 Accuracy assessment

The data for accuracy assessment were collected from three sources: field visit to intertidal areas adjacent to Jakhau and Narayan Sarovar, published maps (SAC 2012; Kumar et al. 2012) and high resolution Google Earth images. The accuracy of classified images were evaluated for six classes viz., Mangrove Dense (MD), Mangrove Sparse (MS), Mangrove Degraded (MDeg.), Intertidal Mudflats (IM), Subtidal Mudflats (SM) and Salt Encrustation

(SE). Sea water (SW) was omitted from this exercise as it would have yielded much higher accuracy relative to other land cover classes (Rahman et al. 2013). A minimum of 50 samples for each class is considered sufficient to provide a good classification accuracy estimate (Congalton 2001, Rahman et al. 2013). Therefore, 50 samples (pixels) for each of the six classes (MD, MS, MDeg, IM, SM, SE) were selected randomly throughout the image. Thus we have a total of 300 pixels for assessing the accuracy of classified images. The accuracy assessment approach followed here is similar to that followed by Rahman et al. (2013). The accuracy assessment of the classified images for the six classes is presented in the form of error matrix in Table 5.3 and Table 5.4.

Table 5.3: Error matrix of 2011 classified image of Kori creek and environs

Classes	**MD**	**MS**	**MDeg**	**IM**	**SM**	**SE**	**Classified Total**	**User's Accuracy (%)**
Mangroves Dense (MD)	44 (88%)	1 (2%)	0	0	0	0	45	97.78
Mangroves Sparse (MS)	6 (12%)	45 (90%)	3 (6%)	0	0	0	54	83.33
Mangroves Degraded (MDeg)	0	4 (8%)	41 (82%)	0	0	0	45	91.11
Intertidal Mudflats (IM)	0	0	4 (8%)	50 (100 %)	0	0	54	92.59
Subtidal Mudflats (SM)	0	0	2 (4%)	0	50 (100 %)	0	52	96.15

Salt Encrustation (SE)	0	0	0	0	0	50	50	100
Reference Total	50	50	50	50	50	50	300	
Producer's Accuracy	88%	90%	82%	100%	100%	100%		

Overall accuracy = (Number of pixels correctly classified/Total number of pixels used in accuracy assessment) x 100 = (280/300) * 100 = 93.33 %, Kappa coefficient = 0.92

Table 5.4: Error matrix of 2017 classified image of Kori creek and environs

Classes	**MD**	**MS**	**MDeg**	**IM**	**SM**	**SE**	**Classified Total**	**User's Accuracy (%)**
Mangroves Dense (MD)	48 (96 %)	1 (2%)	0	0	0	0	49	97.95
Mangroves Sparse (MS)	2 (4%)	47 (94 %)	2 (4%)	0	0	0	51	92.15
Mangroves Degraded (MDeg)	0	2 (4%)	46 (92%)	0	0	0	48	95.83
Intertidal Mudflats (IM)	0	0	2 (4%)	50 (100	0	0	52	96.15

				%)				
Subtidal Mudflats (SM)	0	0	0	0	50 (100%)	0	50	100
Salt Encrustation (SE)	0	0	0	0	0	50 (100%)	50	100
Reference Total	50	50	50	50	50	50	300	
Producer's Accuracy (%)	96	94	92	100	100	100		

Overall accuracy = (Number of pixels correctly classified/Total number of pixels used in accuracy assessment) x 100 = (291/300) * 100 = 97 %, Kappa coefficient = 0.96

5.1.5 Change detection

The area of three mangrove classes viz., Dense (MD), Sparse (MS) and Degraded (MDeg) for 2011 and 2017 are shown in Table 5.5.

Table 5.5: Changes in mangrove area (in sq km) of Kori creek and environs

Time frame	Dense	Sparse	Degraded	Total
2011	28.59	193.56	211.58	433.73
2017	46.55	221.01	214.08	481.64
Change (%)	**62.81**	**14.81**	**1.18**	**11.04**

Results show that mangroves have increased in and around Kori Creek in 2017 as compared to 2011. It is also pertinent to note that mangrove density has also improved during the last six years. Few illustrations of changes in mangrove cover and density between 2011 and 2017 have also been shown in Figure 5.8, 5.9 and 5.10.

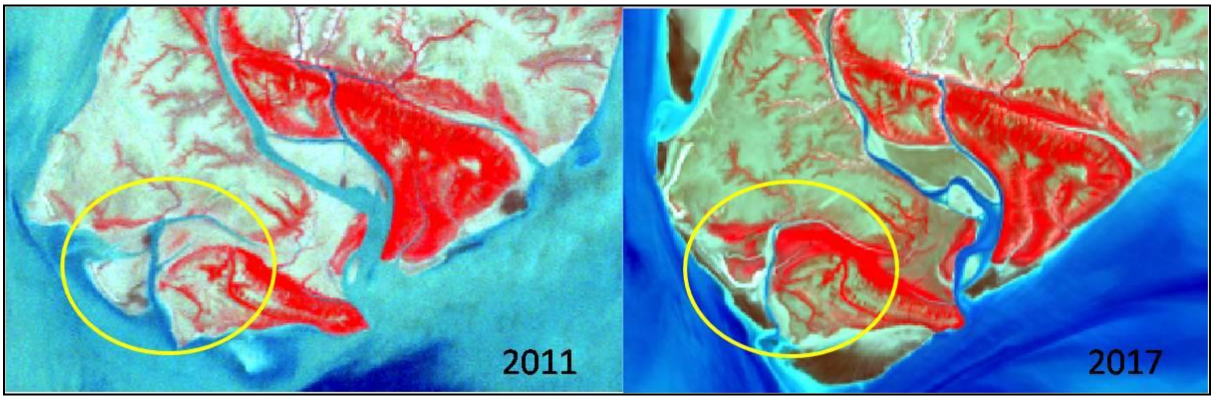

Figure 5.8: Increase in mangrove cover seen in 2017 Landsat FCC image (parts of north-western region of Gulf of Kachchh around Kori Creek)

Most of these mangrove changes have been noticed on creeks which are further away from the nearby coastal areas. Therefore, there appears to be natural growth of mangroves. Artificial plantation of mangroves was carried out during the period 2003-06 close to coastal villages of Lakki, Bhangodi and Ashirawandh (GEC, 2006). An area of 651 hectares (ha) of mangroves was planted by Gujarat Ecology Commission (GEC) at the three sites in collaboration with local communities (GEC, 2006). Changes in the patches of mangroves planted at three sites using satellite images of 2011 and 2017 period were studied.

In general, mangroves have increased around Lakki Creek in 2017 (Figure 5.9). However, if we focus on the mangrove patch that was planted during 2003-06 then during the time frame 2011-2017, no change is observed (Figure 5.11 and Figure 5.12). Mangroves planted around Kharo Creek at Bhangodi site seems to have densified more in 2017 image (Figure 5.13 and Figure 5.14). Among all the three patches planted during 2003-06, the mangrove patch around Kharia Creek at Ashirawand site near Jakhau port could not grow and seems to be in most dilapidated state.

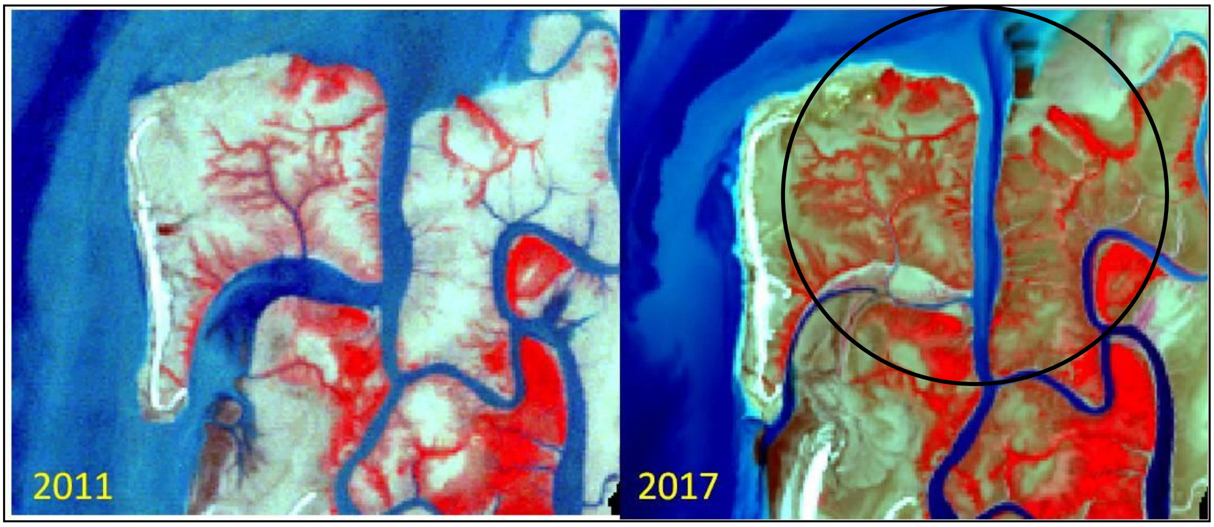

Figure 5.9: Increase observed in mangrove cover around Lakki Creek (parts of north-western region of Gulf of Kachchh around Kori Creek) in 2017 Landsat FCC image

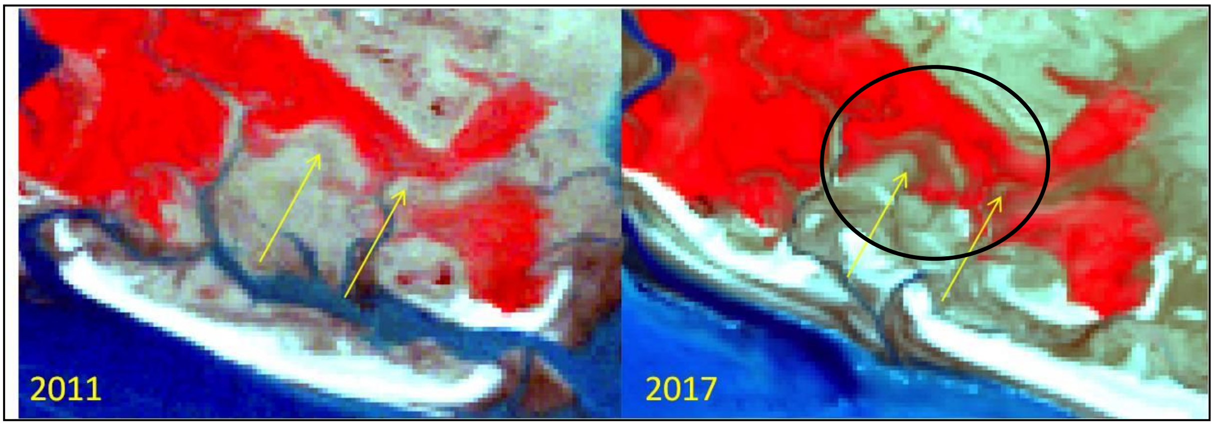

Figure 5.10: Increase observed in mangrove cover in 2017Landsat FCC image (parts of north-western region of Gulf of Kachchh around Kori Creek)

Whatever mangrove patches could be observed in 2011 and 2017 (Figure 5.15 and Figure 5.16), are the natural ones. It is further observed that probably development of salt pans in the region is one of such cause for poor state of mangroves here. In addition, people from nearby coastal villages do collect mangrove leaves and branches for their household needs which may not have provided these newly planted mangroves sufficient time to proliferate. We visited the area and found degraded patches of mangroves (Figure 5.4).

Long term changes in mangrove cover along the coastal stretch between Narayan Sarovar and Jakhau using topographical maps of 1965-66, coastal thematic maps of 1989-91 time frame available in Coastal Zone Information System (CZIS) at SAC and satellite images pertaining to 2001, 2006 and 2010 have been studied in GIS environment (Figure 5.17). It has been observed that during the time frame 1965-66 to 2006 mangrove area has reduced by 11.38 sq km. Most of the degradation took place around Narayan Sarovar, Sindhodic Creek, Chukh Creek, Kharia Creek and Godia Creek (Figures 5.18, 5.19, 5.20 and 5.21). The causes of degradation seem to be dynamic coastal processes occurring in the Indus deltaic environment over 45 years' period and increased anthropogenic influence. Changes in the coastal geomorphology, in particular changes in mudflat regions in Sugar Creek and Sindhodic Creek, and erosion near Narayan Sarovar are observed to have caused reduction of mangrove cover. Development of salt pan activities might have led to mangrove depletion around Kharia (Figure 5.21) and Godia Creek. Mangrove cover in the study region has increased during the time frame 2006-2010 by 8.26 sq km, in particular in regions such as east of Sethwaraand Ogata bet (Figure 5.22). This might be because these areas are relatively sheltered and less affected by the influence of dynamic coastal processes and anthropogenic activities (Kumar et al. 2012).

There is significant loss of mangroves around Narayan Sarovar-Koteshwar. The region around Narayan Sarovar-Koteshwar is conspicuous by the absence of mangroves from1989 onwards as observed in satellite data whereas there were three patches of mangrove covering an area of approximately 6.13 sq km in1965-66 (Figure 5.18).

Similarly, mangrove cover around all directions of Sindhodhic creek have considerably depleted, the reduction being particularly significant in north-northeast and south-southwest direction (Figure 5.19). The patch in west is dotted with more blank areas relative to that in 1965-66. The area around Sindhodic and Sugar creek is showing highly transformed morphology (Figure 5.19) over the study period (1965-66 to 2010), as a result of dynamic coastal processes such as erosion and deposition. The area close to Sethwara bet was completely devoid of mangroves in 1965-66. From 1989 onwards, however, mangrove growth has been observed. The mangrove patch near top-north direction has reduced from 1989 to 2006 before recovering to some extent in 2010.

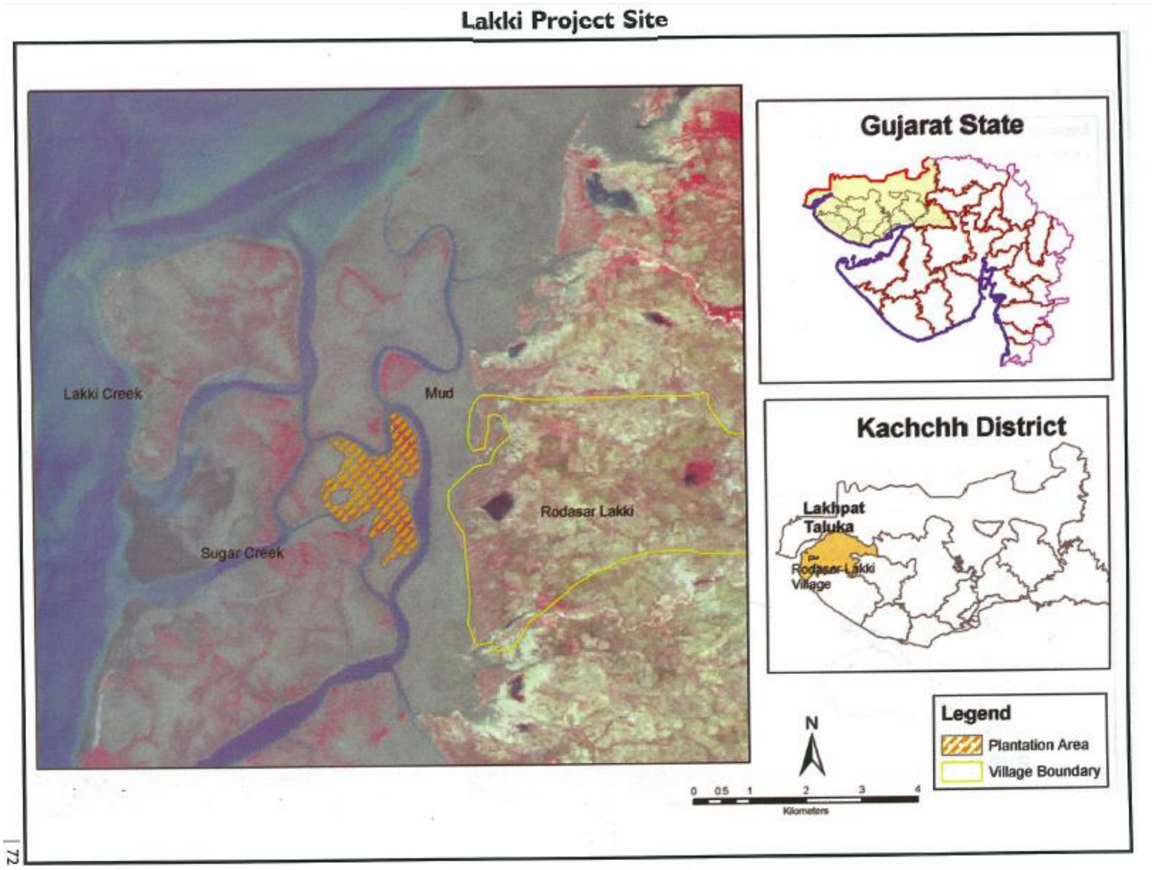

Figure 5.11: Map of mangrove plantation carried out near Lakki, creek in parts of north-western region of Gulf of Kachchh (Source: GEC, 2006)

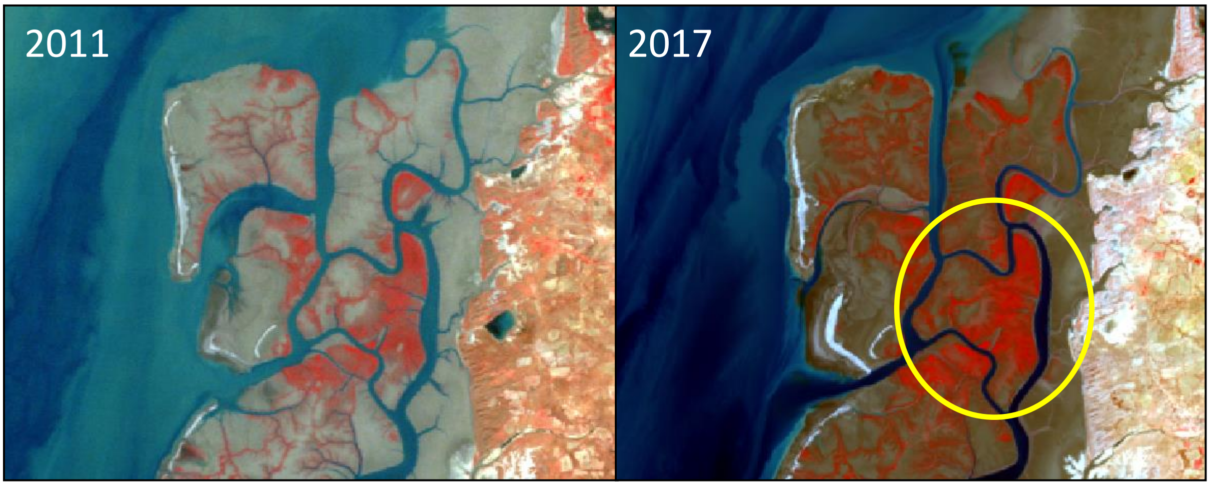

Figure 5.12: No change in mangrove cover at the plantation site near Lakki Creek in parts of north-western region of Gulf of Kachchhduring 2011-2017 as observed on Landsat FCC image

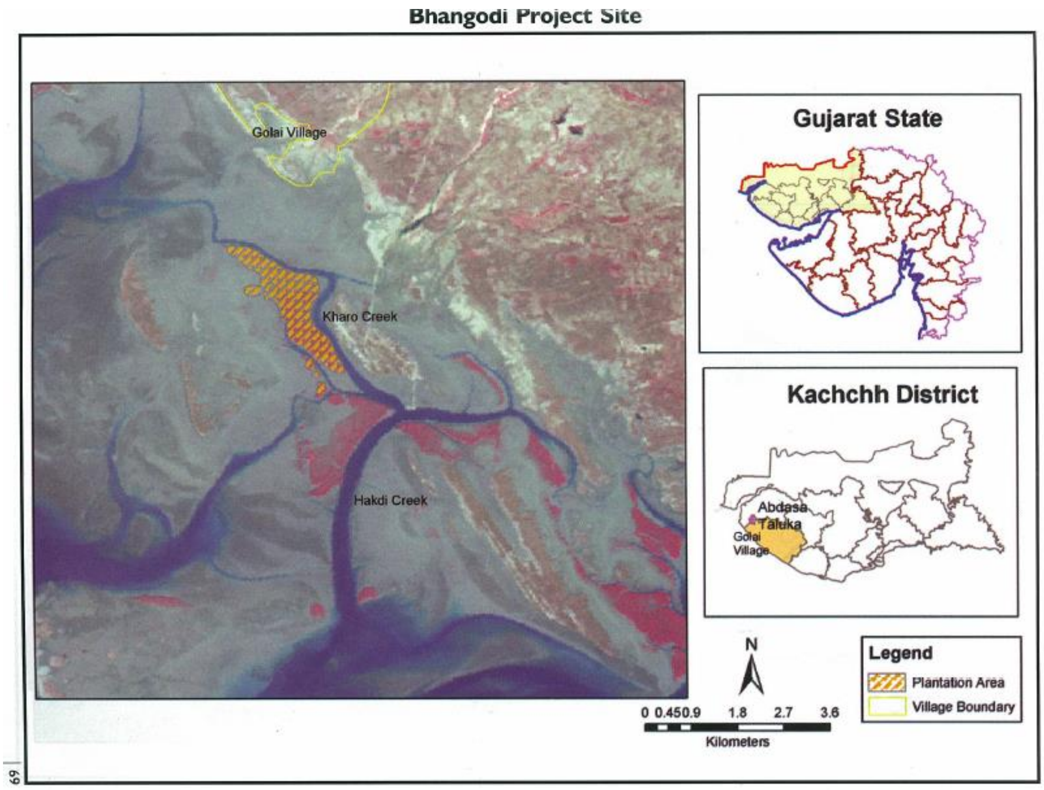

Figure 5.13: Map of mangrove planted at Bhangodi Project Site (Source: GEC, 2006)

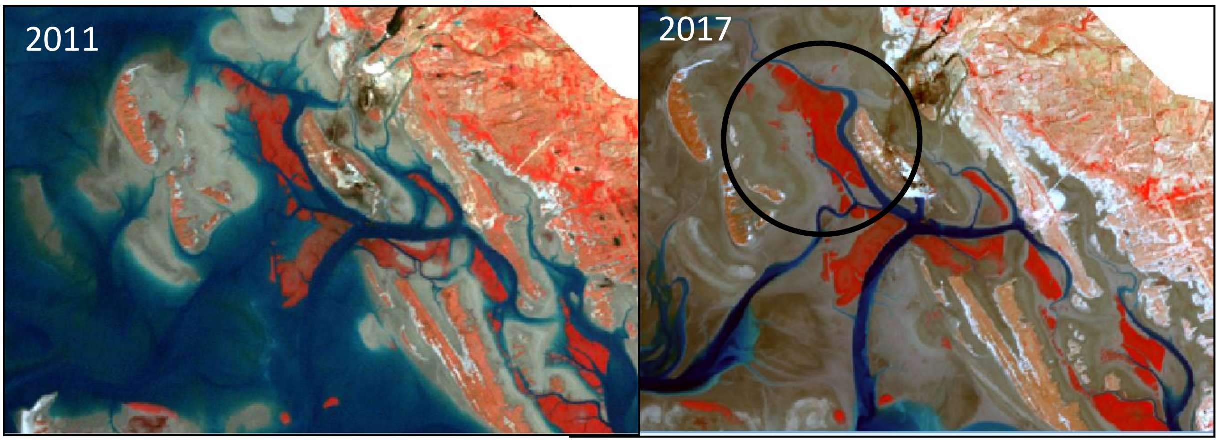

Figure 5.14: Mangroves planted around Bhangodiaround Kharo Creek in parts of north-western region of Gulf of Kachchh during 2011-2017 have become denser as observed on Landsat FCC image

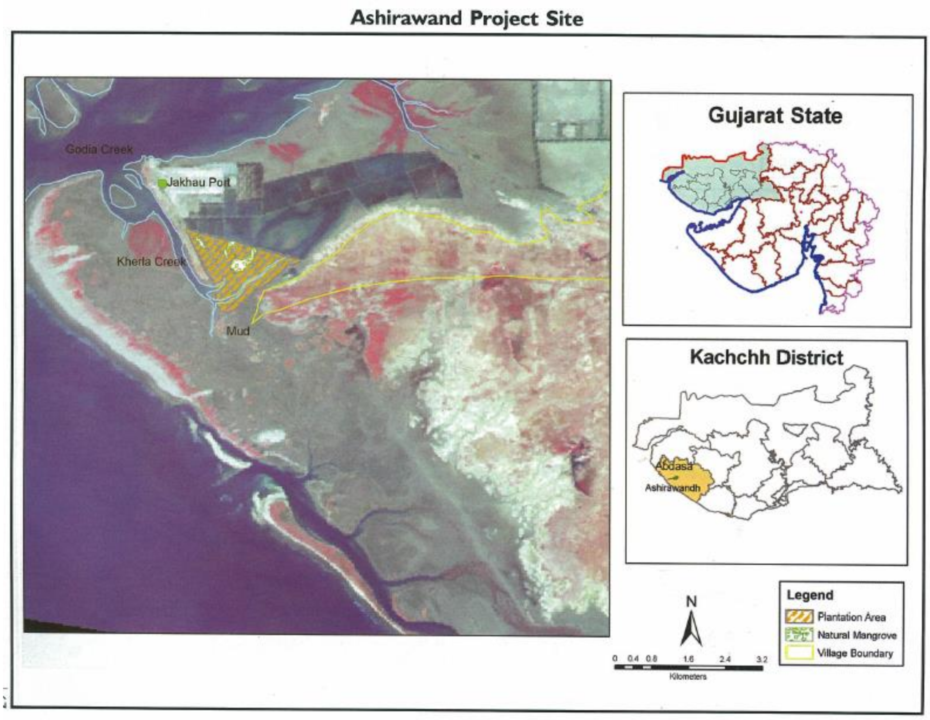

Figure 5.15: Map of mangroves planted at Ashirawand Project Site (Source: GEC, 2006)

Figure 5.16: Mangroves planted (shown in circle) near Kharia Creek at Ashirawand site in parts of north-western region of Gulf of Kachchh during 2011-2017 show no success as observed on Landsat FCC image

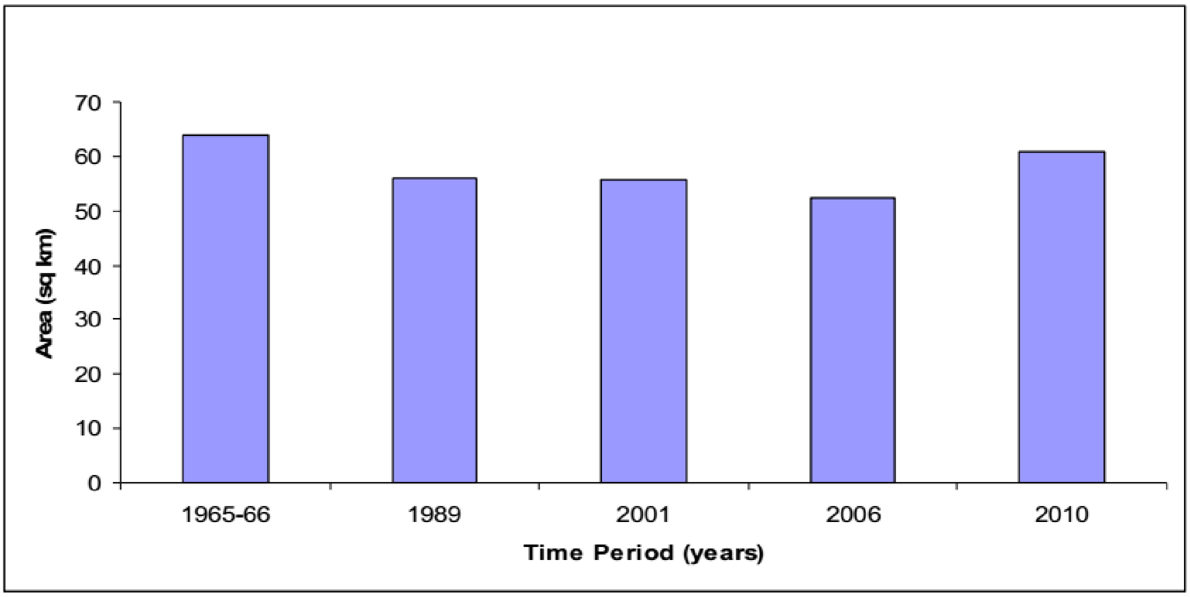

Figure 5.17: Changes in mangrove area during time frame 1965-66 to 2010 in region around Narayan Sarovar - Jakhau (Source: Kumar et al., 2012)

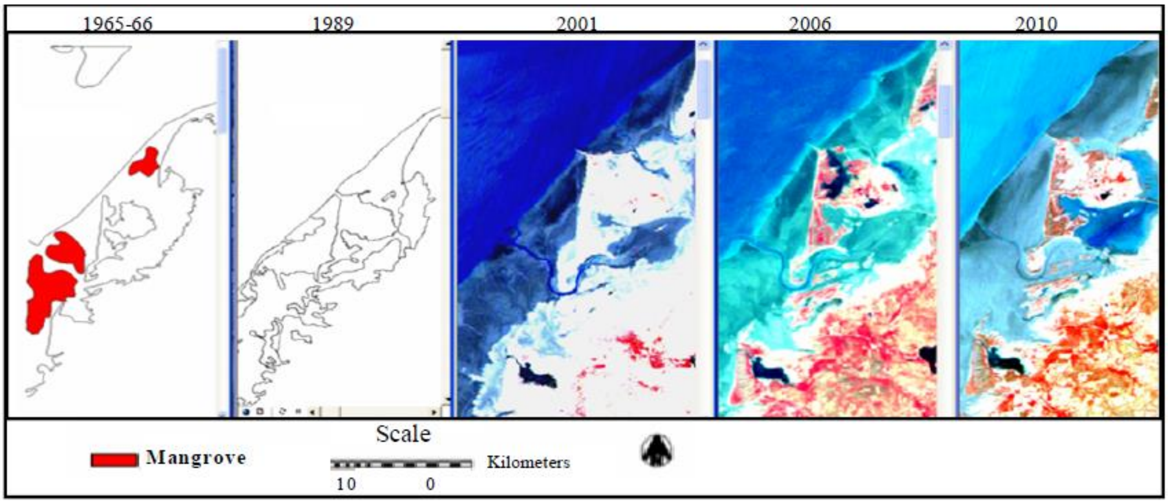

Figure 5.18: Absence of mangrove area (mapped as red patches, left panel using topographical maps of 1965-66) in subsequent coastal thematic maps (1989) and satellite images of 2001, 2006 and 2010 in region around Narayan Sarovar (Source: Kumar et al., 2012)

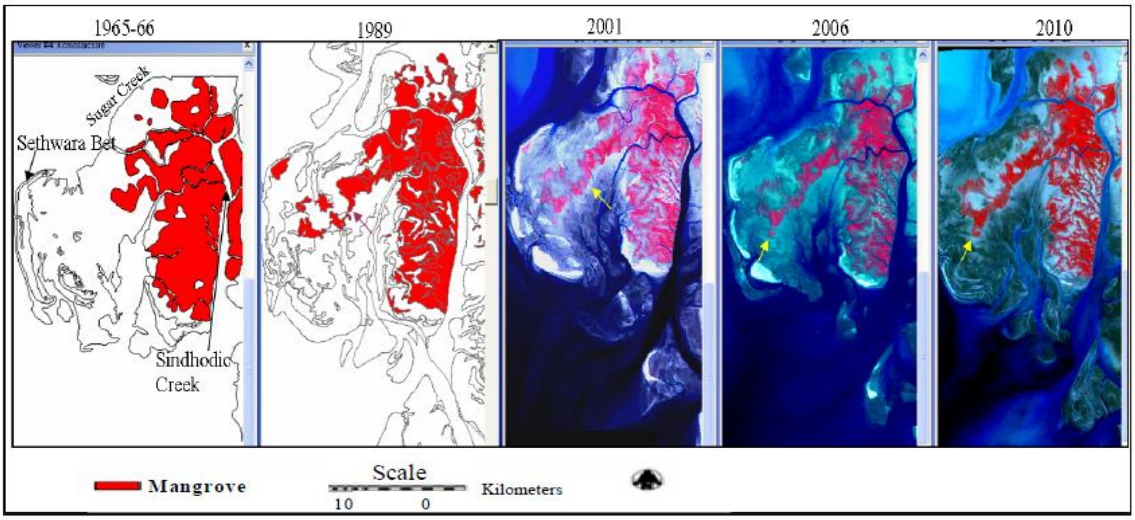

Figure 5.19: Mangrove cover dynamics near Sindhodic Creek in response to dynamic coastal process (Source: Kumar et al., 2012)

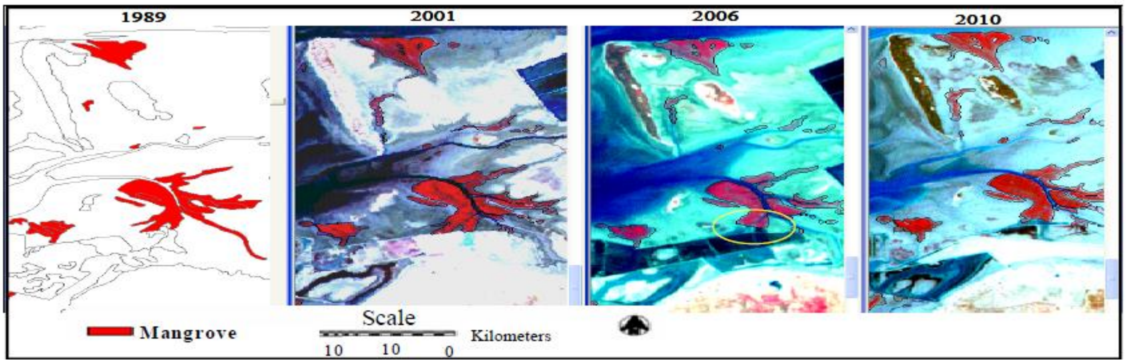

Figure 5.20: Degradation of mangroves due to advancement of saltpans around Jakhau Port (Source: Kumar et al., 2012)

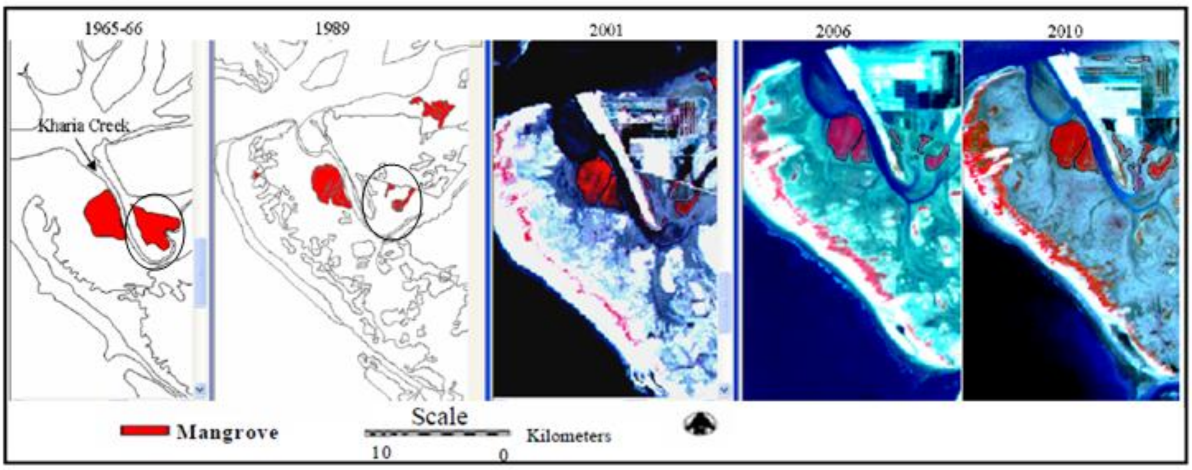

Figure 5.21: Degradation of mangrove near Kharia Creek due to developmental activities (Source: Kumar et al., 2012)

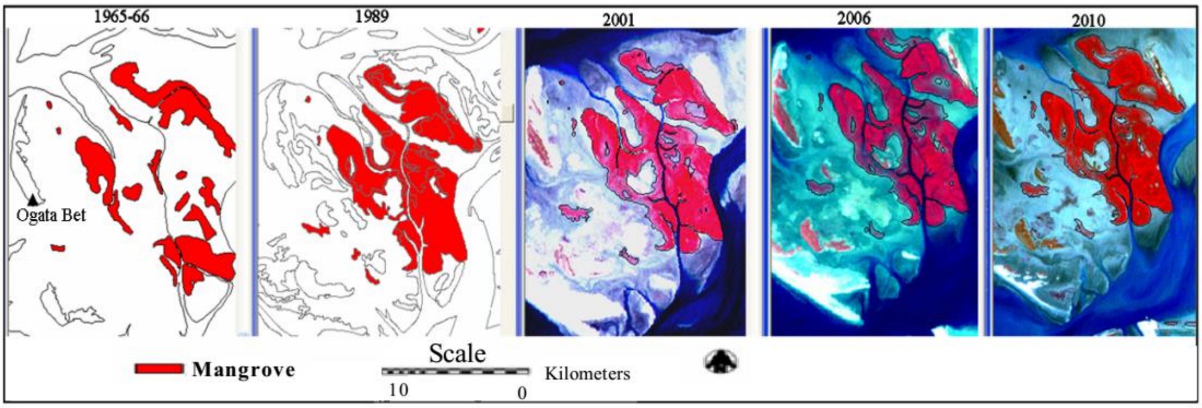

Figure 5.22: Increase in mangrove near Ogata bet (Source: Kumar et al., 2012)

Near middle-eastern side of Sethwara bet there is progressive increase in mangrove coverage throughout the study period (Figure 5.19). It seems that mangroves are expanding from Sindhodic Creek to westward towards Sethwara bet.This could be because of availability of area that is relatively quiet of anthropogenic influences as well as the impacts of dynamic coastal processes. In general, reduction in mangrove cover is due to changes in morphology of islands within creeks, which is primarily due to heavy sedimentation and reworking due to various coastal processes. The region around Lakhpat, Narayan Sarovar-Koteshwar, Godia Creek, Jakhau are experiencing very high erosional rate (SAC, 2012; SAC, 2014; Rajawat et al., 2015) as depicted in Figure 5.23.

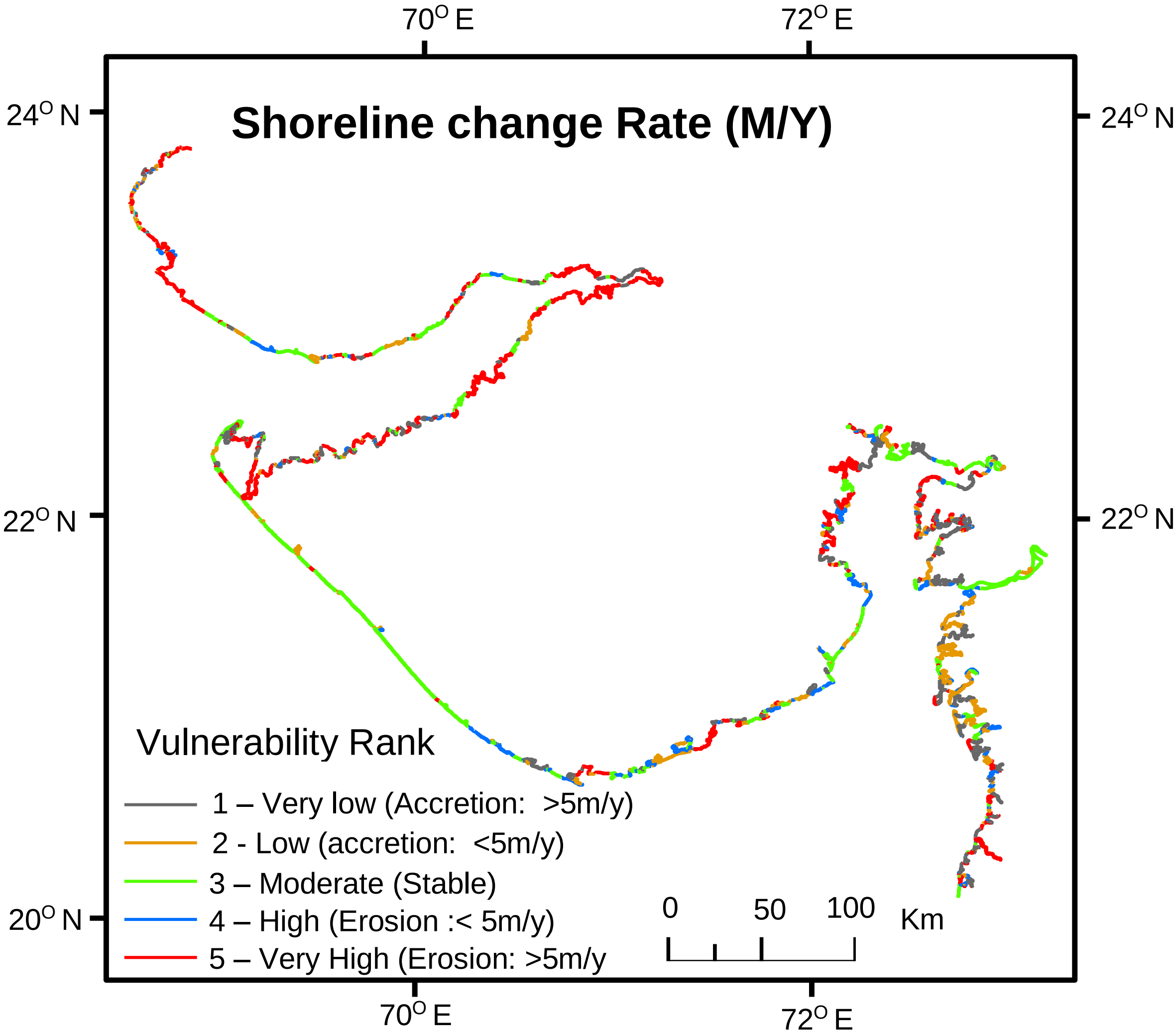

Figure 5.23: Shoreline change along the Gujarat coast (Source: SAC, 2012)

5.2 Mangrove cover dynamics around Mundra (Parts of northern coast of Gulf of Kachchh)

Mundra is a coastal taluka of Gujarat. It is located at the northern flank of the Gulf of Kachchh. The inter-tidal zone covered by mangroves in this region as seen on Landsat-8 OLI FCC is shown in Figure 5.24. Mangroves are seen as red tone on FCC. The inter-tidal zone, supports a unique marine ecosystem dominated by mangroves and natural creeks. A port has been developed in the region, known as Mundra Port. The mangrove vegetation is found on the Navinal Island, Bocha Island and the adjoining inter-tidal mudflats.

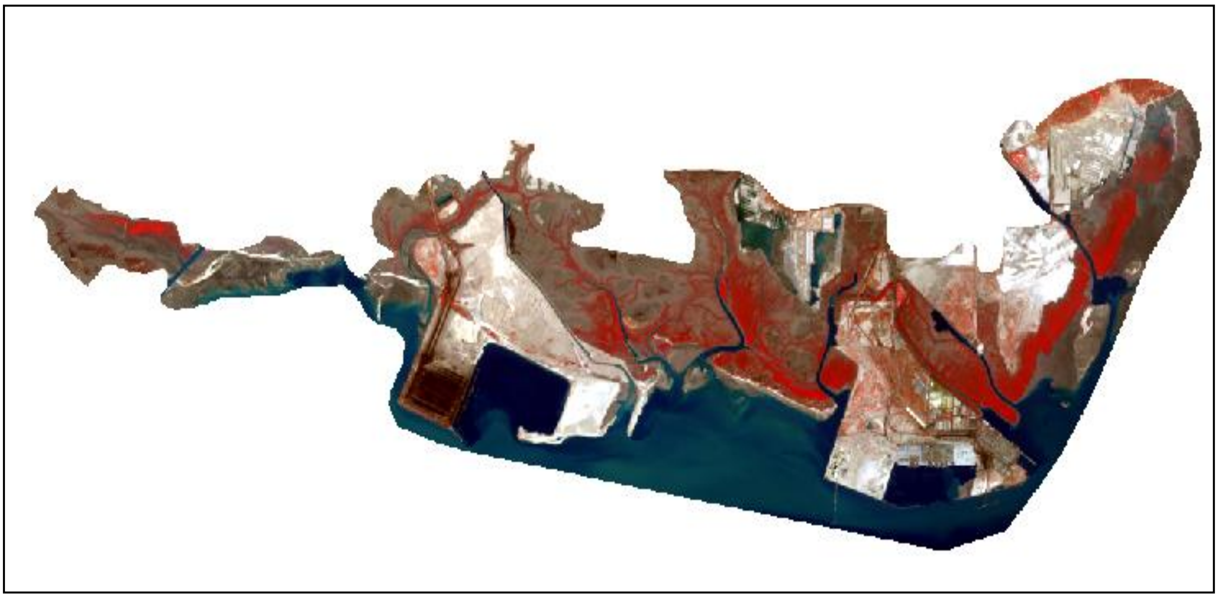

Figure 5.24: Landsat-8 OLI FCC image of 2017 showing mangroves around Mundra (Parts of northern coast of Gulf of Kachchh)

The islands of Bocha and the adjoining mangrove areas including the Bharadi-Mata creek area support dense mangroves on the fringe areas only. Most of the other areas have sparse mangroves. Only one species of true mangrove is found here (SAC, 2012). The species is *Avicennia marina*. In addition to the true mangrove species, several mangrove associates and salt marsh species have been observed in this area, *eg*., *Suaeda fruticosa, Suaeda nudiflora, Suaeda maritima, Urochondra setulosa, Cyperus sp.*, *Salvadora persica, Salicornia sp.*

5.2.1 Class separability analysis

The spectral separability of training signatures of seven intertidal classes, *viz.*, mangrove dense, mangrove sparse, mangrove degraded, intertidal mudflat, subtidal mudflat, salt encrustation, and sea water is shown in Table 5.6 and 5.7.

Table 5.6: Class separability analysis for classified image of 2011 covering Mundra region

Classes	MD	MS	MDeg	IM	SM	SE	SW
Mangroves Dense (MD)	0	1992.19	2000	2000	2000	2000	2000
Mangroves Sparse (MS)	1992.19	0	1999.72	1999.99	2000	2000	2000
Mangroves Degraded (MDeg)	2000	1999.72	0	1998.56	1999.99	2000	2000
Intertidal Mudflats (IM)	2000	1999.99	1998.56	0	1999.99	2000	2000
Subtidal Mudflats (SM)	2000	2000	1999.99	1999.99	0	2000	2000
Salt Encrustation (SE)	2000	2000	2000	2000	2000	0	2000
Sea Water (SW)	2000	2000	2000	2000	2000	2000	0

Table 5.7: Class separability analysis for classified image of 2017 covering Mundra region

Classes	**MD**	**MS**	**MDeg**	**IM**	**SM**	**SE**	**SW**
Mangroves Dense (MD)	0	2000	2000	2000	2000	2000	2000
Mangroves Sparse (MS)	2000	0	1999.99	2000	2000	2000	2000
Mangroves Degraded (MDeg)	2000	1999.99	0	2000	2000	2000	2000
Intertidal Mudflats (IM)	2000	2000	2000	0	2000	2000	2000
Subtidal Mudflats (SM)	2000	2000	2000	2000	0	2000	2000
Salt Encrustation (SE)	2000	2000	2000	2000	2000	0	2000
Sea Water (SW)	2000	2000	2000	2000	2000	2000	0

5.2.2 Accuracy assessment of classified images

Accuracy assessment of classified images of Mundra pertaining to 2011 and 2017 is presented in Table 5.8 and 5.9.

Table 5.8: Error matrix of 2011 classified image of Mundra region

Classes	**MD**	**MS**	**MDeg**	**IM**	**SM**	**SE**	**Classified Total**	**User's Accuracy (%)**
Mangroves Dense (MD)	48 (96%)	2 (3.70 %)	0	0	0	0	50	96
Mangroves Sparse (MS)	2 (4%)	46 (85.18 %)	0	4 (8.16 %)	0	0	52	88.46
Mangroves Degraded (MDeg)	0	2 (3.70 %)	22 (91.67 %)	1 (2.04 %)	0	0	25	88
Intertidal Mudflats (IM)	0	4 (7.41 %)	2 (8.33 %)	44 (89.80 %)	0	0	50	88
Subtidal Mudflats (SM)	0	0	0	0	25 (100 %)	0	25	100
Salt Encrustation (SE)	0	0	0	0	0	30 (100 %)	30	100
Reference Total	50	54	24	49	25	30	232	
Producer's Accuracy (%)	96	85.18	91.67	89.80	100	100		

Overall accuracy = (Number of pixels correctly classified/Total number of pixels used in accuracy assessment) x 100 = (215/232) * 100 = 92.67 %, Kappa coefficient = 0.91

Table 5.9: Error matrix of 2017 classified image of Mundra region

Classes	**MD**	**MS**	**MDeg**	**IM**	**SM**	**SE**	**Classified Total**	**User's Accuracy (%)**
Mangroves Dense (MD)	45 (91.83%)	5 (9.09%)	0	0	0	0	50	90
Mangroves Sparse (MS)	4 (8.16 %)	42 (76.36%)	4 (10.81 %)	0	0	0	50	84
Mangroves Degraded (MDeg)	0	5 (9.09%)	31 (83.78 %)	2 (4%)	0	0	38	81.56
Intertidal Mudflats (IM)	0	3 (5.45%)	2 (5.41)	45 (90 %)	0	2	52	90
Subtidal Mudflats (SM)	0	0	0	0	50 (100%)	0	50	100
Salt Encrustation (SE)	0	0	0	3 (6%)	0	33 (94.28%)	36	91.67
Reference Total	49	55	37	50	50	35	276	
Producer's Accuracy (%)	91.83	76.36	83.78	90	100	94.28		

Overall accuracy = (Number of pixels correctly classified/Total number of pixels used in accuracy assessment) x 100 = (246/276) x100 = 89.13%, Kappa Coefficient = 0.87

5.2.3 Change detection

Classified images of 2011 and 2017 are shown in Figure 5.25. The change detection matrix of mangroves is shown in Table 5.10.

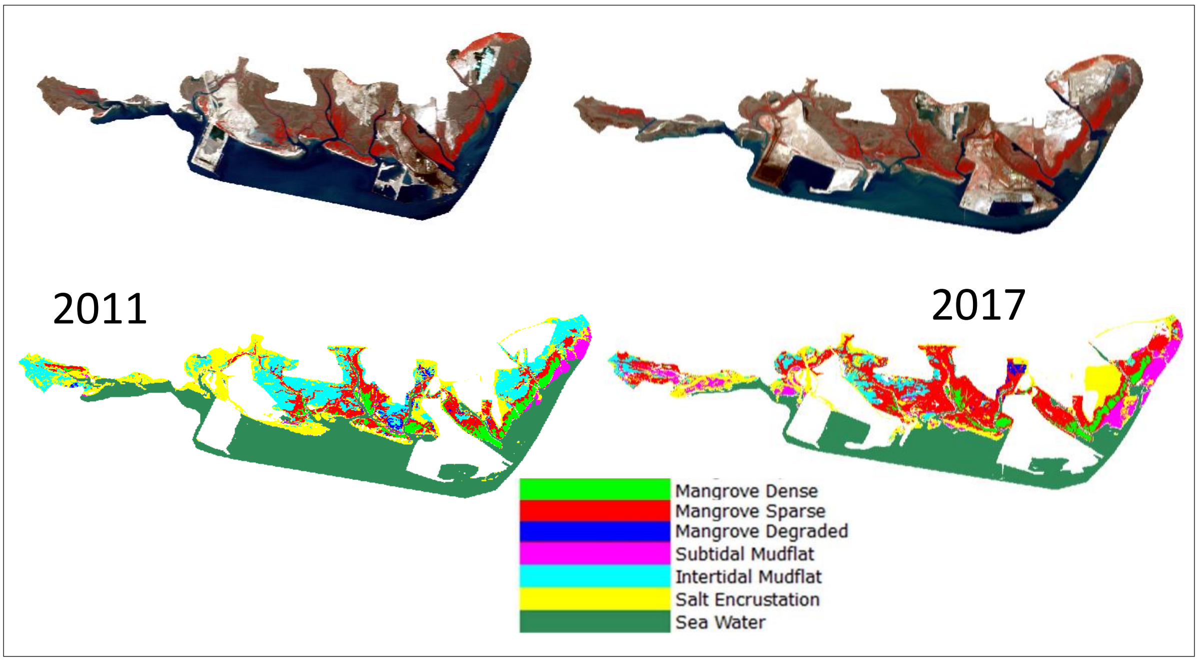

Figure 5.25: Landsat FCC and corresponding mangrove and other inter-tidal classes as per supervised classification for time frame 2011 and 2017 covering Mundra region and environs in northern parts of the Gulf of Kachchh

Table 5.10:Changes in mangrove area (in sq km) of Mundra region

Year → / **Area (sq km)↓**	**2011**	**2017**	**Change (%)**
Mangrove dense	5.44	4.61	- 15.25
Mangrove sparse	12.91	29.63	129.51
Mangrove degraded	1.46	0.77	-47.26
Total Mangrove	**19.81**	**35.01**	**76.72**

Some illustrations of the changes in mangrove area are shown in Figures 5.26, 5.27, 5.28 and 5.29. There has been substantial increase in sparse mangroves at Mundra in 2017 compared to 2011. However, some mangrove patches have been destroyed due to expansion of Mundra Port (Figure 5.28).

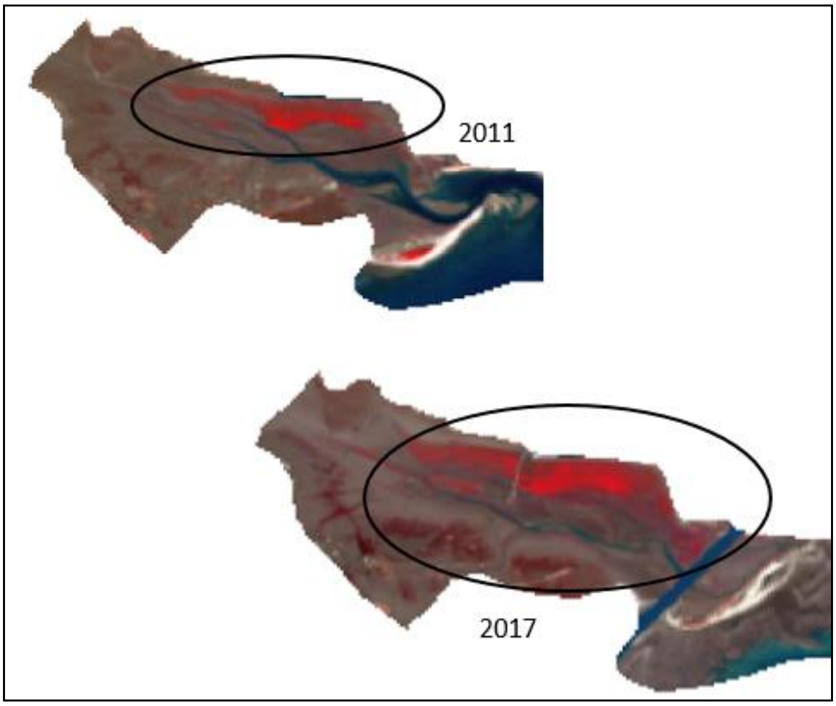

Figure 5. 26: Increase in mangrove cover in region west of Mundra Port in 2017 as seen on Landsat FCC images

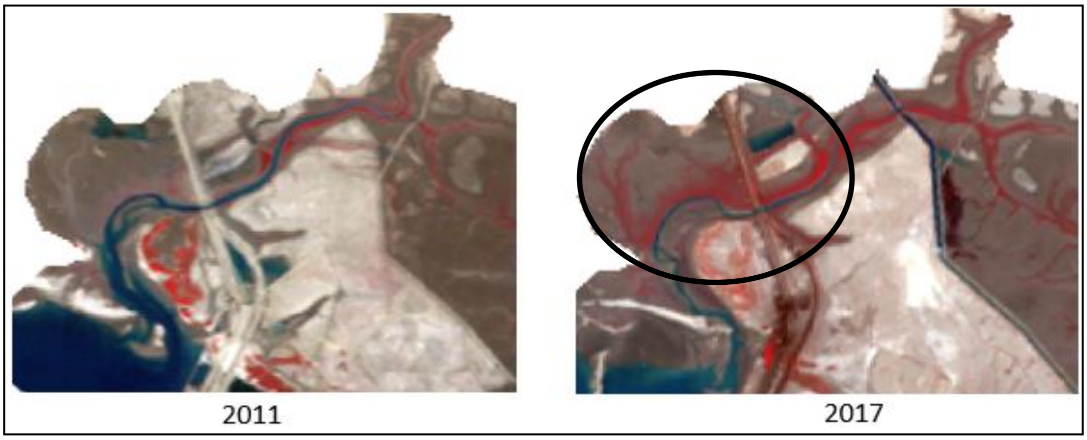

Figure 5.27: Increase in mangrove cover in region north of Mundra Port in 2017 as observed on Landsat FCC images

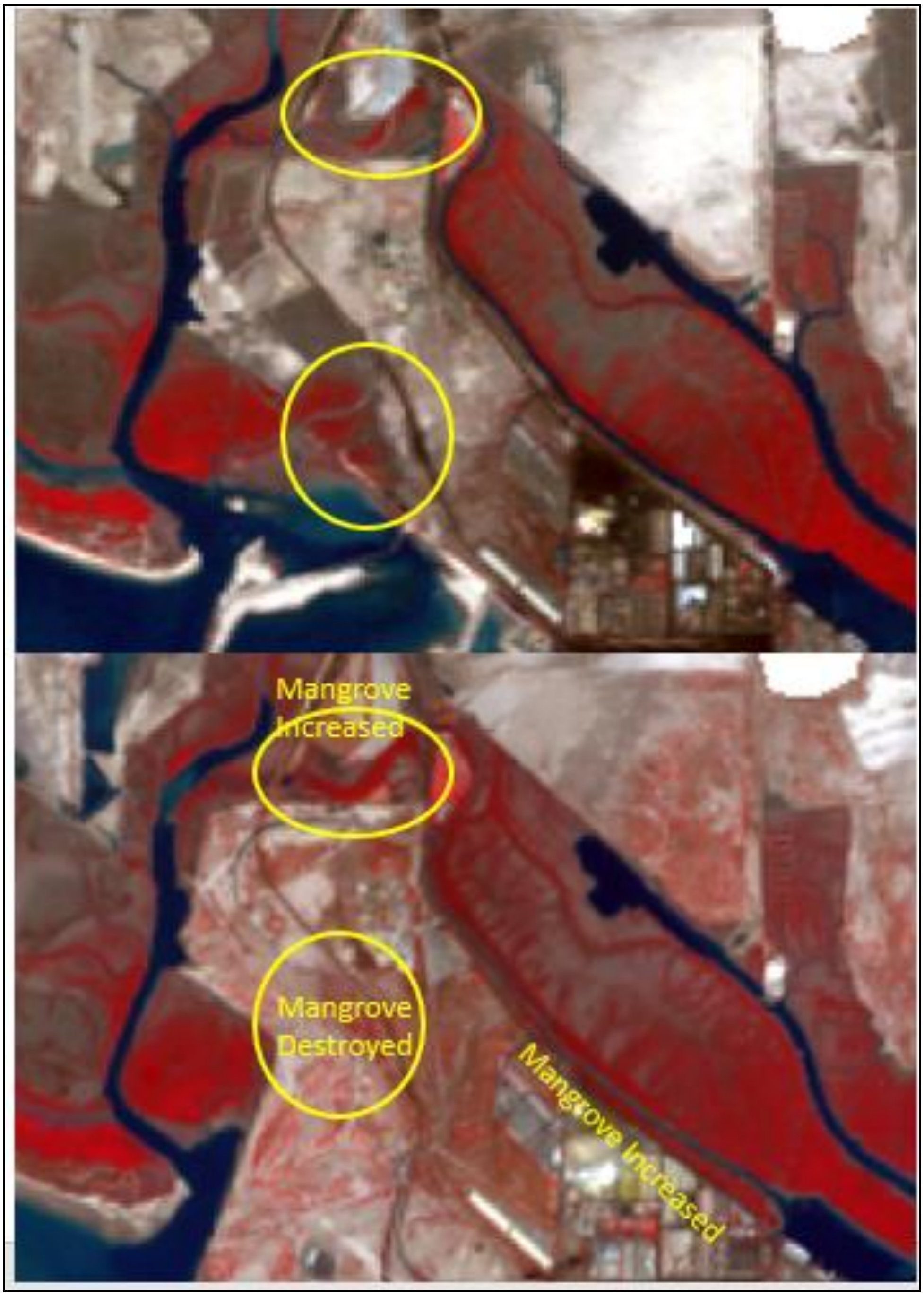

Figure 5.28: Changes in mangrove cover around Mundra Port in 2017 as observed on Landsat FCC images

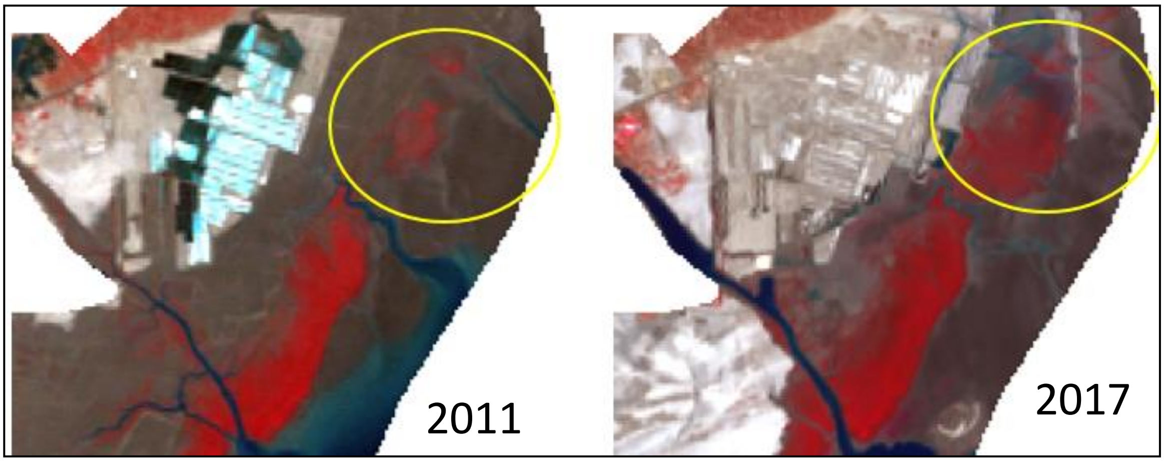

Figure 5.29: Increase in mangroves at Mundra in 2017 as observed on Landsat FCC images

5.3 Mangrove cover dynamics at Kandla and environs (Parts of northern coast of Gulf of Kachchh)

Kandla is a small port town in Anjar taluka of Gujarat. Kandla Port is one of the major ports on the west coast of India. The area has two proposed Special Economic Zones (SEZs), one at Kandla and another Southwest of Kandla near Tuna Port (GUIDE, 2015). Figure 5.30 shows Landsat-5 FCC image of 2011 covering region around Kandla Port (Parts of northern coast of Gulf of Kachchh). Mangrove areas are seen as red tone on FCC images mostly around creeks. The mudflats around Kandla and Tuna support *A. marina* only. The mangroves of Kandla and Tuna exist under heavy pressures from adjoining saltpans and port development activities. These mangroves were mapped for 2011 and 2017 and the changes have been reported hereafter.

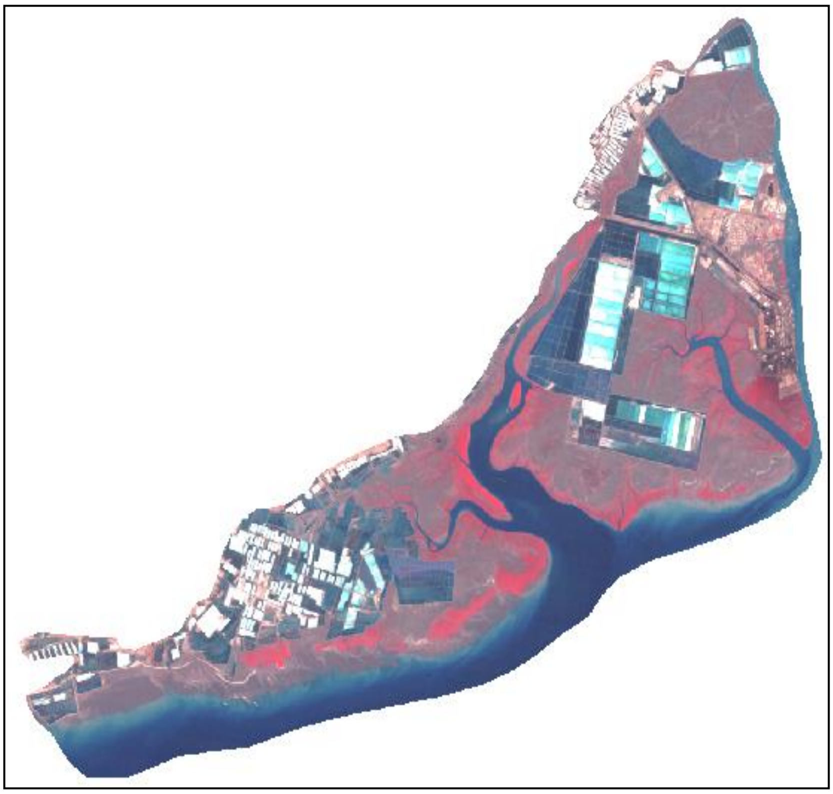

Figure 5.30: Landsat-5 FCC image of 2011 showing mangroves around Kandla Port and environs (Parts of northern coast of Gulf of Kachchh)

5.3.1 Class separability analysis

The signatures of intertidal categories were collected using literature, GE images and limited field visits. In this region, it was not possible to identify mangrove degraded category so only two categories were mapped (mangrove dense and mangrove sparse). Also, salt encrustation was not observed in the 2017 image. The spectral separability of training signatures of six intertidal categories, *viz.*, mangrove dense, mangrove sparse, intertidal mudflats, subtidal mudflats, salt encrustation, and sea water is shown in Table 5.11 and 5.12.

Table 5.11: Class separability analysis for 2011 classified image of Kandla region and environs

Classes	**MD**	**MS**	**IM**	**SM**	**SE**	**SW**
Mangroves Dense (MD)	0	1916.78	2000	2000	2000	2000
Mangroves Sparse (MS)	1916.78	0	1999.99	2000	1999.99	2000
Intertidal Mudflats (IM)	2000	1999.99	0	2000	1999.35	2000
Subtidal Mudflats (SM)	2000	2000	2000	0	2000	2000
Salt Encrustation (SE)	2000	1999.99	1999.35	2000	0	1999.98
Sea Water (SW)	2000	2000	2000	2000	1999.98	0

Table 5.12: Class separability analysis for 2017 classified image of Kandla region and environs

Classes	**MD**	**MS**	**IM**	**SM**	**SW**
Mangroves Dense (MD)	0	1999.99	2000	2000	2000
Mangroves Sparse (MS)	1999.99	0	2000	2000	2000
Intertidal Mudflats (IM)	2000	2000	0	2000	2000
Subtidal Mudflats(SM)	2000	2000	2000	0	2000
Sea Water (SW)	2000	2000	2000	2000	0

5.3.2 Accuracy assessment of classified images

Accuracy assessment of classified images of study area is shown in Table 5.13 and 5.14.

Table 5.13: Error matrix showing classification accuracy of 2011 classified image of Kandla region and environs

Classes	**MD**	**MS**	**IM**	**SM**	**SE**	**Classified Total**	**User's Accuracy (%)**
Mangroves Dense (MD)	46 (92 %)	2 (4%)	0	0	0	48	95.83
Mangroves Sparse (MS)	4 (8%)	48 (96 %)	0	0	0	52	92.31
Intertidal Mudflats (IM)	0	0	50 (100%)	0	0	50	100
Subtidal Mudflats (SM)	0	0	0	20 (100%)	0	20	100
Salt Encrustation (SE)	0	0	0	0	15 (100 %)	15	100
Reference Total	50	50	50	20	15	185	
Producer's Accuracy (%)	92	96	100	100	100		

Overall accuracy = (Number of pixels correctly classified/Total number of pixels used in accuracy assessment) x 100 = (179/185) * 100 = 96.76 %, Kappa coefficient = 0.96

Table 5.14: Error matrix showing classification accuracy of 2017 classified image of Kandla region and environs

Classes	MD	MS	IM	SM	Classified Total	User's Accuracy (%)
Mangroves Dense (MD)	47 (94%)	1 (2%)	0	0	48	97.92
Mangroves Sparse (MS)	3 (6%)	49 (98%)	0	0	52	94.23
Intertidal Mudflats (IM)	0	0	50 (100%)	0	50	100
Subtidal Mudflats (SM)	0	0	0	20 (100%)	20	100
Reference Total	50	50	50	20	170	
Producer's Accuracy (%)	94	98	100	100		

Overall accuracy = (Number of pixels correctly classified/Total number of pixels used in accuracy assessment) x 100 = (166/170) x 100 = 97.64 %, Kappa Coefficient = 0.92

5.3.3 Change detection

Changes in mangrove and other inter-tidal classes as per supervised classification of Landsat data of 2011 and 2017 covering Kandla Port and environs is shown in Figure 5.31. There has been an increase of roughly 19 sq km of mangroves in this region in the six years' period of 2011 and 2017. This is mainly because of increase of 19 sq km of sparse mangroves.

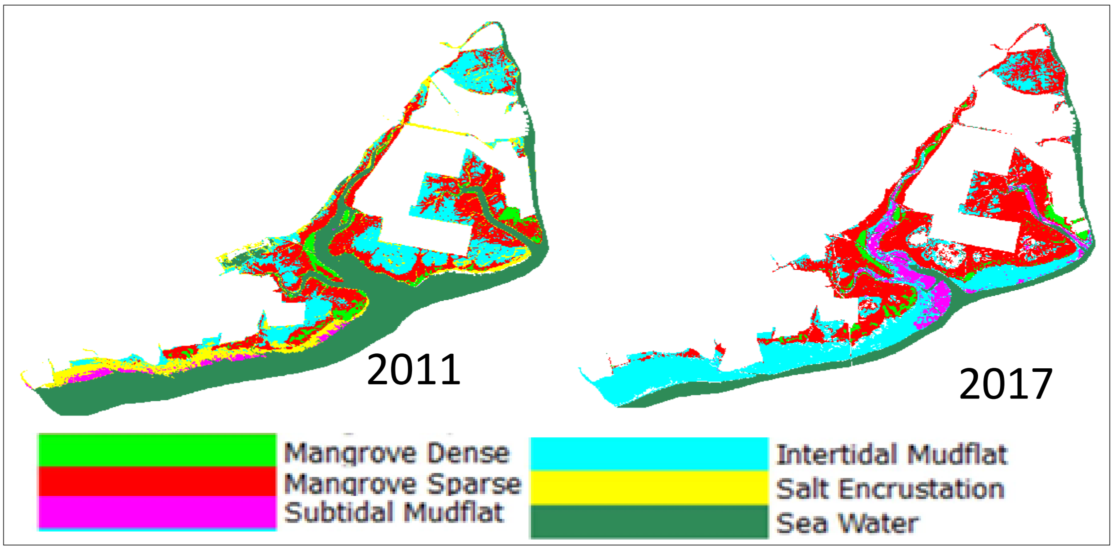

Figure 5.31: Mangrove and other inter-tidal classes as per supervised classification of Landsat data of 2011 and 2017 covering Kandla Port and environs (Parts of northern coast of Gulf of Kachchh)

The change detection matrix of mangroves is shown in Table 5.15.

Table 5.15: Changes in mangrove area (in sq km) of Kandla region

Year → / **Area (sq km)↓**	**2011**	**2017**	**Change (%)**
Mangroves dense	6.23	5.89	-5.45
Mangroves sparse	35.56	54.57	53.45
Total Mangrove	**41.79**	**60.46**	**44.67**

Some illustrations of changes in mangrove are shown in Figures 5.32 and 5.33.

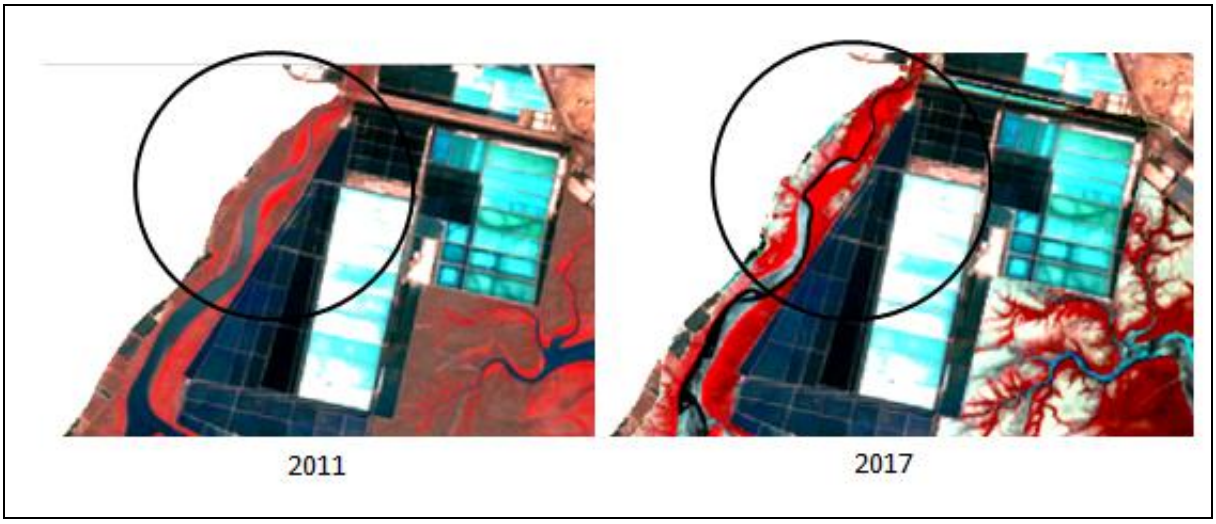

Figure 5.32: Increase in mangrove cover west of Kandla Port in 2017 as observed on Landsat FCC images

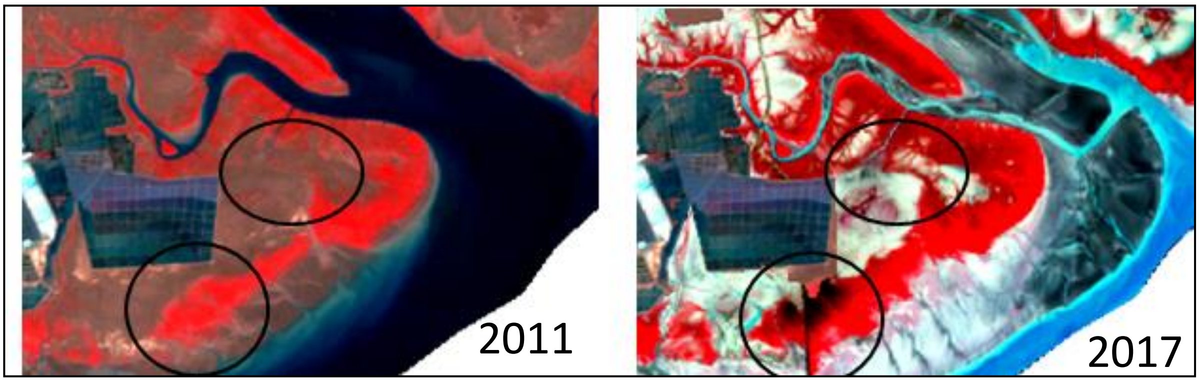

Figure 5.33: Increase in mangrove cover south west of Kandla Port in 2017 as observed on Landsat FCC images

The study also observed decline of about half sq km of dense mangroves in this region because of port-related activities and construction of saltpans. The increase here is chiefly attributed to mangrove plantation carried out near Tuna.

5.4 Mangrove cover dynamics near Satsaida Bet and environs (north-eastern parts of the Gulf of Kachchh)

Satsaida bet and environs located in north-eastern parts of the Gulf of Kachchh has intricate network of creeks, dissecting large intertidal mudflats and has luxuriant growth of mangroves at many parts (Figure 5.34). The region is characterised by extensive inter-tidal zone along with development of salt pans all along the coastal mainland. The mapping done in this work for 2011 and 2017, reveal a significant increase in mangrove cover in this region.

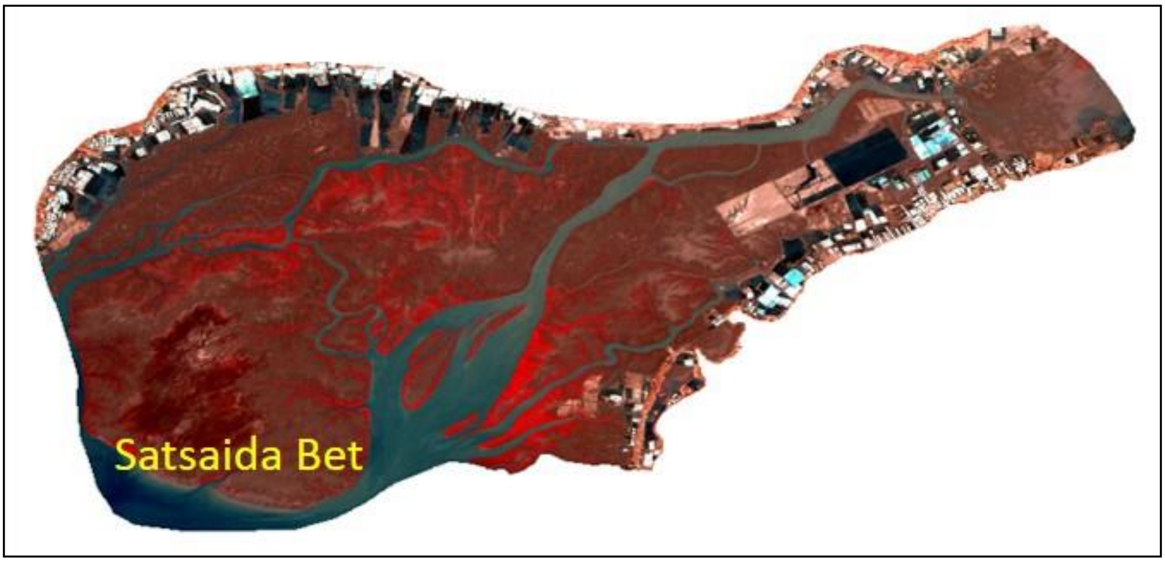

Figure 5.34: Landsat-5 FCC image of 2011 showing mangroves around Satsaida bet and environs (Parts of north-eastern coast of Gulf of Kachchh)

5.4.1 Class separability analysis

The spectral separability of training signatures of seven intertidal classes, *viz.*, mangrove dense, mangrove sparse, mangrove degraded, intertidal mudflats, subtidal mudflats, salt encrustation, and sea water is shown in Table 5.16 and 5.17.

Table 5.16: Class separability analysis for 2011 classified image of Satsaida bet and environs

Classes	MD	MS	MDeg	IM	SM	SE	SW
Mangroves Dense (MD)	0	1988.65	2000	2000	2000	2000	2000
Mangroves Sparse (MS)	1988.65	0	1997.36	1999.99	2000	1999.99	2000
Mangroves Degraded (MDeg)	2000	1997.36	0	1960.70	2000	2000	2000
Intertidal Mudflats (IM)	2000	1999.99	1960.70	0	1999.99	1997.07	2000
Subtidal Mudflats (SM)	2000	2000	2000	1999.99	0	1999.99	2000
Salt Encrustation (SE)	2000	1999.99	2000	1997.07	1999.99	0	2000
Sea Water (SW)	2000	2000	2000	2000	2000	2000	0

Table 5.17: Class separability analysis for 2017 classified image of Satsaida bet and environs

Classes	MD	MS	MDeg	IM	SM	SE	SW
Mangroves Dense (MD)	0	1999.98	2000	2000	2000	2000	2000
Mangroves Sparse (MS)	1999.98	0	2000	2000	2000	2000	2000
Mangroves Degraded (MDeg)	2000	2000	0	2000	2000	2000	2000
Intertidal Mudflats (IM)	2000	2000	2000	0	2000	2000	2000
Subtidal Mudflats (SM)	2000	2000	2000	2000	0	2000	2000
Salt Encrustation (SE)	2000	2000	2000	2000	2000	0	2000
Sea Water (SW)	2000	2000	2000	2000	2000	2000	0

5.4.2 Accuracy assessment of classified images

Accuracy assessment of classified images of study area is shown in Table 5.18 and 5.19.

Table 5.18: Error matrix showing classification accuracy of 2011 classified image of Satsaida bet and environs

Classes	**MD**	**MS**	**MDeg**	**IM**	**SM**	**SE**	**Classified Total**	**User's Accuracy (%)**
Mangroves Dense (MD)	40 (80%)	6 (12%)	0	0	0	0	46	86.95
Mangroves Sparse (MS)	10 (20%)	39 (78%)	7 (14 %)	0	0	0	56	69.94
Mangroves Degraded (MDeg)	0	5 (10%)	41 (82 %)	0	0	0	46	89.13
Intertidal Mudflats (IM)	0	0	2 (4%)	50 (100%)	0	0	52	96.15
Subtidal Mudflats (SM)	0	0	0	0	50 (100 %)	0	50	100
Salt Encrustation (SE)	0	0	0	0	0	50 (100%)	50	100
Reference Total	50	50	50	50	50	50	300	
Producer's Accuracy (%)	80	78	82	100	100	100		

Overall accuracy = (Number of pixels correctly classified/Total number of pixels used in accuracy assessment) x 100 = (270/300) * 100 = 90%, Kappa coefficient = 0.88

Table 5.19: Error matrix showing classification accuracy of 2017 classified image of Satsaida bet and environs

Classes	**MD**	**MS**	**MDeg**	**IM**	**SM**	**SE**	**Classified Total**	**User's Accuracy (%)**
Mangroves Dense (MD)	41 (82%)	4 (8%)	0	0	0	0	45	91.11
Mangroves Sparse (MS)	9 (18%)	40 (80%)	5 (10%)	2 (4%)	0	0	56	71.43
Mangroves Degraded (MDeg)	0	3 (6%)	41 (82%)	3 (6%)	0	0	47	87.23
Intertidal Mudflats (IM)	0	3 (6%)	4 (8%)	45 (90%)	0	0	52	86.53
Subtidal Mudflats (SM)	0	0	0	0	50 (100 %)	0	50	100
Salt Encrustation (SE)	0	0	0	0	0	50 (100%)	50	100
Reference Total	50	50	50	50	50	50	300	
Producer's Accuracy(%)	82	80	82	90	100	100		

Overall accuracy = (Number of pixels correctly classified/Total number of pixels used in accuracy assessment) x 100 = (267/300) * 100 = 89%, Kappa Coefficient = 0.87

5.4.3 Change detection

The classified images of mangrove habitat around Satsaida bet are shown below in Figure 5.35. Overall, the mangroves have increased by 145.62 sq km in 2017 around Satsaida bet in the inner Gulf compared to 2011. This increase is primarily because of plantation efforts of local Forest Development Agencies and Gujarat Ecology Commission (Upadhyay et al., 2015).

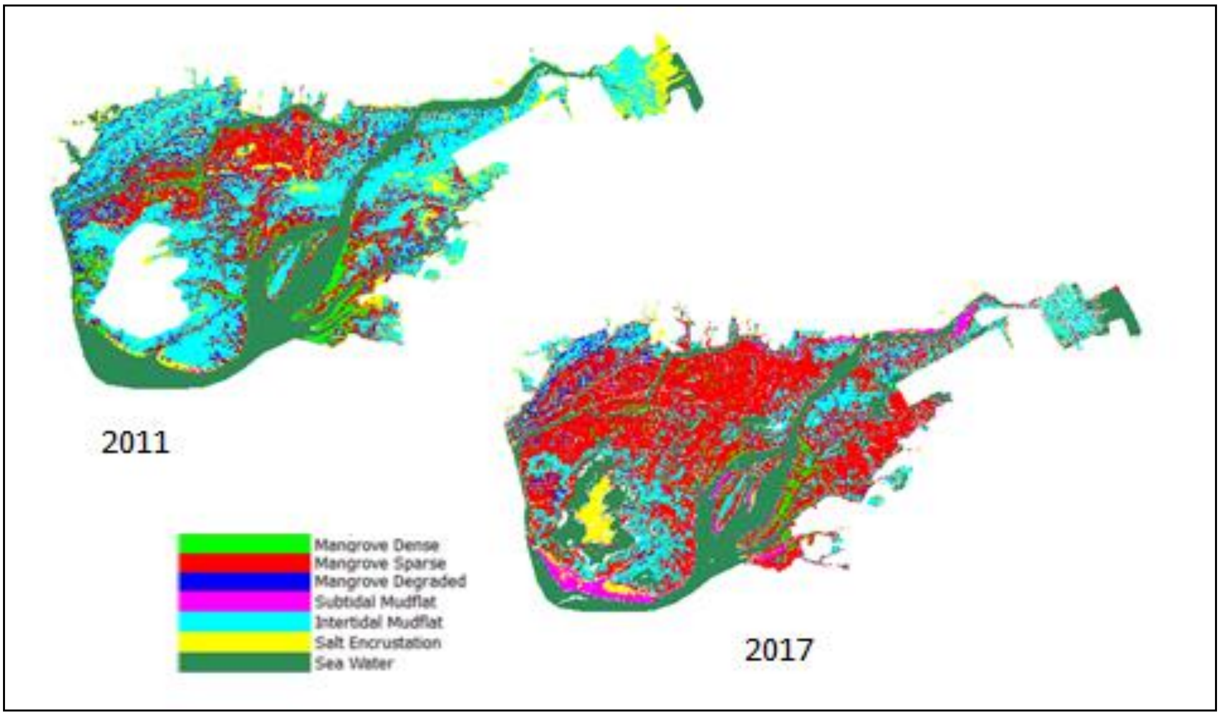

Figure 5.35: Mangrove and other inter-tidal classes as per supervised classification of Landsat data of 2011 and 2017 covering Satsaida bet and environs (north-eastern parts of Gulf of Kachchh)

The change detection matrix of mangroves is shown in Table 5.20.

Table 5.20: Changes in mangrove area (in sq km) near Satsaida Bet

Year → **Area (sq km)↓**	**2011**	**2017**	**Change (%)**
Mangrove Dense	39.54	19.80	- 49.92
Mangrove Sparse	177.29	379.09	113.82
Mangrove Degraded	60.95	24.50	- 59.80
Total Mangrove	**277.77**	**423.39**	**52.43**

Some illustrations of the changes in mangrove cover near Satsaida Bet and environs are shown in Figures 5.36 and 5.37. Major increase is observed in sparse mangrove category whereas some decline is noticed in dense mangrove category due to development of saltpans (Figure 5.36)

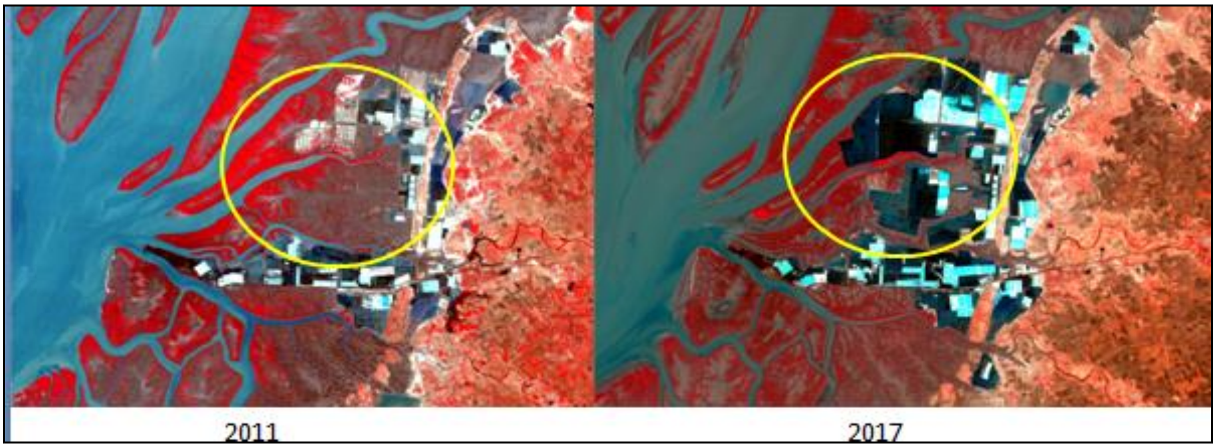

Figure 5.36: Degradation of mangroves around Satsaidabet observed in 2017 in the circled area of Landsat FCC image

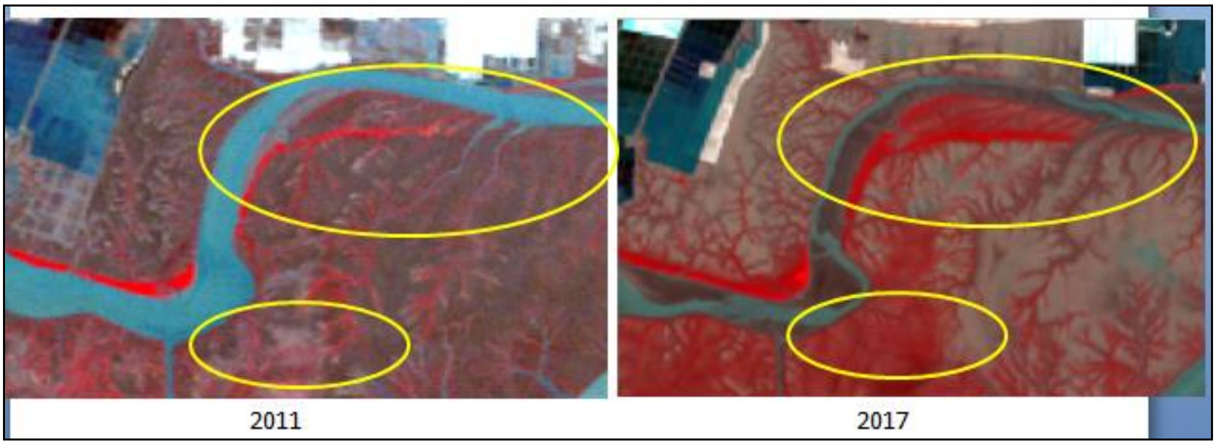

Figure 5.37: Increase in mangrove cover observed in the encircled area in 2017 in the Landsat FCC image

5.5 Mangrove Cover Dynamics in Marine National Park and Sanctuary (MNP&S), southern coast of Gulf of Kachchh

The southern coast of Gulf of Kachchh (GoK) which is also the northern coast of Saurashtra Peninsula, boasts of a diversity of coastal and marine life; and realizing the importance of this zone, the State Government declared some part of this coast as Marine Sanctuary in 1980. In 1982, the area under marine sanctuary was expanded and some of the areas of the marine sanctuary were raised to the level of Marine National Park to provide more protection to these areas. Thus though Marine Sanctuary (MS) and Marine National Park (MNP) are two legal units, they are part of the same ecological area or Marine Protected Area (MPA in the Gulf (Singh, 2003) (Figure 3.2 of Chapter 3). Marine Sanctuary (MS) covers an area of 457.92 sq. km whereas the Marine National Park (MNP) is established in an area of 162.89 sq. km. The MNP is situated along the southern coast of Gulf of Kachchh in Jamnagar and Devbhumi Dwarka districts between 20° 15' N to 23° 40' N latitudes and 68°20' to 70°40' E longitudes. There are 42 islands, out of which 37 islands are covered under National park and the rest 5 islands are covered under Sanctuary area. Mangroves of MNP&S were mapped at community level using Landsat data of 2011 and 2017.

5.5.1 Spectral profile of mangrove communities

The spectral profile of mangrove communities provides distinct separation in visible/infrared bands of Landsat data (Figure 5.38 & 5.39). The *Avicennia* community comprise majorly of *A. marina*, with smaller patches of *A. officinalis* and *A. alba* (SAC, 2003). This community occupies approx. 98% of all mangroves in MNP&S (SAC, 2012). *Rhizophora-Ceriops* community includes closely spaced stands of *R. mucronata* and *C. tagal*. The reflectance received from RCD is lower compared to that received from AD in NIR band. This is because leaves of *Rhizophora* have higher pigment concentration that *Avicennia* (Oswin and Kathiresan, 1994; SAC, 2003). Morphologically also, leaves of *Rhizophora* and *Ceriops* are darker in colour, broad and more thick than *Avicennia* leaves (Figure 5.40). The leaves of *Avicennia* are bright green and its canopy is globose in shape with irregular branching (SAC, 2003).

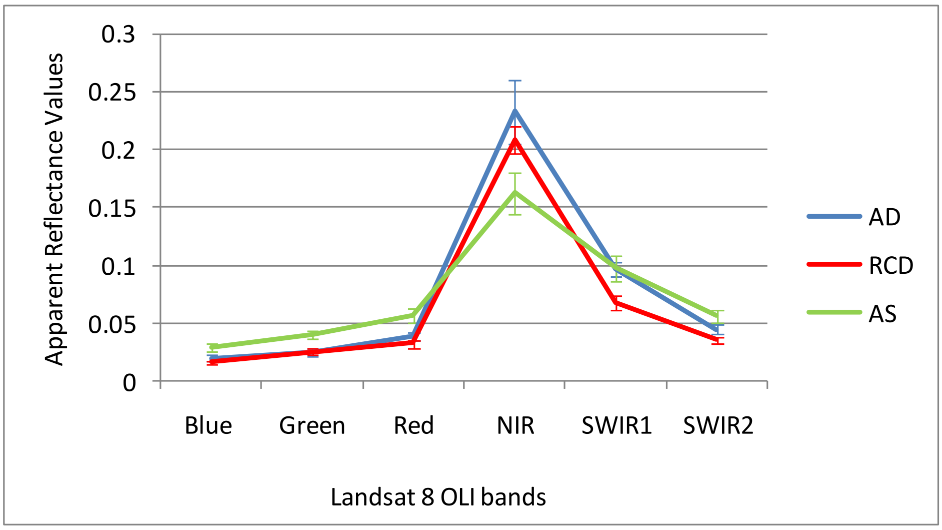

Figure 5.38: Mean spectral reflectance (along with standard deviation bar) of mangrove communities (AD: *Avicennia* dense; RCD: *Rhizophora-Ceriops* dense; AS: *Avicennia* sparse) derived from Landsat-8 OLI data of March 01, 2017 for Marine National Park & Sanctuary (MNP&S) in Gulf of Kachchh.

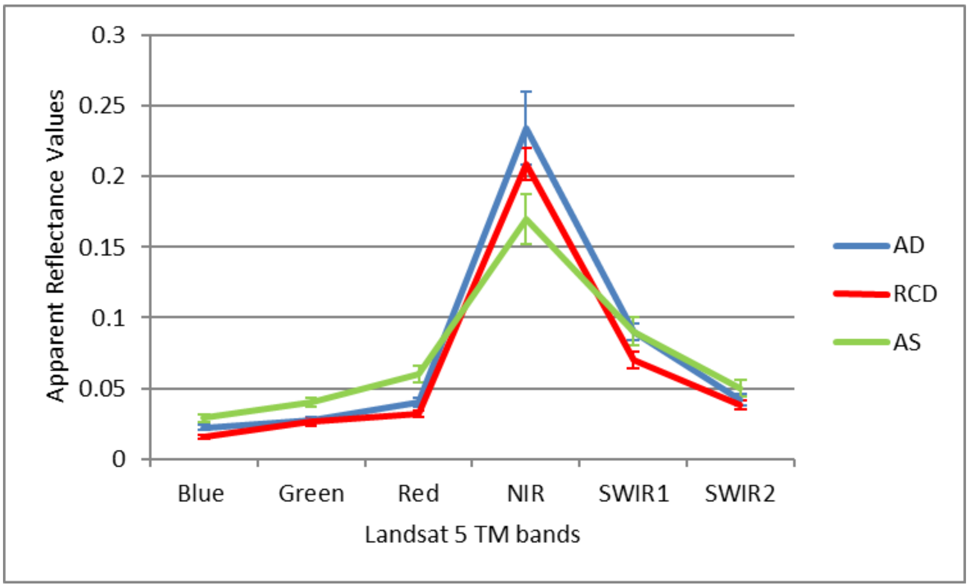

Figure 5.39: Mean spectral reflectance (along with standard deviation bar) of mangrove communities (AD: *Avicennia* dense; RCD: *Rhizophora-Ceriops* dense; AS: *Avicennia* sparse) derived from Landsat-5 TM data of February 13, 2011 for Marine National Park & Sanctuary (MNP&S) in Gulf of Kachchh.

Figure 5.40: *Rhizophora* and *Avicennia* plants in MNP&S

The sparse density *Avicennia* shows high reflectance values in visible and SWIR bands, compared to the other two mangrove communities. This is because AS has more open spaces between plants which causes significant amount of reflectance from muddy background to influence the overall reflectance received at sensor.

5.5.2 Class separability analysis

Published literature (Singh et al., 2002; Venkatraman, 2004; SAC, 2003; SAC, 2012; Ajai et al., 2013; Prerna, 2015), Google Earth (GE) images, ground visit to MNP&S and understanding of the spectral profile mentioned above were employed to identify the dominant community classes and accordingly collect the training signatures. Finally, the training signatures were collected for *Avicennia* Dense (AD), *Rhizophora-Ceriops* Dense (RCD), *Avicennia* Sparse (AS), Intertidal Mudflat (IM) and Salt Encrustation (SE). Tables 5.21 and 5.22 give salient results of class separability analysis for Landsat data of 2011 and 2017 respectively covering MNP&S.

Table 5.21: Class separability analysis for 2011 classified image covering MNP&S

Classes	AD	RCD	AS	IM	SE
Avicennia Dense (AD)	0	1823.62	1964.36	2000	2000
Rhizophora-Ceriops Dense (RCD)	1823.62	0	1999.99	2000	2000
Avicennia Sparse (AS)	1964.36	1999.99	0	2000	2000
Intertidal Mudflat (IM)	2000	2000	2000	0	1999.99
Salt Encrustation (SE)	2000	2000	2000	1999.99	0

Table 5.22: Class separability analysis for 2017 classified image covering MNP&S

Classes	AD	RCD	AS	IM	SE
Avicennia Dense (AD)	0	1958.68	1995.88	2000	2000
Rhizophora-Ceriops Dense (RCD)	1958.68	0	1999.99	2000	2000
Avicennia Sparse (AS)	1995.88	1999.99	0	1999.99	2000
Intertidal Mudflat (IM)	2000	2000	1999.99	0	2000
Salt Encrustation (SE)	2000	2000	2000	2000	0

It is observed that the separability values obtained for (AD and RCD) classes are relatively lower than other pair of classes. This is expected because both AD and RCD are dense mangrove communities.

5.5.3 Accuracy assessment

The ground truth data was collected from field visit, published literature and high resolution GE images. Field visit was conducted around Pirotan, Jindra-Chhad and Narara islands. In addition, adjoining coastal belts of Sikka, Bedi Port, Jodiya and Pindara were also visited. Garmin GPS was used to record co-ordinates of ground features. The error matrix for 2011 and 2017 assessments are shown in Table 5.23 and 5.24.

Table 5.23: Error matrix showing classification accuracy of 2011 classified image covering MNP&S

Classes	**AD**	**RCD**	**AS**	**IM**	**Classified Total**	**User's Accuracy (%)**
Avicennia Dense (AD)	47 (94%)	2 (4%)	2 (4%)	0	51	92.15
Rhizophora-Ceriops Dense (RCD)	3 (6%)	48 (96%)	2 (4%)	0	53	90.56
Avicennia Sparse (AS)	0	0	46 (92%)	2 (4%)	48	95.83
Intertidal Mudflat (IM)	0	0	0	48 (96%)	48	100
Reference Total	50	50	50	50	200	
Producer's Accuracy (%)	94	96	92	96		

Overall accuracy = (Number of pixels correctly classified/Total number of pixels used in accuracy assessment) x 100 = (189/200) * 100 = 94.5%, Kappa Coefficient = 0.93

Table 5.24: Error matrix showing classification accuracy of 2017 classified image covering MNP&S

Classes	AD	RCD	AS	IM	Classified Total	User's Accuracy (%)
Avicennia Dense (AD)	48 (96%)	2 (4%)	3 (6%)	0	53	90.56
Rhizophora-Ceriops Dense (RCD)	1(2%)	47 (94%)	1 (2%)	0	49	95.92
Avicennia Sparse (AS)	1 (2%)	1 (2%)	44 (88%)	3 (6%)	49	89.79
Intertidal Mudflat (IM)	0	0	2 (4%)	47 (94%)	49	95.92
Reference Total	50	50	50	50	200	
Producer's Accuracy(%)	96	94	88	94	94	

Overall accuracy = (Number of pixels correctly classified/Total number of pixels used in accuracy assessment) x 100 = (186/200) * 100 = 93%, Kappa Coefficient = 0.91

5.5.4 Change detection

The classified images showing mangrove community zonation for 2011 and 2017 is provided in Figure 5.41. Enlarged parts for boxes shown in Figure 5.41 are shown in Figure 5.42 and Figure 5.43. The analysis shows that there has been an increase of 27.33 sq km of mangroves in MNP&S in the six years duration of 2011-2017. The increase is mainly in *Avicennia* sparse mangrove category (of roughly 25 sq km). The increase is observed mainly on islands such as Pirotan, Mundeka-Dideka, Kalubhar, Dhani and on coastal belts adjoining Balachadi, Jodiya, near Hansthal Creek and Sikka. All this development is attributed to mangrove plantations carried out by MNP authorities in the last several years. Around 2 sq km of increase was also noticed in *Rhizophora-Ceriops* Dense. During the field visit, it was confirmed by the CCF, MNP Circle, Jamnagar that mangrove plantation has been going on every year for the last several years and apart from *Avicennia*, *Rhizophora* has also been planted on mudflats of MNP&S. This fact also supports the results presented in this study.

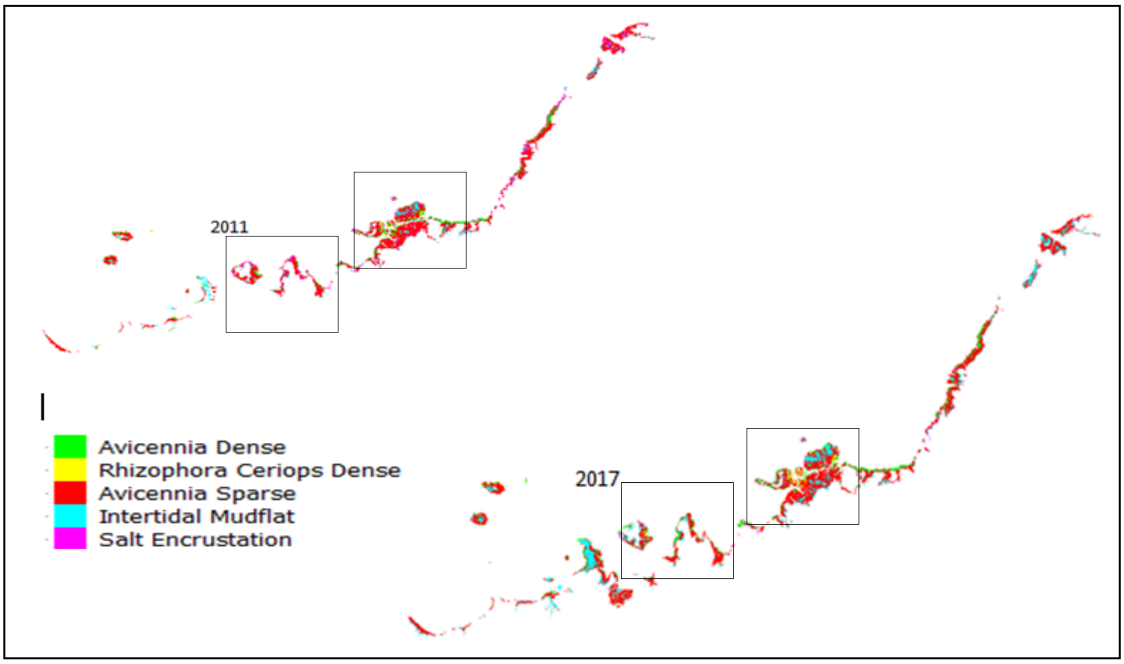

Figure 5.41: Mangrove community zonation in MNP&S as per supervised classification of Landsat data of 2011 and 2017. Enlarged parts for locations shown in boxes are shown in Figure 5.42 and Figure 5.43.

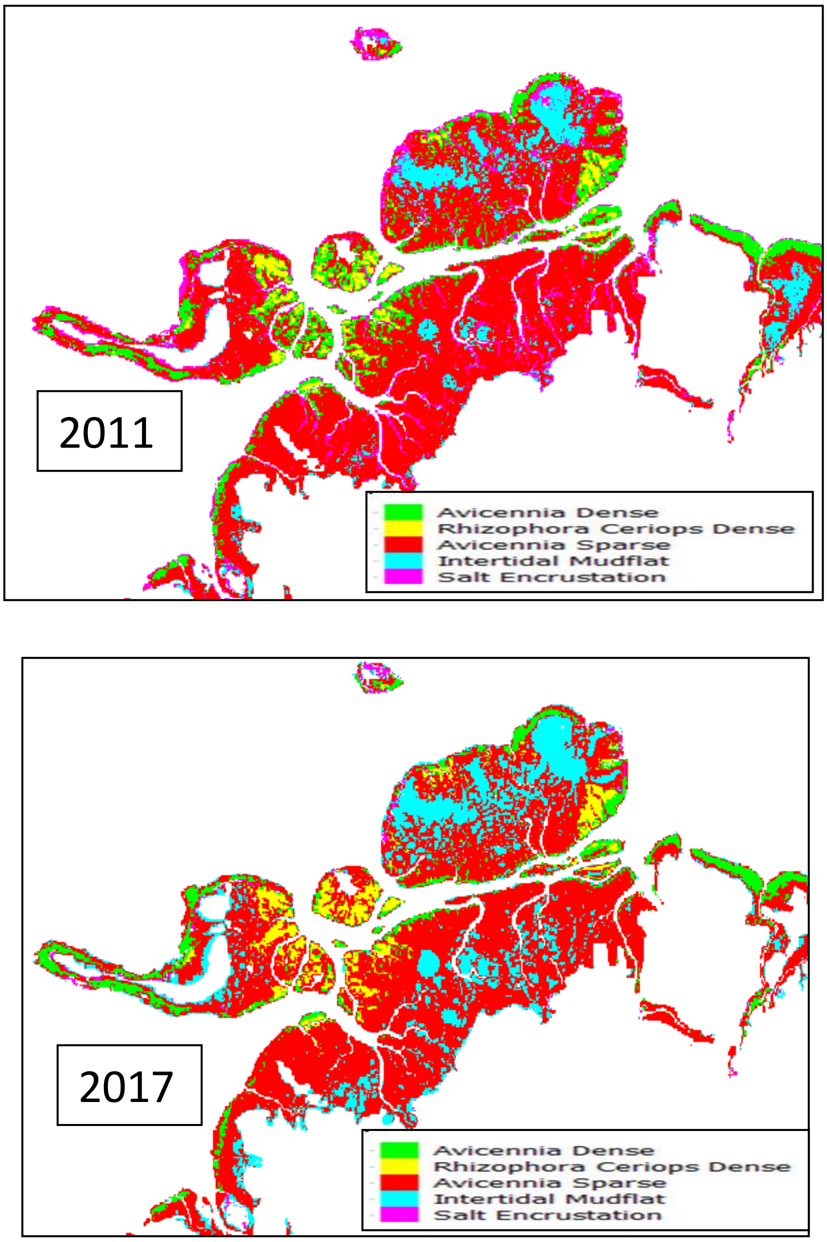

Figure 5.42: Mangrove community zonation covering Core Marine National Park (islands like Piotan, Jindra-Chhad, Mundeka-dideka bet) as per supervised classification of Landsat data of 2011 and 2017

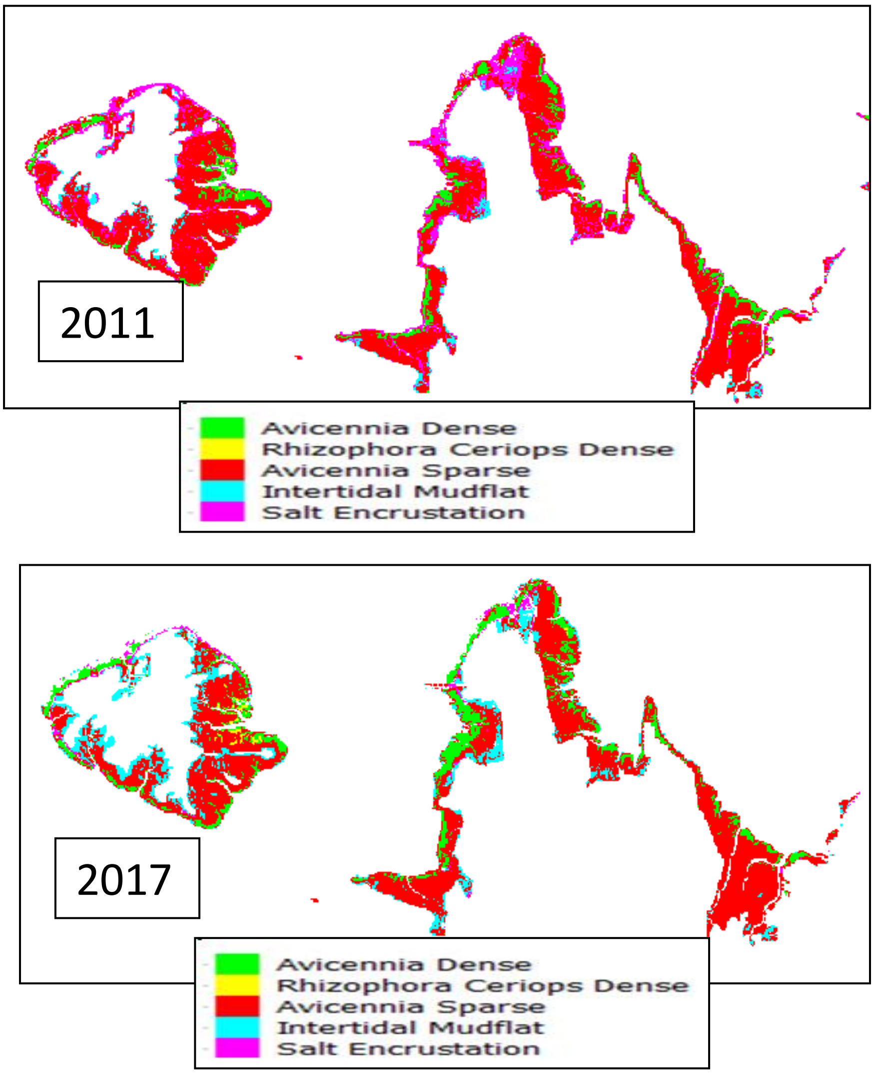

Figure 5.43: Mangrove community zonation covering parts of Marine National Park (Kalubhar and Narara regions) as per supervised classification of Landsat data of 2011 and 2017

Change detection matrix of mangrove communities is shown in Table 5.25. *Rhizophora-Ceriops* community is found on Pirotan, Jindra-Chhad, Mundeka-Dideka, Kalubhar, Bhaidar, Noru and Chank Islands. Majority of mangroves in MNP&S belong to *Avicennia marina*. Small and mixed patches of *A. officinalis* and *A.alba* have also been reported from this region.

Table 5.25: Changes in mangrove area (in sq km) in MNP&S

Year → **Area (sq km)↓**	**2011**	**2017**	**Change (%)**
*Avicennia*Dense	29.52	29.3	-0.74
*Rhizophora-Ceriops*Dense	3.84	5.86	52.64
*Avicennia*Sparse	157.16	182.69	16.24
Total Mangrove	**190.52**	**217.85**	**14.34**

5.6 Discussion

5.6.1 Mangrove classification

The Gulf of Kachchh is a highly energetic macro-tidal system with tidal range reaching upto 7.2 m located in arid to semi-arid environment. It is characterised by the presence of large inter-tidal region and encompasses shoals, islands, creeks, mudflats, mangroves coral reefs etc. *Avicennia marina* is the dominant species at all five regions of GoK, with smaller patches of *Rhizophora mucronata*, *Rhizophora apiculata*, *Acanthus ilicifolius* and *Ceriops tagal* encountered in MNP&S.

Textural and spectral characteristics of the canopy and leaves are the main features employed to differentiate mangrove communities (Ramsey and Jensen, 1996). Their structural appearance depends on several factors, such as species composition, distribution pattern, growth form, density growth, and stand height (Kuenzer et al., 2011). The spectral variations of the canopy reflectance vary as a function of several optical properties, such as leaf area index (LAI), background reflectance, and leaf inclination (Meza Diaz and Blackburn, 2003). The spectral signature of a single species is defined by age, vitality, and phenological and physiological characteristics (Blasco et al., 1998). Periodic climatic changes that influence the leaf dynamics of foliation and leaf senescence may also have an impact on the spectral response (Wang et al., 2008). The optical differences observed among various species is attributed mainly to their biophysical and chemical properties (Figure 5.44) such as water, cellulose, lignin, and protein content, as well as the key leaf pigments chlorophyll a and b and carotenoids (Jones et al., 2004; Kuenzer et al., 2011). The spectral-response signal also depends on the internal leaf structure, which is mainly composed of palisade parenchyma and spongy mesophyll, as well as a number of cell layers, intercellular spaces, air–water interfaces, and cell size (Kuenzer et al., 2011).

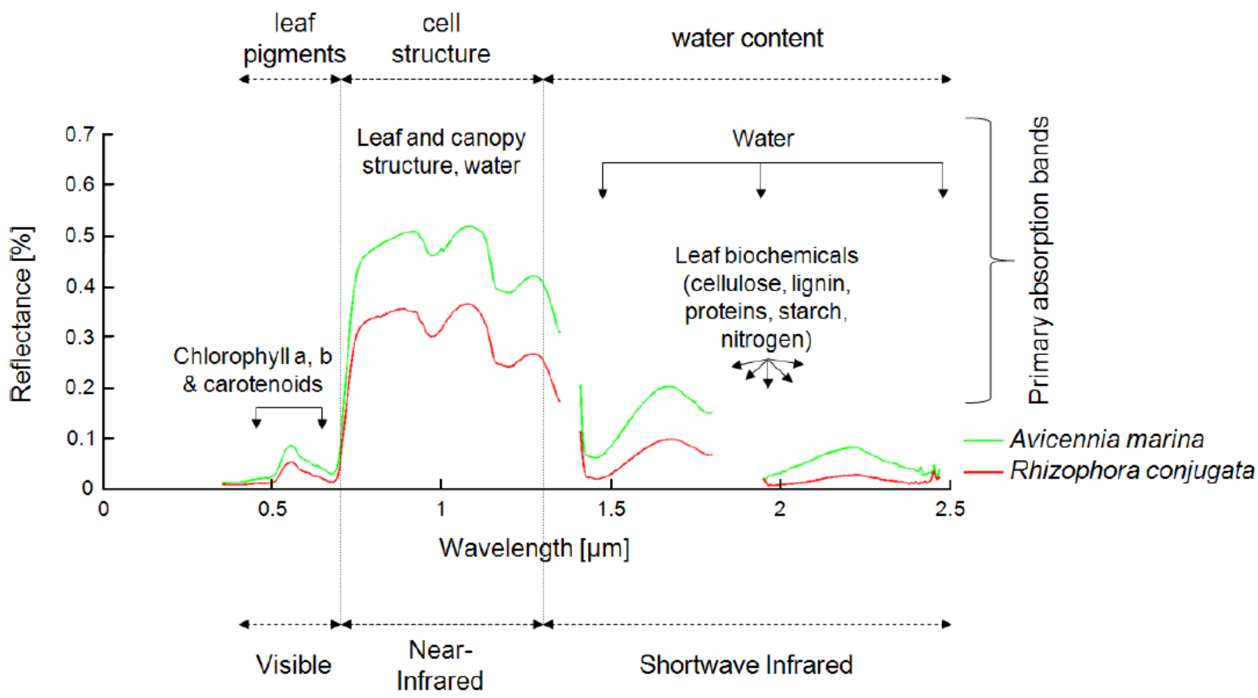

Figure 5.44: Spectral characteristics and their influencing parameters of the mangrove species *Avicennia marina* and *Rhizophora conjugate* as measured with a field spectrometer (Source: Kuenzer et al., 2011)

Additionally, the spectral signal of these plant communities is also influenced by periodic inundation and soil type. In particular, mangroves with lower-stand density are affected more by the changes in the inundation pattern. In Gulf of Kachchh due to high tidal range, the inter-tidal region consisting of large mud flats is regularly inundated due to tidal processes. Mangrove species comprising dominantly of *Avicennia marina* occurs in mud flat regions and along intricate creeks of the inter-tidal regions. In such situation, canopy cover based digital density classification has been observed to be more suitable. Satellite data used are broad channel, medium resolution multispectral data sets best suited for adopting maximum likelihood supervised classification. Based on existing knowledge about various classes in the inter-tidal zone, and understanding of spectral signatures, field visits, seven classes were chosen for supervised classification viz., Mangrove Dense (MD), Mangrove Sparse (MS), Mangrove Degraded (MDeg), Intertidal Mudflat (IM), Subtidal Mudflat (SM), Salt Encrustation (SE) and Sea Water (SW). Class separability has been evaluated using transformed divergence method, which involves computation of spectral distance between signatures of various classes by taking into account their statistical parameters such as mean, variance and covariance. Class separability value is well above the threshold 1700 (i.e., 1823.6 – 2000) for all seven classes used in this study. In fact, mostly the range in near to 2000, except locations where attempt to discriminate mangrove species within MNP&S was made, the value is relatively lower (1823.6). Accuracy assessment for all the classified images shows overall accuracy range 89%-97.64% and corresponding Kappa values ranges 0.87-0.96. Overall this accuracy is acceptable for a medium resolution multispectral data set with an objective of rapid regional change detection as the previous studies have reported 85-90 % accuracy levels (SAC, 2003). A summary of overall accuracy and Kappa coefficient achieved for five different regions for 2011 and 2017 is presented in the Table 5.26. There are limited detailed studies providing classification accuracy for mangrove discrimination in the Gulf of Kachchh using satellite data. Shah et al. (2005) have investigated Jindra and surrounding area (parts of MNP&S) located along southern coast of the Gulf of Kachchh using IRS LISS-III data and classification accuracy achieved is 92 % with Kappa coefficient 0.91 using supervised classification after digital image enhancements such as band ratio and PCA.

Among all five areas Kori creek and Kandla regions have shown relatively higher accuracy ranging from 93.33 to 97.64% with Kappa coefficient ranging between 0.92 to 0.96 whereas the region around Satsaida bet has registered relatively lower accuracies of 89 and 90% with Kappa coefficient values being 0.88 and 0.87. Mostly, the spectral confusion is observed between Mangrove Sparse (MS) and Mangrove Degraded (MDeg). Both these mangrove categories have open spaces comprising of inter-tidal mud flats among the individual plants and therefore changes due to tidal processes influences the overall reflectance received at the sensor.

Table 5.26: Overall accuracy and Kappa coefficient of mangrove classification for the year 2011 and 2017 for five mangrove occupying regions in the Gulf of Kachchh

Mangrove occupying regions in the GoK	**Overall Accuracy**		**Kappa Coefficient**	
	2011	**2017**	**2011**	**2017**
i) around Kori creek along north-west coast	93.33	97	0.92	0.96
ii) around Mundra along northern coast	92.67	89.13	0.91	0.87
iii) around Kandla along northern coast	96.76	97.64	0.96	0.92
iv) around Satsaida bet in north-eastern coast	90.00	89.00	0.88	0.87
v) Marine National Park and Sanctuary (MNP&S) along southern coast of the Gulf of Kachchh	94.50	93.00	0.93	0.91

5.6.2 Mangrove change detection

Spatial changes in different mangrove covered regions of the Gulf of Kachchh during 2011-2017 are given in Table 5.27. The mangrove area comes out to be 963.62 sq km for 2011 and 1218.35 sq km for 2017 for the entire study area. There is an increase of 254.73 sq km of mangrove cover during the period 2011-2017. Changes in Mangrove categories and total mangrove cover in the five region of the Gulf of Kachchh during 2011 and 2017 are depicted in Figure 5.45 and 5.46. Among all five regions, Kori creek and environs and Satsaidabet and environs have shown large changes in dense mangrove cover i.e., increase by about 18 sq km in Kori creek region and decrease by 19.7 sq km in Satsaidabet region. Sparse mangrove cover has increased by 201.8 sq km in Satsaidabet region. Degraded mangrove are not observed in Kandla and Marine National Park & Sanctuary. Satsaida bet and environs have shown maximum reduction in mangrove degraded class by 36.5 sq km.

Table 5.27: Spatial changes in different mangrove covered regions of the Gulf of Kachchh during 2011-2017

Regions covering the Gulf of Kachchh	**Mangrove dense**		**Mangrove sparse**		**Mangrove degraded**		**Total mangrove cover**	
	2011	**2017**	**2011**	**2017**	**2011**	**2017**	**2011**	**2017**
Kori creek and environs	28.59	46.55	193.56	221.01	211.58	214.08	433.73	481.64
Mundra and environs	5.44	4.61	12.91	29.63	1.46	0.77	19.81	35.01
Kandla and environs	6.23	5.89	35.56	54.57	0	0	41.79	60.46
Satsaida bet and environs	39.54	19.80	177.29	379.09	60.95	24.50	277.77	423.39
Marine National Park and Sanctuary	33.36	35.16	157.16	182.69	0	0	190.52	217.85
Total	**113.16**	**112.01**	**576.48**	**866.99**	**273.99**	**239.35**	**963.62**	**1218.35**

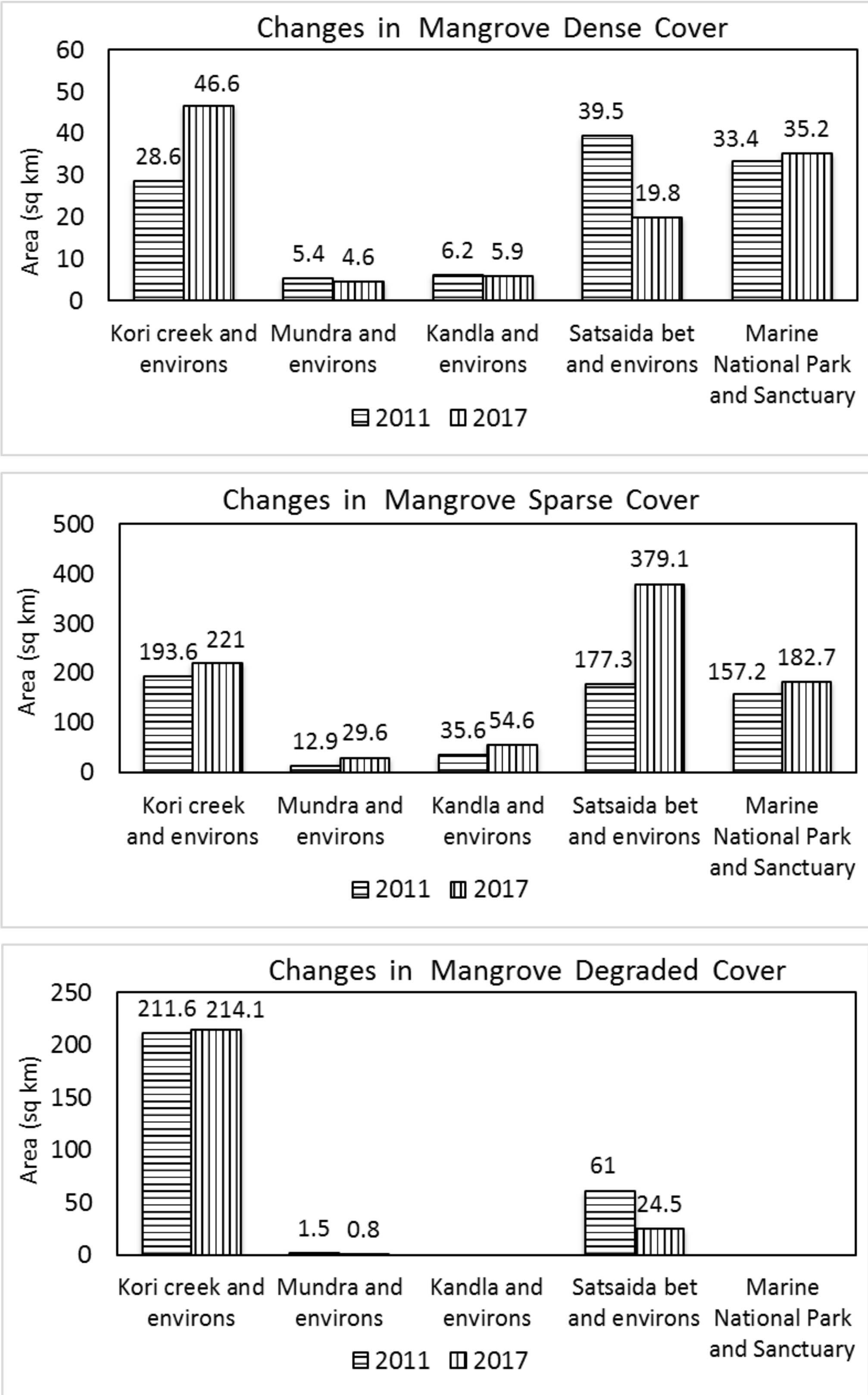

Figure 5.45: Changes in Mangrove categories in the five region of the Gulf of Kachchh during 2011 and 2017

All five regions in the Gulf of Kachchh have shown increase in total mangrove cover during 2011 and 2017 (Figure 5.46). Maximum increase in total mangrove cover is observed in Satsaidabet and environs (145.6 sq km).

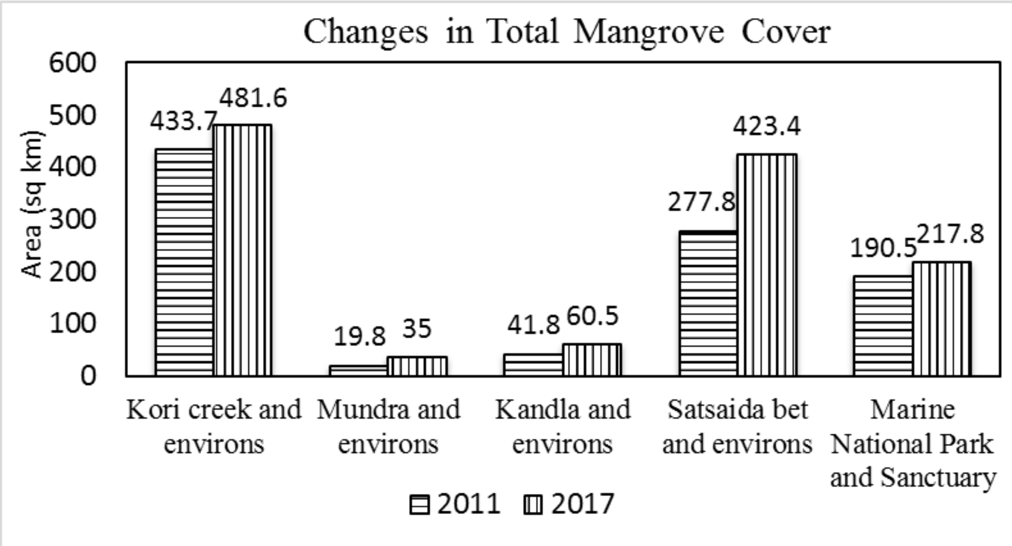

Figure 5.46: Changes in total mangrove cover in the five region of the Gulf of Kachchh during 2011 and 2017

Changes in mangrove cover (in %) for each of the specific region is summarised in Table 5.28. It is noted that Mundra region has shown highest overall improvement of around 76.72 % in mangrove cover and Kori creek has shown lowest improvement of around 11.04 % during 2011 to 2017 among the five study regions in the Gulf of Kachchh. There has been increase in mangrove cover around Satsaida Bet by 52.43% during 2011 to 2017.

Table 5.28: Changes in the mangrove cover (in %) between 2011-2017

Mangrove Area in GoK	Dense	Sparse	Degraded	Total
Kori Creek	62.81	14.81	1.18	11.04
Mundra	-15.25	129.51	-47.26	76.72
Kandla	-5.45	53.45	---	44.67
Satsaida Bet	-49.92	113.82	-59.80	52.43
MNP&S	51.90	16.24	---	14.34

5.6.3 Causes of mangrove dynamics

This study has revealed that there has been a net increase of 254.73 sq km area under mangroves in the Gulf of Kachchh during time frame 2011-2017. Primary reason is due to serious plantation efforts carried out by various agencies such as Gujarat Forest Department, Marine National Park (MNP) authorities, Gujarat Ecology Commission etc. in collaboration with local communities and organizations.

In the Kori creek region, it has been previously reported that total area under mangrove cover was 597.83 sq km in 1990, which was reduced to 407.77 sq km in 2006 (SAC, 2012) and as per this study the area under mangrove cover is 433.73 sq km in 2011 and 481.64 sq km in 2017. Decrease in mangrove cover during 1990 to 2006 is reported to be primarily due to increase in sedimentation (SAC, 2012), while subsequently increase in mangrove cover area is due to plantation efforts as well as natural growth of mangroves.

Mangrove cover in the Kachchh district except Kori creek and environs (includes Mundra and environs, Kandla and environs and Satsaida bet and environs) is reported as 197.55 sq km in 2005-2007 time frame (SAC, 2012), while as per this study area under mangrove cover is 339.37 sq km in 2011 and 518.86 sq km in 2017. Cause of increase in mangrove cover is primarily due to plantation efforts.

Mangrove cover in the MNP&S is reported as 149.62 sq km in 2005-2007 time frame (SAC, 2012), while as per this study area under mangrove cover is 190.52 sq km in 2011 and 217.85 sq km in 2017. Cause of increase in mangrove cover is primarily due to plantation efforts. These plantations were carried out under various schemes such as Cher Plantation, Coastal Border Plantation etc.

There has been lot of developmental activities along the inter-tidal region of Gulf of Kachchh, major ones being development of Ports such as Mundra and massive expansion of salt industry, which led to destruction of mangroves at some locations. However as per this study, efforts and care being taken on mangrove plantation by concerned authorities is delivering positive results and there is substantial increase in mangrove cover during last decade.

Chapter 6

Community Zonation of Mangroves in Marine National Park and Sanctuary (MNP&S), Gulf of Kachchh

Mangrove communities are made up of either one mangrove genus/species or an association of few mangrove genera/species. Such mangrove community zones display distinct spectral behaviour. This chapter provides details of community zonation of mangroves carried out using synergistic employment of optical and SAR data in Jindra-Chhad Island complex of Marine National Park and Sanctuary, Gulf of Kachchh. In this study, the potential of C-band HH RISAT-1 MRS (Medium Resolution ScanSAR mode) data has been explored, in conjunction with Resourcesat-2 LISS-IV (Linear Imaging Self Scanning-IV) data, for identifying mangrove communities in parts of the Marine National Park and Sanctuary (MNP&S) located along the southern coast of the Gulf of Kachchh (GoK) in Jamnagar district, Gujarat, India. Technique and findings reported in this Chapter have been published by the author (Kumar et al., 2017).

6.1 Mangrove community zonation for parts of Marine National Park and Sanctuary (MNP&S), Gulf of Kachchh using optical and SAR data

Here the objective was to evaluate the potentials of optical as well SAR data and develop an approach for improving discrimination of mangrove communities. The study was carried out for mangrove communities of Jindra-Chhad Island complex of MNP&S. Jindra-Chhad island complex is situated in one of the core areas of MNP&S (Figure6.1).

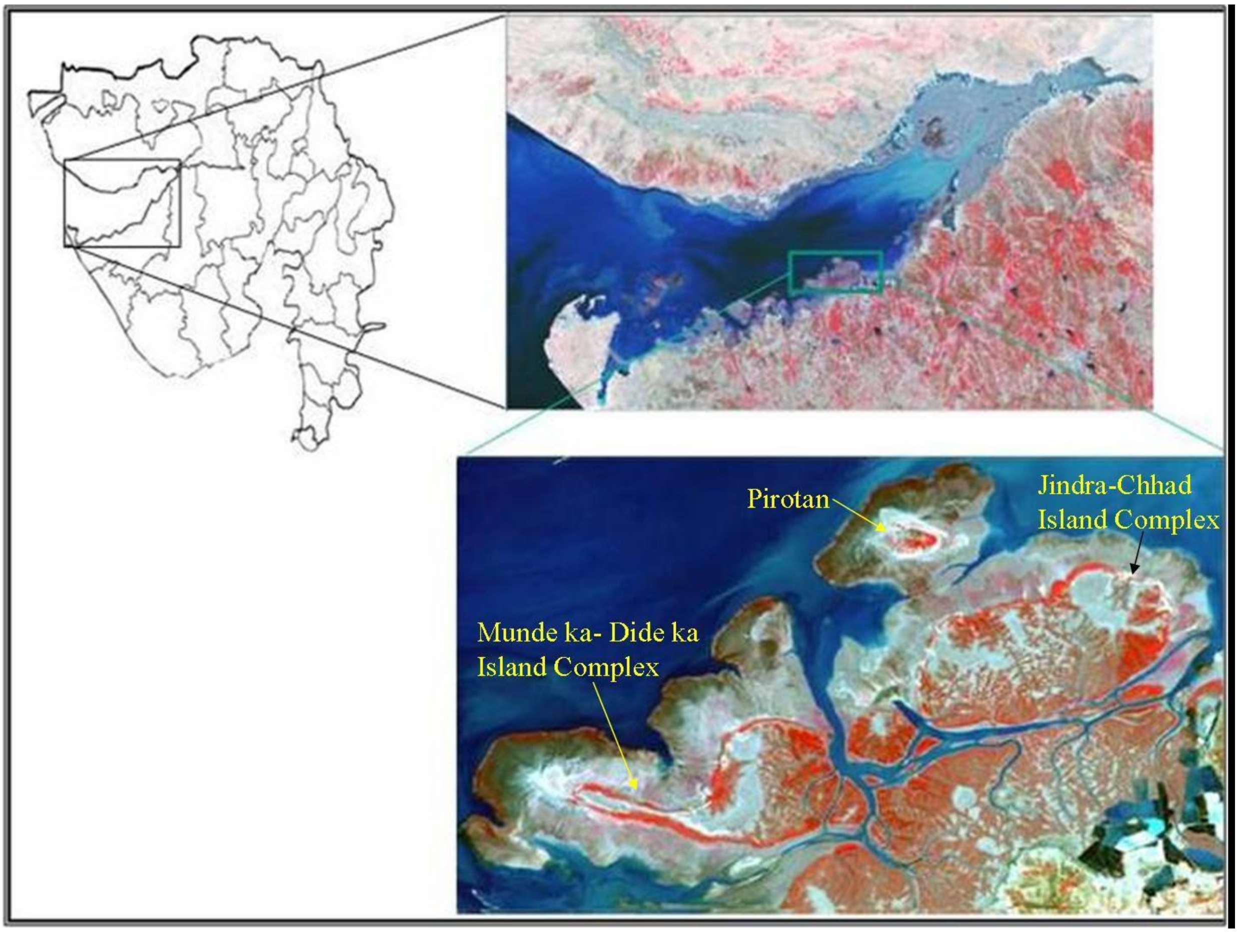

Figure 6.1: Jindra-Chhad Island complex in Marine National Park and Sanctuary, Gulf of Kachchh

Three major mangrove communities have been identified here: *Avicennia* dense, *Rhizophora-Ceriops* dense and *Avicennia* sparse (SAC, 2003; Nayak and Bahuguna, 2001, SAC, 2012, Ajai et al., 2013). *Avicennia* dense occupied the seaward fringing areas having frequent tidal influence, followed by *Avicennia* sparse towards the interior of the island complex. *Rhizophora-Ceriops* community was restricted to relatively sheltered areas along the creek (SAC, 2003).

6.1.1 Mangrove community zonation using LISS-IV data

First of all, an attempt was made to understand spectral characteristics of mangroves communities in the inter-tidal zone based on field observations and existing knowledge. Using the ground photographs (Figure 6.2, 6.3, 6.4,6.5, 6.6) and the maps published by previous studies in this region (Nayak et al., 2003, Shah et al., 2005), the dominant mangrove communities were carefully identified in the satellite images and their reflectance was plotted in the visible and NIR regions. It was observed that '*Avicennia* Dense' [comprising *A. marina, A. officinalis and A.alba* (Nayak et al., 2003)] has highest values in NIR region, followed by '*Rhizophora-Ceriops* Dense'. '*Avicennia* sparse' recorded highest values in Green and Red channels, but lowest in NIR (Figure 6.7).

Figure 6.2: *Avicennia* Dense at Jindra-Chhad, parts of MNP&S, southern coast of Gulf of Kachchh

Figure 6.3: *Rhizophora-Ceriops* Dense at Jindra-Chhadd, parts of MNP&S, southern coast of Gulf of Kachchh

Figure 6.4: Mangrove communities along a creek near Chhad Island, parts of MNP&S, southern coast of Gulf of Kachchh

Figure 6.5: *Rhizophora-Ceriops* Dense, parts of MNP&S, southern coast of Gulf of Kachchh

Figure 6.6: *Rhizophora* plantations in parts of MNP&S, southern coast of Gulf of Kachchh

After signature generation, the LISS-IV data was classified into following categories using theMaximum Likelihood Algorithm (MLA): *Avicennia* Dense (AD), *Avicennia* Sparse (AS), *Rhizophora-Ceriops* Dense (RCD), Intertidal Mudflat (IM), Hightidal Mudflat (HM), Sand and Sea (Figure6.8).

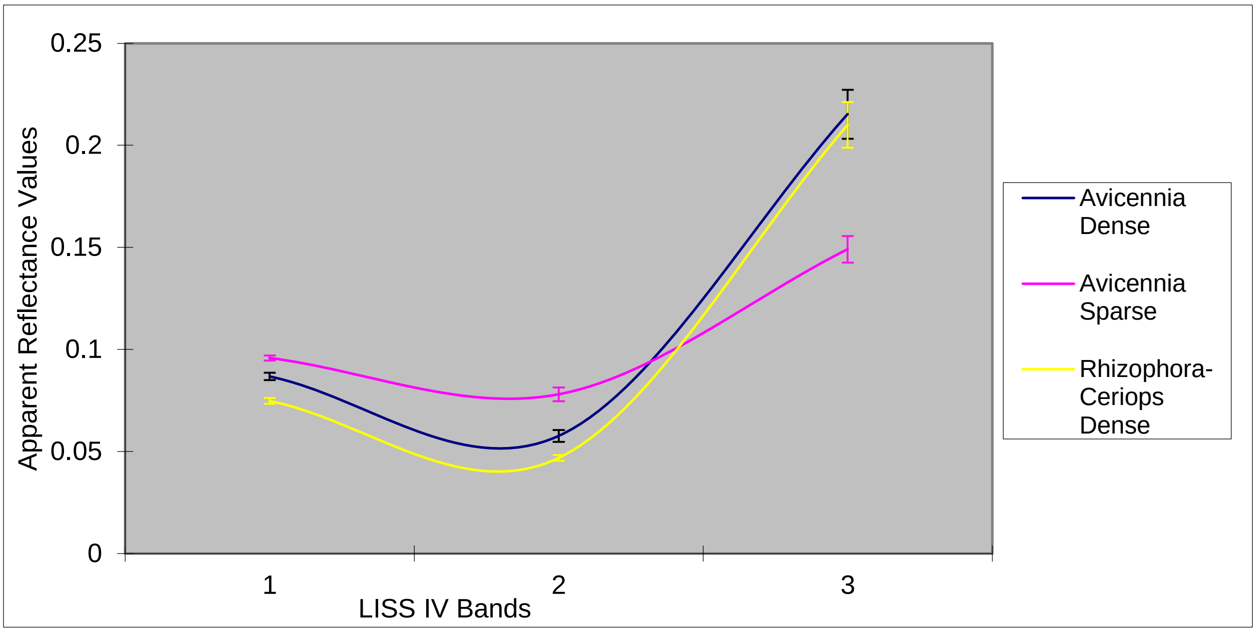

Figure 6.7: Mean spectral reflectance (along with standard deviation bar) of mangrove communities of Jindra-Chhad Island Complex in MNP&S derived from Resourcesat-2 LISS-IV (1= Green, 2= Red, and 3= NIR) data of December 25, 2011.

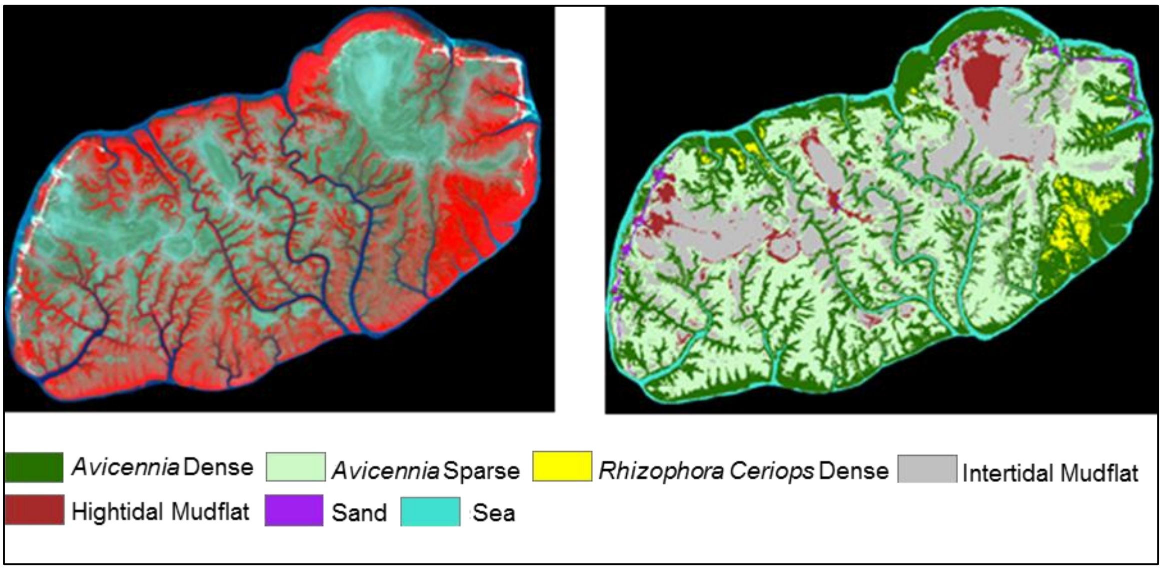

Figure 6.8: Jindra-Chhad Island Complex, as observed in LISS-IV data [NIR (R), Red (G) and Green (B)] (Left) and its classified image (Right) [R=Red, G=Green and B=Blue]

6.1.2 Mangrove community zonation using RISAT-1 SAR data

As the RISAT-1 data was geo-registered with LISS-IV data, the AOI (Area of Interest) polygons, used to generate the signatures for different categories of classification on LISS-IV data, could be employed to study the backscatter values of different communities on RISAT-1 data. Thus the same AOI polygons were used to obtain signatures from RISAT-1 data for various categories under study, which were used to derive signatures from LISS-IV data. It was observed that the three mangrove communities indeed have distinct behaviour in SAR data as represented by the mean backscatter (σ°) plot (Figure 6.9). The classified image of RISAT-1 data is provided in Figure6.10.

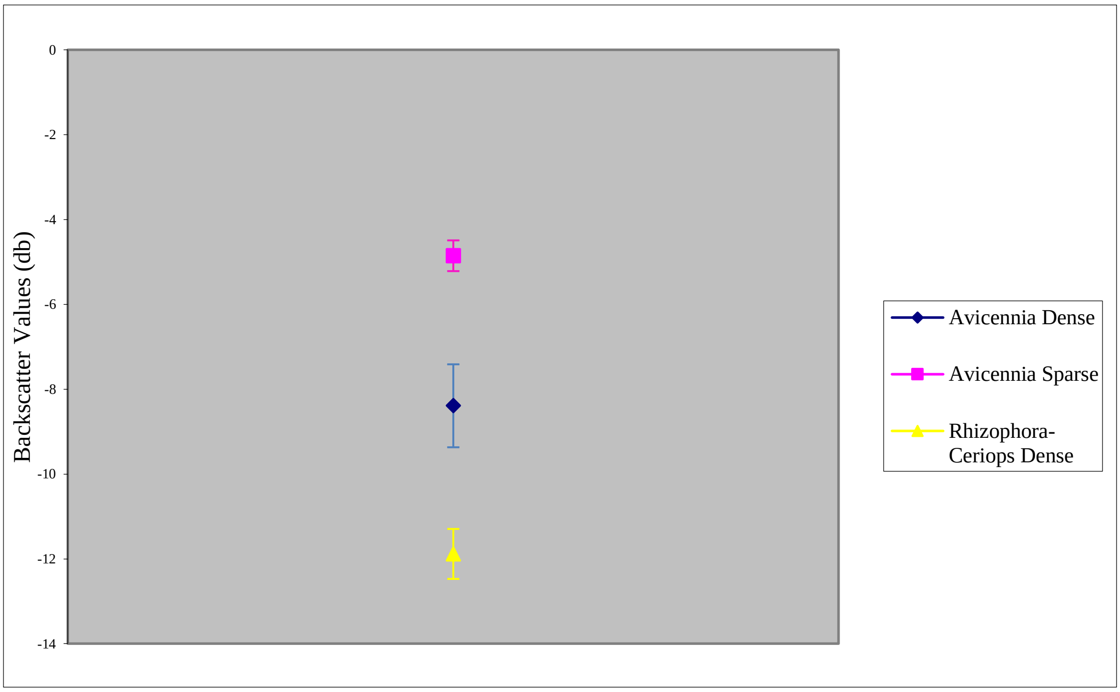

Figure 6.9: Mean backscatter values (σ°) (expressed in db and depicted on Y-axis) with standard deviation bars of major mangrove communities of Jindra-Chhad Island Complex in MNP&S derived from RISAT-1 MRS data of 24 September, 2012.

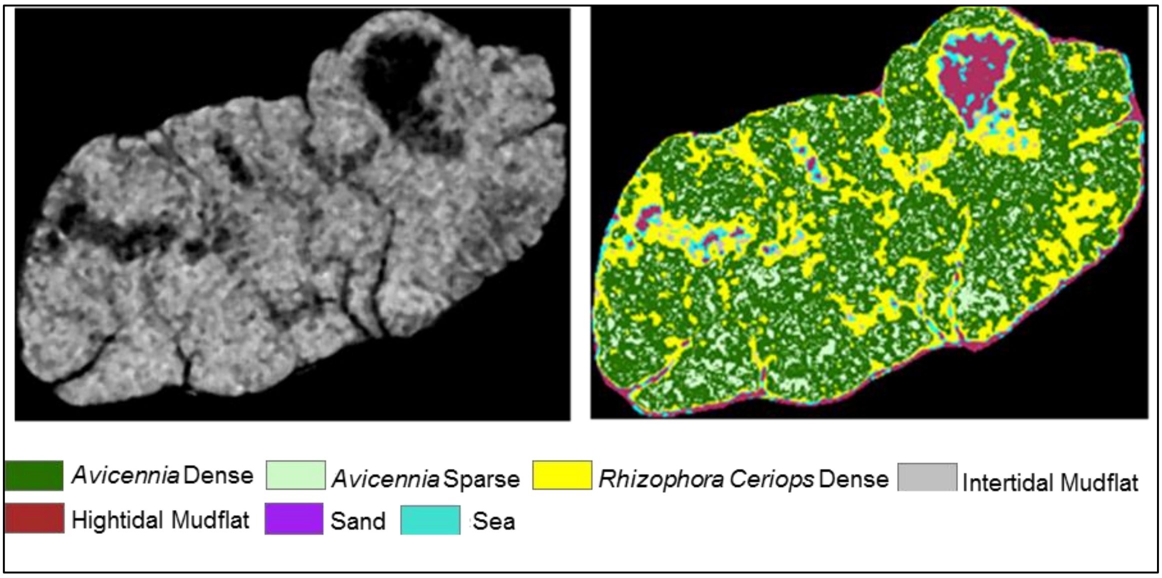

Figure 6.10: Jindra-Chhad Island Complex, as observed in RISAT-1 (Left) and its classified image (Right)

6.1.3 Mangrove community zonation using combined products of LISS-IV and RISAT-1 SAR data

The two data sets, *viz.*, LISS-IV and RISAT-1 were combined together using three different approaches, the results of which are described below.

6.1.3.1 Integrating RISAT-1 SAR and three LISS-IV bands

The geo-registeredsubset of RISAT-1 was layer-stacked as a separate band/layer/channel to the three LISS-IV bands/layers/channels. The three 3-band combinations [False Colour composites(FCC)] possible out of the four available bands, with the condition of having RISAT-1 common to them, were: SAR+NIR+Red, SAR+Red+Green and SAR+NIR+Green (Figure6.11). All these three 3-band combinations were classified into the pre-decided seven categories using Maximum Likelihood Algorithm (Figure 6.11).

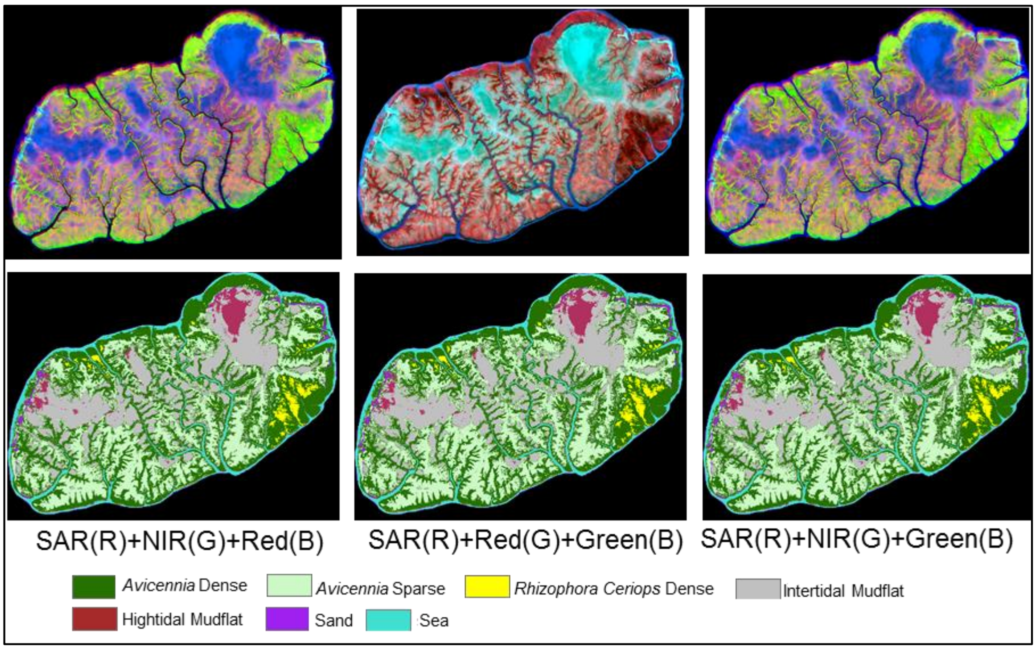

Figure 6.11: The three 3-band combinations of RISAT-1 and LISS-IV (top) and their respective classified images showing mangrove communities (bottom) [R=Red, G=Green and B=Blue]

In addition, the only four band combination, *viz.*, Green+Red+NIR+SAR, was also classified in the similar manner.

6.1.3.2 Merging RISAT-1 SAR and LISS-IV using IHS method

Intensity (I)-Hue (H)-Saturation (S), probably one of the most widely employed techniques to merge two images corresponding to different regions of electromagnetic spectrum, effectively separates the spatial component (I) of an RGB image from its spectral components (H and S). Intensity correspond to the total brightness or total energy of the colour, hue defines the dominant wavelength of the light responsible for the colour, and saturation refers to the purity of the colour relative to white (Mather and Koch, 2011). While merging, one of the three components (I, H or S) of an image is replaced by another image (which is to be merged) and the resulting image is then transformed back to the RGB system of display. Mostly the “I” component is replaced to take advantage of high spatial resolution of the data to be merged, and simultaneously retaining the spectral information of original data. However, in the present study, all the three components, *viz.* I, H and S derived from LISS-IV data, were replaced one-by-one by RISAT-1 data. Thus the three IHS-based combinations generated were: I+H+SAR, H+S+SAR and I+S+SAR (Figure6.12). These three IHS-based combinations were then classified into the seven categories under consideration using Maximum Likelihood Algorithm (MLA).

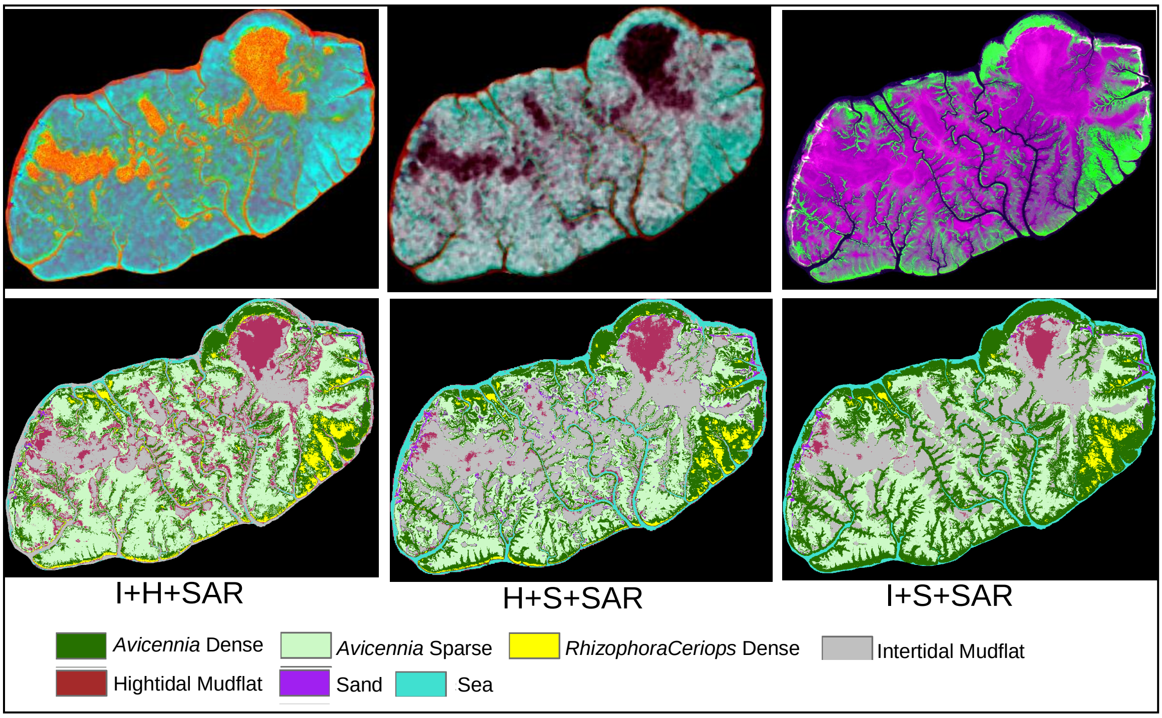

Figure 6.12: Combined products of LISS-IV and RISAT-1 using IHS approach (top), and their classified images (bottom)

6.1.3.3 Integrating RISAT-1 to the band ratios derived from LISS-IV bands

The abstract bands of an optical data may be manipulated with a view to highlight a particular component of the interest in the remotely sensed images. Band ratios are one of the most common ways to study a particular component of the image. A variety of band ratios are found in the literature, some of which are: Simple Ratio (SR), Normalized Difference Vegetation Index (NDVI), Transformed Vegetation Index (TVI), Normalized Difference Water Index (NDWI), Normalized Difference Snow Index (NDSI), Normalized Difference Pond Index (NDPI), Normalized Difference Turbidity Index (NDTI) etc. In the present study, NDVI and Optical Brightness (OB) were the band ratios generated from the LISS-IV bands, which were then layerstacked with RISAT-1 data. NDVI is calculated as [(Reflectance in NIR - Reflectance in Red) / (Reflectance in NIR + Reflectance in Red)] whereas OB is achieved as [(Reflectance in Green + Reflectance in Red) / 2]. NDVI highlights the vegetative component of the image while OB is effective in highlighting the sedimentary component. The combined image of NDVI, OB and SAR is depicted in Figure6.13, along with its classified image.

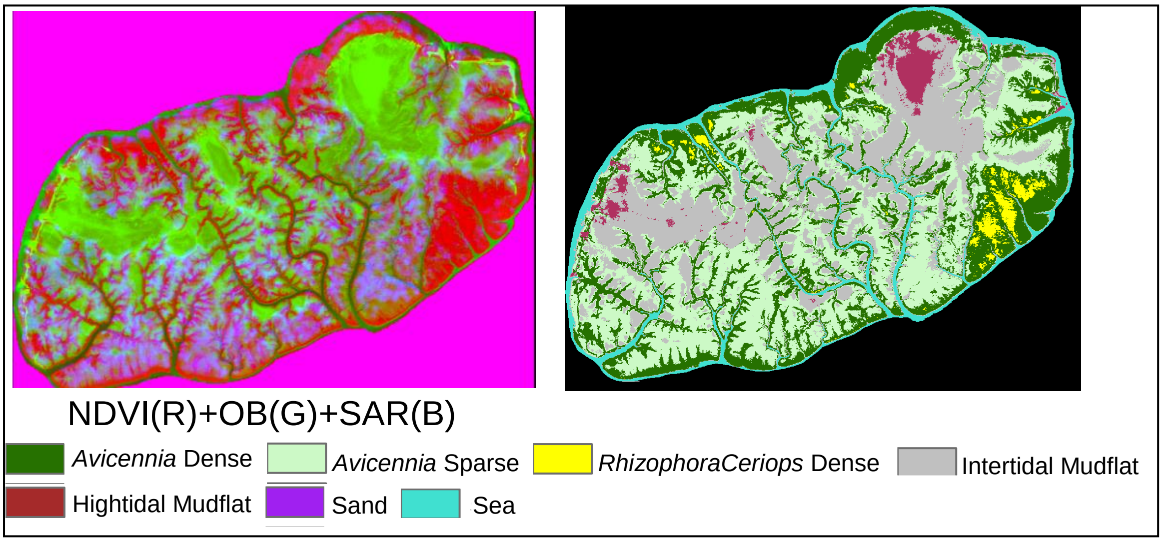

Figure 6.13: Combined product of LISS-IV and RISAT-1 using band ratio approach (left), and its classified image (right) [R=Red, G=Green and B=Blue]

6.2Evaluation of integrated/merged images

6.2.1 Qualitative evaluation

Qualitatively the images were visually inspected with a view to identify the different classes of mangrove communities. Visual interpretation of LISS-IV and RISAT-1 data is described first, and used later in comparative visual evaluation of integrated/merged images.

In the LISS-IV data, mangroves could be delineated into dense and sparse through visual analysis. Dense mangroves (having closed canopies) appear bright red and sparse mangroves (with open canopies) appear pale red in an FCC (NIR, Red and Green displayed as RGB) shown in Figure6.8. However, mangrove communities could not be identified through visual inspection alone. Among the non-mangrove categories, intertidal mudflat could be separated from the hightidal mudflat, as the former appears dark (due to high moisture content) relative to later (Figure6.8). Sand appears white whereas sea water appears blue (Figure6.8), thus making it quite easy to distinguish them from the rest.

The visual distinction among various classes was difficult while interpreting RISAT-1 HH data. Often, there is confusion between mangrove and mudflat categories (Figure6.10). The differentiation between sea, sand and mudflat is also very poor (Figure6.10). Identification of mangrove communities through visual inspection of RISAT-1 data alone seems not possible.Integrating RISAT-1 with LISS-IV bands offers exciting perspective of the region (Figure 6.14).

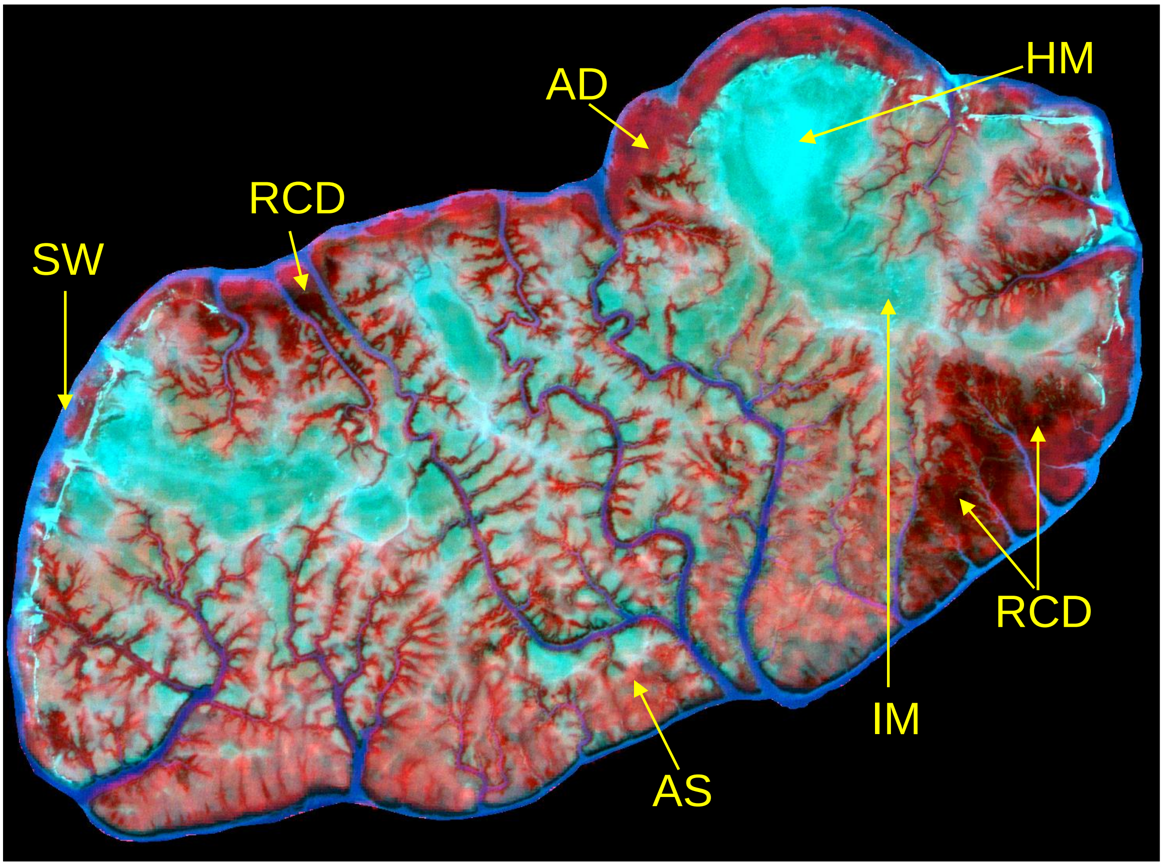

Figure 6.14: Mangrove habitat of Jindra-Chhad island complex, as observed in an FCC prepared by integrating RISAT-1 with Red and Green bands of LISS-IV [SAR(R), Red (G) and Green (B)] (AD=*Avicennia* Dense, AS=*Avicennia* sparse, RCD=*Rhizophora-Ceriops* Dense, IM=Intertidal Mudflat, HM=Hightidal Mudflat, SW=Sea Water)

FCC of SAR, Red and Green displayed in RGB respectively, highlights the various mangrove communities effectively (Figure 6.14).It is observed that dense mangroves could be separated from sparse mangroves. Hightidal mudflat (bright blue) and intertidal mudflat (dark blue) are easily discriminated. However, sand could not be separated from mudflat on the basis of colour only as both appear blue in colour. Integrating RISAT-1 with NIR and Red (Figure6.11), andwith NIR and Green (Figure6.11) does not help in discriminating mangrove communities visually, but dense and sparse mangroves can be demarcated easily. Conclusively, integrating RISAT-1 with Red and Green bands of LISS-IV provides an FCC which appears visually better for our purpose of mangrove community zonation. This may be because, C-band SAR data closely resemble NIR band of optical data in terms of radiometry, image contrast and discernible terrain features (Kushwaha et al., 2000); using RISAT-1 with Red and Green band of LISS-IV data provides more contrast variation and therefore highlights the different communities effectively.

Among the IHS-related combinations, merging RISAT-1 SAR with intensity (I) and saturation (S) derived from LISS-IV data (Figure6.15), offered better discrimination among mangrove habitat categories than merging SAR with, intensity (I) and hue (H) or hue (H) and saturation (S) (Figure6.12). Though the image generated by merging RISAT-1 with I and S, could not provide visual discrimination among mangrove communities, it offered better differentiation among rest of the mangrove habitat categories such as dense and sparse mangroves, sand and mudflat.

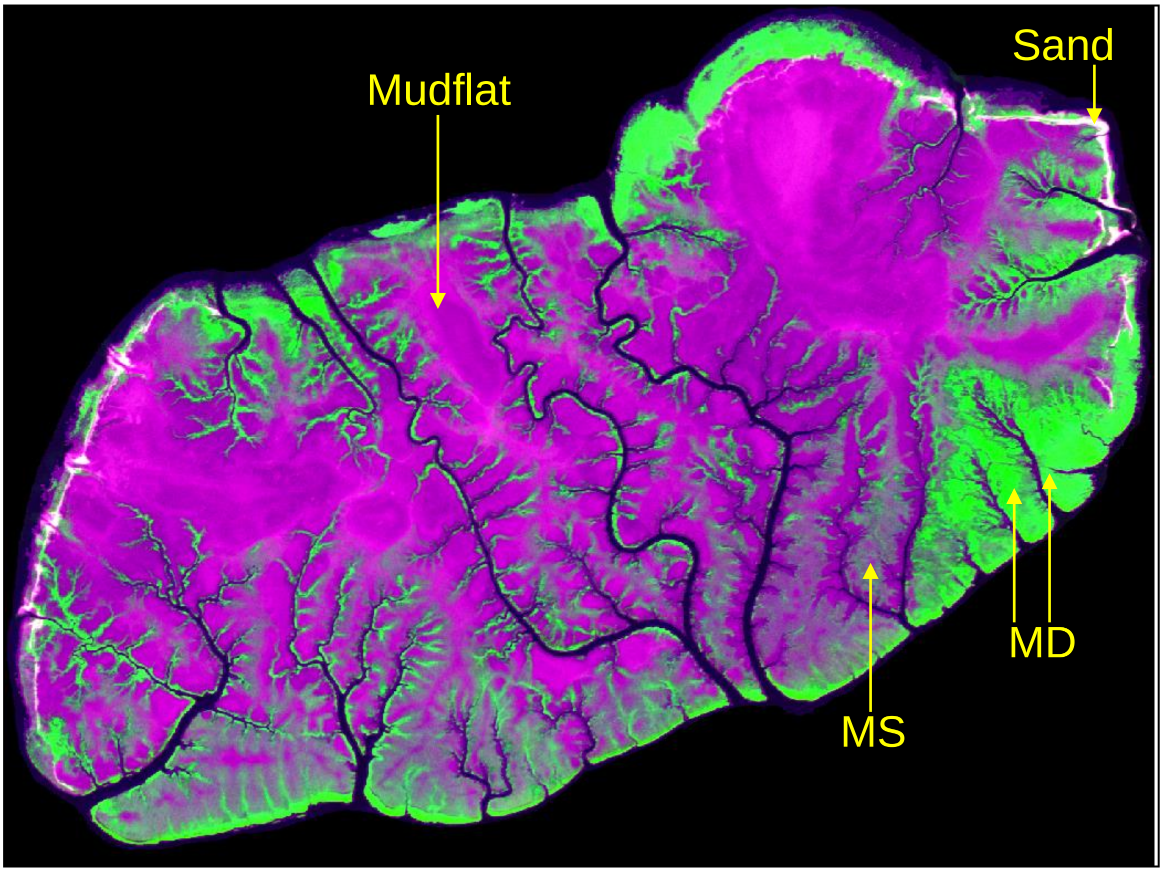

Figure 6.15: Mangrove habitat of Jindra-Chhad island complex, as observed in an image prepared by merging RISAT-1 with Intensity and Saturation derived from LISS-IV data (MD= Mangrove Dense, MS= Mangrove Sparse)

6.2.2 Quantitative evaluation

As the objective of the entire exercise was to study separability/discrimination among the seven categories of classification used (in particular the three mangrove communities), the quantitative evaluation of the images was done through a class separability analysis. For this purpose, Transformed Divergence (TD) algorithm was employed. The advantages associated with the TD algorithm relative to similar other algorithms are:

- It takes into account the mean, variance and covariance of the classes while calculating the inter-class spectral distance whereas other methods such as Euclidean Distance do not.
- It represents the inter-class spectral distance on a transformed scale to enable comparisons from different such exercises.

- This method can work on multiple bands simultaneously, whereas other measures such as M-Statistics can work with only one band at a time.

The idea was to study the performance of a single classifier, in this case MLA, when different inputs are provided to it.

All the classified images obtained from the classification of, RISAT-1, LISS-IV as well as the different combinations of RISAT-1 and LISS-IV, were put to class separability analysis using TD measure. As mentioned previously, the TD analysis provides separability values ranging from 0 to 2000. A separability value above 1700 indicates fairly good separabilityamongthe classes. On the other hand, any value below 1500 is an indication of poor separability between the classes.

This evaluation exercise was performed, on the samples of the seven classification classes (parametric signatures) selected for training the classifier.

6.2.2.1 TD evaluation of parametric signatures

A parametric signature comprises of a set of statistical parameters (such as mean and co-variance matrix) of the pixels. This information is then used to train the classifier for grouping the image pixels into desired set of clusters/classes. The information set comprising the parametric signature include:

- the number of bands in the input image.
- the minimum and maximum data value for each band, for each sample.
- the mean data value for each band, for each sample.
- the covariance matrix for each sample.
- the number of pixels in the sample.

These statistics of parametric signatures were used to compute the TD matrix to evaluate the separability among the various classification categories. A graph showing the comparison of class separability values obtained for various images (individual as well as merged) is shown in Figure6.16.

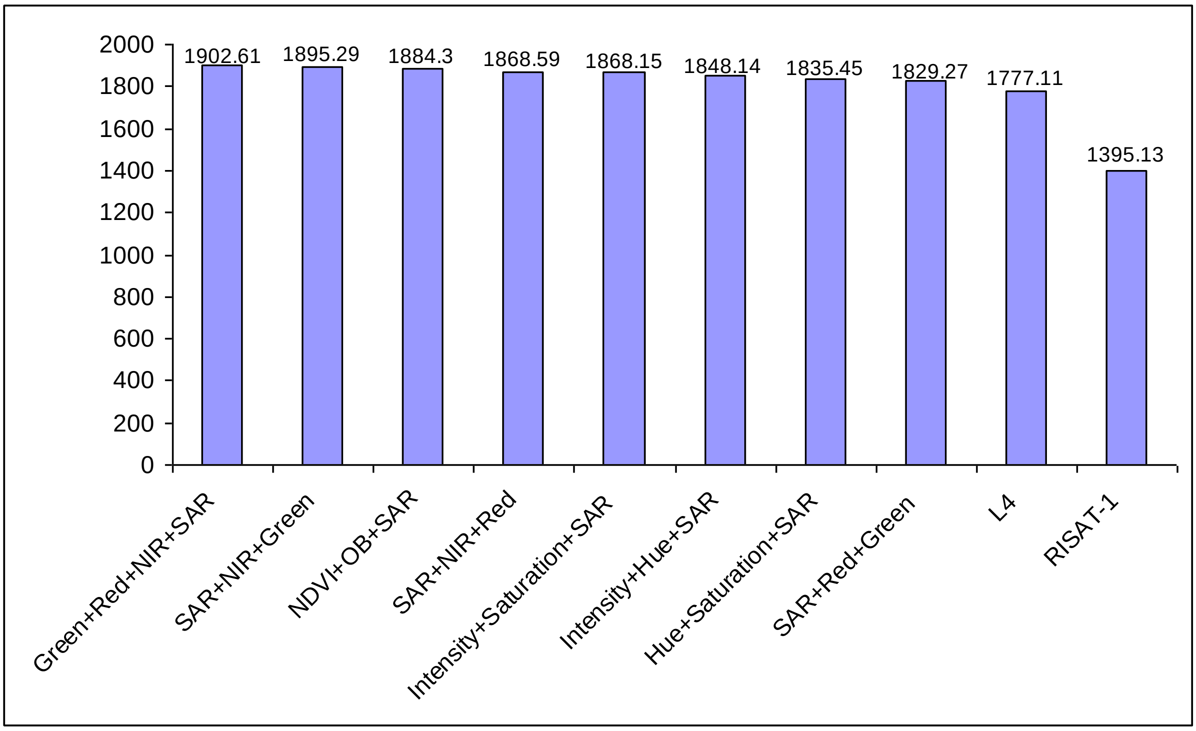

Figure 6.16: Class separability values (from 0 to 2000, depicted on vertical Y-axis) for different images (represented on horizontal X-axis) used in the study for all the seven categories

By looking at the graph, it can be inferred that addition of RISAT-1 significantly improves the class separability. All the combinations employing optical and SAR data, have shown increased class separability compared to either LISS-IV or RISAT-1 when used alone. In addition, when all the four channels (two visible, one NIR and one microwave) are integrated and used together, the separability obtained is highest. This inference suggests that microwave data, in particular the C-band HH data, can be used synergistically with optical data, in the form of an additional band, at least for discrimination of coastal features.

Now, as the prime objective was to evaluate the discrimination among the three mangrove communities of the study area, the TD matrix was also computed for studying the separability among the three mangrove communities. Figure6.17 shows the class separability values obtained employing different images for AD, AS and RCD.

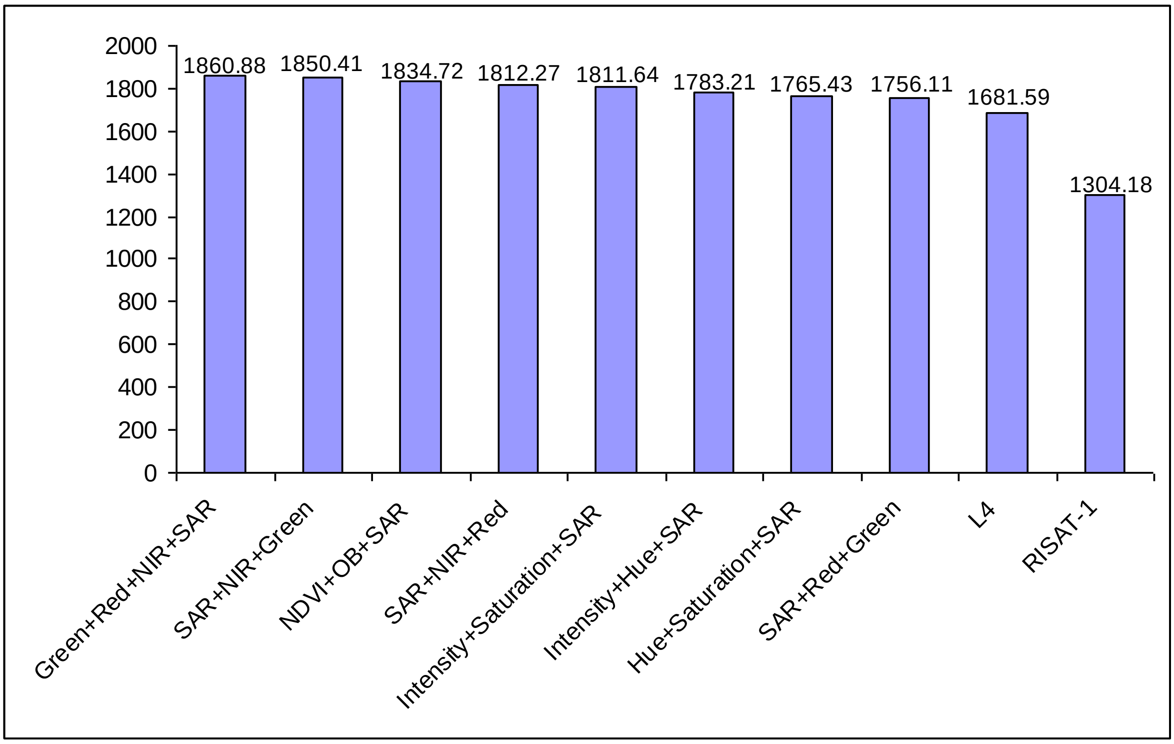

Figure 6.17: Class separability values (from 0 to 2000, depicted on vertical Y-axis) for different images (represented on horizontal X-axis) used in the study for the three mangrove categories, *viz.* AD, AS and RCD

The graph shown above has decreased separability values than that obtained when all the seven classes were used for all the images studied. This is expected as the separability is bound to reduce in case of mangrove communities which behave spectrally similar than the other classes such as mudflat, sand and sea water. However, the trend is identical to what was observed in Figure 6.16. The class discrimination among the three mangrove categories is significantly improved when RISAT-1 data is used synergistically toLISS-IV data. The same trend is observed for AD and AS also (Figure6.18). However, the trend is little altered in case of AD and RCD (Figure6.19), and for AS and RCD (Figure6.20). Though the separation has increased by employing both microwave and optical data, in the case of AD and RCD (Figure6.19) L4 data alone has provided the second best separability value. In the case of AS and RCD (Figure6.20), RISAT-1 has scored slightly better than LISS-IV in terms of separability value. One possible reason for this could be the more sensitive nature of RISAT-1 to the canopy structure of mangroves relative to LISS-IV.

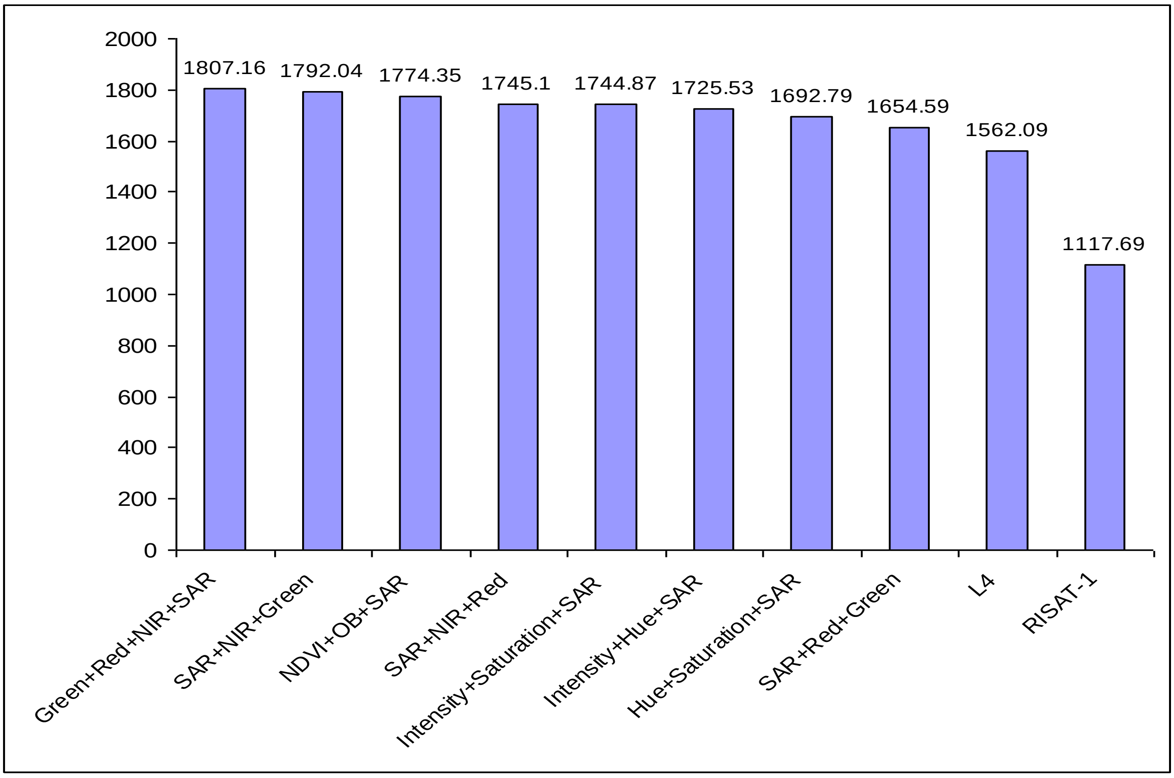

Figure 6.18: Class separability values (from 0 to 2000, depicted on vertical Y-axis) for different images (represented on horizontal X-axis) used in the study for the two mangrove categories, *viz.* AD and AS

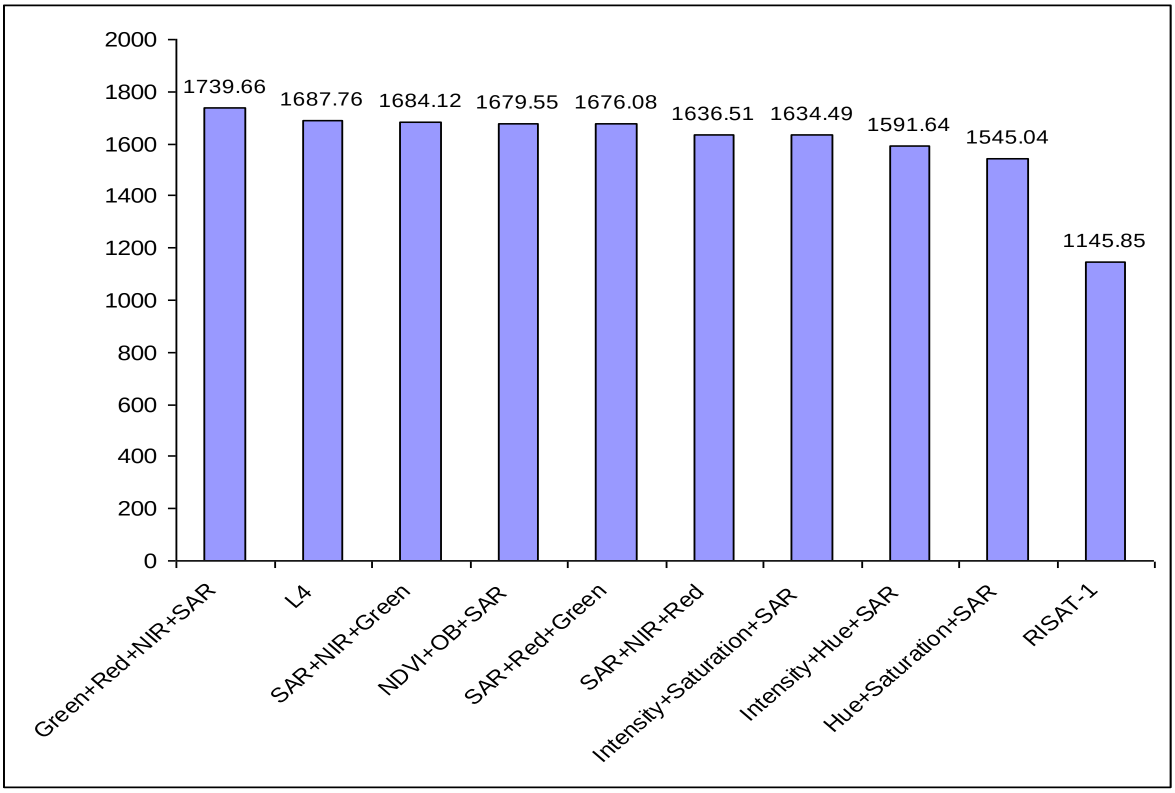

Figure 6.19: Class separability values (from 0 to 2000, depicted on Y-axis) for different images (represented on X-axis) used in the study for the two mangrove categories, *viz.* AD and RCD

Among the IHS-related combinations, in all the TD analyses, combining intensity and saturation obtained from LISS-IV data with RISAT-1 data provided more separability than combining either hue and saturation, or, intensity and hue with RISAT-1 data.

Also worth mentioning is that the band ratio approach yielded better result than IHS-associated approaches, however, simple integration of LISS-IV bands with RISAT-1 provided the highest class separability value.

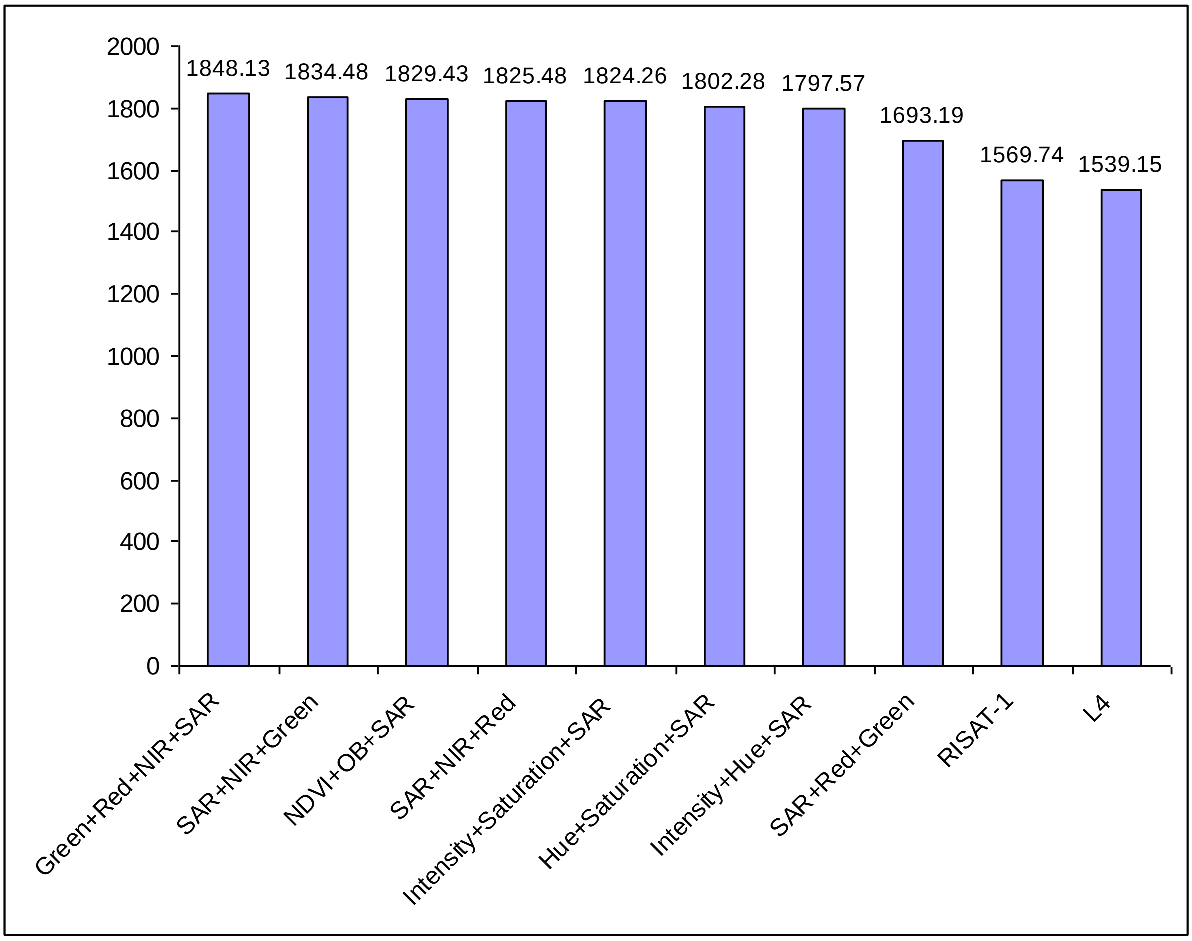

Figure 6.20: Class separability values (from 0 to 2000, depicted on Y-axis) for different images (represented on X-axis) used in the study for the two mangrove categories, *viz.* AS and RCD

6.2.2.2 Accuracy assessment

As the area of the island is small, 20 points were selected per class for assessing the accuracy of classified images (Table 6.1 to 6.10)

Table 6.1: Accuracy assessment of LISS-IV classified image (shown in Figure 6.8)

Classes	**AD**	**RCD**	**AS**	**IM**	**HM**	**Sand**	**Sea**	**Classified Total**	**User's Accuracy (%)**
Avicennia Dense (AD)	18 (90 %)	2 (10 %)	2 (10 %)	0	0	0	0	22	81.81
Rhizophora-Ceriops Dense (RCD)	0	17 (85 %)	0	0	0	0	0	17	100
Avicennia Sparse (AS)	2 (10 %)	1 (5%)	16 (80 %)	2 (10 %)	0	0	0	21	76.19
Intertidal Mudflat (IM)	0	0	2 (10 %)	16 (80 %)	3 (15 %)	0	0	21	76.19
Hightidal Mudflat (HM)	0	0	0	2 (10 %)	17 (85 %)	0	0	19	89.47
Sand	0	0	0	0	0	20 (100 %)	0	20	100
Sea	0	0	0	0	0	0	20 (100 %)	20	100
Reference Total	20	20	20	20	20	20	20	140	
Producer's Accuracy (%)	90	85	80	80	85	100	100		

Overall accuracy = (Number of pixels correctly classified/Total number of pixels used in accuracy assessment) x 100 = (124/140) x 100 = 88.57 %, Kappa Coefficient = 0.87

Table 6.2: Accuracy assessment of RISAT SAR classified image (shown in Figure 6.10)

Classes	**AD**	**RCD**	**AS**	**IM**	**HM**	**Sand**	**Sea**	**Classified Total**	**User's Accuracy (%)**
Avicennia Dense (AD)	5 (25 %)	3 (15 %)	8 (40 %)	10 (50 %)	1 (5%)	6 (30 %)	2 (10 %)	35	14.29
Rhizophora-Ceriops Dense (RCD)	3 (15 %)	6 (30 %)	2 (10 %)	3 (15 %)	1 (5%)	4 (20 %)	1 (5%)	20	30
Avicennia Sparse (AS)	7 (35 %)	4 (20 %)	4 (20 %)	1 (5%)	1 (5%)	0	1 (5%)	18	22.22
Intertidal Mudflat (IM)	3 (15 %)	3 (15 %)	3 (15 %)	2 (10 %)	1 (5%)	0	0	12	16.67
Hightidal Mudflat (HM)	1 (5%)	2 (10 %)	1 (5%)	2 (10 %)	12 (60 %)	3 (15 %)	8 (40 %)	29	41.38
Sand	1 (5%)	2 (10 %)	1 (5%)	1 (5%)	0	4 (20 %)	2 (10 %)	11	36.36
Sea	0	0	1 (5%)	1 (5%)	4 (20 %)	3 (15 %)	6 (30 %)	15	40
Reference Total	20	20	20	20	20	20	20	140	
Producer's Accuracy (%)	25	30	20	10	60	20	30		

Overall accuracy = (Number of pixels correctly classified/Total number of pixels used in accuracy assessment) x 100 = (39/140) x 100 = 27.86 %, Kappa Coefficient = 0.16

Table 6.3: Accuracy assessment of integrated classified image generate by layerstacking Green, Red and NIR bands of LISS IV data with RISAT SAR data

Classes	**AD**	**RCD**	**AS**	**IM**	**HM**	**Sand**	**Sea**	**Classified Total**	**User's Accuracy (%)**
Avicennia Dense (AD)	18 (90 %)	1 (5%)	1 (5%)	0	0	0	0	20	90
Rhizophora-Ceriops Dense (RCD)	0	19 (95 %)	0	0	0	0	0	19	100
Avicennia Sparse (AS)	1 (5%)	0	18 (90 %)	1 (5%)	0	0	0	20	90
Intertidal Mudflat (IM)	1 (5%)	0	1 (5%)	18 (90 %)	0	0	0	20	90
Hightidal Mudflat (HM)	0	0	0	1 (5%)	20 (100 %)	0	0	21	95.24
Sand	0	0	0	0	0	20 (100 %)	0	20	100
Sea	0	0	0	0	0	0	20 (100 %)	20	100
Reference Total	20	20	20	20	20	20	20	140	
Producer's Accuracy (%)	90	95	90	90	100	100	100		

Overall accuracy = (Number of pixels correctly classified/Total number of pixels used in accuracy assessment) x 100 = (133/140) x 100 = 95 %, Kappa Coefficient = 0.94

Table 6.4:Accuracy assessment of integrated classified image generate by layer stacking Green, and NIR bands of LISS IV data with RISAT SAR data (shown in Figure 6.11, right, bottom)

Classes	**AD**	**RCD**	**AS**	**IM**	**HM**	**Sand**	**Sea**	**Classified Total**	**User's Accuracy (%)**
Avicennia Dense (AD)	17 (85 %)	1 (5%)	2 (10 %)	0	0	0	0	20	85
Rhizophora-Ceriops Dense (RCD)	0	19 (95 %)	0	0	0	0	0	19	100
Avicennia Sparse (AS)	2 (10 %)	0	17 (85 %)	1 (5%)	0	0	0	20	85
Intertidal Mudflat (IM)	1 (5%)	0	1 (5%)	18 (90 %)	0	0	0	20	90
Hightidal Mudflat (HM)	0	0	0	1 (5%)	20 (100 %)	0	0	21	95.24
Sand	0	0	0	0	0	20 (100 %)	0	20	100
Sea	0	0	0	0	0	0	20 (100 %)	20	100
Reference Total	20	20	20	20	20	20	20	140	
Producer's Accuracy (%)	85	95	85	90	100	100	100		

Overall accuracy = (Number of pixels correctly classified/Total number of pixels used in accuracy assessment) x 100 = (131/140) x 100 = 93.57 %, Kappa Coefficient = 0.925

Table 6.5:Accuracy assessment of integrated classified image generate by layer stacking Red, and NIR bands of LISS IV data with RISAT SAR data (shown in Figure 6.11, left, bottom)

Classes	**AD**	**RCD**	**AS**	**IM**	**HM**	**Sand**	**Sea**	**Classified Total**	**User's Accuracy (%)**
Avicennia Dense (AD)	17 (85 %)	1 (5%)	2 (10 %)	0	0	0	0	20	85
Rhizophora-Ceriops Dense (RCD)	1 (5%)	18 (90 %)	0	0	0	0	0	19	94.74
Avicennia Sparse (AS)	1 (5%)	1 (5%)	16 (80 %)	2 (10 %)	0	0	0	20	80
Intertidal Mudflat (IM)	1 (5%)	0	2 (10 %)	17 (85 %)	0	0	0	20	85
Hightidal Mudflat (HM)	0	0	0	1 (5%)	20 (100 %)	0	0	21	95.24
Sand	0	0	0	0	0	20 (100 %)	0	20	100
Sea	0	0	0	0	0	0	20 (100 %)	20	100
Reference Total	20	20	20	20	20	20	20	140	
Producer's Accuracy (%)	85	90	80	85	100	100	100		

Overall accuracy = (Number of pixels correctly classified/Total number of pixels used in accuracy assessment) x 100 = (128/140) x 100 = 91.43%, Kappa Coefficient = 0.90

Table 6.6:Accuracy assessment of integrated classified image generate by layer stacking Green, and Red bands of LISS IV data with RISAT SAR data (shown in Figure 6.11, central, bottom)

Classes	**AD**	**RCD**	**AS**	**IM**	**HM**	**Sand**	**Sea**	**Classified Total**	**User's Accuracy (%)**
Avicennia Dense (AD)	17 (85%)	1 (5%)	2 (10%)	0	0	0	0	20	85
Rhizophora-Ceriops Dense (RCD)	1 (5%)	18 (90%)	0	0	0	0	0	19	94.74
Avicennia Sparse (AS)	1 (5%)	1 (5%)	15 (75%)	3 (15%)	0	0	0	20	75
Intertidal Mudflat (IM)	1 (5%)	0	3 (15%)	16 (80%)	0	0	0	20	80
Hightidal Mudflat (HM)	0	0	0	1 (5%)	20 (100%)	0	0	21	95.24
Sand	0	0	0	0	0	20 (100%)	0	20	100
Sea	0	0	0	0	0	0	20 (100%)	20	100
Reference Total	20	20	20	20	20	20	20	140	
Producer's Accuracy (%)	85	90	75	80	100	100	100		

Overall accuracy = (Number of pixels correctly classified/Total number of pixels used in accuracy assessment) x 100 = (126/140) x 100 = 90 %, Kappa Coefficient = 0.88

Table 6.7: Accuracy assessment of integrated classified image generated by merging intensity and hue derived from LISS IV data with RISAT SAR data (shown in Figure 6.12, left, bottom)

Classes	**AD**	**RCD**	**AS**	**IM**	**HM**	**Sand**	**Sea**	**Classified Total**	**User's Accuracy (%)**
Avicennia Dense (AD)	17 (85%)	1 (5%)	1 (5%)	0	0	0	0	19	89.47
Rhizophora-Ceriops Dense (RCD)	2 (10%)	17 (85%)	0	0	0	0	0	19	89.47
Avicennia Sparse (AS)	0	1 (5%)	16 (80%)	3 (15%)	0	0	0	20	80
Intertidal Mudflat (IM)	1 (5%)	1 (5%)	2 (10%)	14 (70%)	2 (10%)	0	0	20	70
Hightidal Mudflat (HM)	0	0	1 (5%)	3 (15%)	18 (90%)	0	0	22	81.82
Sand	0	0	0	0	0	20 (100%)	0	20	100
Sea	0	0	0	0	0	0	20 (100%)	20	100
Reference Total	20	20	20	20	20	20	20	140	
Producer's Accuracy (%)	85	85	80	70	90	100	100		

Overall accuracy = (Number of pixels correctly classified/Total number of pixels used in accuracy assessment) x 100 = (122/140) x 100 = 87.14 %, Kappa Coefficient = 0.85

Table 6.8:Accuracy assessment of integrated classified image generated by merging hue and saturation derived from LISS IV data with RISAT SAR data (shown in Figure 6.12, central, bottom)

Classes	**AD**	**RCD**	**AS**	**IM**	**HM**	**Sand**	**Sea**	**Classified Total**	**User's Accuracy (%)**
Avicennia Dense (AD)	16 (80%)	1 (5%)	1 (5%)	0	0	0	0	18	88.89
Rhizophora-Ceriops Dense (RCD)	1 (5%)	15 (75%)	1 (5%)	0	0	0	0	17	88.23
Avicennia Sparse (AS)	2 (10%)	2 (10%)	15 (75%)	2 (10%)	1 (5%)	0	0	22	68.18
Intertidal Mudflat (IM)	1 (5%)	2 (10%)	2 (10%)	15 (75%)	4 (20%)	0	0	24	62.5
Hightidal Mudflat (HM)	0	0	1 (5%)	2 (10%)	14 (70%)	2 (10%)	1 (5%)	20	70
Sand	0	0	0	1 (5%)	1 (5%)	18 (90%)	0	20	90
Sea	0	0	0	0	0	0	19 (95%)	19	100
Reference Total	20	20	20	20	20	20	20	140	
Producer's Accuracy (%)	80	75	75	75	70	90	95		

Overall accuracy = (Number of pixels correctly classified/Total number of pixels used in accuracy assessment) x 100 = (112/140) x 100 = 80%, Kappa Coefficient = 0.77

Table 6.9:Accuracy assessment of integrated classified image generated by merging intensity and saturation derived from LISS IV data with RISAT SAR data (shown in Figure 6.12, right, bottom)

Classes	**AD**	**RCD**	**AS**	**IM**	**HM**	**Sand**	**Sea**	**Classified Total**	**User's Accuracy (%)**
Avicennia Dense (AD)	17 (85%)	1 (5%)	1 (5%)	0	0	0	0	19	89.47
Rhizophora-Ceriops Dense (RCD)	1 (5%)	16 (80%)	1 (5%)	0	0	0	0	18	88.89
Avicennia Sparse (AS)	1 (5%)	1 (5%)	16 (80%)	2 (10%)	1 (5%)	0	0	21	76.19
Intertidal Mudflat (IM)	1 (5%)	2 (10%)	1 (5%)	16 (80%)	2 (10%)	0	0	22	72.73
Hightidal Mudflat (HM)	0	0	1 (5%)	1 (5%)	16 (80%)	1 (5%)	1 (5%)	20	80
Sand	0	0	0	1 (5%)	1 (5%)	18 (90%)	1 (5%)	21	85.71
Sea	0	0	0	0	0	1 (5%)	18 (90%)	19	94.74
Reference Total	20	20	20	20	20	20	20	140	
Producer's Accuracy (%)	85	80	80	80	80	90	95		

Overall accuracy = (Number of pixels correctly classified/Total number of pixels used in accuracy assessment) x 100 = (117/140) x 100 = 83.57%, Kappa Coefficient = 0. 81

Table 6.10: Accuracy assessment of integrated classified image generated by merging NDVI and optical brightness derived from LISS IV data with RISAT SAR data (shown in Figure 6.13, right)

Classes	**AD**	**RCD**	**AS**	**IM**	**HM**	**Sand**	**Sea**	**Classified Total**	**User's Accuracy (%)**
Avicennia Dense (AD)	19 (95%)	1 (5%)	2 (10%)	0	0	0	0	22	86.36
Rhizophora-Ceriops Dense (RCD)	0	19 (95%)	0	0	0	0	0	19	100
Avicennia Sparse (AS)	1 (5%)	0	16 (80%)	1 (5%)	0	0	0	18	86.89
Intertidal Mudflat (IM)	0	0	1 (5%)	18 (90%)	1 (5%)	0	0	20	90
Hightidal Mudflat (HM)	0	0	1 (5%)	1 (5%)	19 (95%)	0	0	21	90.48
Sand	0	0	0	0	0	20 (100%)	0	20	100
Sea	0	0	0	0	0	0	20 (100%)	20	100
Reference Total	20	20	20	20	20	20	20	140	
Producer's Accuracy (%)	95	95	80	90	95	100	100		

Overall accuracy = (Number of pixels correctly classified/Total number of pixels used in accuracy assessment) x 100 = (131/140) x 100 = 93.57%, Kappa Coefficient = 0.925

A summary of overall accuracy and Kappa coefficient achieved with various datasets for mangrove community zonation is presented in the Table 6.11.

Table 6.11: Summary of overall accuracy and Kappa coefficient obtained using various datasets for mangrove community zonation

Various data sets of classified images showing mangrove community classes	Overall Accuracy	Kappa Coefficient
G+R+NIR+SAR	95.00	0.94
SAR+NIR+Green	93.57	0.93
Band Ratio	93.57	0.93
SAR+NIR+Red	91.43	0.90
SAR+Red+Green	90.00	0.88
optical data	88.57	0.87
I+H+SAR	87.14	0.85
I+S+SAR	83.57	0.81
H+S+SAR	80.00	0.77
SAR data	27.86	0.16

Looking at the above table, it is clear that combining SAR data with optical data is very useful for mangrove community zonation. SAR data alone (C-band HH) is not sufficient for the purpose of mangrove community zonation. Combining SAR with various band ratios derived from optical bands also proved to be useful.

6.3 Discussions

Community zonation of mangroves is an attempt to understand the spatial relationship between mangroves and their immediate environment (Ajai et al., 2013, Blasco et al., 1998, Bahuguna and Nayak, 1996). These communities are made up of either one mangrove genus/species or an association of few mangrove genera/species. Such mangrove community zones display distinct spectral behaviour and the potential of optical (Indian Remote Sensing Satellite) data in discriminating the mangrove communities was earlier demonstrated by

Nayak and Bahuguna (2001), SAC (2003), Shah et al. (2005) and SAC (2012). It was observed that for regions such as Gulf of Kachchh, where mangrove diversity is very low (SAC, 2003, SAC, 2012 and Ajai et al., 2013), utility of moderate resolution optical data is limited because of smaller patches of mangrove species. Their relatively coarser resolution limits discrimination of smaller mangrove patches.

In the Gulf of Kachchh which has predominant distribution of *Avicennia* species, identification and zonation of smaller patches of mangrove communities/species require use of high resolution multi-spectral satellite data (SAC, 2012). Therefore, in this study comparatively, higher resolution data of LISS IV (with spatial resolution of 5.8 m) has been utilised for mangrove community zonation.

Three major mangrove communities/species have been identified in the study area, viz., *Avicennia Dense, Avicennia Sparse* and *Rhizophora-Ceriops Dense* (SAC, 2003, Shah et al., 2005 and SAC, 2012). *Avicennia* zone (dense having >40% canopy closure and sparse having <40% canopy closure) consists of three species, viz., *A. marina*, *A. officinalis* and *A. alba* (Nayak et al. 2003). *Rhizophora-Ceriops* zone comprises of *Rhizophoramucronata* and *Ceriopstagal*, with the latter being the dominant species (Shah et al. 2005). During field visits, same three communities were observed in the Jindra-Chhad island complex in the Gulf of Kachchh.

It was observed that '*Avicennia* Dense' (comprising *A. marina*, *A. officinalis* and *A.alba)* has highest reflectance values in NIR region, followed by '*Rhizophora-Ceriops* Dense'. '*Avicennia* sparse' recorded highest reflectance values in Green and Red channels, but lowest in NIR (Figure 6.7). In visible region, the spectral response is because of pigments present inside the cell; in NIR (Near Infra-Red) region, the spectral behaviour is affected by the anatomy of leaves and how the leaves are stacked one above the other. For sparse mangroves (<40% canopy closure), the reflectance from the muddy substrata also adds to the overall response received at the sensor.

In this study, RISAT-1 C-band SAR data has been integrated with LISS-IV data, which has led to improvement in discriminating the above mentioned classes. In SAR data, the backscatter signal of mangrove ecosystems is influenced by the geometric properties of the stand (canopy closure, canopy geometry, leaf structure, cell structure, stem structure and the underlying surface component and its roughness: soil mudflats water) and dielectric properties which vary depending on the soil moisture, plant moisture, and underlying water surfaces (Kuenzer et al., 2011).

C-band is more sensitive to crown characteristics, (number, density, size and leaf orientation) and canopy structure (architecture and heterogeneity) and has more information about the top canopy part of the mangroves (Figure 6.21). Whereas, the longer L-band microwaves have a greater likelihood of penetrating the foliage and small branches of the upper canopies of the forest and interacting with woody trunk and larger branch components as well as the underlying surface (Lucas et al., 2004) and are extremely useful for biomass estimation. Since the objective here was to map mangrove communities RISAT-1 C-band SAR data could serve the purpose. However, since LISS-IV is limited by its spectral capabilities (it has only three bands, Red, Green and NIR), it has been further demonstrated that synergistic use of optical (LISS-IV) and microwave (RISAT-1 SAR) data is more helpful in mangrove community zonation in low diversity regions of Gulf of Kachchh.

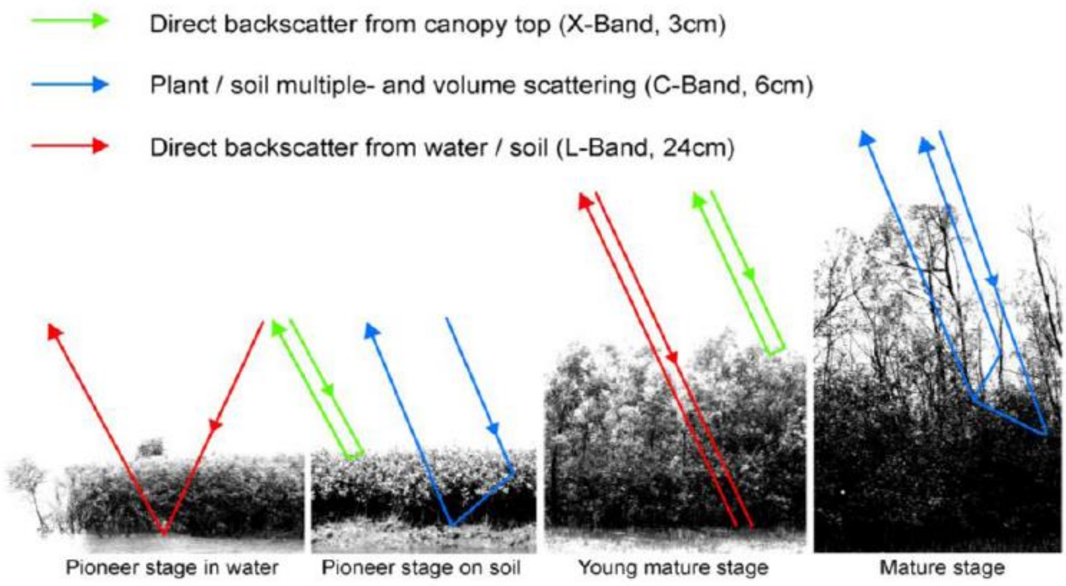

Figure 6.21: Dominating backscatter mechanisms at different stages of mangrove growth depending on bandwidth of the radar beam (Source: Kuenzer et al., 2011)

Integrating RISAT-1 as an additional band to LISS-IV bands has been observed to be extremely useful. In particular, an FCC of SAR, Red and Green displayed in RGB respectively, highlights the various mangrove communities effectively (Fig 6.14). This combination appears visually better for our purpose of mangrove community zonation. RISAT-1 with Red and Green bands of LISS-IV data provides more contrast variation and therefore highlights the different communities effectively. Among the IHS-related combinations, merging RISAT-1 SAR with intensity (I) and saturation (S) derived from LISS-IV data (Figure 6.12) offered better discrimination among mangrove habitat categories than merging SAR with, intensity (I) and hue (H) or hue (H) and saturation (S) (Figure 6.12). Though the image generated by merging RISAT-1 with I and S could not provide visual discrimination among mangrove communities, it offered better differentiation among rest of the mangrove habitat categories such as 'dense and sparse mangroves' and 'sand and mudflat' (Fig 6.15).

Quantitatively also, it was observed that addition of RISAT-1 significantly improves the class separability. All the combinations employing optical and SAR data, have shown increased class separability compared to either LISS-IV or RISAT-1 when used alone. In addition, when all the four channels (two visible, one NIR and one microwave) are integrated and used together, the separability obtained is highest. This inference suggests that microwave data, in particular the C-band HH data, can be used synergistically with optical data, in the form of an additional band, at least for discrimination of coastal features.

Differences in canopy structure resulted in different backscatter responses recorded by the three mangrove communities on RISAT-1 data used in this study (Fig 6.9). However, single band microwave data used here did not provide good mangrove classification using MLC. The possible reason is that classes such as mud flats and mangrove communities having similar surface roughness are getting mixed in single band RISAT-1 SAR data. Another reason could be different spatial resolutions of LISS-IV and RISAT-1 SAR data.

The study demonstrated that the synergistic use of RISAT-1 C-band MRS and Resourcesat-2 LISS-IV data improves mangrove community discrimination. The mangrove communities discriminated are *Avicennia* Dense, *Avicennia* Sparse, and *Rhizophora-Ceriops* Dense in the Marine National Park, Jamnagar, Gujarat. Among the different approaches of merging SAR with optical data, maximum separability among mangrove community classes could be obtained by integrating SAR data with Red, Green and NIR bands of optical data. RISAT SAR data, due to its sensitivity to the canopy geometry and heterogeneity provides detailed information regarding the composition of mangrove communities.

Chapter 7

Conclusions and Future Work

This Chapter summarizes the salient findings and also provides scope of future work.

- This research work has demonstrated efficacy of digital classification techniques using both optical as well microwave satellite data in inventory and monitoring of mangrove cover and community classes of the mangrove covered regions of the Gulf of Kachchh, Gujarat, India and has attempted to understand causes for changes in the mangrove habitats.
- Mangrove cover dynamics has been studied separately for five mangrove occupying regions of the Gulf of Kachchh viz., i) around Kori creek along north-west coast, ii) around Mundra along northern coast, iii) around Kandla along northern coast, iv) around Satsaida bet in north-eastern coast, and v) Marine National Park and Sanctuary (MNP&S) along southern coast of the Gulf of Kachchh.
- The mangroves in the Gulf of Kachchh show spatial variability in extent, composition and condition based on dominant coastal processes, geomorphological setting and amount of protection from anthropogenic influences.

- Maximum likelihood supervised classification has been observed to be useful for classifying dominant mangrove communities based on understanding of spectral properties, evaluation of class separability and accuracy assessment.
- This study has observed that in all the five study regions mentioned above, *Avicennia marina* is the only dominant species, with smaller patches of *Rhizophora mucronata*, *Rhizophora apiculata*, *Acanthus ilicifolius* and *Ceriops tagal*. Therefore, density based mangrove community classes have been taken up viz., mangrove dense (> 40 % canopy cover), mangrove sparse (10-40% canopy cover) and mangrove degraded (<10 % canopy cover). It has been possible to digitally classify mangroves as per density for all the regions.
- Based on existing knowledge about various classes in the inter-tidal zone, and understanding of spectral signatures, field visits, seven classes were chosen for supervised classification viz., Mangrove Dense (MD), Mangrove Sparse (MS), Mangrove Degraded (MDeg), Intertidal Mudflat (IM), Subtidal Mudflat (SM), Salt Encrustation (SE) and Sea Water (SW)
- Class separabilityhas been evaluated using transformed divergence method, which involves computation of spectral distance between signatures of various classes by taking into account their statistical parameters such as mean, variance and covariance and evaluating in a scale of values between 0 to 2000. A separability value above 1700 indicates fairly good separability among the classes, where as any value below 1500 is an indicationof poor separability among the classes. Class separability value iswell abovethe threshold 1700 (i.e., 1823.6 – 2000) for all seven classes used in this study. In fact mostly the range in near to 2000, except locations where attempt to discriminate mangrove species within MNP&S was made, the value is relatively lower (1823.6).
- Accuracy assessment for all the classified images shows overall accuracy range 89%-97.64% and corresponding Kappa values ranges 0.87-0.96.
- Temporal changes in extent and condition of mangrove classes during time frame 2011 and 2017 have been quantified based on the corresponding classified Landsat images.

- The results show that mangrove covered area in the entire Gulf of Kachchh has increased by 254.73 sq km during time frame 2011-2017. Mangrove covered area mapped is 963.62 sq km for 2011 and 1218.35 sq km for 2017 for the entire study area. Out of five regions, Satsaida bet and environs has shown 57.18 % increase, Kori creek and environs 18.81 % increase, Marine National Park and Sanctuary 10.70 % increase, Kandla and environs 7.33 % increase and Mundra and environs 5.98 % increase in mangrove cover. In general, there is decrease in area under degraded mangrove class and increase in area under sparse mangrove class.
- Primary reason of increase in mangrove cover is due to serious plantation efforts carried out by various agencies such as Gujarat Forest Department, Marine National Park (MNP) authorities, Gujarat Ecology Commission etc. in collaboration with local communities and organizations.
- There has been lot of developmental activities along the inter-tidal region of Gulf of Kachchh, major ones being development of Ports such as Mundra and massive expansion of salt industry, which led to destruction of mangroves at some locations prior to 2011, however as per this study, efforts and care being taken on mangrove plantation is resulting into positive results and there is substantial increase in mangrove cover during current decade.
- Most of the mangrove in Kori creek and environs are *Avicennia marina*, with smaller patches of *Rhizophoramucronata*, *Rhizophoraapiculata*,*Acanthusilicifolius* and *Ceriopstagal*. However, in this region due to less canopy cover of other species, only *A. marina* could be classified and mapped.
- There has been an increase of about 48 sq km of mangroves around Kori Creek in 2017 compared to 2011. Dense mangroves have increased by about 18 sq km, sparse mangroves have shown an increase of about 27 sq km and mangroves under degraded class have increased by 2.5 sq km.The increase is more in the category of dense mangroves (63% increase) which reflects concomitant improvement of mangrove density in this region.It seems that due to lot of nutrients being brought out along with the sediments of Indus river and less anthropogenic activities due to its proximity to International border, growth of mangroves in this region is more due to natural processes rather than plantation efforts.

- Long term changes observed using old topographical maps (1965-66), available coastal thematic maps (1989-91) and multi-temporal satellite data of 2001, 2006 and 2010 have shown that mangroves close to Narayan Sarovar-Koteshwar, and those around Sindhodic Creek and Chukh Creek along north-west coast of Gulf of Kachchhhave been damaged.
- Reduction in mangrove cover is due to changes in morphology of islands within creeks, which is primarily due to heavy sedimentation and reworking due to various coastal processes. The region around Lakhpat, Narayan Sarovar-Koteshwar, Godia Creek, Jakhau are experiencing very high erosional ratebecause of high erosion in the area which has even modified shape of the mudflats.
- The study has also observed that natural disasters like cyclones during 1999 and 2001 and associated strong winds coupled with storm surges have considerable damaged mangroves by uprooting the trees and depositing thick layer of sediments on them. However, subsequently, over a period of time mangroves could regenerate
- Mangroves are observed to be growing around Sethwara and Ogata Bet as these areas are relatively sheltered from the influence of dynamic coastal processes.
- The study has also assessed condition of artificially planted mangroves in north-west parts of the Gulf of Kachchh using satellite images. Artificial plantation of mangroves was carried out during the period 2003-06 close to coastal villages of Lakki, Bhangodi and Ashirawandh. An area of 651 hectares (ha) of mangroves was planted by Gujarat Ecology Commission (GEC) at the three sites in collaboration with local communities. Although there has been increase in mangrove cover due to these efforts, the mangrove patch around Kharia Creek at Ashirawand site near Jakhau port could not grow due to anthropogenic pressures.
- The study shows an increase of about 15 sq km of mangroves at Mundra during the period 2011-2017, largely because of approx. 17 sq km of increase in the sparse mangrove category, which is probably result of plantation activities. However, around1sq km of dense mangroves and 0.69 sq km of degraded mangroves were destroyed in this region due to expansion of port-related activities.
- In Kandla region, there has been an increase of roughly 19 sq km of sparse mangroves during 2011 and 2017, which is also probably result of plantation activities. However,

the study has also observed decline of about half sq km of dense mangroves in this region because of port-related activities and construction of saltpans.

- The mudflats around Satsaida bet showed an increase of 145.62 sq km of mangrove during the mapping period of 2011-2017, which is around 57.18 % increase among the five regions studied. Here, the increase is mainly because of increase of 201 sq km of sparse mangroves. This large increaseis due to serious plantation efforts carried out by Gujarat Forest Department in collaboration with local communities and organizations. However, the study also observed reduction of approx. 20 sq km of dense mangroves due to construction of saltpans. The area under ‘mangrove degraded’ category declined by about 36 sq km as their condition improved and they were categorized as sparse mangroves in 2017.
- Mangrove cover in the Marine National Park and Sanctuary (MNP&S), located along southern coast of the Gulf of Kachchh is 190.52 sq km in 2011 and 217.85 sq km in 2017. There has been an increase in mangrove cover of about 27.23 sq km (10.69% among five regions studied). The increase is mainly in *Avicennia*sparse mangrove class (~ 25 sq km). The increase is observed mainly on islands such as Pirotan, Mundeka-Dideka, Kalubhar, Dhani and on coastal belts adjoining Balachadi, Jodiya, near Hansthal Creek and Sikka.Cause of increase in mangrove cover is primarily due to plantation efforts by authorities of the MNP&S. These plantations were carried out under various schemes such as Cher Plantation, Coastal Border Plantation etc.
- An attempt has been made to evaluate potentials of C-band HH RISAT-1 MRS (Medium Resolution ScanSAR mode) data in conjunction with Resourcesat-2 LISS-IV (Linear Imaging Self Scanner-IV) datafor identifying mangrove communities in Jindra-Chhad Island complex located within Marine National Park and Sanctuary (MNP&S), with a primary focus on developing approach for improving discrimination of mangrove communities by synergistic use of multi-sensor data.
- Three different approaches were used to combine the SAR and optical data to explore the synergistic potential of the SAR data with optical data, for discriminating different mangrove communities in the study region.
- The study has carried supervised classification for mangrove community zonation using Maximum Likelihood Classifier i) using LISS-IV data, ii) using RISAT-1 SAR data, iii) Integrating RISAT-1 SAR and three LISS-IV bands, iv) Merging RISAT-1

SAR and LISS-IV using IHS method and v) Integrating RISAT-1 to the band ratios derived from LISS-IV bands and has subsequently evaluated the results qualitatively as well quantitatively.

- All approaches resulted into classified images showing seven classes viz., *Avicennia* Dense (AD), *Avicennia* Sparse (AS), *Rhizophora-Ceriops* Dense (RCD), Intertidal Mudflat (IM), Hightidal Mudflat (HM), Sand and Sea.
- Quantitative evaluation of classified images was done through class separability analysis using transformed divergence method and accuracy assessment.
- The results indicate that addition of RISAT-1 SAR significantly improves the class separability. All the combinations employing optical and SAR data, have shown increased class separability compared to either LISS-IV or RISAT-1 when used alone. In addition, when all the four channels (two visible, one NIR and one microwave) are integrated and used together, the separability obtained is highest.
- All merged/integrated images provided classified images with higher best average class separability values than those obtained by using either optical (1777.11) or SAR (1372.74) data alone.
- The classification obtained using SAR data alone yielded worst class separability value (1372.74) among the various approaches studied.
- Highest class separability value (1898.45) was obtained by classifying the image produced by integrating the SAR data with NIR, Red and Green bands of optical data. Visually also this image was found better in highlighting the mangrove communities.
- Replacing hue with SAR data yielded image that provided better class separability value (1847.51) than replacing either intensity (1811.78) or saturation (1829.72).
- The band ratio approach which segregated the non-vegetative component from the vegetative one in the image, yielded image with relatively lower class separability value (1867.27) than those obtained by integration method, but this approach provided relatively higher class separability value than those obtained by IHS method.
- The study demonstrated that the synergistic use of RISAT-1 C-band MRS and Resourcesat-2 LISS-IV data improves mangrove community discrimination. The mangrove communities discriminated are *Avicennia* Dense, *Avicennia* Sparse, and *Rhizophora-Ceriops* Dense. Among the different approaches of merging SAR with

optical data, maximumseparability among mangrove community classes could be obtained by integrating SAR data with Red, Green and NIR bands of optical data. RISAT SAR data, due to its sensitivity to the canopy geometry and heterogeneity provides detailed information regarding the composition of mangrove communities.

- This study has been constrained as the diversity of mangroves in Gulf of Kachchh is very low. Mostly monospecific stands of *A. marina* comprise the mangrove communities in the Gulf of Kachchh.

Following are suggestions for future work:

- The study provides an approach that should be replicated in more mangrove diverse regions such as Sundarbans in West Bengal or Bhitarkanika National Park in Odisha.
- Polarimetric techniques should be explored for mangrove community zonation.
- Microwaves of different frequencies and polarizations should be combined using different image fusion algorithms with optical, hyperspectral and Lidar data for mangrove community zonation.
- Carbon stock assessments of mangroves at community level should be carried out.
- Climate change impacts on mangroves should be studied. In particular, an assessment or prediction should be made about possible changes in mangrove distribution in the Gulf in response to sea level rise.
- Very high resolution satellite images (spatial resolution close to sub-meter) should be used to identify smaller mangrove patches as well as to improve the mapping accuracies.
- Impact of increase in soil salinity on mangroves should be investigated.
- The co-dependency of mangroves and coral reefs in the MNP&S and the interactions between these coastal habitats existing together should be explored.

References

1. Adhavan, D., et al. “Status of Intertidal Biodiversity of Narara Reef, Marine National Park, Gulf of Kachchh, Gujarat.” *Journal of Marine Biology and Oceanography* 3.3 (2014): 1-2.

2. Ajai, et al. “Mangrove inventory of India at community level.” *National Academy Science Letters* 36.1 (2013): 67-77.

3. Alongi, D.M. “Present state and future of the world’s mangrove forests.” *Environmental Conservation* 29.3 (2002): 331–349.

4. Asbridge, E., et al. “Mangrove response to environmental change in Australia’s Gulf of Carpentaria.” *Ecology and Evolution* 6 (2016): 3523–3539.

5. Aschbacher, J., et al. “An integrated comparative approach to mangrove vegetation mapping using advanced remote sensing and GIS technologies: Preliminary results.” *Hydrologica* 295 (1995): 285-295.

6. Bahuguna A. and S. Nayak. “Mangrove community discrimination using IRS-1C data.” *National Symposium on Remote Sensing for Natural Resources with special emphasis to Water Management.* Pune, India. 1996.

7. Bahuguna, A., et al. *Coastal habitat of selected Marine Protected Areas: Atlas of India*. SAC/RESIPA/MESG/PR/59/2007, Space Applications Centre, Ahmedabad. 2007.

8. Bhatt, J. R. and K. Kathiresan. *Biodiversity of mangrove ecosystems in India*. In: Towards conservation and management of mangrove ecosystem in India, ed. by Bhatt J. R., Macintosh D. J., Nayar T. S., Pandey C. N. and B. P. Nilaratna, IUCN India (2011): 1-34.

9. Benfield, S.L., H. M. Guzman, and J. M. Mair. “Temporal mangrove dynamics in relation to coastal development in Pacific Panama.” *Journal of Environmental Management* 76 (2005): 263-276.

10. Beys-da-Silva, L. Santi, and J .A. Guimaraes. "Mangroves: A threatened ecosystem under-utilized as a resource for scientific research." *Journal of Sustainable Development* 7.5 (2014): 40-51.

11. Binh, T., et al. "Land cover changes between 1968 and 2003 in Cai Nuoc, Ca Mau Peninsula, Vietnam." *Environment, Development and Sustainability* 7 (2005): 519-536.

12. Blasco, F. and M. Aizpuru. "Mangroves along the coastal stretch of Bay of Bengal: present status." *Indian Journal of Marine Science* 31.1 (2002): 9-20.

13. Blasco, F., M. Aizpuru, and C. Gers. "Depletion of the mangroves of continential Asia." *Wetlands Ecology and Management* 9 (2001): 245-256.

14. Blasco, F., M. F. Bellan, and M. U. Chaudhury. "Estimating the Extent of Floods in Bangladesh—Using SPOT Data." *Remote Sensing of Environment* 39 (1992): 167-178.

15. Blasco F., et al. "Recent advances in mangrove studies using remote sensing data, *Marine and Freshwater Research*, 49.4 (1998): 287–296.

16. Campbell, J.B. *Introduction to Remote Sensing*. The Guilford Press, 2007: 667.

17. Cebrain, J. "Variability and control of carbon consumption, export, and accumulation in marine communities." *Limnology and Oceanography* 47 (2002): 11-22.

18. Chakraborty, M., et al. "Initial results using RISAT-1 C-band SAR data." *Current Science* 104.4 (2013): 490-501.

19. Chakravortty, S. "Application of hyperspectral data for development of spectral library of mangrove species in the Sunderban Delta." *International Journal of Geomatics and Geosciences* 4.2 (2013): 305-312.

20. Chakravortty, S., E. Shah, and A.S. Chowdhury. "Application of Spectral Unmixing Algorithm on Hyperspectral Data for Mangrove Species Classification"; in Gupta, P.

and Zaroliagis, C. (Eds) *Applied Algorithms, First International Conference, ICAA* 2014, Kolkata, India, January 13-15, 2014: 223-236.

21. Chakravortty, S and D. Sinha. “Development of higher-order model for nonlinear interactions in hyperspectral data of mangrove forests.” *Current Science* 111.6 (2016): 1055-1062.

22. Chauhan, H.B., et al. *Synergistic application of radar and optical Data for studying the coastal habitats: A case study in Gulf of Kachchh, Gujarat, India*, in RISAT UTILISATION PROGRAMME: Status Report, SAC/EPSA/ATGDG/ATD/RISAT-UP/03/2013: LU12-LU27.

23. Classification accuracy assessment, https://www.e-education.psu.edu/geog883/node/524, page accessed on 09 March 2017.

24. Cohen, J. “A coefficient of agreement for nominal scales.” *Educ. Psych. Measurement* 20.1 (1960): 37-46.

25. Conchedda, G., L. Durieux, and P. Mayaux. “An object-based method for mapping and change analysis in mangrove ecosystems.” *ISPRS Journal of Photogrammetry and Remote Sensing* 63 (2008): 578-589.

26. Congalton, R.G. “A review of assessing the accuracy of classifications of remotely sensed data.” *Remote Sensing of Environment* 37 (1991): 35-46.

27. Congalton R. “Accuracy and validation of remotely sensed and other spatial information.” *International Journal of Wildland Fire* 10 (2001): 321-328.

28. Cornforth, A., et al. “Advanced Land Observing Satellite Phased Array Type L-Band SAR (ALOS PALSAR) to Inform the Conservation of Mangroves: Sundarbans as a Case Study.” *Remote Sensing* 5 (2013): 224-237.

29. Costanza, R., et al. “The value of the world’s ecosystem services and natural capital.” *Nature*, 387 (1997): 253-260.

30. Cougo, M., et al. “Radarsat-2 backscattering for the modeling of biophysical parameters of regenerating mangrove forests.” *Remote Sensing* 7 (2015): 17097–17112.

31. Dale, P.E., A. L. Chandica, and M. Evans. “Using image subtraction and classification to evaluate change in sub-tropical intertidal wetlands.” *International Journal of Remote Sensing* 17 (1996): 703-719.

32. Das S. and R. Vincent. “Mangroves protected villages and reduced death toll during Indian super cyclone.” *Proceedings of National Academy of Sciences of United States of America (PNAS)* (2009): 1-4.

33. Dahdouh-Guebas, F.,et al. “Qualitative distinction of congeneric and introgressive mangrove species in mixed patchy forest assemblages using high spatial resolution remotely sensed imagery (IKONOS)”. *Systematics and Biodiversity* 2 (2005): 113-119.

34. Dahdouh-Guebas, F., et al. “Recent changes in land-use in the Pambala-Chilaw Lagoon complex (Sri Lanka) investigated using remote sensing and GIS: Conservation of mangroves vs. development of shrimp farming.” *Environment, Development and Sustainability* 4 (2002): 185-200.

35. Darmawan, S., et al. “Characterization and spatial distribution of mangrove forest types based on ALOS-PALSAR mosaic 25m-resolution in Southeast Asia.” *8th IGRSM International Conference and Exhibition on Remote Sensing & GIS (IGRSM 2016) IOP Conf. Series: Earth and Environmental Science* 37 (2016): 1-11.

36. Demuro, M. and L. Chisholm. “Assessment of Hyperion for Characterizing Mangrove Communities.” *Proceedings of the 12th JPL AVIRIS Airborne Earth Science Workshop*, Pasadena, CA, USA, 24–28 February 2003.

37. De Santiago, F.F., J. M. Kovacs, and P. Lafrance. “An object-oriented classification method for mapping mangroves in Guinea, West Africa, using multipolarized ALOS PLASAR L-band data.” *International Journal of Remote Sensing* 34.2 (2013): 563-586.

38. Devi, V., et al. “Water and sediment quality characteristics near an industrial vicinity, Vadinar, Gulf of Kachchh, Gujarat, India.” *International Journal of Plant, Animal and Environmental Sciences* 4.3 (2014): 219-226.

39. Dittmar, T., et al. "Mangroves, a major source of dissolved organic carbon to the oceans." *Global Biogeochemical Cycles* 20.1 (2006): 1-7.

40. Dixit, A.M., et al. *Economic valuation of coral reef ecosystem in Gulf of Kachchh.* Gujarat Ecology Commission, Gandhinagar, 2010.

41. Durand, M.J., B. J. Gimonet, and J. R. Perbos. "SAR Data Filtering for Classification." IEE, GE25 5 (1987): 629-637.

42. Dwivedi, R.S., B. R. Rao, and S. Bhattacharya. "Mapping wetlands of the Sundaban Delta and its environs using ERS-1 SAR data." *International Journal of Remote Sensing* 20 (1999): 2235-2247.

43. Evaluating Signatures, https://wiki.hexagongeospatial.com/index.php?title=Evaluating_Signatures, page accessed on 07 March 2017.

44. Everitt, J.H., D. E. Escobar, and F. W. Judd. "Evaluation of airborne video imagery for distinguishing black mangrove (*Avicennia germinans*) on the lower Texas Gulf Coast." *Journal of Coastal Research* 7 (1991): 1169-1173.

45. Everitt, J.H. and F. W. Judd. "Using remote sensing techniques to distinguish and monitor black mangrove (*Avicennia germinans*)." *Journal of Coastal Research 5* (1989): 737-745.

46. Everitt, J.H., et al. "Integration of remote sensing and spatial information technologies for mapping black mangrove on the Texas Gulf Coast." *Journal of Coastal Research* 12 (1996): 64-69.

47. Everitt, J.H., et al. "Evaluation of color-infrared photography and digital imagery to map black mangrove on Texas Gulf Coast." *Journal of Coastal Research* 23 (2007): 230-235.

48. Everitt, J.H., et al. "Using high resolution satellite imagery to map black mangrove on the Texas Gulf Coast." *Journal of Coastal Research* 24 (2008): 1582-1586.

49. Fatoyinbo, T.E. and M. Simard. “Height and biomass of mangroves in Africa from ICESat/GLAS and SRTM.” *International Journal of Remote Sensing* 34.2 (2013): 668-681.

50. Fromard, F., C. Vega, and C. Proisy. “Half a century of dynamic coastal change affecting mangrove shorelines of French Guiana. A case study based on remote sensing data analyses and field surveys.” *Marine Geology* 208 (2004): 265-280.

51. Frost V.S., et al. “A model for RADAR images and its application to adaptive digital filtering of multiplicative noise.” *IEEE Transactions on Pattern Analysis and Machine Intelligence*, PAMI-4.2 (1982): 157-165.

52. FSI. *India State of Forest Report*. Forest Survey of India, Dehra Dun, 2015.

53. Fujimoto, K. “Belowground carbon sequestration of mangrove forests in the Asia Pacific region.” *Proceedings of Asia Pacific Cooperation on Research for Conservation of Mangroves*, Okinawa, Japan, 2000: 87-96.

54. Gang, P.O. and J. L. Agatsiva. “The current status of mangroves along the Kenyan coast: A case study of Mida creek mangroves based on remote sensing.” *Hydrobiologia*, 247 (1992): 29-36.

55. GES. *Ecological profile for coastal talukas of Gulf of Kachchh. Overview. Final Report.* Gujarat Ecological Society, Vadodara, 2014.

56. Gilman, E., et al. “Adapting to Pacific Island mangrove responses to sea level rise and other climate change effects.” *Climate Research* 32 (2006): 161–176.

57. Giri, C. P. and J. P. Delsol. “Mangrove forest cover mapping in Phangnga Bay, Thailand, Using SPOT HRV and JERS-1 data in conjunction with GIS.” *International Seminar on Remote Sensing for Coastal Zone and Coral Reef Applications*, Bangkok, Thailand, 25 October–1 November 1993.

58. Giri C., et al. “Status and distribution of mangrove forests of the world using earth observation satellite data.” *Global Ecology and Biogeography*, 20 (2011): 154-159.

59. Govender, M., K. Chetty, and H. Bulcock. “A review of hyper-spectral remote sensing and its application in vegetation and water resource studies.” *Water S.A* 33.2 (2007):145-151.

60. Green, E.P., et al. “Remote sensing techniques for mangrove mapping.” *International Journal of Remote Sensing*, 19 (1998): 935-956.

61. GUIDE. *Final Environmental Impact Assessment (EIA) Report for Port based Multiproduct SEZ at Kandla Port, Kachchh district, Gujarat*. Report prepared by Gujarat Institute of Desert Ecology (GUIDE). 2015.

62. Gupta M.C., et al. *Coastal Zone Information System – Gujarat*, Technical Report, SAC/RESA/MWRD/TR/04/2000: 32.

63. Held, A., et al. “High resolution mapping of tropical mangrove ecosystems using hyperspectral and radar remote sensing.” *International Journal of Remote Sensing*, 24.13 (2003): 2739-2759.

64. Hirano, A., M. Madden, and R. Welch. “Hyperspectral image data for mapping wetland vegetation.” *Wetland* 23 (2003): 436-448.

65. Huang Y. and J. L. Van Genderen. “Evaluation of several speckle filtering techniques for ERS-1 & 2 imagery.” *International Archives of Photogrammetry and Remote Sensing*, XXXI (B2) (1996): 164-169.

66. Hue, Saturation and Intensity, http://www.colorado.edu/physics/phys1230/phys1230_fa01/topic45.html, page accessed on 24 Feb 2017.

67. ICMAM. *Geographical Information System for the Gulf of Kachchh*. Technical Report. Integrated Coastal and Marine Area Management, Chennai, 2002.

68. Inam A., et al. *The geographic, geological and oceanographic settings of the Indus River*, in Large Rivers: Geomorphology and Management (Ed. A. Gupta) (2008): 333-346.

69. Ingle, K.K., et al. *An Account of Lichen Diversity in Islands of Marine Protected Area, Jamnagar, Gujarat*. Paper presented at the conference “Island Biodiversity

(International Day for Biological Diversity)", Uttar Pradesh State Biodiversity Board, Lucknow. 2014. 23-30.

70. IRADe. *Review of Marine National Park, Jamnagar: Evolving Vision Statement for Management of MNP*. Project Report, published by Integrated Research and Action for Development (IRADe), New Delhi. 2016.

71. IRS-P6, https://earth.esa.int/web/guest/missions/3rd-party-missions/current-missions/irs-p6, page accessed on 01 March 2017.

72. Jagtap, T.G., V. S. Chavan, and A. G. Untawale. "Mangrove Ecosystems of India: A Need for Protection." *Ambio*, 22.4 (1993): 252-254.

73. Jennerjahn, T.C. and V. Ittekot. "Relevance of mangroves for the production and deposition of organic matter along tropical continental margins." *Naturwissenschaften*, 89.1 (2002): 23-30.

74. Jensen, J. R. *Introductory Digital Image Processing: A Remote Sensing Perspective*. Englewood Cliffs, New Jersey: Prentice-Hall. 1986.

75. Jones, J., et al. "Changes in distribution of grey mangrove *Avicennia marina* (Forsk.) using large scale aerial color infrared photographs: Are changes related to habitat modification for mosquito control?" *Estuarine Coastal and Shelf Science* 61 (2004): 45-54.

76. Joseph, G. *Fundamentals of Remote Sensing*. Universities Press, Hyderabad, India. 2003.

77. Kairo, J.G., B. Kivyatu, and N. Koedam. "Application of remote sensing and GIS in the management of mangrove forests within and adjacent to Kiunga Marine Protected Area, Lamu, Kenya." *Environment, Development and Sustainability* 4 (2002): 153-166.

78. Kamal, M. and S. Phinn. "Hyperspectral data for mangrove species mapping: A comparison of pixel-based and object-based approach." *Remote Sensing* 3 (2011): 2222-2242.

79. Kamboj, R.D. "Biology and status of seagrasses in Gulf of Kachchh Marine National Park and Sanctuary, India." *Indian Ocean Turtle Newsletter* 19 (2014): 8-11.

80. Kanniah, K.D., et al. "Satellite images for monitoring mangrove cover changes in a fast growing economic region in Southern Peninsular Malaysia." *Remote Sensing* 7 (2015): 14360-14385.

81. Kanniah, K.D., et al. "Per-pixel and sub-pixel classifications of high-resolution satellite data for mangrove species mapping." *Applied GIS* 3 (2007): 1-22.

82. Kathiresan, K. "Importance of Mangrove Ecosystem." *International Journal of Marine Science* 2.10 (2012): 70-89.

83. Kovacs, J.M., et al. "The use of multipolarized spaceborne SAR backscatter for monitoring the health of a degraded mangrove forest. *Journal of Coastal Research* 24.1 (2008): 248 – 254.

84. Kovacs, J.M., et al. "Estimating leaf area index of a degraded mangrove forest using high spatial resolution satellite data." *Aquatic Botany* 80 (2004): 13-22.

85. Kovacs, J.M., et al. "Assessing relationships between Radarsat-2 C-band and structural parameters of a degraded mangrove forest." *International Journal of Remote Sensing* 34 (2013): 7002–7019.

86. Kovacs, J.M., et al. "Applications of ALOS PALSAR for monitoring biophysical parameters of a degraded black mangrove (*Avicennia germinans*) forest." *ISPRS Journal of Photogrammetry and Remote Sensing* 82 (2013): 102–111.

87. Kovacs, J.M., C. V. Vandenberg, and F. Flores-Verdugo. "Assessing fine beam RADARSAT-1 backscatter from a white mangrove (*Laguncularia racemosa* (Gaertner)) canopy." *Wetlands Ecology and Management* 14 (2006): 401-408.

88. Kovacs, J.M., J. Wang, and F. Flores-Verdugo. "Mapping mangrove leaf area index at the species level using IKONOS and LAI-2000 sensors for the Agua Brava Lagoon, Mexican Pacific." *Estuarine Coastal and Shelf Sciences* 62 (2005): 377-384.

89. Kuenzer, C., et al. “Remote sensing of mangrove ecosystems: a review.” *Remote Sensing* 3 (2011): 878-928.

90. Kumar, Mohit, et al. “Application of remote sensing and GIS techniques in understanding changes in mangrove cover in parts of Indus delta around Kori Creek, Gujarat, India. *Journal of Environmental Research and Development*, 7.1A (2012): 504-511.

91. Kumar, Mohit, et al. “Monitoring Marine Protected Areas (MPAs) using Geomatics: A case study in Gulf of Kachchh, Gujarat, India”. *ISG Newsletter (special issue on Marine and Coastal Dynamics)* 19.3 (2013): 56-62.

92. Kumar, Mohit, et al. “Study of mangrove communities in Marine National Park and Sanctuary, Jamnagar, Gujarat, India, by fusing RISAT-1 SAR and Resourcesat-2 LISS-IV images.” *International Journal of Image and Data Fusion* 8.1 (2017a): 73-91.

93. Kumar, Mohit, et al. “Changing landscape of Marine National Park & Sanctuary, Gulf of Kachchh: Ecological assessment of mangroves and coral reefs.” *Proceedings of National Academy of Sciences India Section A Physical Sciences (special issue on Remote Sensing)* 87.4 (2017b): 889-900.

94. Kumar, Mohit, A. S. Rajawat, and Ajai. “Mangrove cover dynamics in Kachchh, Gujarat, India”. *Proceedings of 38th Asian Conference on Remote Sensing*. Delhi, India. 2017.

95. Kumar, T., et al. “Classification of floristic composition of mangrove forests using hyperspectral data: case study of Bhitarkanika National Park, India.” *Journal of Coastal Conservation* 17.1 (2013): 121-132.

96. Kunte P. D., B. G. Wagle, and Y. Sugimori. “Sediment transport and depth variation study of the Gulf of Kachchh using remote sensing.” *International Journal of Remote Sensing* 24 (2003): 2253-2263.

97. Kushwaha, S.P.S., R. S. Dwivedi, and B.R.M. Rao. “Evaluation of various digital image processing techniques for detection of coastal wetlands using ERS-1 SAR data.” *International Journal of Remote Sensing* 21.3 (2000): 565-579.

98. Lee, J.S. “Digital Image Smoothing and Sigma Filter.” *Computer Vision Graphics and Image Processing* 17 (1983): 24-32.

99. Lee, T. M. and H. C. Yeh. “Applying remote sensing techniques to monitor shifting wetland vegetation: A case study of Danshui River estuary mangrove communities, Taiwan.” *Ecological Engineering* 35 (2009): 487-496.

100. Leempoel, K., et al. “Dynamics in mangroves assessed by high-resolution and multi-temporal satellite data: a case study in Zhanjiang Mangrove National Nature Reserve (ZMNNR), P. R. China.” *Biogeosciences* 10 (2013): 5681–5689.

101. Li. X., et al. “Regression and analytical models for estimating mangrove wetland biomass in South China using Radarsat images.” *International Journal of Remote Sensing* 28.24 (2007): 5567-5582.

102. Lopes A., et al. “Maximum A Posteriori speckle filtering and first order texture models in SAR images.” *International Geoscience and Remote Sensing Symposium (IGARSS)*. 1990.

103. Lucas, R.M., et al. “ALOS PALSAR Applications in the Tropics and Subtropics: Characterisation, Mapping and Detecting Change in Forests and Coastal Wetlands.” *Proceedings of Second ALOS PI Symposium*, Rhodes, Greece, 3–7 November 2008. Available online: http://amapmed.free.fr/AMAPMED_fichiers/Publications_fichiers/Lucas08.pdf (accessed on 13 February 2017).

104. Lucas, R. M. et al. “The potential of L-band SAR for quantifying mangrove characteristics and change: Case studies from the tropics.” *Aquatic Conservation* 17 (2007): 245-264.

105. Lucas, R. M., M. Moghaddam, and N. Cronin. “Microwave scattering from mixed-species forest, Queensland, Australia.” *IEEE Transaction on Geoscience and Remote Sensing* 42 (2004): 2142-2159.

106. Lucas, R.M., A. Mitchell, and C. Proisy. “The Use of Polarimetric AIRSAR (POLSAR) Data for Characterising Mangrove Communities.” *Proceedings of AIRSAR Earth Science and Application Workshop,* Pasadena, CA, USA, 4–6 March 2002.

107. Mallat, S. G. “A theory for multiresolution signal decomposition: The wavelet representation.” *I.E.E.E. Transactions on Pattern Analysis and Machine Intelligence* 11 (1989): 674-693.

108. Manjunath, K., et al. “Discrimination of mangrove species and mudflat classes using in situ hyperspectral data: a case study of Indian Sundarbans.” *GIScience and Remote Sensing* 50.4 (2013): 400–417.

109. Manson, F.J., et al. “Assessing techniques for estimating the extent of mangroves: topographic maps; aerial photographs and Landsat TM images.” *Marine and Freshwater Research* 52 (2001): 787–792.

110. Mansourpour, M., M. A. Rajabi, and J. A. R. Blais. “Effects and Performance of Speckle Noise Reduction Filters on Active Radar and SAR imageries.” ISPRS Proceedings, XXXVI. 2006.

111. Mather P.M. and M. Koch. *Computer processing of remotely-sensed images: An introduction.* John Wiley & Sons. 2011. 171-172.

112. McCoy, E.D., et al. “Mangrove damage caused by Hurricane Andrew on the south-western coast of Florida.” *Bulletin of Marine Science* 59.1 (1996): 1-8.

113. Memon, A. A., “Devastation of the Indus river delta.” *Proceedings of World Water & Environmental Resources Congress 2005.* American Society of Civil Engineers, Environmental and Water Resources Institute, Anchorage, Alaska, May 14-19, 2005 (Note – Expanded version).

114. Monzon, A.K., et al. "Synergy of optical and SAR data for mapping and monitoring mangroves." *The International Archives of the Photogrammetry, Remote Sensing and Spatial Information Sciences*. XLI-B6. 2016 XXIII ISPRS Congress, Prague, Czech Republic. 12–19 July 2016. 259-266.

115. Mouat, D. A., G. G. Mahin, and J. Lancaster. "Remote sensing techniques in the analysis of change detection." *Geocarto International* 2 (1993): 39- 50.

116. Mougin, E., et al. "Multifrequency and multipolarization radar backscattering from mangrove forests." *IEEE Transactions on Geoscience and Remote Sensing* 37 (1999): 94-102.

117. Myint, S.W., et al. "Identifying mangrove species and their surrounding land use and land cover classes using an object-oriented approach with a lacunarity spatial measure." *GIScience and Remote Sensing* 45 (2008): 188–208.

118. Nair, V. *Status of the flora and fauna of Gulf of Kachchh, India*. National Institute of Oceanography (NIO), Goa. 2002. 27.

119. Navalgund, R.R. and A. Bahuguna. "Applications of remote sensing and GIS in coastal zone management and conservation: Indian experience." *Proc: U.N. ESCAP/ISRO Science Symposium, On Space Technology for improving Quality of Life in Developing Countries: a perspective for the next millennium*, held at New Delhi from Nov. 15-17 1999. 121-146.

120. Nayak, S. and A. Bahuguna. "Application of remote sensing data to monitor mangroves and other coastal vegetation of India." *Indian Journal of Marine Sciences* 30.4 (2001): 195-213.

121. Nayak, S.R., et al. "Application of satellite data for monitoring degradation of tidal wetlands of Gulf of Kachchh, Western India." *Acta Astronautica* 20 (1989): 171-178.

122. Neukermans, G., et al. “Mangrove species and stand mapping in Gazi Bay (Kenya) using Quickbird satellite imagery.” *Journal of Spatial Sciences* 53 (2008): 75-86.

123. Olwig, M.F., et al. “Using remote sensing to assess the protective role of coastal woody vegetation against tsunami waves.” *International Journal of Remote Sensing* 28 (2007): 3153-3169.

124. Ong, C.C., et al. “Deriving quantitative dust measurements related to iron ore handling from airborne hyperspectral data.” *Mining Tech. Trans. Inst. Min. Metall. A,* 112 (2003):158-163.

125. Padia, K. and R. Mehra. *RISAT-1 Data Product Format*. Space Applications Centre (SAC), Indian Space Research Organization (ISRO), Ahmedabad, Gujarat, India. 2013.

126. Pasqualini, V., et al. “Mangrove mapping in North-Western Madagascar using SPOT-XS and SIR-C radar data.” *Hydrobiologica* 413 (1999): 127-133.

127. Patterson, W.G. *Mangrove community boundary interpretation and detection of areal changes in Marco Island, Florida: application of digital image processing and remote sensing technique*. US Fish & Wildlife Service. Biological Report. 1986.

128. Pohl, C. and J. L. Van Genderen. “Multisensor image fusion in remote sensing: Concepts, methods and applications.” *International Journal of Remote Sensing* 19.5 (1998): 823-854.

129. Polidoro, B. A., et al. “The loss of species: mangrove extinction risk and geographic areas of global concern.” *PLOS One* 5 (2010): e10095.

130. Porwal, M.C., et al. “Importance of middle infrared band for classifying mangrove vegetation and plantation in Middle Andaman Islands.” *Proceedings of National Symposium on Remote Sensing for Sustainable Development.* Lucknow, India. 1992.

131. Pratt W.K. *Digital Image Processing*. Wiley. New York. 1978.

132. Proisy, C., et al. “Interpretation of polarimetric radar signatures of mangrove forests.” *Remote Sensing of Environment* 71 (2000): 56-66.

133. Proisy, C., E. Mougin, and F. Fromard. “Radar remote sensing of mangroves: results and perspectives. *Proceedings of IGARSS Conference*. Sydney, Australia. 9–13 July 2001.

134. Proisy, C., et al. “On the influence of canopy structure on the radar backscattering mangrove forests.” *International Journal of Remote Sensing* 23 (2002): 4197-4210.

135. Proisy, C., P. Couteron, and F. Fromard. “Predicting and mapping mangrove biomass from canopy grain analysis using Fourier-based textural ordination of IKONOS images.” *Remote Sensing of Environment* 109 (2007): 379-392.

136. RADAR and SAR Glossary, https://earth.esa.int/handbooks/asar/CNTR5-2.html, page accessed on 06 March 2017.

137. Radar Imaging Satellite (RISAT-1), https://nrsc.gov.in/sites/all/pdf/RISAT-1BROCHUREV4.pdf, accessed on 01 March 2017.

138. Radiance, https://en.wikipedia.org/wiki/Radiance, page accessed on 04 March 2017.

139. Rahman, M.M., et al. “Comparison of Landsat image classification methods for detecting mangrove forests in Sundarbans.” *International Journal of Remote Sensing* 34.4 (2013): 1041-1056.

140. Rajawat, A.S., et al. “Assessment of coastal erosion along the Indian coast on 1: 25,000 scale using satellite data of 1989–1991 and 2004–2006 time frames.” *Current Science* 109.2 (2015): 347-353.

141. Ramachandran, S., et al. “Application of remote sensing and GIS to coastal wetland ecology of Tamil Nadu and Andaman and Nicobar group of islands with special reference to mangroves.” *Current Science* 75 (1998): 236-244.

142. Ramachandran, S., et al. “Ecological impact of tsunami on Nicobar Islands (Camorta, Katchal,Nancowry and Trinkat).” *Current Science* 89 (2005): 195-200.

143. Ramsey, E.W., and J. R. Jensen. “Remote sensing of mangrove wetlands: Relating canopy spectra to site-specific data.” *Photogrammetric Engineering and Remote Sensing* 62 (1996): 939-948.

144. Ranchin, T., and L. Wald. “The wavelet transform for the analysis of remotely sensed images.” *International Journal of Remote Sensing* 14 (1993): 615-619.

145. Raney, R.K. *Radar Fundamentals: Technical Perspective.* In Principle and Application of Imaging Radar, Manual of Remote Sensing, Third Edition, Volume 2, ASPRS, John Wiley and Sons, Inc., Toronto. 1998.

146. Raouf, A., and J. Lichtenegger. “Integrated Use of SAR and Optical Data for Coastal Zone Management.” available on earthnet online https://earth.esa.int/workshops/ers97/papers/lichtenegg/231c.html. 1997.

147. Rasolofoharinoro, M., et al. “A remote sensing based methodology for mangrove studies in Madagascar.” *International Journal of Remote Sensing*, 19 (1998): 1873-1886.

148. Resourcesat-2, https://directory.eoportal.org/web/eoportal/satellite-missions/r/resourcesat-2, page accessed on 01 March 2017.

149. RISAT-1. https://directory.eoportal.org/web/eoportal/satellite-missions/r/risat-1, page accessed on 01 March 2017

150. Rhyma, P.P., et al. “A review of uses of satellite imagery in monitoring mangrove forests.” *IOP Conference Series: Earth and Environmental Sciences* 37 (2016):1-14.

151. Richards, J.A. and X. Jia. *Remote Sensing Digital Image Analysis: An Introduction*. Springer. 2006.

152. Rodriguez, W. and I. C. Feller. “Mangrove landscape characterization and change in Twin Cays, Belize using aerial photography and IKONOS satellite data.” *Atoll Research Bulletin* 513 (2004): 1-22.

153. Rosenquist, A., M. Shimada, and M. Watanbe. “ALOS PALSAR: Technical outline and mission concepts.” *4th International Symposium on Retrieval of Bio- and Geophysical Parameters from SAR data for Land Applications*. Innsbruck, Austria, Nov. 16-19, 2004.

154. Roy, S. D. and P. Krishanan. “Mangrove stands of Andamans *vis-à-vis* tsunami.” *Current Science* 89 (2005): 1800-1804.

155. Roy, P.S., et al. “Tropical forest type mapping and monitoring using remote sensing.” *International Journal of Remote Sensing* 12 (1991): 2205-2225.

156. Sabins, F.F. *Remote Sensing: Principles and Interpretation*. W. H. Freeman. ISBN. 0716700239. 1978. 426.

157. Space Applications Centre. *Community zonation of selected mangrove habitats of India using satellite data*. Scientific Note. SAC/RESIPA/MWRG/MSCED/SN/2003. 92.

158. Space Applications Centre. *Coastal habitat of selected Marine Protected Areas: Atlas of India*. SAC/RESIPA/MESG/PR/59/2007.

159. Space Applications Centre. *Coastal Zones of India*. Published by Space Applications Centre, Ahmedabad. 2012. 609.

160. Sahu, S.C., et al. “Mangrove area assessment in India: Implications of loss of Mangroves.” *Journal of Earth Science & Climate Change* 6.5 (2015): 1-7.

161. Saleh, M.A. Mangrove vegetation on Abu Minqar Island of the Red Sea. *International Journal of Remote Sensing* 28 (2007): 5191-5194.

162. Sandilyan, S. and K. Kathiresan. “Mangrove conservation: A global perspective.” *Biodiversity and Conservation* 21 (2012): 3523-3542. http://dx.doi.org/10.1007/s10531-012-0388-x.

163. Sari, S.P. and D. Rosalina. “Mapping and Monitoring of Mangrove Density Changes on tin Mining Area.” *Procedia Environmental Sciences* 33 (2016): 436–442.

164. Sathirathai, S. and E.B. Barbier. “Valuing mangrove conservation in Southern Thailand.” *Contemporary Economic Policy* 19.2 (2001): 109-122.

165. Satyanarayana C. & Ramakrishna. *Handbook on hard corals of Gulf of Kachchh*. Zoological Survey of India. 2009.

166. Selvam, V., et al. “Assessment of community-based restoration of Pichavaram mangrove wetland using remote sensing data.” *Current Science* 85 (2003): 794-798.

167. Seto, K.C. and M. Fragkias. “Mangrove conversion and aquaculture development in Vietnam: A remote sensing-based approach for evaluating the Ramsar Convention on Wetlands.” *Global Environment Change* 17 (2007): 486-500.

168. Shah A.A., I. Kasawani and J. Kamaruzaman. “Degradation of Indus Delta mangroves in Pakistan.” *International Journal of Geology* 1.3 (2007): 27-34.

169. Shah, D.G., et al. “Zoning and monitoring dominant mangrove communities of a part of the Marine National Park, Gulf of Kachchh.” *Journal of Indian Society of Remote Sensing* 33.1 (2005): 155-163.

170. Shanmugam, P., et al. “Application of mulitsensor fusion techniques in remote sensing of coastal mangrove wetlands.” *International Journal of Geoinformatics* 1 (2005): 1-17.

171. Shettigara, V. K. “A generalized component substitution technique for spatial enhancement of multispectral images using a higher resolution data set.” *Photogrammetric Engineering and Remote Sensing* 58 (1992): 561-567.

172. Shukla, S. B., et al. “Coastal geomorphology and tsunami hazard scenario along the Kachchh coast, Western India.” *Indian Journal of Geo-Marine Sciences* 39.4 (2010): 549-556.

173. Shukla, S. B., A. K. Patidar and N. Bhatt. “Application of GPR in the study of shallow subsurface sedimentary architecture of Modwa spit, Gulf of Kachchh.” *Journal of Earth System Sciences* 117.1 (2008): 33-40.

174. Simard, M., et al. “Mapping tropical coastal vegetation using JERS-1 and ERS-1 radar data with a decision tree classifier.” *International Journal of Remote Sensing* 23 (2002): 1461-1474.

175. Singh, H.S. “Marine protected areas in India.” *Indian Journal of Marine Sciences* 32.3 (2003): 226-233.

176. Singh, H.S., et al. *An Ecological and Socio-Economic Study in Marine National Park and Sanctuary in the Gulf of Kachchh (A Comprehensive Study on Biodiversity and Management Issues)*. GEER Foundation. 2002. 347.

177. Singh, H.S. *Mangroves in Gujarat, Current status and strategy for conservation*. 2000. 128.

178. Singh, H.S. *Protected Areas in India: Status of Coastal Wetlands and their Conservation in India*. GEER Foundation, Gandhinagar. 2002.

179. Spalding, M., F. Blasco. And C. Field. *World Mangrove Atlas*. The International Society for Mangrove Ecosystems: Okinawa, Japan. 1997.

180. Souza Filho, P.W. and W. R. Paradella. “Recognition of the main geobotanical features along the Braganca mangrove coast (Brazilian Amazon Region) from Landsat TM and RADARSAT-1 data.” *Wetlands* 10 (2002): 123-132.

181. Souza Filho, P.W. and W.R. Paradella. “Use of RADARSAT-1 fine mode and Landsat-5 TM selective principal component analysis for geomorphological mapping in a macrotidal mangrove coast in the Amazon Region.” *Canadian Journal of Remote Sensing* 31 (2005): 214-224.

182. Sridhar, R., et al. “Rapid assessment on the impact of tsunami on mangrove vegetation of the Great Nicobar Island.” *Journal of the Indian Society of Remote Sensing* 34 (2006): 89-93.

183. Swain, P. K. and N. R. Rao. *Floral diversity and vegetation ecology of mangrove ecosystems in the states of Goa, Karnataka and Andhra Pradesh, India*. In Mangroves in India: their biology and uses. 2013. 95-110.

184. Tarakanadha, B., B. T. Singh, and K. S. Rao. *Coastal vegetation of Nellore district, Andhra Pradesh, East Coast of India*. In Mangroves in India: their biology and uses. 2013. 233-244.

185. Times News Network. "*Four held in Tata Chemicals leakage case*". 25 Oct 2003.

186. Tomlinsosn, P.B. *The Botany of Mangroves*. Cambridge University Press. 1986. 413.

187. Tong, P.H., et al. “Assessment from space of mangroves evolution in the Mekong Delta; in relation to extensive shrimp farming.” *International Journal of Remote Sensing*, 25 (2004): 4795-4812.

188. Touzi, R., A. Lopes, and P. Bousquet. (1998). “A statistical and geometrical edge detector for SAR image.” I*EEE Transactions on Geoscience and Remote Sensing*, 26.6 (1998): 764-773.

189. Down to Earth. *Toxic destruction*. 15 July 2001.

190. Untawale, A.G. *Restoration of mangroves along the Central West Coast of India*. In Restoration of mangrove ecosystems. Japan, ISME. 1996. 111-112.

191. Upadhyay, R., et al. “Mangrove restoration and regeneration monitoring in Gulf of Kachchh, Gujarat State, India, using remote sensing and Geo-Informatics.” *International Journal of Geosciences* 6 (2015): 299-310.

192. Vaiphasa, C., et al. “Tropical mangrove species discrimination using hyperspectral data: A laboratory study.” *Estuarine Coastal Shelf Science* 65 (2005): 371-379.

193. Vaiphasa, C., A. K. Skidmore. and W. F. de Boer. “A post-classifier for mangrove mapping using ecological data.” *ISPRS Journal of Photogrammetry and Remote Sensing* 61 (2006): 1-10.

194. Valiela, I., J. L. Bowen. and J. K. York. “Mangrove Forests: One of the World’s Threatened Major Tropical Environments.” *Bioscience* 51 (2001): 807–815.

195. Vethamony, P. and M. T. Babu. “Physical processes in the Gulf of Kachchh: A Review.” *Indian Journal of Geo-Marine Sciences* 39.4 (2010): 497-503.

196. Vyas, P. *Sundarban Biosphere Reserve, India: Conservation and management of mangrove ecosystem*. In: Mangroves in India: their biology and uses. 2013. 33-56.

197. Wang, Y., et al. “Remote sensing of mangrove change along the Tanzania Coast.” *Marine Geodesy* 26 (2003): 35-48.

198. Wang, L., L. Silván-Cárdenas, and W. P. Sousa. “Neural network classification of mangrove species from multi-seasonal IKONOS imagery.” *Photogrammetric Engineering and Remote Sensing*. 74 (2008): 921-927.

199. Wang, L.,et al. “Comparison of IKONOS and QuickBird imagery for mapping mangrove species on the Caribbean coast of Panama.” *Remote Sensing of Environment* 91 (2004): 432-440.

200. Wang, L. and W.P. Sousa. “Distinguishing mangrove species with laboratory measurements of hyperspectral leaf reflectance.” *International Journal of Remote Sensing* 30 (2009): 1267-1281.

201. Wickramasinghe, C.H., et al. “Mangrove mapping analysis on optical and Synthetic Aperture Radar data using ALOS/PLASAR and ALOS/ AVNIR-2.” *The 33rd Asian Conference of Remote Sensing*, Nov. 26-30, 2012, Thailand. Downloaded from: http://a-a-r-s.org/acrs/administrator/components/com_jresearch/files/publications/D4-2.pdf (accessed on 14 Feb 2017).

202. www.mnpcs.gov.in, page accessed on 14/08/2015 and 17/08/2015.

203. Yang, C., et al. “Evaluating AISA+ hyperspectral imagery for mapping black mangrove along the South Texas Gulf Coast.” *Photogrammetric Engineering and Remote Sensing* 75 (2009): 425-435.